

Elham Khalilzadeh Shirazi

**Investigations on the applicability of
bentonite, dolomite and vermicompost
as natural adsorbents for the
decolorization of textile wastewater**

FORSCHUNGS- UND ENTWICKLUNGSINSTITUT FÜR
INDUSTRIE- UND SIEDLUNGSWASSERWIRTSCHAFT SOWIE
ABFALLWIRTSCHAFT E.V. (FEI)

Elham Khalilzadeh Shirazi

**Investigations on the applicability of
bentonite, dolomite and vermicompost as
natural adsorbents for the decolorization
of textile wastewater**

D 93

IMPRESSUM

Bibliographische Information der Deutschen Bibliothek

Die Deutsche Bibliothek verzeichnet die Publikation in der Deutschen Nationalbibliographie; detaillierte bibliographische Daten sind im Internet über <http://dnb.ddb.de> abrufbar

Elham Khalilzadeh Shirazi

Investigations on the applicability of bentonite, dolomite and vermicompost as natural adsorbents for the decolorization of textile wastewater

Forschungs- und Entwicklungsinstitut für Industrie- und Siedlungswasserwirtschaft sowie Abfallwirtschaft e.V. (FEI)

Stuttgarter Berichte zur Siedlungswasserwirtschaft, Band 253



Layout:

Institut für Siedlungswasserbau, Wassergüte- und Abfallwirtschaft
der Universität Stuttgart ISWA
Bandtäle 2, 70569 Stuttgart

Druck:

e.kurz + co. druck und medientechnik gmbh
Kernerstr. 5, 70182 Stuttgart

©2023 Alle Rechte vorbehalten

Printed in Germany

Investigations on the applicability of bentonite, dolomite and vermicompost as natural adsorbents for the decolorization of textile wastewater

Von der Fakultät für Bau - und Umweltingenieurwissenschaften
der Universität Stuttgart zur Erlangung der Würde einer Doktor-Ingenieurin (Dr.-Ing.)
genehmigte Abhandlung

Vorgelegt von
Elham Khalilzadeh Shirazi
Aus Teheran, Iran

Hauptberichter: Prof. Dr. rer. nat. habil. Jörg W. Metzger

Mitberichter: PD Dr.-Ing. habil. Harald Schönberger

Mitberichter: Prof. Amir Hessam Hassani

Tag der mündlichen Prüfung: 20.04.2023

Institut für Siedlungswasserbau, Wassergüte - und Abfallwirtschaft
der Universität Stuttgart

2023

Acknowledgments

This dissertation work could not have been accomplished without the assistance and support of many individuals and institutions.

I am very thankful to my supervisor Prof. Jörg W. Metzger for recognizing my potential and giving me the opportunity to pursue this doctorate, for his great commitment, guidance, patience, support and sense of responsibility throughout the research process. I am genuinely appreciative of all his kind support.

I am really grateful to Dr. Harald Schönberger as the co-supervisor of this doctoral thesis and would like to thank him for investing his time in the case that he was extremely busy and for the critical and constructive input and guidance, which certainly improved the quality of this work. Without his support and co-supervision, this research work could not have been possible to come to an end successfully.

I would like to express my deep gratitude to my Iranian co-supervisor Prof. Amir Hessem Hassani at Azad University (Tehran Science and Research Branch). I really thank him for hosting me in his department and laboratory premises throughout all these years. Thank you for being extremely supportive and reliable, and for sharing your valuable experience and knowledge.

I appreciate the contribution of Dr. Klaus Fischer in the preliminary studies phase of this doctoral thesis, for his guidance, and for sharing his valuable experience.

My grateful thanks go to all the staff of the Acryl Tab company and the LECA company, including managers and engineers for their fantastic cooperation. Also, I am thankful to the laboratory personnel and all the staff of Azad University and to different industries in Iran who provided me with different materials that were necessary for this research work.

I acknowledge gratefully Mrs. Katja Jenkner, the supervisor for international doctoral candidates and DAAD-scholarship holders at the Department of International Students (IZ) at the University of Stuttgart, and Mrs. Anne Weiss, the course director of the WAREM program, and Mrs. Claudia Hojak for their kind support.

I would like to acknowledge also the direct and indirect contribution and support of the scientific, administrative and secretarial staff of ISWA (Institute for Sanitary Engineering, Water Quality and Waste Management), in particular the assistance of Dr. Bertram Kuch, Dr. Michael Koch, Mr. Carsten Meyer, Mrs. Dörte Hahn, Mrs. Renate Schill, Mrs. Christine Schulmeister, Mrs. Gertrud Joas and Mrs. Cornelia Orth.

Nothing could be more important to me than my family. My final and profound gratitude goes to my loving family, my mother and my brother for their immense patience and unconditional support throughout this long and strenuous process with a lot of ups and downs.

Published papers covering parts of the dissertation

- 1) Elham Khalilzadeh Shirazi, Jörg W. Metzger, Klaus Fischer, Amir Hessam Hassani
Removal of cationic and anionic dyes from single and binary dye systems with Persian charred dolomite using the first-order derivative spectrophotometer analysis method
International Journal of Advances in Science, Engineering and Technology (IJASEAT), 6 (4) suppl. 1 (2018) 17-21.
- 2) Elham Khalilzadeh Shirazi, Jörg W. Metzger, Klaus Fischer, Amir Hessam Hassani
Simultaneous removal of a cationic and an anionic textile dye from water by a mixed sorbent of vermicompost and Persian charred dolomite
Chemosphere, 234 (2019) 618-629.
<https://doi.org/10.1016/j.chemosphere.2019.05.224>
- 3) Elham Khalilzadeh Shirazi, Jörg W. Metzger, Klaus Fischer, Amir Hessam Hassani
Removal of textile dyes from single and binary component systems by Persian bentonite and a mixed adsorbent of bentonite/charred dolomite
Colloids and Surfaces A: Physicochemical and Engineering Aspects, 598 (2020) 124807.
<https://doi.org/10.1016/j.colsurfa.2020.124807>
- 4) Elham Khalilzadeh Shirazi, Jörg W. Metzger, Klaus Fischer, Amir Hessam Hassani
Design and cost analysis of batch adsorber systems for removal of dyes from contaminated groundwater using natural low-cost adsorbents
International Journal of Industrial Chemistry, 11 (2020) 101-110.
<https://doi.org/10.1007/s40090-020-00205-1>

Oral presentations at conferences:

- 1) Elham Khalilzadeh Shirazi, Jörg W. Metzger, Klaus Fischer, Amir Hessam Hassani
Removal of cationic and anionic dyes from single and binary dye systems with Persian charred dolomite using first-order derivative spectrophotometer analysis method
Oral presentation at International Conference on Natural Science and Environment, Copenhagen, Denmark (Proceedings of 189th The IIER International Conference, Copenhagen, Denmark, 15th-16th September 2018).

- 2) Elham Khalilzadeh Shirazi, Jörg W. Metzger, Klaus Fischer, Amir Hessam Hassani

Green materials for sustainable remediation of dyes in water

Theme for the seminar: An innovative outlook in the fields of hydraulic engineering, groundwater management and sanitary engineering through professional and research activities

Oral presentation at a professional seminar by IAHR-BW International Association for Hydro-Environment Engineering and Research-Baden Württemberg, 25th January 2019, University of Stuttgart, Germany.

- 3) Elham Khalilzadeh Shirazi, Jörg W. Metzger, Klaus Fischer, Amir Hessam Hassani

Biosorptive removal of a textile dye basic violet 16 on the green adsorbent vermicompost: sustainable environmentally friendly clean up technique

4th Green and Sustainable Chemistry Conference (Elsevier conference), 5th-8th May 2019, Dresden, Germany.

Poster presentation:

- 1) Elham Khalilzadeh Shirazi, Jörg W. Metzger, Klaus Fischer, Amir Hessam Hassani

Batch adsorber design and cost analysis for removal of dyes from contaminated groundwater using natural low-cost adsorbents

Poster presented at Industrial Water, Dechema Haus, 27th-29th November 2018, Frankfurt am Main, Germany.

Relation to the published works

The following chapters of this thesis including abstract, motivation and chapters 1 to 4 are based on the publications mentioned above and contain similar information. The references are declared at the end of each chapter (summary part) as well.

Abstract

This thesis focused on the applicability of bentonite, dolomite and vermicompost as natural adsorbents for the removal of cationic and anionic textile dyes from colored wastewater. The application of natural granular bentonite in a fixed-bed column for the treatment of wastewater resulting from the acrylic fiber dyeing process pretreated with the coagulation-flocculation process in the wastewater treatment plant of the Iranian textile company of Acryl Tab was studied. The potential reuse of the treated wastewater in the studied company was investigated. Furthermore, the application of the spent bentonite in the production of lightweight aggregates (LWAs) was studied as possibility to minimize the environmental impacts of the disposal of the produced waste material. Natural granular bentonite and other natural materials were studied in this thesis in terms of their color removal efficiency and the possibility to be applied as adsorbent in a fixed-bed column. Granular bentonite was selected for further detailed studies. Adsorption experiments included batch and fixed-bed column experiments. The evaluation of efficiencies of the studied treatment systems was based on decolorization and COD reduction. A series of pilot-scale fixed-bed column (diameter 5 cm/ height 1 m) tests were conducted to examine the breakthrough curves and to evaluate the efficiency of granular bentonite to remove color and COD under different set-up and operating conditions, including bed height and flow rate.

The X-ray diffractogram of the natural granular bentonite showed that it was primarily composed of montmorillonite as the main mineral phase. The textile wastewater which beforehand had been subjected to coagulation-flocculation and sedimentation processes had a yellowish-orange color which corresponded to 20.2 m^{-1} for $\text{SAC}_{436 \text{ nm}}$, 6.4 m^{-1} for $\text{SAC}_{525 \text{ nm}}$, 3.9 m^{-1} for $\text{SAC}_{620 \text{ nm}}$ and to $456 \text{ mg Pt-Co L}^{-1}$ (The Pt-Co method was used only for the comparison with the Iranian discharge limit standard). These color parameters of the pretreated wastewater neither comply with Iranian nor with German discharge limits into water bodies for textile wastewaters, which are in Iran: $75 \text{ mg Pt-Co L}^{-1}$, in Germany: 7 m^{-1} for $\text{SAC}_{436 \text{ nm}}$, 5 m^{-1} for $\text{SAC}_{525 \text{ nm}}$ and 3 m^{-1} for $\text{SAC}_{620 \text{ nm}}$, nor with water reuse requirements for textile processing, i.e. non-visible color (with reference to the European AquaFit4Use project). The pretreated wastewater was characterized by an alkaline pH of 11.6, a COD value of 890 mg L^{-1} and a conductivity of $2213 \text{ }\mu\text{S m}^{-1}$.

In the batch studies, granular bentonite showed an effective removal for color and COD. 5 g granular bentonite/L was found to be the optimized amount for maximum color and COD reduction. In the batch experiments, the color reduction was 88.1% ($\text{SAC}_{436 \text{ nm}}$), 70.3% ($\text{SAC}_{525 \text{ nm}}$) and 71.8% ($\text{SAC}_{620 \text{ nm}}$), respectively. The Langmuir model efficiently described the adsorption process of color on granular bentonite for all three wavelengths (SAC_{436} , 525 and 620 nm). This suggests that the removal of color using natural granular bentonite occurred

via monolayer adsorption. Moreover, the results showed that the adsorption process followed more satisfactorily a pseudo-second-order model than a pseudo-first-order model indicating that the adsorption process is presumably chemical adsorption. Under optimum conditions, results illustrated that the COD could be lowered from initial 890 mg L^{-1} to 403 mg L^{-1} (removal efficiency 54.7%). The Freundlich model can effectively describes the adsorption process of COD on granular bentonite, and the COD removal on granular bentonite followed the pseudo-second-order kinetics.

In continuous adsorption experiments using a fixed-bed column packed with granular bentonite, the effect of the different flow rates 5, 10 and 20 ml min^{-1} and bed heights 5, 10 and 20 cm on the removal efficiency of color and COD was studied. The highest bed height and the lowest influent flow rate were found to be the best condition for color adsorption, i.e. color was effectively removed in a fixed-bed column with 20 cm bed height at a flow rate of 5 ml min^{-1} . The color of the treated effluent was lowered from 20.2 to 3.9 for $\text{SAC}_{436 \text{ nm}}$, 6.4 to 1.5 for $\text{SAC}_{525 \text{ nm}}$, and 3.9 to 1.4 for $\text{SAC}_{620 \text{ nm}}$, respectively. Decolorization efficiencies of 93% (Pt-Co method), 80% ($\text{SAC}_{436 \text{ nm}}$), 67% ($\text{SAC}_{525 \text{ nm}}$) and 64% ($\text{SAC}_{620 \text{ nm}}$) were reached. COD of the treated effluent from the fixed-bed column was lowered from 890 mg L^{-1} to 382 mg L^{-1} , i.e. 57% of the COD was eliminated. These results show that granular bentonite for the decolorization of the textile wastewater is effective.

The treated wastewater at a breakthrough point from the fixed-bed column (20 cm adsorbent height, 5 ml min^{-1} flow rate) not only fulfils the requirement for reuse in the textile wet processing (“non-visible” color) but also reached the German and Iranian discharge limits in terms of the color of the treated effluent. The results show that the treated wastewater from the fixed-bed adsorption column has $32 \text{ mg Pt-Co L}^{-1}$ which is below the determined limited value in Iran for discharging the treated effluent into the environment. The color parameters of the treated wastewater resulted below 7 m^{-1} for $\text{SAC}_{436 \text{ nm}}$, 5 m^{-1} for $\text{SAC}_{525 \text{ nm}}$ and 3 m^{-1} for $\text{SAC}_{620 \text{ nm}}$, which fulfilled German minimum discharge limits into water bodies for textile wastewaters. The COD of the treated effluent from the fixed-bed column (382 mg L^{-1}) can meet the COD range limit of “low-quality water” for reuse purposes (with reference to the European AquaFit4Use project). The conductivity and pH of the wastewater after treatment reached $1565 \text{ } \mu\text{S m}^{-1}$ and 8.15, respectively, fulfilled limits for the “general water reuse” for the conductivity, and “medium- to low-quality water” requirement for pH. Therefore, the treated textile wastewater can be proposed to be reused in the production process of the studied textile industry for rinsing/washing applications (washing down the equipment and washing the floors) as well as for washing the fibers for part of the pretreatment before dyeing. In conclusion, the adsorption using granular bentonite can be applied as a treatment step combined with the other conventional treatment methods in the studied industry to remove color and to reduce COD sufficiently from the wastewater of the acrylic fiber dyeing process to be reused for washing purposes. The reuse of the treated wastewater in the studied company can reduce

water consumption. Therefore, the solution of water closed-loop recycling is suggested for achieving sustainability in water consumption in this textile finishing industry. Moreover, the treatment with the natural adsorbent can decrease the contamination of surface and ground waters since the studied industry (Acryl Tab CO.) usually discharges the pretreated textile effluent from its wastewater treatment plant into the municipal wastewater sewer and/or on agricultural lands (rice fields).

Based on the scale-up method developed by Forntwalt and Hutchins (1966), the parameters to design and implement a fixed-bed column at an industrial scale were calculated as: area $A = 0.84 \text{ m}^2$, diameter $d = 1.04 \text{ m}$ and height between 3.12 and 5.12 m. According to the results from 5 cm, 10 cm and 20 cm bentonite bed heights at pilot-scale, the design column can treat 37.5 m^3 , 56.25 m^3 and 100 m^3 of wastewater, respectively in 6 h, 9 h and 16 h (at breakthrough points) using 2287 kg, 4569.6 kg and 9150.4 kg of bentonite which is required for the treatment of wastewater with a flow rate of $150 \text{ m}^3 \text{ d}^{-1}$. As the company works mainly in 2 working shifts, 6098 kg bentonite (5 cm bed height), 8123.73 kg bentonite (10 cm bed height) and 9150.4 kg bentonite (20 cm bed height) is required per day to treat the generated wastewater.

As the quality of the treated wastewater at breakthrough points of all bentonite bed heights (5, 10 and 20 cm) fulfilled the requirements for water reuse (low-quality water for washing purposes based on the Aquafit4use project), the amount of bentonite scaled up from the pilot-scale column with 5 cm bed height will be reasonable to be considered in practice for the studied industry from the economic point of view. Accordingly, as the company works mainly in 2 working shifts (16 h), 6098 kg of bentonite is needed to treat the produced wastewater per day. Considering the price of the natural bentonite provided from an Iranian company, only 83 euro should be spent to supply this amount of bentonite per day. However, the amount of bentonite can be a considerable quantity to handle and to process.

With reference to the life cycle impact assessment (LCIA) and Monte Carlo analysis results, the ratio of the mean price of wastewater treatment with 86.6 kg bentonite per hour to the mean price of wastewater treatment with 3.8 kg activated carbon per hour concluded 0.06. Therefore, natural bentonite was concluded as a much more environmentally friendly and cheaper alternative compared to activated carbon, a common adsorbent in wastewater treatment, for the treatment of the pretreated acrylic fiber dyeing wastewater in Iran.

Another aim of this thesis was to investigate the possibility of using the spent adsorbent as a new raw material source in the production of construction materials. In other words, to convert waste (the used adsorbent) into a usable resource. In this thesis, spent bentonite was applied in the production of LWAs such as LECA (lightweight expanded clay aggregate). This solution can help to avoid producing secondary pollution and to increase the value of the produced waste by converting it into an efficient material. The properties of the generated LWAs from

the spent waste were compared to the conventional LWAs, i.e. LECA produced at LECA CO. using natural clay.

To produce LWAs using spent bentonite, the mixtures were blended with water and an additive (1% mazut), then shaped into pellets and oven-dried, and finally sintered at 1140 °C for 4 min in a muffle furnace. The main technical features of the aggregates (water absorption after 24 h, density and mechanical strength) were determined. As there is a positive correlation between an increase in organic matter and porosity in the produced LWAs, the organic matters in the effluent contributed to a higher porosity in the sintering process, thereby lowering the density as well as increasing the water absorption of the produced LWAs.

It was found that the use of spent adsorbent can yield a reasonably high-performance LWA which can reduce the cost of the waste treatment and the cost of LWAs production leading a more circular economy.

In preliminary studies, different low-cost natural materials such as vermicompost (organic), dolomite and bentonite (inorganic) were used as adsorbents in single and binary sorbent systems to remove fabric dyes from single and binary dye solutions. The two dyes selected were the cationic dye basic violet 16 (BV₁₆) and the anionic dye reactive red 195 (RR₁₉₅), two commonly used dyes in the textile industry in Iran. Groundwater samples were spiked with the two dyes and used in this thesis.

Firstly, a series of preliminary bench-scale experiments were performed to study the feasibility of removing BV₁₆ and RR₁₉₅, from single-component solutions using the inorganic materials Persian charred (i.e. treated at 800 °C) dolomite, Persian natural bentonite, organic material vermicompost (all of them adsorbents locally available in Iran) and commercially available 'standard' bentonite.

Batch experiments with single sorbent single dye solutions were carried out to examine and optimize the process parameters, including the effect of the initial dye concentration, contact time, adsorbent amount and stirring speed on the adsorption of the dyes. The effect of the above-mentioned parameters was investigated to adjust the process variables and to determine the adsorption isotherms and kinetics curves as well as using the optimized parameters in a single sorbent binary dye solution system and binary sorbent binary dye system. Groundwater samples containing one or both of these dyes ('single' or 'binary dye solutions') were treated with vermicompost and charred dolomite either alone or mixed, or with bentonite and charred dolomite either alone or mixed. In single sorbent single dye experiments, the maximum adsorption capacity of vermicompost, natural bentonite and standard bentonite for BV₁₆ was found to be 16 mg g⁻¹, 434.78 mg g⁻¹ and 500 mg g⁻¹, respectively, and the adsorption capacity of charred dolomite for RR₁₉₅ was 7.34 mg g⁻¹. Anionic RR₁₉₅ was not noticeably adsorbed by vermicompost, natural bentonite and standard bentonite (having a negative surface charge) and cationic BV₁₆, not by charred dolomite (having a positive surface charge) but adsorbed by the

oppositely charged adsorbents which indicates a selective electrostatic adsorption mechanism. The equilibrium and kinetic data from single dye experiments showed that the adsorption process satisfactorily fitted to the Langmuir isotherm model and pseudo-second-order kinetics which implies that chemisorption dominates the dye-uptake processes.

Secondly, analyzing BV₁₆ and RR₁₉₅ in binary solutions using zero-order derivative spectrophotometry (λ_{max} adsorption of BV₁₆ and RR₁₉₅ is at 548 nm and 540 nm, respectively), the severe overlapping of the individual dye absorptions impeded the direct determination of the concentrations of each dye from the total absorbance. Therefore, first-order derivative spectrophotometry was used and developed to quantify the concentration of each of the dyes RR₁₉₅ and BV₁₆ in binary solutions. Various measurements of first-order derivative absorption spectra of binary solutions of BV₁₆ and RR₁₉₅ led to the result that BV₁₆ can be quantified in the presence of RR₁₉₅ at 580 nm, at which the absorbance of RR₁₉₅ is zero; on the other hand, RR₁₉₅ can be determined in the presence of BV₁₆ at 308 nm, at which the absorbance of BV₁₆ is zero.

For adsorption experiments with dye mixtures in principle, there are three possibilities for the interaction of dyes: antagonism, synergism and non-interaction. In binary dye solution, BV₁₆ adsorption onto charred dolomite increased in the presence of RR₁₉₅ (synergistic effect), yet RR₁₉₅ adsorption on charred dolomite was not influenced by BV₁₆. An antagonistic effect of RR₁₉₅ can be concluded for BV₁₆ adsorption onto vermicompost. The amount of RR₁₉₅ adsorbed on bentonite remarkably increased in the presence of the cationic dye BV₁₆. Moreover, the adsorption capacity for BV₁₆ doubled (833.33 mg g⁻¹) in the presence of the anionic dye demonstrating synergistic effects due to the possible formation of water-insoluble ion pairs of anionic and cationic dyes. Another series of experiments where commercially available 'standard' bentonite was used instead of natural bentonite led to similar results for both dyes. The adsorption equilibrium data for all adsorbents fitted more acceptable to the Langmuir isotherm model than to the Freundlich model in binary solutions, other than the adsorption of BV₁₆ on vermicompost which followed the Freundlich model. The kinetic data from binary dye experiments concluded that the adsorption process suitably fitted to pseudo-second-order kinetics.

In the next step, the potential of a mixed sorbent consisting of vermicompost and Persian charred dolomite, and the adsorption potential of natural bentonite and charred dolomite for simultaneous adsorption of basic violet 16 (BV₁₆) and reactive red 195 (RR₁₉₅) was investigated. More than half of the removal efficiencies determined for both dyes onto the mixed sorbents (vermicompost and charred dolomite (VC + CD); natural bentonite and charred dolomite (NB + CD)) were >70% which highlights that the mixed sorbents investigated are highly efficacious for simultaneous removal of cationic and anionic dyes from contaminated groundwater. In conclusion, a mixture of bentonite and charred dolomite as well as a mixed

sorbent consisting of vermicompost and charred dolomite are highly promising and efficacious natural sorbent systems for the simultaneous removal of cationic and anionic dyes from water.

Kurzfassung

Diese Arbeit konzentrierte sich auf die Anwendbarkeit von Bentonit, Dolomit und Vermicompost als natürliche Sorbentien für die Entfernung von kationischen und anionischen Textilfarbstoffen aus gefärbtem Abwasser. Untersucht wurde die Anwendung von natürlichem granuliertem Bentonit in einer Festbettkolonne zur Behandlung von Abwässern aus dem Acrylfaser-Färbeprozess, die mit dem Koagulations-Flockungsprozess in der Kläranlage des iranischen Textilunternehmens *Acryl Tab* vorbehandelt wurden. Die Möglichkeiten der Wiederverwendung des behandelten Abwassers in dem Unternehmen wurde untersucht. Darüber hinaus wurde die Verwendung des verbrauchten Sorptionsmittels bei der Herstellung von Leichtzuschlägen (LWA; engl. light weight aggregates) als Möglichkeit zur Minimierung der Umweltauswirkungen der Entsorgung des produzierten Abfallmaterials untersucht. Granulierter Bentonit und andere natürliche Materialien wurden hinsichtlich ihrer Farbentfernungseffizienz und der Möglichkeit, als Sorptionsmittel in einer Festbettkolonne eingesetzt zu werden, untersucht und für weitere detaillierte Studien ausgewählt. Die Sorptionsexperimente umfassten Batch- und Festbettsäulenexperimente. Die Bewertung der Effizienz der untersuchten Aufbereitungssysteme erfolgte anhand der Entfärbung und der CSB-Reduktion. Eine Reihe von Versuchen mit einer Festbettkolonne im Pilotmaßstab (Höhe 1 m, Durchmesser 5 cm) wurde durchgeführt, um Durchbruchkurven zu bestimmen und die Effizienz von granuliertem Bentonit zur Entfernung von Farbe und CSB unter verschiedenen Betriebsbedingungen und Versuchsparametern wie Betthöhe und Durchflussrate zu bewerten.

Wie das Röntgendiffraktogramm des natürlichen granulierten Bentonits zeigte, bestand er hauptsächlich aus Montmorillonit als Hauptmineralphase. Das untersuchte, mittels Koagulations-Flockung und Sedimentation vorbehandelte Textilabwasser, hatte eine orangegelbe Farbe, charakterisiert durch $20,2 \text{ m}^{-1}$ für $\text{SAC}_{436 \text{ nm}}$, $6,4 \text{ m}^{-1}$ für $\text{SAC}_{525 \text{ nm}}$, $3,9 \text{ m}^{-1}$ für $\text{SAC}_{620 \text{ nm}}$ und $456 \text{ mg Pt-Co L}^{-1}$ (letzterer Wert war für den Vergleich mit der iranischen Einleitgrenzwertnorm nötig). Diese Farbparameter des vorbehandelten Abwassers genügen weder den iranischen noch den deutschen Einleitgrenzwerten in Gewässer für Textilabwasser, die im Iran gelten ($75 \text{ mg Pt-Co L}^{-1}$, in Deutschland: 7 m^{-1} für $\text{SAC}_{436 \text{ nm}}$, 5 m^{-1} für $\text{SAC}_{525 \text{ nm}}$ und 3 m^{-1} für $\text{SAC}_{620 \text{ nm}}$), noch den Anforderungen, die an die Wasserwiederverwendung in der Textilverarbeitung gestellt werden, d.h. "nicht sichtbare Farbe" (in Anlehnung an das europäische Projekt *AquaFit4Use*). Das vorbehandelte Abwasser war durch einen alkalischen pH von 11,6, einen CSB-Wert von 890 mg L^{-1} und eine Leitfähigkeit von $2213 \text{ }\mu\text{S m}^{-1}$ gekennzeichnet.

In Batch-Versuchen mit granuliertem Bentonit wurde Farbe und CSB effektiv entfernt. Die optimale Menge von Sorbens für die maximale Farb- und CSB-Reduktion lag bei $0,5 \text{ g pro } 0,1$

L. Die Effizienz für Farbreduktion betrug 88,1 % ($SAC_{436\text{ nm}}$), 70,3 % ($SAC_{525\text{ nm}}$) bzw. 71,8 % ($SAC_{620\text{ nm}}$). Das Langmuir-Modell beschrieb effizient den Sorptionsprozess der Farbstoffe an granulierten Bentonit für alle drei Wellenlängen (SAC 436, 525 und 620 nm). Dies deutet darauf hin, dass eine Monoschicht Sorption vorliegt. Darüber hinaus zeigten die Ergebnisse, dass der Sorptionsprozess eher einem Modell pseudo-zweiter Ordnung als einem Modell pseudo-erster Ordnung folgte, was darauf hindeutet, dass der Sorptionsprozess vermutlich eine chemische Sorption ist. Unter optimalen Bedingungen konnte der CSB von anfänglich 890 mg L^{-1} auf 403 mg L^{-1} gesenkt werden (Entfernungseffizienz 54,7 %). Der Sorptionsprozess von CSB an granulierten Bentonit kann effektiv mit dem Freundlich-Modell beschrieben werden und folgt einer Kinetik pseudo-zweiter Ordnung.

In kontinuierlichen Sorptionsexperimenten mit einer Festbettkolonne, die mit granuliertem Bentonit gefüllt war, wurde die Auswirkung der verschiedenen Durchflussraten ($5, 10$ und 20 ml min^{-1}) und Betthöhen ($5, 10$ und 20 cm) auf die Entfernungseffizienz von Farbe und CSB untersucht. Die höchste Betthöhe (20 cm) bei geringster Durchflussrate des Zulaufs (5 ml min^{-1}) erwiesen sich als beste Bedingung für die FarbadSORption. Die Farbe des behandelten Abwassers wurde von $20,2$ auf $3,9$ für $SAC_{436\text{ nm}}$, $6,4$ auf $1,5$ für $SAC_{525\text{ nm}}$ bzw. $3,9$ auf $1,4$ für $SAC_{620\text{ nm}}$ gesenkt. Es wurden Entfärbungseffizienzen von 93 % (Pt-Co-Methode), 80 % ($SAC_{436\text{ nm}}$), 67 % ($SAC_{525\text{ nm}}$) und 64 % ($SAC_{620\text{ nm}}$) erreicht. Der CSB des behandelten Abwassers aus der Festbettkolonne wurde von 890 mg L^{-1} auf 382 mg L^{-1} gemindert, d.h. 57% des CSB wurden eliminiert. Diese Ergebnisse zeigen, dass granulierter Bentonit das untersuchte Textilabwasser effektiv entfärbt.

Das behandelte Abwasser aus der Festbettkolonne (20 cm Betthöhe, 5 ml min^{-1} Durchflussrate) an einem Durchbruchpunkt erfüllt nicht nur die Anforderung ("nicht sichtbar") für eine Wiederverwendung in der Textilverarbeitung, sondern erreichte auch die deutschen und iranischen Einleitgrenzwerte hinsichtlich der Farbe des gereinigten Abwassers. Das gereinigte Abwasser aus der Festbett-Sorptionskolonne wies $32\text{ mg Pt-Co L}^{-1}$ auf, was unterhalb des im Iran festgelegten Grenzwertes für die Einleitung des gereinigten Abwassers in die Umwelt liegt. Die Farbparameter des behandelten Abwassers ergaben $< 7\text{ m}^{-1}$ für $SAC_{436\text{ nm}}$, 5 m^{-1} für $SAC_{525\text{ nm}}$ und 3 m^{-1} für $SAC_{620\text{ nm}}$, womit die deutschen Grenzwerte für die Einleitung in Gewässer für Textilabwasser erfüllt sind. Der CSB des behandelten Abwassers aus der Festbettkolonne (382 mg L^{-1}) liegt unter dem Grenzwert des CSB von "Wasser geringer Qualität" für Wiederverwendungszwecke (entsprechend dem europäischen Projekt AquaFit4Use). Leitfähigkeit und pH des Abwassers nach sorptiver Behandlung lagen bei $1565\text{ }\mu\text{S m}^{-1}$ bzw. $8,15$; die Leitfähigkeit erfüllt damit das Kriterium für eine "allgemeine Wasserwiederverwendung" und der pH die Anforderung "Wasser mittlerer bis geringe Qualität". Daher kann das behandelte Textilabwasser zur Wiederverwendung im

Produktionsprozess der untersuchten Textilindustrie für Spül- und Waschanwendungen (Abwaschen der Gerätschaften und Wischen der Böden) sowie zum Waschen der Fasern zur Vorbehandlung vor dem Färben vorgeschlagen werden. Zusammenfassend lässt sich sagen, dass die Sorption mit granuliertem Bentonit als weiterer Behandlungsschritt in Kombination mit den anderen bereits angewandten Behandlungsmethoden in der untersuchten Textilfirma eingesetzt werden kann, um die Farbstoffe und den CSB soweit aus dem Abwasser des Acrylfaser-Färbeprozesses zu entfernen, dass es für die genannten Waschw Zwecke wiederverwendet werden kann. Mit der Schaffung eines solchen Wasser-Recycling-Kreislaufs kann der Verbrauch von knappem Wasser reduziert werden und so eine höhere Nachhaltigkeit erreicht werden. Außerdem kann die Behandlung mit dem natürlichen Sorptionsmittel die Verschmutzung von Oberflächen- und Grundwasser verringern, da die untersuchte Firma (*Acryl Tab CO.*) das vorbehandelte Textilabwasser aus ihrer betriebseigenen Kläranlage normalerweise in die kommunale Abwasserkanalisation einleitet und/oder auf landwirtschaftliche Flächen (Reisfelder) ausbringt.

Aufbauend auf der von Forntwalt und Hutchins (1966) entwickelten Scale-up Methode wurden die Parameter für die Planung und Umsetzung einer Festbettkolonne im industriellen Maßstab wie folgt berechnet: Fläche $A=0,84 \text{ m}^2$, Durchmesser $d=1,04 \text{ m}$ und Höhe zwischen 3,12 und 5,12 m. Gemäß den Ergebnissen für Bentonitbetthöhen von 5 cm, 10 cm und 20 cm im Maßstab eines Pilotprojektes kann die Entwurfskolonne $37,5 \text{ m}^3$, $56,25 \text{ m}^3$ bzw. 100 m^3 Abwasser in 6 h, 9 h und 16 h (an Durchbruchpunkten) unter Verwendung von 2287 kg, 4569,6 kg und 9150,4 kg Bentonit behandeln, was erforderlich ist für die Abwasserbehandlung eines täglichen Volumenstroms von $150 \text{ m}^3 \text{ d}^{-1}$. Da das Unternehmen vorwiegend 2 Arbeitsschichten täglich fährt, werden pro Tag 6098 kg Bentonit (5 cm Schütthöhe), 8123,73 kg Bentonit (10 cm Schütthöhe) und 9150,4 kg Bentonit (20 cm Schütthöhe) zur Behandlung des anfallenden Abwassers benötigt.

Da die Qualität des gereinigten Abwassers an den Durchbruchpunkten aller Bentonitbetthöhen (5, 10 und 20 cm) die Anforderungen für die Wiederverwendung von gereinigtem Abwasser (Wasser mit geringer Qualität für Waschw Zwecke auf der Grundlage des Aquafit4use-Projekts) erfüllt, ist die aus der Pilotkolonne mit 5 cm Betthöhe hochkalierte Bentonitmenge wirtschaftlich gesehen die effizienteste für die untersuchte Industrie. Da das Unternehmen vorwiegend 2 Arbeitsschichten (16 h) täglich fährt, werden folglich 6098 kg Bentonit pro Tag benötigt, um die anfallenden Abwässer zu behandeln. In Betrachtung der Preise für natürliches Bentonit, welches von einem iranischen Unternehmen geliefert wird, müssten lediglich 83 Euro täglich investiert werden, um diese Menge Bentonit pro Tag bereitzustellen.

Jedoch kann die Menge an Bentonit die zu behandeln und zu verarbeiten ist, beträchtlich sein. Bezüglich der Ergebnisse der Ökobilanz und der Monte-Carlo-Analyse ergab sich ein Verhältnis von 0,06 zwischen dem mittleren Preis der Abwasserreinigung mit 86.6 kg Bentonit pro Stunde und dem mittleren Preis der Abwasserreinigung mit 3.8 kg Aktivkohle pro Stunde. Daraus wurde geschlussfolgerd, dass natürlicher Bentonit eine sehr umweltfreundliche und günstige Alternative zu Aktivkohle darstellt, einem gängigen Adsorptionsmittel in der Abwasserbehandlung, für die Behandlung von vorbehandeltem Abwasser aus Acrylfaserfärbereien im Iran darstellt.

Ein weiteres Ziel dieser Arbeit war es, die Möglichkeit zu untersuchen, das verbrauchte bentonite als neue Rohstoffquelle bei der Herstellung von Baumaterialien zu nutzen. Mit anderen Worten, um Abfall (das verbrauchte Sorptionsmittel) in eine nutzbare Ressource umzuwandeln, wurde das verbrauchte Sorptionsmittel in der Produktion von LWA wie LECA (Leichtblähtonaggregat) eingesetzt. Dieser Ansatz kann dazu beitragen, die Entstehung von Sekundärverschmutzung zu vermeiden sowie den Wert des erzeugten Abfalls zu erhöhen, indem er in ein nützliches Material umgewandelt wird. Die Eigenschaften der erzeugten LWA aus den verbrauchten Abfällen wurden mit konventionellen LWA, (hier: LECA, die bei der iranischen Firma *LECA CO.* unter Verwendung von natürlichem Ton hergestellt wurden, verglichen.

Zur Herstellung von LWA aus verbrauchtem Sorptionsmittel wurden die Mischungen mit Wasser und einem Additiv (1% mazut) vermengt, anschließend zu Pellets geformt und ofengetrocknet und schließlich bei 1140 °C für 4 min in einem Muffelofen gesintert. Die wichtigsten technischen Eigenschaften der Aggregate (Wasseraufnahme nach 24 h, Dichte und mechanische Festigkeit) wurden bestimmt. Da es eine positive Korrelation zwischen der Menge an organischer Substanz im Zuschlag und der Porosität in den hergestellten LWA gibt, trugen die organischen Stoffe im Abwasser zu einer höheren Porosität im Sinterprozess bei, wodurch die Dichte gesenkt und die Wasseraufnahme der hergestellten LWA erhöht wurde.

Es konnte gezeigt werden, dass die positiven Eigenschaften von LWA auch bei der Verwendung von verbrauchtem Sorptionsmittel weitgehend erhalten bleiben, und dadurch die Kosten für die Abfallbehandlung und die Produktionskosten reduzieren werden können.

Die genannten Ergebnisse beruhen auf Vorversuchen, in denen verschiedene kostengünstige natürliche Materialien wie Vermicompost (organisch) sowie Dolomit und Bentonit (anorganisch) als Sorbentien in einfachen und binären Sorbenssystemen verwendet wurden, um Textilfarbstoffe aus Wasserproben mit einem bzw. zwei Farbstoffen zu entfernen. Bei den beiden ausgewählten Farbstoffen handelte es sich um den kationischen Farbstoff Basic Violet

16 (BV₁₆) und dem anionischen Farbstoff Reactive Red 195 (RR₁₉₅), zwei in der Textilindustrie im Iran häufig eingesetzte Farbstoffe. Mit diesen wurden Grundwasserproben dotiert, die in dieser Arbeit systematisch untersucht wurden.

Zunächst wurde eine Reihe von Vorversuchen im Labormaßstab durchgeführt, um das Potenzial von thermisch (bei 800 °C) behandeltem Dolomit ("halbgebranntem Dolomit"), natürlichem Bentonit, sowie Wurmkompost (all diese Sorbentien sind im Iran lokal verfügbar) und auch kommerziell erhältlichem "Standard"-Bentonit, die Farbstoffe BV₁₆ und RR₁₉₅ aus Lösungen mit jeweils nur einem Textilfarbstoff ("Einzelfarbstoffsystem") zu entfernen, zu untersuchen.

Zur Untersuchung und Optimierung von Parametern, die potenziell die Sorption der Farbstoffe beeinflussen könnten, einschließlich der Kontaktzeit, der anfänglichen Farbstoffkonzentration, der Rührgeschwindigkeit und der Sorptionsmittelmenge, wurden Batch-Experimente mit Einzelfarbstoffsystemen behandelt mit jeweils einem Sorbens durchgeführt. Ziel war es dabei, die Prozessvariablen einzustellen und die Sorptionsisothermen und kinetischen Kurven zu bestimmen. Daneben wurden die optimierten Parameter für ein binäres Zweifarbstoffsystem mit jeweils einem Sorptionsmittel zu verwenden. Grundwasserproben, die einen ("Einzelfarbstoffsystem") oder beide Farbstoffe ("binäres Farbstoffsystem") enthielten, wurden mit Vermicompost und/oder halbgebranntem Dolomit (jeweils allein oder gemischt) oder mit Bentonit und/oder halbgebranntem Dolomit (jeweils alleine oder gemischt) behandelt. In den Experimenten mit Vermicompost, natürlichem Bentonit bzw. Standard-Bentonit als einzigem Sorptionsmittel betrug die maximale Sorptionskapazität für BV₁₆ 16 mg g⁻¹ bzw. 434,78 mg g⁻¹ bzw. 500 mg g⁻¹. Die Sorptionskapazität von halbgebranntem Dolomit betrug für RR₁₉₅ 7,34 mg g⁻¹. Anionisches RR₁₉₅ wurde nicht merklich von den Sorbentien mit negativer Oberflächenladung Vermicompost, natürlichem Bentonit und Standard-Bentonit sorbiert. Kationisches BV₁₆ wurde nicht von halbgebranntem Dolomit (mit positiver Oberflächenladung) sorbiert, jedoch von den entgegengesetzt geladenen Sorbentien, was auf einen selektiven elektrostatischen Sorptionsmechanismus hinweist. Die Gleichgewichts- und kinetischen Daten aus den Einzelfarbstoff-Experimenten zeigten, dass der Sorptionsprozess zufriedenstellend zum Langmuir-Isothermenmodell passte und einer Kinetik pseudo-zweiter Ordnung entsprach, was impliziert, dass Chemisorption die Farbstoff-Aufnahmeprozesse dominiert.

Bei der Analyse von BV₁₆ (λ_{\max} 548 nm) und RR₁₉₅ (540 nm) in binären Lösungen mittels Sorptionsspektroskopie kommt es zu einer Überlagerung der individuellen Farbstoffabsorptionen. Um dennoch die Einzelkonzentrationen der Farbstoffe in binären Lösungen bestimmen zu können, wurde eine Methode beruhend auf

Derivatspektrophotometrie erster Ordnung entwickelt Verschiedene Messungen von "herkömmlichen" Absorptionsspektren erster Ordnung von binären Lösungen von BV₁₆ und RR₁₉₅ führten zu dem Ergebnis, dass BV₁₆ in Gegenwart von RR₁₉₅ bei 580 nm quantifiziert werden kann, da die Absorption von RR₁₉₅ hier Null ist; andererseits kann RR₁₉₅ in Gegenwart von BV₁₆ bei 308 nm bestimmt werden, da BV₁₆ hier nicht sorbiert.

Bei Versuchen mit Farbstoffgemischen können prinzipiell drei Möglichkeiten für die Wechselwirkung der Farbstoffe mit dem Sorbens erwartet werden: Nicht-Wechselwirkung, erhöhte Sorption (Synergismus) und geminderte Sorption (Antagonismus). In binärer Farbstofflösung wurde in Anwesenheit von RR₁₉₅ mehr BV₁₆ an halbgebranntem Dolomit gebunden (synergistischer Effekt), dagegen wurde die Sorption von RR₁₉₅ an halbgebranntem Dolomit durch die Anwesenheit von BV₁₆ nicht beeinflusst. Für die Sorption von BV₁₆ an Vermicompost kann auf einen antagonistischen Effekt von RR₁₉₅ geschlossen werden. Die Menge an RR₁₉₅, die an Bentonit sorbiert wurde, stieg in Gegenwart des kationischen Farbstoffs BV₁₆ deutlich an. Darüber hinaus verdoppelte sich die Sorptionskapazität für BV₁₆ (833,33 mg g⁻¹) in Anwesenheit des anionischen Farbstoffs, was als synergistischer Effekt gedeutet werden kann. Eine weitere Versuchsreihe, bei der anstelle von natürlichem Bentonit handelsüblicher "Standard"-Bentonit verwendet wurde, führte zu ähnlichen Ergebnissen für beide Farbstoffe. Die Sorptionsgleichgewichtsdaten für alle Sorbentien und binären Lösungen passten eher zum Langmuir-Isothermenmodell als zum Freundlich-Modell, nur die Sorption von BV₁₆ auf Vermicompost folgte dem Freundlich-Modell. Die aus den Experimenten mit binären Farbstoffsystemen erhaltenen kinetischen Daten sprechen für eine Kinetik pseudo-zweiter Ordnung.

Im letzten Schritt wurde das Potenzial einer Sorptionsmittelmischung, bestehend aus Vermicompost und halbgebranntem Dolomit, sowie einer Mischung aus natürlichem Bentonit und halbgebranntem Dolomit für die Sorption von gleichzeitig vorhandenem BV₁₆ und RR₁₉₅ untersucht. Mehr als die Hälfte der für beide Farbstoffe auf den gemischten Sorptionsmitteln (Vermicompost und halbgebrannter Dolomit (VC + CD); natürlicher Bentonit und halbgebrannter Dolomit (NB + CD)) ermittelten Sorptionseffizienzen lagen bei >70%. Dies unterstreicht, dass diese Mischungen für die gleichzeitige Entfernung von kationischen und anionischen Farbstoffen aus kontaminiertem Grundwasser hocheffizient sind. Zusammenfassend lässt sich sagen, dass Mischungen aus Bentonit und halbgebranntem Dolomit und auch Vermicompost und halbgebranntem Dolomit, sehr vielversprechende und wirksame natürliche Sorptionsmittelsysteme für die gleichzeitige Entfernung von kationischen und anionischen Farbstoffen aus Wasser sind.

Table of Contents

Acknowledgments	III
Published papers covering parts of the dissertation	V
Abstract	VII
Kurzfassung	XIII
List of Tables	XXIII
List of Figures	XXV
Abbreviations	XXXI
Motivation	1
1. Fundamentals	7
1.1 Dyes in textile industry	7
1.1.1 Chemical characteristics, applicability and properties of cationic dyes.....	10
1.1.2 Chemical characteristics, applicability and properties of reactive dyes.....	17
1.2 Textile industry	18
1.2.1 Raw materials	19
1.2.2 Pretreatment of fibers	21
1.2.3 Dyeing	21
1.3 Environmental issues of the textile industry	23
1.4 Conventional wastewater treatment methods of textile wastewater	30
1.4.1 Biological methods.....	30
1.4.2 Chemical methods	31
1.4.3 Physical methods.....	31
1.4.3.1 Adsorption.....	35
1.4.3.2 Natural adsorbents.....	37
1.5 Fixed-bed adsorber design	41
1.6 Scale-up approach.....	42
1.7 Iran water situation	42
1.8 Textile industry in Iran.....	44
1.9 Reuse of the treated wastewater in the textile industry.....	45
1.10 Reuse of the spent adsorbent in the production of LWAs	48
1.10.1 Lightweight aggregates (LWAs)	48

1.10.2	Life cycle assessment and Monte Carlo analysis	51
2.	Materials and Methods.....	57
2.1	Material characterization	57
2.1.1	Adsorbents.....	57
2.1.2	Fabric dyes and stock solutions.....	59
2.1.3	Textile wastewater from Acryl Tab textile company	61
2.1.4	Characterization of the wastewaters from different baths (dark, medium and pale shade) in cationic exhaust dyeing.....	63
2.2	Analytical and experimental methods.....	63
2.3	Dye analysis	64
2.3.1	Analysis of BV ₁₆ and RR ₁₉₅ in single and binary dye solutions using zero-order spectrophotometry	64
2.3.2	Simultaneous analysis of BV ₁₆ and RR ₁₉₅ in binary mixtures using first-order derivative spectrophotometry	65
2.4	Adsorption in batch experiments	68
2.4.1	Equilibrium isotherms	70
2.4.2	Adsorption kinetics.....	71
2.5	Fixed-bed column adsorption experiments.....	72
2.5.1	Effect of various operating parameters	74
2.5.1.1	Effect of feed flow rate.....	74
2.5.1.2	Effect of bed height	74
2.5.1.3	Analysis of fixed-bed adsorption	74
2.6	Scale-up approach.....	75
2.7	Reuse of the spent adsorbent in the production of LWAs	77
2.7.1	Production process in the LECA company	77
2.7.2	Preparation and characterization of LWAs	80
2.7.3	Life cycle assessment (LCA) and Monte Carlo analysis for comparing textile wastewater treatment with bentonite and activated carbon.....	81
3.	Results and Discussion	87
3.1	Characterization of the adsorbents.....	88
3.1.1	Characterization of natural granular bentonite as the adsorbent used for the treatment of textile wastewater.....	93
3.2	Characterization of the raw textile wastewater from Acryl Tab CO.	97

3.3	Characterization of the wastewaters from different baths (dark, medium and pale shade) in cationic exhaust dyeing.....	99
3.4	Batch adsorption studies on real textile wastewater	102
3.4.1	Effect of the amount of granular bentonite on the removal of color as determined by measurement of the SAC number at different wavelengths.....	102
3.4.2	Effect of the amount of granular bentonite on COD removal	106
3.4.3	Equilibrium isotherm studies.....	108
3.4.4	Kinetic analysis	114
3.4.5	Fixed-bed column adsorption experiments	118
3.4.5.1	Experimental breakthrough curves for different bed heights and flow rates.....	120
3.4.5.2	Analysis of fixed-bed adsorption data.....	124
3.4.5.2.1	Dependence of adsorption efficiency on the flow rate	124
3.4.5.2.2	Dependence of adsorption efficiency on the bed height.....	126
3.4.6	Reuse of the treated textile wastewater in the studied textile industry	128
3.4.7	Fixed-bed column design by the scale-up approach	131
3.5	Reuse of the spent adsorbent in the production of LWAs	136
3.6	Life cycle assessment (LCA) and Monte Carlo analysis for comparing textile wastewater treatment with bentonite and activated carbon	143
3.7	Batch adsorption studies on dye-spiked groundwater	147
3.7.1	Equilibrium isotherms in single and binary dye systems	147
3.7.2	Dye interactions in binary dye experiments	153
3.7.3	Kinetic analysis	156
3.7.4	Adsorption of dyes on the mixed sorbent in binary dye solutions	160
4.	Summary and Outlook	179
5.	References.....	185
	Appendix	199
A1.	Recovery studies for the first-order derivative spectrophotometry experiments.....	199
A2.	Studies on the reuse of adsorbents	200
A3.	pH points of zero charge (pH_{pzc}) of the adsorbents	200
A4.	Effect of pH on absorbance and λ_{max}	201
A5.	Reuse studies.....	202
A6.	pH points of zero charge (pH_{pzc}) of the adsorbents	203

List of Tables

Table 1 Classification of dyes based on the chemical structure	8
Table 2 Classification of dyes based on the chemical nature	9
Table 3 General categories of fibers used in the textile industry	20
Table 4 The most common dyestuffs and dyeing techniques for polyacrylic fibers	23
Table 5 Overview of the typical emissions generated in dyeing processes	26
Table 6 List of carcinogenic amines	27
Table 7 Advantages and disadvantages of existing and emerging technologies for dye removal	32
Table 8 Most commonly used dyes in the textile industry of Iran.....	44
Table 9 Main requirements in reuse purposes in the textile industry	47
Table 10 Characteristics of the two fabric dyes basic violet 16, reactive red 195.....	60
Table 11 Adsorption of dyes on different adsorbents in single dye experiments.....	69
Table 12 Characterization of vermicompost; chemical constituents as determined with XRF and elemental analysis (in ppm).....	88
Table 13 Characterization of Persian charred dolomite, natural bentonite and standard bentonite; chemical constituents as determined with XRF and elemental analysis (in weight %)	89
Table 14 Product specification of standard bentonite (Sigma-Aldrich (Merck))	91
Table 15 Characterization of natural granular bentonite; chemical constituents as determined with XRF and elemental analysis (in weight %).....	93
Table 16 Characterization of the raw textile wastewater from the Acryl Tab CO.	97
Table 17 Characterization of different baths (dark, medium and light shade) in cationic exhaust dyeing.....	100
Table 18 Isotherm parameters of the adsorption of color determined as SAC on granular bentonite	111
Table 19 Parameters of the pseudo-second-order kinetics of dye adsorption on granular bentonite.....	114
Table 20 Isotherm parameters of the adsorption of COD on granular bentonite from textile wastewater	116
Table 21 Kinetic constants of the adsorption of COD from textile wastewater onto granular bentonite	117

Table 22 Characterization of the natural granular bentonite before and after adsorption; chemical constituents as determined with XRF and elemental analysis (in weight %)	137
Table 23 Properties of lightweight aggregates produced with different percentages of natural clay (LECA CO; standard) and granular bentonite (granular bentonite; before and after usage for adsorption)	140
Table 24 Heavy metals in the produced sintered lightweight aggregate made of the spent adsorbent (determined by ICP-OES)	141
Table 25 Emitted carbon dioxide in different scenarios of the spent adsorbents disposal ...	146
Table 26 Isotherm parameters of the adsorption of BV ₁₆ and RR ₁₉₅ on charred dolomite (CD), vermicompost (VC), natural bentonite (NB) and standard bentonite (SB) in single and binary dye solution (* no data fit)	151
Table 27 Parameters of the pseudo-second-order kinetics of dye adsorption on vermicompost (VC), charred dolomite (CD), natural bentonite (NB) and standard bentonite (SB)	157
Table 28 Efficiencies of mixed adsorbents (VC+CD) for removal of BV ₁₆ and RR ₁₉₅ in single and binary dye solutions	161
Table 29 Removal efficiencies of mixed adsorbents (NB+CD)/(SB+CD) for BV ₁₆ and RR ₁₉₅ in single and binary dye solutions	162
Table A.1 Results of the percentage recovery, error and average error values for the concentrations of BV ₁₆ and RR ₁₉₅ in binary mixtures obtained from first-order derivative spectra	199

List of Figures

Fig. 1 Basic blue 3 C.I. 510041	11
Fig. 2 Basic red 18 C.I. 110852	11
Fig. 3 Cationic dye with localized positive charge	11
Fig. 4 Diazahemicyanine dye with delocalized positive charge	12
Fig. 5 Enamine dye	12
Fig. 6 Styryl dye.....	13
Fig. 7 Zeromethine dye	13
Fig. 8 Monoazamethine dye.....	13
Fig. 9 Azo dye with a localized charge which resides in the coupling component	14
Fig. 10 An azo dye with a localized charge which resides in the diazo moiety	14
Fig. 11 Anthraquinone dye	15
Fig. 12 Phthalocyanine dye.....	15
Fig. 13 Perinone dye	15
Fig. 14 Naphthalimide dye.....	16
Fig. 15 Quinophthalone dye.....	16
Fig. 16 Neutrocyanine dye.....	16
Fig. 17 Nitro dye	17
Fig. 18 Basic terms of adsorption	36
Fig. 19 Selected low-cost adsorbents.....	38
Fig. 20 Lightweight aggregate	49
Fig. 21 (a), Vermicompost farm (Golbang Yas CO.) (b), dried vermicompost	57
Fig. 22 Charred dolomite from Iranian Refractories Procurement & Production CO.....	58
Fig. 23 Persian natural bentonite and standard bentonite from the Iran Barite Falat CO.....	58
Fig. 24 Natural granular bentonite from Iran mineral products CO.	59
Fig. 25 Structural formulae of (a) basic violet 16 (BV ₁₆) and (b) reactive red 195 (RR ₁₉₅)	59
Fig. 26 Wastewater treatment plant in the Acryl Tab company	61
Fig. 27 Sedimentation basin before adding chlorine in the Acryl Tab company	62
Fig. 28 Addition of chlorine to the treated wastewater in the last basin in the Acryl Tab industry	62
Fig. 29 Zero-order absorption spectra of BV ₁₆ (10 mg L ⁻¹ , λ _{max} = 548 nm), RR ₁₉₅ (10 mg L ⁻¹ , λ _{max} = 540 nm), and a 1:1 mixture of both (10 mg L ⁻¹ each).....	65
Fig. 30 First-order absorption spectra of BV ₁₆ (10 mg L ⁻¹), RR ₁₉₅ (10 mg L ⁻¹), and a 1:1 mixture of both (10 mg L ⁻¹ each)	66
Fig. 31 First-order derivative spectra of 1:1 mixture of BV ₁₆ and RR ₁₉₅ (each in concentrations of 2, 4, 6, 8 or 10 mg L ⁻¹).....	67

Fig. 32 First-order derivative spectra of 1:1 mixture of BV ₁₆ and RR ₁₉₅ (fixed concentration of 2 mg L ⁻¹ BV ₁₆ and varying concentrations of 2, 4, 6, 8 or 10 mg L ⁻¹ RR ₁₉₅).....	67
Fig. 33 First-order derivative spectra of 1:1 mixture of BV ₁₆ and RR ₁₉₅ (fixed concentration of 2 mg L ⁻¹ RR ₁₉₅ and varying concentrations of 2, 4, 6, 8, or 10 mg L ⁻¹ BV ₁₆)	68
Fig. 34 Batch experiments using granular bentonite for the treatment of real textile wastewater	70
Fig. 35 Treatment of acrylic fiber dyeing wastewater using natural granular bentonite in a fixed-bed continuous system	73
Fig. 36 Natural clay deposit in the LEAC CO. in Iran	77
Fig. 37 Green granules made of the spent adsorbent, water and additive (quality control laboratory at LECA CO.).....	78
Fig. 38 (a, b) Thermal treatment of green granules in a muffle furnace (quality control laboratory at LECA CO.).....	78
Fig. 39 The temperature profile of the LECA production process at LECA CO.	79
Fig. 40 Installations for heat treatment of the green granules in different phases of drying, burning and cooling at the LECA CO.	80
Fig. 41 Field emission scanning electron microscopic (FESEM) images of the pristine <i>vermicompost</i>	89
Fig. 42 Field emission scanning electron microscopic (FESEM) images of the pristine <i>charred dolomite</i>	91
Fig. 43 Field emission scanning electron microscopic (FESEM) images of the pristine <i>natural bentonite</i>	92
Fig. 44 Field emission scanning electron microscopic (FESEM) images of the pristine <i>standard bentonite</i>	92
Fig. 45 Field emission scanning electron microscopic (FESEM) images of the pristine <i>granular bentonite</i> (before adsorption).....	95
Fig. 46 X-ray diffractograms of natural granular bentonite (Position °2 Theta, Cu K α radiation);	96
Fig. 47 Different vessels in the dye house of the Acryl Tab company in Iran	99
Fig. 48 Wastewater from different baths (dark, medium and pale shade) from cationic exhaust dyeing	101
Fig. 49 Effect of the amount of granular bentonite on color removal, measured as spectral absorption coefficient (SAC) in m ⁻¹ at a wavelength of 436 nm (experimental conditions: stirring speed of 250 rpm, no pH adjustment, ambient temperature, volume = 100 ml)	102
Fig. 50 Effect of the amount of granular bentonite on color removal, measured as spectral absorption coefficient (SAC) in m ⁻¹ at a wavelength of 525 nm (experimental	

conditions: stirring speed of 250 rpm, no pH adjustment, ambient temperature, volume = 100 ml)	103
Fig. 51 Effect of the amount of granular bentonite on color removal, measured as spectral absorption coefficient (SAC) in m^{-1} at a wavelength of 620 nm (experimental conditions: stirring speed of 250 rpm, no pH adjustment, ambient temperature, volume = 100 ml)	103
Fig. 52 Effect of the amount of granular bentonite on color removal efficiency, measured as spectral absorption coefficient (SAC) in m^{-1} at a wavelength of 436 nm (experimental conditions: stirring speed of 250 rpm, no pH adjustment, ambient temperature, volume = 100 ml)	104
Fig. 53 Effect of the amount of granular bentonite on color removal efficiency, measured as spectral absorption coefficient (SAC) in m^{-1} at a wavelength of 525 nm (experimental conditions: stirring speed of 250 rpm, no pH adjustment, ambient temperature, volume = 100 ml)	105
Fig. 54 Effect of the amount of granular bentonite on color removal efficiency, measured as spectral absorption coefficient (SAC) in m^{-1} at a wavelength of 620 nm (experimental conditions: stirring speed of 250 rpm, no pH adjustment, ambient temperature, volume = 100 ml)	105
Fig. 55 Effect of the amount of granular bentonite on COD removal (experimental conditions: stirring speed of 250 rpm, no pH adjustment, ambient temperature, volume = 100 ml)	106
Fig. 56 Effect of the amount of granular bentonite on color removal efficiency (experimental conditions: stirring speed of 250 rpm, no pH adjustment, ambient temperature, volume = 100 ml)	107
Fig. 57 Langmuir isotherm of the adsorption of color (determined as $SAC_{436\text{ nm}}$) on granular bentonite	108
Fig. 58 Freundlich isotherm of the adsorption of color (determined as $SAC_{436\text{ nm}}$) on granular bentonite	108
Fig. 59 Langmuir isotherm of the adsorption of color (determined as $SAC_{525\text{ nm}}$) on granular bentonite.....	109
Fig. 60 Freundlich isotherm of the adsorption of color (determined as $SAC_{525\text{ nm}}$) on granular bentonite	109
Fig. 61 Langmuir isotherm of the adsorption of color (determined as $SAC_{620\text{ nm}}$) on granular bentonite	110
Fig. 62 Freundlich isotherm of the adsorption of color (determined as $SAC_{620\text{ nm}}$) on granular bentonite	110
Fig. 63 Removal of color (determined via $SAC_{436\text{ nm}}$) from textile wastewater applying granular bentonite, a pseudo-second-order equation was used	112

Fig. 64 Removal of color (determined via SAC _{525 nm}) from textile wastewater applying granular bentonite, a pseudo-second-order equation was used	113
Fig. 65 Removal of color (determined via SAC _{620 nm}) from textile wastewater applying granular bentonite, a pseudo-second-order equation was used.	113
Fig. 66 Langmuir isotherm of the adsorption of COD on granular bentonite	115
Fig. 67 Freundlich isotherm of the adsorption of COD on granular bentonite.....	116
Fig. 68 Removal of COD from textile wastewater applying granular bentonite using a pseudo-second-order equation	117
Fig. 69 Field emission scanning electron microscopic (FESEM) images of the spent <i>granular bentonite</i> (after adsorption).....	118
Fig. 70 Comparison of different breakthrough curves (C/C_0 versus time) at a constant bed height of 5 cm with different flow rates of 5, 10 and 20 ml min ⁻¹ , absorbance at SAC _{436 nm} (no pH adjustment, ambient temperature).....	120
Fig. 71 Comparison of different breakthrough curves (C/C_0 versus throughput volume) at a constant bed height of 5 cm with different flow rates of 5, 10 and 20 ml min ⁻¹ , absorbance at SAC _{436 nm} (no pH adjustment, ambient temperature).....	120
Fig. 72 Comparison of different breakthrough curves (C/C_0 versus time) at a constant bed height of 5 cm with different flow rates of 5, 10 and 20 ml min ⁻¹ , absorbance at SAC _{525 nm} (no pH adjustment, ambient temperature).....	121
Fig. 73 Comparison of different breakthrough curves (C/C_0 versus time) at a constant bed height of 5 cm with different flow rates of 5, 10 and 20 ml min ⁻¹ , absorbance at SAC _{620 nm} (no pH adjustment, ambient temperature)	122
Fig. 74 Comparison of different breakthrough curves (C/C_0 versus time) at a constant flow rate of 5 ml min ⁻¹ with different bed heights of 5, 10 and 20 cm, absorbance at SAC _{436 nm} (no pH adjustment, ambient temperature).....	122
Fig. 75 Comparison of different breakthrough curves (C/C_0 versus throughput volume) at a constant flow rate of 5 ml min ⁻¹ with different bed heights of 5, 10 and 20 cm, absorbance at SAC _{436 nm} (no pH adjustment, ambient temperature).....	123
Fig. 76 Comparison of different breakthrough curves (C/C_0 versus time) at a constant flow rate of 5 ml min ⁻¹ with different bed heights of 5, 10 and 20 cm, absorbance at SAC _{525 nm} (no pH adjustment, ambient temperature).....	123
Fig. 77 Comparison of different breakthrough curves (C/C_0 versus time) at a constant flow rate of 5 ml min ⁻¹ with different bed heights of 5, 10, and 20 cm, absorbance at SAC _{620 nm} (no pH adjustment, ambient temperature).....	124
Fig. 78 Dependence of the COD removal efficiency of natural granular bentonite in columns of different bed heights (5, 10 and 20 cm) operated at various flow rates (5, 10 and 20 mL), (no pH adjustment, ambient temperature)	127
Fig. 79 Treated real acrylic fiber dyeing wastewater using fixed-bed column.....	130

Fig. 80 Pretreatment of the fibers in the Acryl Tab CO.....	130
Fig. 81 (a) Produced LWAs from the natural clay (standard LECA), (b) from the spent adsorbent (granular bentonite), (c) from the pristine adsorbent (granular bentonite)	139
Fig. 82 Comparison of the scenarios - Impact characterization with ReCiPe 2016 v1.1 Endpoint (H).....	144
Fig. 83 Comparison of the scenarios - Impact characterization with ReCiPe 2016 v1.1 Endpoint (H).....	145
Fig. 84 Isotherms of the adsorption of BV ₁₆ (10-50 mg L ⁻¹) and RR ₁₉₅ (5-30 mg L ⁻¹) on <i>vermicompost</i> in single dye solution at 25 C°	147
Fig. 85 Freundlich isotherm of the adsorption of BV ₁₆ (10-50 mg L ⁻¹) in the presence of a fixed RR ₁₉₅ concentration (20 mg L ⁻¹) on <i>vermicompost</i> at 25 C°	147
Fig. 86 Isotherms of the adsorption of BV ₁₆ (5-30 mg L ⁻¹) and RR ₁₉₅ (10-40 mg L ⁻¹) on <i>charred dolomite</i> in single dye solutions at 25 C°	148
Fig. 87 Isotherms of the adsorption of RR ₁₉₅ (10-50 mg L ⁻¹) in the presence of a fixed BV ₁₆ concentration (20 mg L ⁻¹) on <i>charred dolomite</i> at 25 C°	148
Fig. 88 Isotherms of the adsorption of BV ₁₆ (10-40 mg L ⁻¹) and RR ₁₉₅ (5-30 mg L ⁻¹) on <i>natural bentonite</i> in single dye solutions at 25 C°	149
Fig. 89 Isotherms of the adsorption of BV ₁₆ (10-50 mg L ⁻¹) in the presence of a constant RR ₁₉₅ concentration (20 mg L ⁻¹) on <i>natural bentonite</i> at 25 C°	149
Fig. 90 Isotherms of the adsorption of BV ₁₆ (10-40 mg L ⁻¹) and RR ₁₉₅ (5-30 mg L ⁻¹) on <i>standard bentonite</i> in single dye solutions at 25 C°	150
Fig. 91 Isotherms of the adsorption of BV ₁₆ (10-50 mg L ⁻¹) in the presence of a constant RR ₁₉₅ concentration (20 mg L ⁻¹) on <i>standard bentonite</i> at 25 C°	150
Fig. 92 Adsorption capacities of the different adsorbents for dyes:	154
Fig. 93 Interaction of dyes in binary dye experiments.....	156
Fig. 94 Kinetics of the adsorption of BV ₁₆ (20 mg L ⁻¹) on <i>vermicompost</i> in single and binary dye solution at 25 C°	158
Fig. 95 Kinetics of the adsorption of RR ₁₉₅ (20 mg L ⁻¹) on <i>charred dolomite</i> in single and binary dye solution at 25 C°	158
Fig. 96 Kinetics of the adsorption of BV ₁₆ (20 mg L ⁻¹) on <i>natural bentonite</i> in single and binary dye solution at 25 C°	159
Fig. 97 Kinetics of the adsorption of BV ₁₆ (20 mg L ⁻¹) on <i>standard bentonite</i> in single and binary dye solution at 25 C°	159
Fig. 98 Adsorption capacity of BV ₁₆ (A) and RR ₁₉₅ (B) to single and mixed sorbent systems	160
Fig. 99 Conceptual scheme of the proposed method for dye elimination from water with mixed sorbents in single and binary dye solutions.....	164

Fig. 100 Field emission scanning electron microscopic (FESEM) images of vermicompost (negative surface charge) before (A) and after (B) adsorption of the positively charged dye (BV ₁₆).....	165
Fig. 101 FTIR spectra of vermicompost (VC) before and after adsorption of BV ₁₆ and/or RR ₁₉₅	166
Fig. 102 Field emission scanning electron microscopic (FESEM) images of <i>charred dolomite</i> before (A, C) and after (B, D, E) adsorption of the oppositely charged dye RR ₁₉₅	167
Fig. 103 FTIR spectra of <i>charred dolomite</i> (CD) before and after adsorption of BV ₁₆ and/or RR ₁₉₅	168
Fig. 104 Field emission scanning electron microscopic (FESEM) images of <i>natural bentonite</i> before (A) and after (B) adsorption of the oppositely charged dye (BV ₁₆)	169
Fig. 105 Field emission scanning electron microscopic (FESEM) images of <i>standard bentonite</i> before (A) and after (B) adsorption of the oppositely charged dye (BV ₁₆)	169
Fig. 106 FTIR spectra of <i>natural bentonite</i> before and after adsorption of BV ₁₆ and/or RR ₁₉₅	170
Fig. 107 FTIR spectra of <i>standard bentonite</i> before and after adsorption of BV ₁₆ and/or RR ₁₉₅	170
Fig. 108 Adsorption of BV ₁₆ on charred dolomite (A), adsorption of RR ₁₉₅ on charred dolomite (B), adsorption of RR ₁₉₅ on vermicompost (C), adsorption of BV ₁₆ on vermicompost (D)	172
Fig. 109 Removal of RR ₁₉₅ with charred dolomite by stirring the suspension in a Jar Tester	172

Abbreviations

AC	Activated carbon
AO	Anodic oxidation
AOPs	Advanced oxidation processes
AOX	Adsorbable organic halides
ASTM	American Standard Test Method
bcm	Billion cubic meters
BET	Brunauer-Emmett-Teller
BOD ₅	Five-day biochemical oxygen demand
BTC	Breakthrough curve
BV	Bed volume
BV ₁₆	Basic violet 16
CD	Charred dolomite
CEC	Cationic exchange capacity
COD	Chemical oxygen demand
CS	Chitosan
DFZ	Durchsichtsfarbzahl (= SAC)
DIN	Deutsches Institut für Normung
DMF	Dimethylformamide
DO	Dissolved oxygen
DOC	Dissolved organic carbon
DTPA	Diethylenetriaminepentaacetic acid
ECO ₂	Embodied carbon
EDTA	Ethylenediaminetetraacetic acid
EL	Elastane
EO	Ethylene oxide
EPA	Environmental Protection Agency
ETAD	Ecological and Toxicological Association of the Dyes and Organic Pigments Manufacturers
FESEM	Field emission scanning electron microscope
FTIR	Fourier transform infrared
GAC	Granular activated carbon
IR	Infrared
ISWA	Institut für Siedlungswasserbau, Wassergüte- und Abfallwirtschaft
LCA	Life cycle assessment
LCI	Life cycle inventory
LCIA	Life cycle impact assessment

LECA	Lightweight expanded clay aggregate
LOI	Loss on ignition
LWA	Lightweight aggregate
MCT	Monochlorotriazinyl
NACE	Nomenclature statistique des activités économiques dans la Communauté européenne
NB	Natural bentonite
NTA	Nitrilotriacetic acid
PA	Polyamide
PAC	Acrylic/Acrylic fibers
PAN	Polyacrylonitrile
PES	Polyester
PO	Propylene oxide
PP	Polypropylene fiber
Pt-Co	Platinum-Cobalt
PZC	Point of zero charge
RPM	Revolution per minute
RR ₁₉₅	Reactive red 195
SAC	Spectral absorption coefficient
SB	Standard bentonite
SEM	Scanning electron microscope
SMEs	Small and medium enterprises
TDS	Total dissolved solids
TOC	Total organic carbon
TOM	Total organic matter
UV	Ultraviolet
VC	Vermicompost
VS	Vinyl sulfone
WWTP	Wastewater treatment plant
XRD	X-ray diffraction
XRF	X-ray fluorescence

Motivation

Stricter restrictions on wastewater discharges and the question of water shortage put the textile wet processing industries under pressure to treat and reuse their effluents. On the other hand, the commonly used treatment methods and even some new advancements in treatment technologies still have limitations from economical, performance (technical) and environmental point of view (1).

Practically almost all industries in the textile wet processing sector use synthetic dyes, which most of them are non-biodegradable and are stable to oxidizing agents, light and heat, thereby challenging to decolorize respective wastewaters (2). Hence, most textile dyes have been found to be one of the most problematic constituents of the textile wastewaters to treat with widely used conventional treatment systems such as biological and physico-chemical methods (3, 4). To specify, the coagulation-flocculation and biological treatment methods do not always represent a viable technique for the complete removal of color from the colored textile effluents (3). Although the coagulation-flocculation process can remove many dyes, there are some limitations, especially against the highly soluble, low molecular, cationic and anionic (mainly reactive) dyes. The wastewater with residual dyes after this treatment requires further treatment using advanced methods such as adsorption or chemical oxidation (2).

On the other hand, irrespective of the widespread use of activated carbon in industries for dye removal (2, 5, 6), there are debates concerning the extent of its application in the long run due to its high price (4, 6). Due to the remarkable adsorption capability, activated carbon is the most widely used adsorbent in water treatment (4, 7, 8). However, the manufacture of activated carbon requires high pressure, high temperature and expensive activation processes. For large plants or facilities, high operational expenses limit the practical applicability of activated carbon (2, 4, 7). Moreover, regeneration of the activated carbon by desorption is a crucial task, resulting in a substantial carbon loss as well as adsorption capacity reduction of the regenerated material. Therefore, even though the activated carbon is a relatively effective adsorbent, it is not cost-effective due to its low pay-back for large-scale treatment plants (2, 7).

These challenges have prompted further in-depth research in using new, more efficient and more cost-effective methods and/or materials, specifically for full-scale installations (4, 7). In fact, an efficient treatment method for the decolorization of the colored effluent is required before it can be discharged into the environment better can be reused in the textile industry. Accordingly, the application of an effective treatment method like adsorption using locally available low-cost natural materials can be promising in terms of cost, performance and environmental standpoint (5, 9, 10). The application of these kinds of adsorbents can be considered as an economical solution compared to activated carbon and other advanced

processes such as photochemical oxidation, sonolysis, ozonation, ion exchange, membrane filtration and the like (2).

Potential commercialization of an adsorbent for full-scale applications requires that it fulfils some important criteria: the material must be available in higher quantities, cheap, non-toxic (5) and should guarantee a simple application with minimal use of additional chemicals and energy consumption. More recently, these features received great heed in the removal of pollutants from contaminated waters (6). Hence, using natural mineral materials where they are locally available such as bentonite in Iran, cheap, abundant and non-toxic can be an effective alternative for the treatment of pretreated textile effluents (5, 10-12). Furthermore, a natural bentonite can be expected to show a considerable efficacy in removal of dyes which stems from its high specific surface area and high chemical and mechanical stability (3, 4, 11, 13, 14).

Based on the previous investigations, clays show a good adsorption performance. They are widely distributed globally and readily available at a low price (4). An additional environmental benefit is that normally neither a high purity nor special (e.g. chemical) modification is required (3).

Additionally, the inclusion of these kinds of natural adsorbents in the wastewater treatment technology can bring about a more efficacious use of the energy and resources, and it can lead to a cleaner and more sustainable production of textile fabrics (15).

Recent studies have shown an excellent capacity of clays in batch studies for dyes applied for textile dyeing processes. However, clay particles need a long settling period due to the micrometric size and are not suitable for separation in the sedimentation process. Continuous fixed-bed sorption is typically applied for the treatment of a greater quantity of wastewater with a higher pollution load and it is also extensively used for industrial purposes (6). So, it appears reasonable to investigate the performance of clays in a continuous fixed-bed column mode which can be used for large-scale wastewater treatment processes (9) in order to demonstrate its potential use for the treatment of real textile wastewater.

With reference to literature, almost all studies using the continuous fixed-bed columns carried out by researchers were associated with the removal of dyes, metals, pharmaceuticals and so forth from synthetic wastewater. However, treating real industrial effluents, including tanning, textile, electroplating, paper and dyeing should be taken more into account for the elimination of the constituents contributing to color, BOD₅, COD and other parameters (16).

The textile industry in Iran faces the problem of a water shortage crisis. Water is scarce and many of the companies have to buy water, or they are doomed to close. In the Iran textile industry, between 100 to 200 L of water per kilogram of finished textile is used leading to polluted wastewater. Thus, owing to the water shortage crisis in Iran and the prospective

problems in many countries, the textile industry needs to save freshwater, decrease the production of wastewater and enhance the recycling rate of the treated wastewater. On the other hand, due to economic problems in Iran, industries are not able to apply expensive treatment methods such as the commonly suggested treatment techniques, including activated carbon or AOPs (advanced oxidation processes). Also, many of them have inefficient biological treatment system. It is therefore important to establish a practical and cost-effective treatment method to improve the quality of the treated wastewater to enable its reuse as required process water.

In the Acryl Tab company in Iran, groundwater is treated with reverse osmosis and/or sand filter. The produced process water is generally used for the pretreatment of the fibers (washing of fibers before dyeing), dyeing, last rinsing and washing down the equipment and floors. The consumed water from the pretreatment step is normally reused several times for washing the fibers. Although the quality of the reused water for fibers washing is reduced significantly, they normally use the used water in order to save water.

The huge consumption of groundwater in textile industry results in a steady decline of groundwater level, an increase in the wastewater treatment cost and an increase in the volume of the colored effluents discharges with high COD. In the Acryl Tab company, the pretreated colored effluent is discharged into the municipal wastewater sewer or on agricultural lands (rice fields). Thus, treatment of the colored effluent with cost-effective technologies and the investigation of the reuse potential of the treated wastewater in the industry are of great importance.

To the best of my knowledge, no research has been reported to date where a natural bentonite has been used for the fixed-bed column studies in treating actual wastewater from acrylic fiber dyeing pretreated only by coagulation-flocculation. Accordingly, this study focuses on the efficiency of granular bentonite as adsorbent in a fixed-bed column for the removal of color and COD.

In the second part of the thesis, the problem of what to do with the natural adsorbent loaded with organic pollutants after use is addressed. The main disposal strategies for spent adsorbents are either incineration or landfilling. Significant economic and environmental factors provide an incentive for industries to utilize recycled materials in the building industry since this can help create a circular economy in which waste materials can be considered as a part of the economic cycle. Production of LWAs has been taken into account for using many different secondary materials as unconventional raw materials such as waste glass, washing aggregate sludge, incinerator bottom ash, combustion ashes, sewage sludge ash, mining residues, contaminated mine soil, lignite coal fly ash, sediments from water reservoirs and harbor dredging, municipal solid waste, mining and quarrying, residues from coal power plants, mineral transformation and metallurgical industry, ornamental stones powders and steel dust

(17). Thermal treatment can result in an environmentally stable material that can be used to make ceramics. It must be stressed that the reduced leachability usually seen with the use of recycling contaminated wastes into synthetic aggregates is an advantage (17-20).

The use of the spent mineral adsorbents in the manufacturing of LWAs is a potential reusing alternative for the wastes generated. Hence, it is suggested to use the loaded granular bentonite as a new raw material source in the production of LWAs. The important environmental advantage is that the production of LWAs involves a sintering process in which almost all the organic compounds are decomposed and totally oxidized (destroyed) at high temperatures. Replacing raw materials commonly used in the production of LWAs will reduce the depletion of resources and also the cost of production. Furthermore, the building sector must comply with new material sources and systems for environmentally sustainable construction.

Summary of motivation

The main aim of this thesis was to remove residual dyes from the colored actual acrylic fiber dyeing wastewater pretreated with coagulation-flocculation from the Iranian textile industry by using cost-effective natural granular bentonite in a continuous fixed-bed adsorption system. This investigation can be considered as a resource-oriented approach in terms of water reuse which will bring about a minimization in water consumption. Furthermore, the proposed treatment can prevent discharging of the colored and polluted wastewater into the environment. The second aim was to investigate the potential reuse of the spent adsorbent in manufacturing LWAs to reduce the consumption of natural resources in the construction industry as well as to minimize the negative impacts of the disposal of the waste material in the environment. The organic compounds in the loaded adsorbent can be destroyed at high temperatures in the sintering process.

References (Published papers):

Khalilzadeh Shirazi E, Metzger J.W, Fischer K, Hassani A.H, Design and cost analysis of batch adsorber systems for removal of dyes from contaminated groundwater using natural low-cost adsorbents, *International Journal of Industrial Chemistry*, Vol. 11, 101–110, 2020.

Khalilzadeh Shirazi E, Metzger J.W, Fischer K, Hassani A.H, Simultaneous removal of a cationic and an anionic textile dye from water by a mixed sorbent of vermicompost and Persian charred dolomite, *Chemosphere*, Vol. 234, 618-629, 2019.

Khalilzadeh Shirazi E, Metzger J.W, Fischer K, Hassani A.H, Removal of cationic and anionic dyes from single and binary dye systems with Persian charred dolomite using first-order derivative spectrophotometer analysis method, *International Journal of Advances in Science Engineering and Technology*, Vol. 6 (4), 2018.

1. Fundamentals

1.1 Dyes in textile industry

Dyes are a diverse group of chemical compounds which can be categorized by either their chemical structure (e.g. methine dyes, azo dyes, etc.) (Table 1) or by their chemical nature as anionic (direct, acid and reactive dyes), cationic (basic dyes) and non-ionic (disperse and vat dyes) (Table 2). There are more than 100,000 different types of dyes and pigments in use, with an estimated 700,000 tons produced globally each year and a growth rate of 3% (21-23).

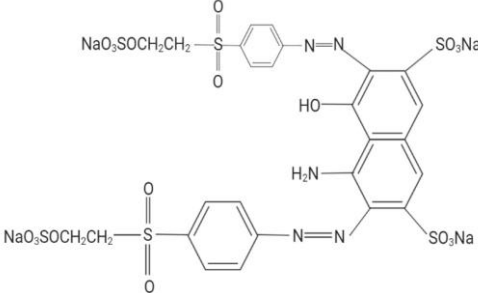
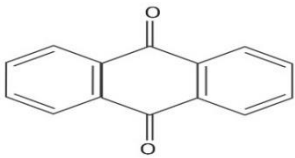
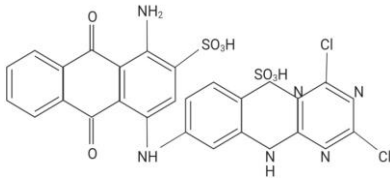
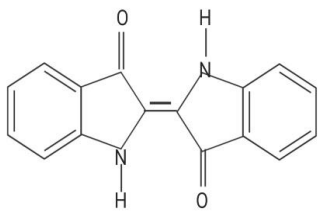
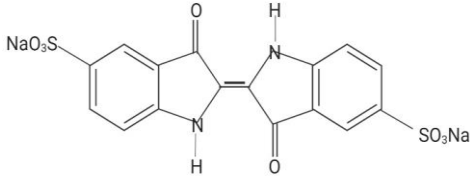
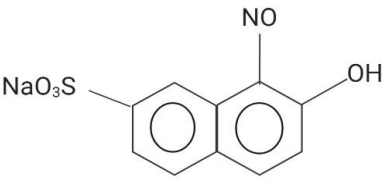
Dye molecules consist of chromophore and auxochrome groups. Chromophores are functional groups or bonds on chemical compounds responsible for the absorption of light. Auxochromes are known as functional groups in dye molecules that shift the absorption maximum of a chromophore into the longer-wave range of the spectrum. Chromophores (NO_2 , NO , $\text{N}=\text{N}$) contribute to the production of colors and auxochromes (OH , NH_2 , NHR , NR_2 , Cl and COOH) improve the affinity of the dye for the fibers. Nonetheless, colored effluents are produced because dyes do not fix to fiber completely throughout the dyeing and finishing processes (23).

Sulfonic acid ($-\text{SO}_3\text{H}$) groups are introduced into the molecule to impart water solubility, hydroxyl ($-\text{OH}$) and carboxylic acid ($-\text{CO}_2\text{H}$) groups are also effective in water-solubilizing, particularly when ionized. Such three different groups are widely used in textile dyes. A quaternary nitrogen atom ($-\text{N}^+\text{R}_4$) also contributes to the solubility of water which can be found in cationic dye (23).

Fundamentals

Table 1 Classification of dyes based on the chemical structure

(Source: Ref (24) Yagub et al. 2014)

Class	Chromophores	Example
Azo dyes	—N=N—	 <p style="text-align: center;">Reactive black 5</p>
Anthraquinone dyes		 <p style="text-align: center;">Reactive blue 4</p>
Indigoid dyes		 <p style="text-align: center;">Acid blue 71</p>
Nitroso dyes	—N=O	 <p style="text-align: center;">Acid green 1</p>

Fundamentals

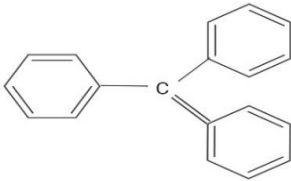
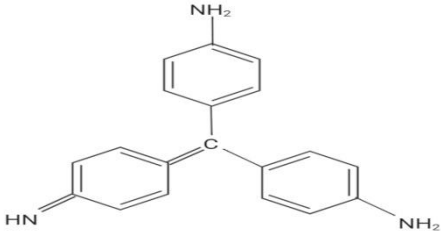
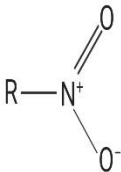
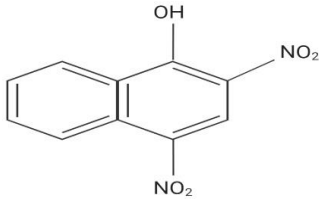
Class	Chromophores	Example
Triarylmethane dyes		 Basic red 9
Nitro dyes		 Acid yellow 24

Table 2 Classification of dyes based on the chemical nature

(Source: Ref (24) Yagub et al. 2014)

Dye class	Substrate	Method of application	Chemical type
Acidic	Wool, nylon, silk, inks, leather and paper	From neutral to acidic bath	Anthraquinone, xanthene, azo (including nitroso, premetallized), nitro and triphenylmethane
Basic	Inks, paper, polyacrylonitrile, treated nylon and polyester	Applied from acidic bath	Hemicyanine, azo, cyanine, diazahemicyanine, azine diphenylmethane, xanthene, triarylmethane, acridine, anthraquinone and oxazine

Fundamentals

Dye class	Substrate	Method of application	Chemical type
Direct	Nylon, rayon, paper, leather and cotton	Applied from neutral or a little alkaline bath containing additional electrolyte	Phthalocyanine, azo, oxazine and stilbene
Disperse	Polyamide, acrylic, polyester, acetate and plastics	Fine aqueous dispersions often applied by high temperature/pressure or lower temperature carrier methods; dye maybe padded on cloth and thermo fixed	Benzodifuranone, azo, anthraquinone, nitro and styryl
Reactive	Wool, cotton, silk and nylon	Reactive site on dye reacts with functional group on fiber to bind dye covalently under influence of heat and pH	Anthraquinone, formazan, phthalocyanine, azo, oxazine and basic
Sulphur	Rayon and cotton	Aromatic substrate vatted with sodium sulfide and reoxidized to insoluble sulfur-containing products on fiber	Indeterminate structures
Vat	Wool and cotton	Water-insoluble dyes solubilized by dropping with sodium hydrogen sulfite, then exhausted on reoxidized and fiber	Indigoids and anthraquinone

1.1.1 Chemical characteristics, applicability and properties of cationic dyes

Cationic dyes, also known as basic dyes, are widely used in nylon, acrylic, wool and silk dyeing (25, 26). Cationic dyes consist of a quaternary amino group. This group can be an essential part (more common). Sometimes instead of nitrogen, a positively charged atom of sulphur or oxygen can be found.

The followings are examples of typical basic dyes which are adapted from Ref (26):

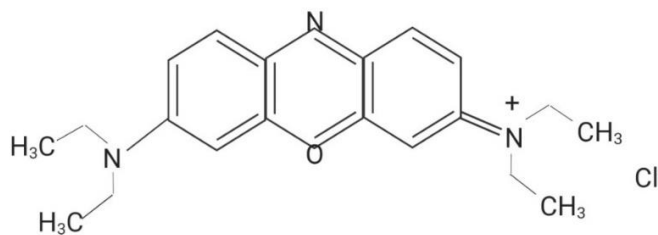


Fig. 1 Basic blue 3 C.I. 510041

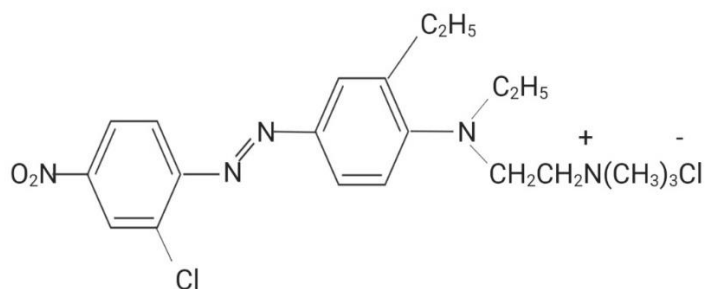


Fig. 2 Basic red 18 C.I. 110852

The positive charge of the cationic dyes may be either delocalized or localized. As can be seen in Fig. 3, the positive charge is localized at the nitrogen atom:

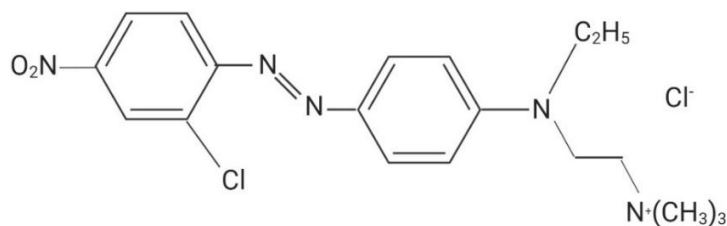


Fig. 3 Cationic dye with localized positive charge

The positive charge is delocalized across the dye cation in the diazahemicyanine dye, which can be seen in Fig. 4:

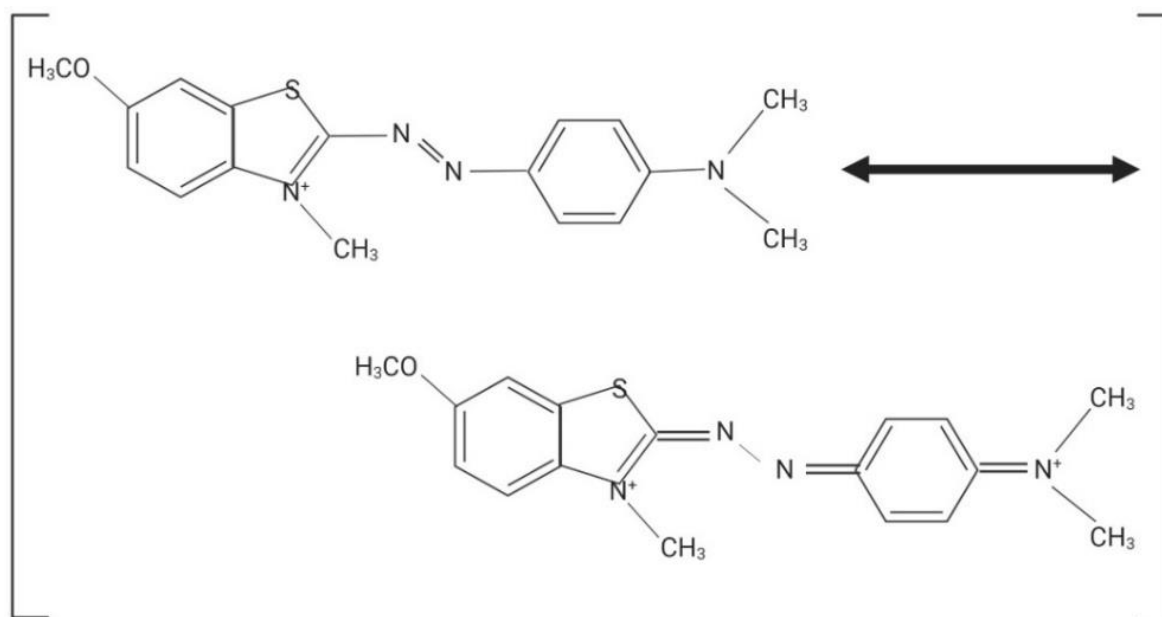


Fig. 4 Diazahemicyanine dye with delocalized positive charge

The methine dyes are categorized into cationic dyes with a delocalized charge. All these dyes can be characterized by different resonance formulae. They are distinguished by high color strength.

Hemicyanine dyes can be introduced as the cationic dyes with a delocalized positive charge, which a nitrogen atom directly linked to the methine chain and one of the charged terminal atoms is part of a heterocyclic ring. Enamine dye is an example of this type of dye which imparts a yellow color to polyacrylonitrile fibers (Fig. 5).

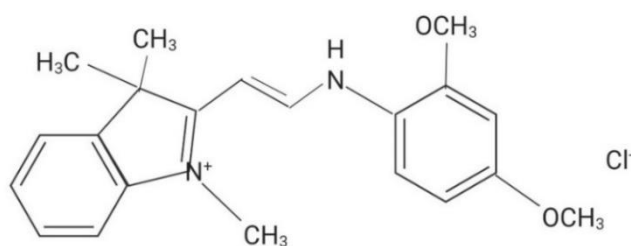


Fig. 5 Enamine dye

Styryl dyes (Fig. 6) can be used to give red and purple shades to polyacrylonitrile. These types of dyes have an aryl residue between the methine chain and the second nitrogen atom.

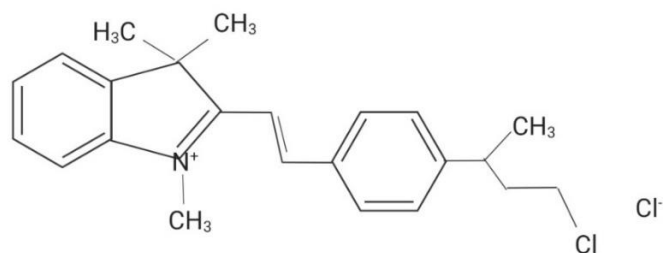


Fig. 6 Styryl dye

The chain may be totally missing in a specific form of this type of dye which results in zeromethine dyes (see Fig. 7). They confer very blue shades and lightfast violet to polyacrylonitrile.

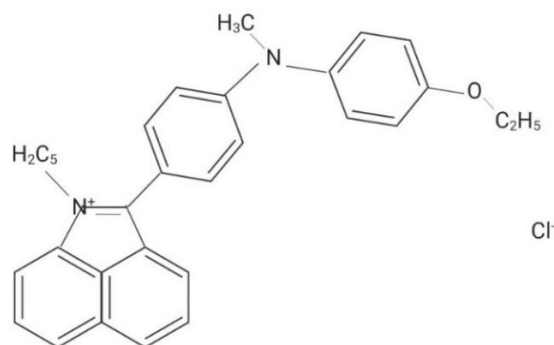


Fig. 7 Zeromethine dye

Nitrogen may replace one or more carbon atoms in the chain, as it is cited by the prefix aza. Mono- (Fig. 8) or diazadimethine dyes are formed depending on the number of nitrogen atoms inserted into the chain. The other known dyes are Tri- and tetraazamethine dyes. An example is a dye below, in which a golden yellow color is conferred to polyacrylonitrile fibers.

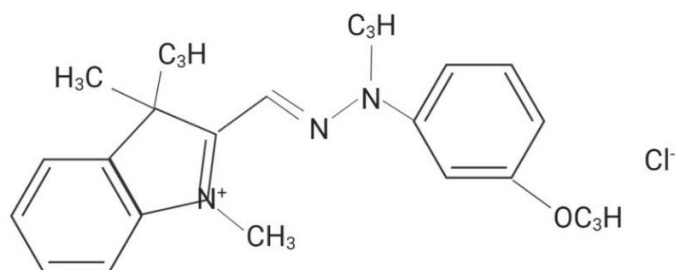


Fig. 8 Monoazamethine dye

Unlike dyes with delocalized charge, where the charge is an integral part of the chromophore, in most cases, the charged atom in dyes with localized charge is isolated from the chromophore by a nonconjugated group. Thus, any chromophore can be used, and the charged atom does not or just slightly affect the spectral properties of this chromophore. Representatives of localized charged cationic dyes with localized charge are found in the following dye classes.

- 1) Azo dyes: The localized charge in cationic azo dyes can reside either in the coupling component (Fig. 9) or diazo moiety (Fig. 10):

(moiety: the principal characteristic parts of molecule is composed of atoms that take part in similar chemical reactions in the majority of the molecules that they make up)

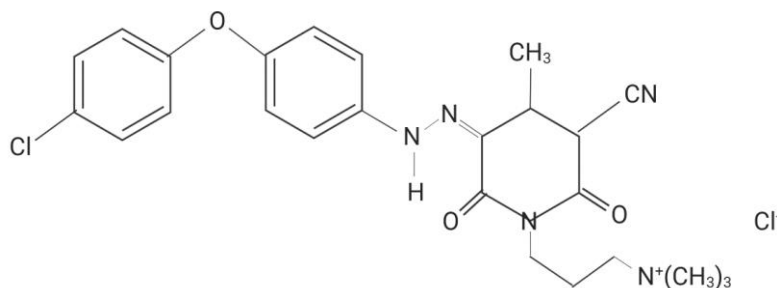


Fig. 9 Azo dye with a localized charge which resides in the coupling component

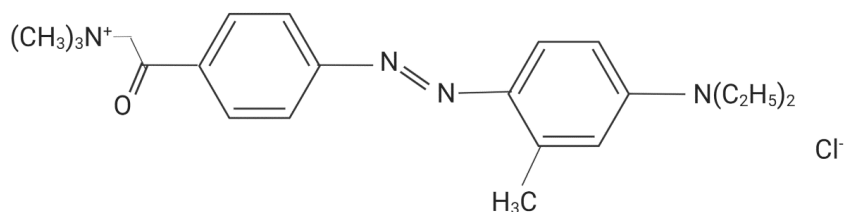


Fig. 10 An azo dye with a localized charge which resides in the diazo moiety

2) An example of anthraquinone dyes:

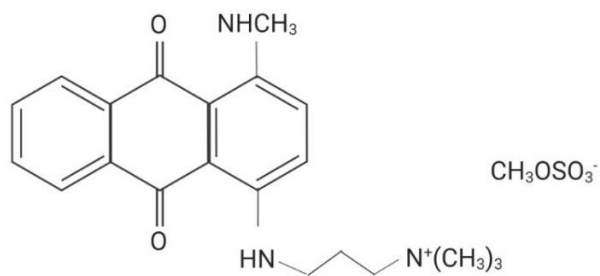


Fig. 11 Anthraquinone dye

3) An example of phthalocyanine dyes:

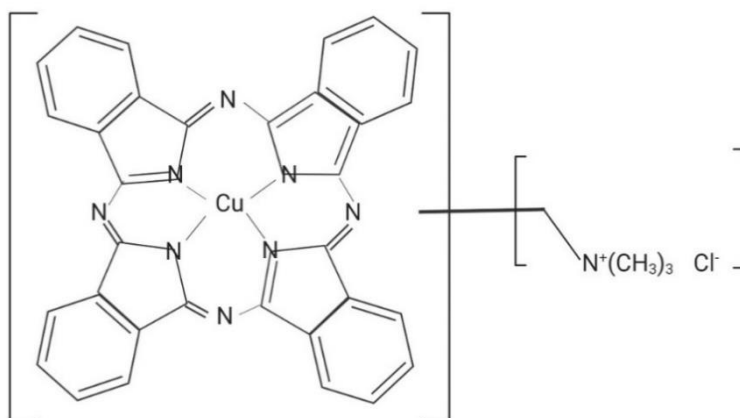


Fig. 12 Phthalocyanine dye

(4) An example of perinone dyes:

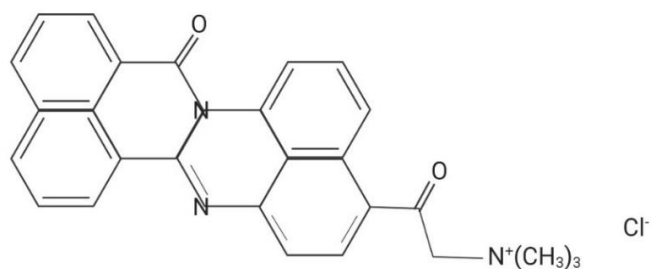


Fig. 13 Perinone dye

5) An example of naphthalimide dyes:

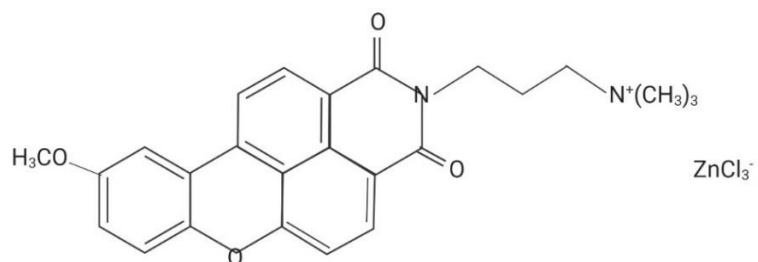


Fig. 14 Naphthalimide dye

6) An example of quinophthalone dyes:

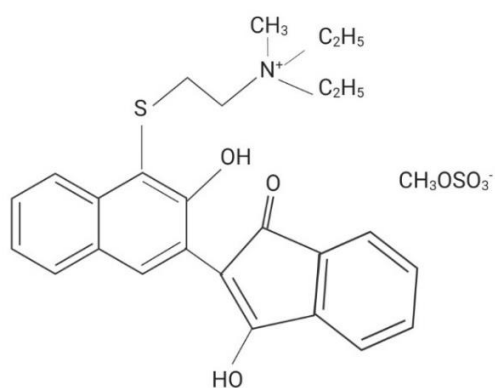


Fig. 15 Quinophthalone dye

7) An example of neutrocyanine dyes:

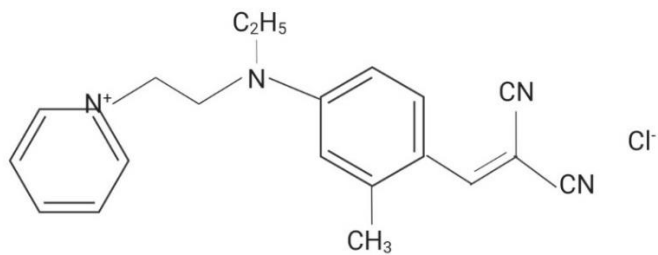


Fig. 16 Neutrocyanine dye

8) An example of nitro dyes:

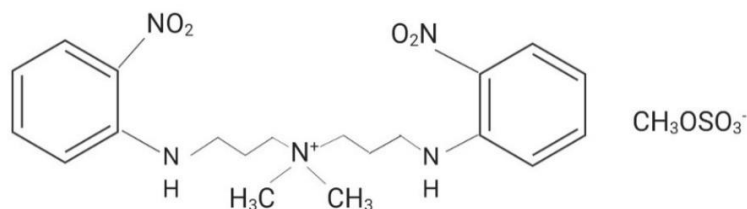


Fig. 17 Nitro dye (Ref (26)).

Ionic bonds are formed between the anionic site on the fiber and the positively charged atom in the dye. Basic dyes were used to dye wool and silk (using a mordant) initially; however, they showed poor fastness features. Currently, cationic dyes are nearly exclusively applied on acrylic fibers, modified polyamide fibers and blends. These dyestuffs have excellent fastness performances on acrylic fibers.

Common cationic dyes show low solubility in water; differently, they have a higher solubility in ethanol, ether, acetic acid and other organic solvents. They are used in weak acid solution in dyeing processes. Basic dyes are tightly bound to the fiber and do not migrate simply. Specific levelling auxiliaries (known as retarders) are usually applied (unless an absorption process with a pH controlled is used) to reach level dyeing. Retarders containing quaternary ammonium compounds with long alkyl side-chains are considered as the most important group (cationic retarders). Electrolytes and anionic condensation products between formaldehyde and naphthalenesulphonic acid can be found as well (26).

1.1.2 Chemical characteristics, applicability and properties of reactive dyes

Reactive dyes constitute 20-30% of the dye market and are extensively used in the textile industry because of their favourable water solubility, low consumption of energy, bright color and straightforward application technique (27-29). Owing to the presence of chemically reactive group of either the triazine or vinyl sulfone type, reactive dyes are called reactive. They are water-soluble due to their sulfonate groups (11).

Reactive dyes are principally applied for dyeing cellulose fibers including viscose and cotton but are also becoming increasingly important for polyamide and wool. They have high wet fastness, but their application is not always feasible due to the difficulties of providing level dyeing. Reactive dyes are distinct since they consist of specific chemical groups that can form

covalent links with the textile substrate. In the case of protein and polyamide fibers, reactive groups of the colorant react with the amino groups of the fiber, and in the case of cellulose, they react with the hydroxyl groups (26).

Reactive dyes for cotton are soluble in water, which comprises a group able to form a covalent bond with the hydroxyl groups in the cellulose polymer during the dyeing process. Two groups of monochlorotriazinyl (MCT) and betasulphatoethylsulphone [masked vinyl sulfone (VS)] are the two major reactive groups, which are either alone or in combination (23).

1.2 Textile industry

The textile industry uses various raw materials/sources such as woolen, cotton and synthetic fibers. It can also be divided into the wet and dry fabric industries. Solid wastes are produced in the dry fabric industry, while liquid wastes are generated in the textile wet processing industry. Scouring, mercerizing, desizing, bleaching, printing, dyeing and finishing stages as processing operations are included in the textile wet processing industry. The water consumption and wastewater production from a wet processing textile business depends on the operations during the formation of fabric. The process of dyeing involves treating a fabric or yarn with a dye in order to impart color (30, 31).

The following pages including tables (3-6) are extracted from a document published by the European commission in 2003 entitled "Integrated Pollution Prevention and Control (IPPC), Reference Document on Best Available Techniques for the Textiles Industry" (26).

The textile industry has been known to be one of the most complicated and longest production chains in the manufacturing industry. It has a demand mainly driven by three major end-uses: clothing, industrial use and home furnishing.

The textile and clothing chain consists of a broad variety of sub-sectors encompasses the entire manufacturing cycle from the production of raw materials (man-made fibers) to semi-processed materials (woven and knitted fabrics, yarns with their finishing processes) and final/consumer products (home textiles, carpets, industrial use textiles and clothing).

In the old nomenclature system, the textile industry activities were divided based on fiber processing. Traditionally, natural fibers dominated by wool and cotton were the only available textile fibers. Currently, these two sectors (cotton and wool) in the textile industry both process all available fibers due to the proliferation of man-made fibers.

As it has become inapplicable to categorize the textile activities with reference to the fiber processing, the new nomenclature system classifies the textile industry activities as follows:

- yarn and thread

- woven fabric
- textile finishing
- home textiles
- industrial and other textiles (this includes carpets and wool scouring)
- knitted fabrics and articles.

Furthermore, textile industry activities can be classified into three sub-sectors which involve wet processes as follows:

- textile finishing
- industrial and other textiles (including carpets and wool scouring)
- home textiles.

The carpet yarn spinning, carpet manufacturing and related dyeing industry can be grouped into a variety of basic sub-sectors, although there may be substantial variations. All sectors may process combinations of 100% natural fiber, 100% synthetic fiber and/or combinations of the two, as many of the techniques and processes applied are not fiber specific.

The reference document on best available techniques for the textiles industry (European Commission) categorizes companies where wet processes are usually carried out into five specific groups of:

- commission loose fiber dyehouses
- commission yarn dyehouses
- integrated yarn manufacturing mills, which in addition to the dyeing processes perform on-site conversion of the loose fiber to yarn, selling the finished yarn as the end-product
- commission piece dyeing mills
- integrated carpet manufacturing mills, which carry out all the mechanical processes, dyeing and finishing operations required to convert natural and synthetic fibers into the finished carpet (26).

1.2.1 Raw materials

A wide range of chemicals and auxiliaries and fibers are the main two groups of raw materials in the textile industry. A significant number of organic dyestuffs/pigments and chemical auxiliaries are used in the textile industry. They can be categorized into the following groups (26, 31, 32):

- dyestuffs and pigments
- basic chemicals (also known as “Commodities”), which encompasses all inorganic chemicals, organic reducing and oxidizing agents as well as the aliphatic organic acids

- auxiliaries, which consist of all textile auxiliaries, including primarily organic materials other than organic reducing and oxidizing agents and organic aliphatic acids.

In the textile industry, two general types of fibers are utilized, including natural and man-made. Man-made fibers consist of both purely synthetic materials of petrochemical origin and regenerative cellulosic materials produced from wood fibers (26). An overview is shown in Table 3.

Table 3 General categories of fibers used in the textile industry
(Source: Ref (26) Integrated Pollution Prevention and Control, 2003)

Type	Origin	Example	
Natural origin fibers	Animal origin	Raw wool Silk fiber Hair	
	Vegetable origin	Raw cotton fiber Flax Jute	
	Mineral origin	Asbestos (not used in the textile industry)	
Chemical fibers (man-made)	Natural polymer fibers	Viscose, Cupro, Lyocell, Acetate, Triacetate	
	Synthetic polymer fibers	Inorganic polymer	Glass for fiber glass Metal for metal fiber
		Organic polymer	Polyester (PES) Polyamide (PA) Polypropylene (PP) Elastane (EL) Polyacrylonitrile (PAN)

As the Iranian textile company “Acryl Tab” only dyes acrylic fibers for manufacturing carpet and knitwear, acrylic fibers will be described in the following section.

Acrylic fibers are formed by radical polymerization of acrylonitrile in a solvent or aqueous emulsion. PAN (Polyacrylonitrile), made of 100% acrylonitrile, gives fibers with inadequate

dye-binding capability, due to the high glass transition temperature (above 100 °C). For this reason, this polymer is no longer used in textile industry. Acrylic fibers (PAC) which are the commonly available fibers on the current market, are anionic copolymers containing 85-89% of acrylonitrile, 4-10% of a non-ionic co-monomer (vinyl chloride, vinyl acetate and methyl acrylate) and 0.5-1% of ionic co-monomers containing sulfonyl or sulphate groups. Techniques of dry and wet spinning can be used to produce the fiber. The polymer is dissolved in dimethylformamide (DMF) when dry spinning is utilized. If the fiber is produced by means of wet spinning, in addition to DMF, dimethylacetamide, dimethylsulphoxide, ethyl carbonate and aqueous solutions of inorganic salts or acids are also applied. Residues of these solvents (0.2-2% of the weight of fiber) are found in the wastewater from pretreatment.

1.2.2 Pretreatment of fibers

Pretreatment processes must assure

- the removal of foreign materials from the fibers to enhance their uniformity, hydrophilic properties and affinity for dyestuffs and finishing treatments
- the improvement of the ability to absorb dyes uniformly
- the relaxation of tensions in synthetic fibers (without this tension relaxation, unevenness and dimensional instability can be developed).

The pretreatment in the manufacturing system is done near the place of dyeing. Pretreatment is carried out before dyeing (and printing).

The pretreatment of synthetic materials before dyeing usually includes washing and thermofixing (heat-setting). Scouring is intended for the elimination of impurities present on the raw fiber. Water scouring is typically a batch process in the equipment in which the textile content is subsequently dyed.

All preparation agents and impurities are normally removed before dyeing to make the fibers more hydrophilic and allow dyestuffs to penetrate the fibers. Nevertheless, this operation is not always required. In some cases, a separate scouring/washing phase can be eliminated if the preparation agents are added in low quantities, and they do not interfere with the dyeing process.

1.2.3 Dyeing

Dyeing is a technique to color a textile material in which a dye is applied uniformly to the substrate in order to achieve an even shade with performance and fastness suitable for its final

usage. A dyestuff is a molecule that comprises a chromophoric group (conjugated electron system) that adsorbs light in a defined range of wavelengths, thereby giving the impression of color. Textile dyeing involves the application of various chemicals and auxiliaries to promote the dyeing process. Some of them are process-specific, although others are also used in other operations. Some auxiliary agents (e.g. dispersing agents) already exist in the dyestuff formulation, yet more commonly used auxiliaries are added to the dye liquor in the subsequent step, auxiliaries are found in the emissions at last as in general they do not remain on the textile substrate.

Different dyeing techniques are used:

- mass dyeing/gel dyeing, in which a dye is applied in the synthetic fiber during its manufacturing (this method is the most widely used technique for PP (polypropylene) fibers and is used also for PAC)
- pigment dyeing, in which an insoluble pigment, without affinity for the fiber, is applied onto the textile substrate and then fixed with a binder
- dyeing processes that incorporate the diffusion of a dissolved or at least partially dissolved dye into the fibers.

Dyeing can be conducted in a batch or in a continuous/semi-continuous system. The choice between the two modes hinges upon the make-up type, dye class, the available equipment and the involved cost. Both continuous and discontinuous dyeing processes consist of the steps as follows:

- preparation of the dye
- dyeing
- fixation
- washing and drying.

In batch dyeing (also known as exhaustion dyeing), a determined amount of textile material is placed into a dyeing machine and brought to equilibrium with a dye-containing solution mixed with auxiliaries lasting for a period of minutes to hours.

The dyeing process begins with the absorption of the colorant on the outer surface of the fiber. Afterwards, it is accompanied by the diffusion and migration of the colorant through the fiber. To accelerate and optimize the exhaustion and fixation of the dye, chemical auxiliaries are used and controlled temperatures are applied. When the dyeing is deemed to be the correct shade, the spent dye bath is drained, and the textile content is washed to eliminate the chemicals and unfixed dyes. Washing is normally carried out in the same equipment. However, separate washing machines can also be used.

Acrylic (PAC) fibers are hydrophobic and comprises anionic groups in the molecule. Therefore, they can be dyed with cationic and disperse dyes. The fiber can also be dyed with acid dyes with the addition of cationic comonomers in the polymer (26).

Table 4 The most common dyestuffs and dyeing techniques for polyacrylic fibers
(Source: Ref (26) Integrated Pollution Prevention and Control, 2003)

Dyestuff	Chemicals and auxiliaries/typical application conditions	Technique
Disperse	<ul style="list-style-type: none"> - dyeing conditions correspond to those used for polyester - addition of carriers is not required 	
Cationic	<ul style="list-style-type: none"> - Acetic acid (pH 3.6 - 4.5) - Salt (sodium sulphate or sodium acetate) - Retardant auxiliaries (usually cationic agents) - Non-ionic dispersing agents 	Batch
	<ul style="list-style-type: none"> - Acetic acid (pH 4.5) - Dye solvent - Steam-resistant and readily soluble dyes (usually liquid) are required - Dye solvent - Rapidly diffusing dyes are required 	Pad-steam process with pressurized steam Pad-steam process with saturated steam

1.3 Environmental issues of the textile industry

Generally, emissions to water and air as well as energy consumption are the major environmental concerns resulting from the activities and processes in the textile industry. Among these, water contamination and consumption are considered the most critical environmental issues. The textile industry consumes water as the main medium for washing, applying finishing agents and dyes and for generating steam. The majority of the water used is discharged as aqueous effluent, aside from the limited amount of water that is evaporated during drying. The key issues are consequently the volume of water discharges and the chemical load that it bears (26).

Textile mills of average size need roughly 200 liters of water per kilogram of fabric processed per day. Textile dyeing and finishing treatment, with reference to the World Bank, is given to a fabric that produces 17 to 20% of industrial effluent (31).

Textile is one of the main industries using water, dyestuffs and other chemicals such as surfactants, fats, oils, waxes, salts, solvents, fabric softeners, pesticides, coupling agents, polishing and coating agents, alkalis, acids, soaps of metals, starch, hydrogen peroxide and dispersing agents which produces large amounts of colored and polluted wastewater. Thus, contamination of water resources caused by textile industry now has become a serious environmental concern (4, 30, 33-35).

Contaminated waters containing dyes affect the ecological system. Thus, they endanger both aquatic life and human life when entering the food web. Some of the dyes are mutagenic, carcinogenic and have other toxic effect (21, 33).

With reference to the Environmental Hazards of Textile Industries, many textile producers utilize dyes that release aromatic amines. The effluents from dye baths may contain ammonia, heavy metals, toxic solids, alkali salts and significant quantities of pigments many of which are toxic. About 40% of globally used colorants contain “organically bound chlorine”, containing substances which are potentially a known carcinogenic (25, 26, 36). Carcinogenic chromium ions can be released into the water by chromium-based dyes, and disperse dyes tend to bioaccumulate (12). Furthermore, some carcinogenic, toxic and mutagenic intermediates are usually generated by various reactions including oxidation and hydrolysis of dyes (37). In addition, any degradation by chemical, physical and biological treatments may produce small carcinogenic and toxic products (25, 26). Furthermore, residual dyestuffs increase the chemical oxygen demand (COD) (30, 38). Textile wastewater has a high color, high salt (total dissolved solids) load and low biodegradability ($BOD_5/COD < 0.1$) (30, 38, 39). Owing to high BOD_5 , raw textile wastewater may cause a rapid depletion of dissolved oxygen if it is directly discharged into surface water bodies. High COD levels in effluent are toxic to biological life (40).

The US Environmental Protection Agency (EPA) categorized textile wastes into four categories that require special pollution prevention approaches. These categories are high-volume, hard-to-treat, dispersible, hazardous or toxic wastes. Colored wastewater generated from dyeing processes can be included in all four categories (41). Therefore, an effective effluent treatment is of great importance.

It is worth mentioning that 2% of dyes that are generated worldwide and discharged directly into aquatic systems are synthetic dyes as prevailed water pollutants (4). Based on the previous studies, about 15% of total dyes used in coloring processes can still be present in wastewater as residuals (21).

Unused dyes specifically reactive dyes (which account for approximately 8-20% of the total pollution load due to incomplete exhaustion) and auxiliary chemicals in addition to a considerable amount of water can be found in wastewater streams from textile dyeing operations (12, 42). As the hydrolysed form of reactive dyes does not have any affinity for

textile fabrics in the alkaline dye bath, approximately a mean of 30% of used reactive dyes end up in effluent (12).

Washing (scouring) and bleaching of the natural fibers as well as dyeing and finishing sections are the primary sources of textile wastewater (1).

The dyeing method, which is possibly the most studied stage in textile manufacturing, produces intensely colored wastewater from the mixture of various forms of dyes and auxiliary materials such as fixing agents, organic acids, diluents and reducing agents (43).

Water-polluting substances in the emissions referred to Table 5 can be derived from:

- dyes (color, metals, toxicity)
- auxiliaries in the dye formulation
- basic chemicals (e.g. salts, alkali, oxidizing and reducing agents) and auxiliaries applied in the dyeing processes
- contaminants present on the fiber upon entering the process (spin finishes are found on synthetic fibers and residues of pesticides on wool can be found in yarn dyeing and loose fiber).

Spent dye baths in discontinuous dyeing, residual dye liquors and water from washing operations always encompass a proportion of unfixed dye. Fixation rates differ greatly among the different dye classes.

Poorly bio-degradable dyestuffs will end up in the discharged effluent after passing through a biological wastewater treatment plant (unless they are subjected to destructive treatment systems) (26). For instance, cotton dyeing industry produces textile wastewater which is polluted due to the presence of reactive dyes which are difficult to treat biologically (44). In other words, since brightly colored reactive and acid dyes are water-soluble, they are usually rendered unaffected by conventional treatment systems. Thus, effluents are usually colored when they leave the wastewater treatment plant (45). Furthermore, the azo and anthraquinone groups are the most prominent groups that causes contamination in textile effluent, resulting in an undesirable color (30, 31).

Color is the first observable effect in the receiving water. Moreover, high concentrations of color cause a negative aesthetic effect and can also disrupt photosynthesis which affects aquatic life. The aquatic toxicity, molecules of metals or halogens which can generate adsorbable organic halides (AOX) emissions and the organic contamination caused by the colorant (typically measurable as BOD₅ and COD, but also as organic carbon, using parameters such as TOC and DOC) are other effects (26).

Fundamentals

Table 5 Overview of the typical emissions generated in dyeing processes
(Source: Ref (26) Integrated Pollution Prevention and Control, 2003)

Operations	Emission sources	Type of emission
Color kitchen operations	Dye preparation	Discontinuous, low-concentration water emission at the end of each batch (cleaning step)
	Auxiliaries' preparation	Discontinuous, low-concentration water emission at the end of each batch (cleaning step)
	Dispensing of dyes and auxiliaries (manual)	Indirect pollution from inaccurate dosing and handling of chemicals (spillage, poor shade repeats, etc.)
	Dispensing of dyes and auxiliaries (automatic)	No emission, provided that the system is regularly calibrated and verified for accuracy
	Dyeing	Discontinuous, low-concentration water emission at the end of each cycle
Batch dyeing	Washing and rinsing operations after dyeing	Discontinuous, low-concentration water emission at the end of each cycle
	Cleaning of equipment	Discontinuous, low-concentration water emission
	Application of the colorant	No emission from the process unless dye bath is drained
	Fixation by steam or dry heat	Continuous emission to air (generally not significant, except for specific situations such as, for example, the thermosol process, drying of carrier dyed fabrics, etc.)
Semi-continuous and continuous dyeing	Washing and rinsing operations after dyeing	Continuous, low-concentration water emission
	Discharging of leftovers in the chassis and feed storage container	Discontinuous, concentrated water emission at the end of each lot
	Cleaning of equipment	Discontinuous, low-concentration water emission (it can contain hazardous substances when reductive agents and hypochlorite are applied)

Moreover, another major concern originates from the discharge of poorly or non-biodegradable substances such as mineral oils, EO-PO adducts, silicone oils and hard surfactants and the like.

In addition, biocides, which are usually found in the aqueous compositions, contribute to the aquatic toxicity of the wastewater.

Textile dyestuffs show aquatic toxicity and/or allergenic effects. It is worth noting that around 60% to 70% of the dyes used are azo dyes. Such dyes generate amines and some of these are carcinogenic under reductive conditions (26). Table 6 lists the carcinogenic amines that can be generated by cleavage of specific azo dyes.

Table 6 List of carcinogenic amines

(Source: Ref (26) Integrated Pollution Prevention and Control, 2003)

No	Carcinogenic amines
1	4-aminodiphenyl
2	o-aminoazotoluene
3	2-amino-4-nitrotoluene
4	4-aminoazobenzene
5	o-anisidine
6	benzidine
7	4-chloro-o-toluidine
8	p-chloroaniline
9	p-cresidine
10	2,4-diaminoanisol
11	4,4'-diaminodiphenylmethane
12	2,4-diaminotoluene
13	3,3'-dichlorobenzidine
14	3,3'-dimethoxybenzidine
15	3,3'-dimethylbenzidine
16	3,3'-dimethyl-4,4'-diaminodiphenylmethane
17	4,4'-methylene-bis-(2-chloraniline)
18	2-naphthylamine
19	o-toluidine
20	4,4'-oxydianiline
21	2,4,5-trimethylaniline
22	4,4'-thiodianiline

The application of azo dyes which may be reduced to one of the 22 potentially carcinogenic aromatic amines given in Table 6 is banned with reference to the 19th amendment of Directive

76/769/EWG on dangerous substances. Nonetheless, more than 100 potential dyes generating carcinogenic amines in the dyeing process are still commercially available.

Regarding environmental issues of cationic dyes, many of them show high aquatic toxicity. However, in the case when they are applied properly, they prove to have fixation degrees close to 100%. Problems mostly arise from inefficient handling processes, spill clean-up and other disruptions.

The following dyestuffs are categorized as toxic by ETAD (Ecological and toxicological association of the dyes and organic pigments manufacturers):

- Basic violet 16
- Basic red 12
- Basic blue 3, 7, 81
- Basic yellow 21 (26).

For instance, basic violet 16 (BV₁₆) is extensively used in the textile industry worldwide. It directly harms the skin, eyes and gastrointestinal respiratory tract. It also provokes phototoxic and photoallergic reactions. Its carcinogenicity, neurotoxicity and chronic toxicity towards humans and animals have also been experimentally proven (6, 46).

According to a research study in Germany and Austria which investigated the major charging loads from the textile industry in Europe, a high portion of the total emission load from the activities of the textile industry is associated to the compounds that already existed on the raw material before entering the finishing process step. Such substances include preparation agents, sizing agents, natural fibers impurities and related materials.

To specify, the potentially harmful additives and impurities that are already on synthetic fibers before they are processed at the finishing mill account for a high proportion of the pollution load arising from the pretreatment step. Some of the impurities are generated during the manufacturing of the fiber. They are by-products of the polymer synthesis including unreacted monomers (e.g. caprolactame, in the production of polyamide), residual catalysts and low-molecular-weight oligomers which are emitted to air during thermal processing. To improve the subsequent processing, other materials are usually added to the fiber. These are the preparation agents applied in fiber, yarn manufacturing and the sizing agents. In various phases of the process, spinning oils and preparation agents are added to fibers from the production of the fiber itself (only for synthetic fibers) to the yarn formation. Such organic substances are eliminated at the finishing mill in the pretreatment step either by heat-setting in the dry processing or through washing in wet processing. In wet processing, the organic load of the final effluent rises as a result of the organic materials while they become airborne in the dry processing. The average quantity of the preparation agents used on man-made fibers (apart from elastomeric fibres, as the load can be substantially higher) is estimated between 2% and

4% of the fiber weight. Approximately 80% of these materials are discharged into the wastewater and in the following high temperature treatments (thermo fixation and drying), the remaining 20% can be emitted to exhaust air. Before the finishing process, sizing agents that are applied to facilitate the weaving process are removed from the woven fabric, which results in the generation of high degrees of the organic load in the water (26).

Natural fibers comprise a proportion of impurities and related materials (the information given in the following two pages is taken from Ref. (26)). Such associated substances are an integral part of the natural fibers (e.g. lignin for flax, hemicellulose and pectin for cotton, sericin for silk and grease for wool). Impurities are mineral, pesticides and metals. Before finishing processes, all these materials must be removed from the fiber. Consequently, they have the potential for major environmental impacts. Based on the data recorded, the largest environmental loads originate from salts, organic acids and detergents which are typically used during the process.

Compared to these substances applied in the process, dyestuffs do not reflect a large load. However, they are responsible for the color of the generated effluent which substantially causes the aesthetic problem, whereas a high amount of color may diminish light transmission to aquatic plants as well. The introduction of wastewater containing dyestuffs into bodies of water is a crucial problem due to color as well as other environmental concerns, including difficult-to-eliminate organic materials, metals and AOX, particularly for specific types of dyestuffs.

Some chemicals reported in the “Reference document on best available techniques for the textiles industry (European Commission)” that may be applied in the textile process and have potential negative impacts on the environment are:

- alkylphenol ethoxylates (leveling agents, wetting agents, detergents, etc.): their metabolites (octyl- and nonylphenols) are substantially toxic to aquatic life; they have been shown to disrupt the reproduction of aquatic species by disturbing their endocrine system (octyl- and nonylphenols and are on the list of “Priority Substances” targeted for priority action under the Water Framework Directive 2000/60/EC, specifically nonylphenol is defined as “Priority Hazardous Substance”)
- halogenated phenols, chlorinated paraffins (flame retardants), polybrominated diphenyl ethers and benzenes (reagents in the production of flame retardants): some members of these classes of substances (e.g. pentabromodiphenylether, C10-13 chloroparaffines) have already been determined as “Priority Hazardous Substances” due to their persistency, toxicity and liability to bioaccumulate or they have been evaluated within the framework of Regulation (EEC) 793/93 on the control and evaluation of the risk of the existing substances. The discussion about their possible detrimental effects on the environment is continuing for other members of these classes

- mothproofing agents based on cyfluthrin (carpet sector), permethrin and other biocides which are extremely toxic to aquatic life
- sequestering agents like DTPA, EDTA and NTA: these agents can produce very stable complexes with metals (DTPA and EDTA are poorly bio eliminable as well)
- chlorine and chlorine-releasing compounds such as sodium dichloroisocyanurate (wool anti-felting agent) and sodium hypochlorite (bleaching agent): these have the ability to interact with organic compounds to form adsorbable organic halogens (AOX)
- compounds which contain metals such as potassium dichromate
- substances with carcinogenic potentials, such as some aromatic amines, formed by cleavage of some azo dyes, or vinylcyclohexene and 1,3-butadiene, which can be found in polymer dispersions as a result of an incomplete reaction during polymerization
- carriers namely o-phenylphenol, trichlorobenzene, etc.

It is estimated that more than 90% of the organic chemicals and auxiliaries used in pretreatment and dyeing processes do not fix on the fiber; nevertheless, the opposite is true in finishing treatment. Moreover, almost 90% of the organic raw material load introducing the textile process ends up in the wastewater, the remaining quantity is emitted to the air (26).

1.4 Conventional wastewater treatment methods of textile wastewater

The main techniques to remove pollutants from the effluents can be categorized as physical, chemical and biological (4). Different technologies are extensively used for the treatment of textile wastewater, including membrane filtration (reverse osmosis, ultrafiltration, nanofiltration, etc.), adsorption, chemical and electrochemical advanced oxidation processes (AOPs/EAOPs) including Fenton, electro-Fenton (EF), photo-Fenton, coagulation-flocculation, anodic oxidation (AO), hydrogen peroxide, photolysis with UVC radiation (H_2O_2/UVC) and the application of pure and mixed cultures under anaerobic and/or aerobic conditions (47).

Different conventional treatment methods are as follows (see Table 7):

1.4.1 Biological methods

Compared with other physical and chemical processes, biological treatment can often be considered as the most economical alternative. Biological methods such as adsorption by (living or dead) microbial biomass, microbial degradation, bioremediation systems and fungal decolorization are widely used for the treatment of textile effluents since many

microorganisms, including algae, bacteria, fungi and yeasts can accumulate and degrade various pollutants.

1.4.2 Chemical methods

The chemical methods used for discoloration of colored wastewater are electroflotation, precipitation-flocculation with Fe(II)/Ca(OH)_2 , conventional oxidation methods by oxidizing agents (ozone), coagulation combined with floatation and filtration, electrochemical processes, electrokinetic coagulation and irradiation.

The process of coagulation-flocculation occurs in successive phases: coagulation, flocculation and sedimentation. The first step is a chemical process that consists of neutralizing the charge of colloidal suspensions in order to destabilize them. The second step is flocculation, a physical process to group the smaller particles.

1.4.3 Physical methods

Various physical methods are commonly used such as membrane-filtration processes (reverse osmosis, nanofiltration, electrodialysis, etc.) and adsorption techniques. The main drawback of the membrane technology is that membrane fouling leads to a limited lifetime. Hence, in any economic viability study, the cost of periodic replacement must be included.

Many conventional treatment methods for dye removal such as ion exchange, coagulation, electroflotation, solvent extraction, filtration, ozonation and biological oxidation are usually inefficient, costly and not adaptable to a broad range of colored wastewaters (21, 34, 48).

Fundamentals

Table 7 Advantages and disadvantages of existing and emerging technologies for dye removal
 (Source: Ref (4, 31, 45, 48, 49) Crini G. (2006), Holkar CR et al. (2016), Anjaneyulu Y et al. (2005), Bhagavathi Pushpa T et al. (2015), Robinson T et al. (2001))

Physical methods	Advantages	Disadvantages
Membrane-filtration process (Established recovery processes)	High potential for recycling hydrolyzed reactive dyes and auxiliaries concurrently decreases BOD ₅ , COD and color Remove all types of dyes/Produce a high-quality treated effluent	Cost of initial investment High pressures/Incapable of treating large volumes Possible fouling of the membrane Formation of additional wastes including starch and water-insoluble dyes such as indigo dye
Adsorption	Effective, low initial expenses, flexible, straightforward design, easy handling and insensitive to toxic contaminants Does not result in the formation of harmful substances	Non-selective for some adsorbents Non-destructive process Generation of waste
Adsorption on activated carbon (Conventional treatment process)	The most effective adsorbent Great capacity Produce a high-quality treated effluent	Non-selective/Ineffective against disperse and vat dyes/ Regeneration is expensive and results in loss of the adsorbent/ Non-destructive process

Fundamentals

Chemical methods	Advantages	Disadvantages
Coagulation-flocculation (Conventional treatment process)	Useful for decolorization of disperse dyes	Low decolorization efficiency for reactive and vat dyes/Does not remove acid and reactive dyes of low-molecular weight
	Simple	Large generation of resultant chemical sludge/Disposal problem
	Economically feasible	The method may occasionally fail to remove the colors from the water because particle flakes do not settle effectively
Advanced oxidation methods (Emerging removal processes)	Pollutant degradation/Easiness of application/Powerful oxidizing agents/Faster rates of oxidation reactions	Possibility of arising a secondary pollution problem because of excessive chemical use
	Using both individually/Synergism (Hybrid AOPs)	Degrading the toxic initial and their by-product chemicals, dyes, pesticides
	Hydroxyl radicals react with most dyes with high-rate reaction constants	Iron sludge generation in Fenton process
	Oxidizing substantial portion of the complex organic and inorganic chemicals found in the textile effluent	Economically unfeasible
	No sludge production/Little or no consumption of chemicals/Efficiency for recalcitrant dyes	Technical constraints
	Useful for breaking down some functional groups including the complex aromatic rings, also efficient in dye chromophores (conjugated double bonds) degradation	High electrical energy demand Consumption of chemical reagents
Chemical oxidation (O ₃ /H ₂ O ₂ ...)	No sludge production and reduction in foul odors in the combination of UV light and H ₂ O ₂ /Less sludge generation in ozonation	Formation of by-products
		Low rate of degradation as equated to the AOPs
		Potential formation of toxic by-products during the ozonation even from biodegradable dyes
		Chemicals are required Cost

Fundamentals

Chemical methods	Advantages	Disadvantages
Chemical oxidation (O ₃ /H ₂ O ₂ ...)	Hybrid techniques have lesser treatment times Rapid and efficient process	Temperature, pH and salts can affect the stability of ozone Continuous monitoring of the textile effluent pH is required for faster ozone decomposition Higher energy cost in hybrid methods

Biological methods	Advantages	Disadvantages
Biological treatments	Often the most economical alternative	Different limitations in application including technical constraints, sensitivity toward diurnal variation and toxicity of some chemicals/ Requires a large land area/Less flexibility in design and operation/ Unable to effectively eliminate color using currently used biodegradation procedures/Many organic dyes are resistant to degradation due to synthetic organic origin as well as complex chemical structures although many of them are degraded/As azo dyes are xenobiotic, they do not totally breakdown
Biodegradation (Conventional treatment process)	Economically attractive Publicly acceptable treatment	Slow process/ Necessary to create an optimal favorable environment/ Maintenance and nutrition requirements
Biomass (Emerging removal process)	Low operating cost/Good efficiency and selectivity/No toxic effect on microorganisms	Slow process/Performance depends on some external factors (pH, salts)
Selective bioadsorbents (Emerging removal process)	Economically attractive Regeneration is not necessary High selectivity	Requires chemical modification Non-destructive process

1.4.3.1 Adsorption

Adsorption has been defined as a phase transfer process that is extensively used in practice for the removal of substances from the fluid phases (gases or liquids). The most common concept defines the adsorption process as an enrichment of chemical species on the surface of a liquid or a solid from a fluid phase. In water treatment, this surface process has been shown as an effective removal method for a multiplicity of solutes. In this process, molecules or ions are removed by adsorption onto solid surfaces from an aqueous solution.

The species that sticks, accumulates or adheres (adsorbed) to the solid surface is known as “adsorbate” and the solid material that provides the surface for adsorbates to be adsorbed is known as an “adsorbent”. Adsorption can be influenced by the nature of the adsorbate and adsorbent, the electrostatic forces between adsorbent and adsorbate, the mass-transfer process, the presence of other species, the atmospheric and experimental conditions (temperature, the concentration of pollutants, pH, the particle size of the adsorbent and contact time).

With modifying the properties of the liquid phase (e.g. pH, concentration, temperature), the adsorbed materials can be transferred back into the liquid phase through release from the surface. Desorption is the term for the reverse process.

At a given temperature, the relationship between the amounts of pollutant adsorbed and that in the water at equilibrium is defined by an “adsorption isotherm”. In other words, adsorption isotherms indicate how adsorption is distributed between the liquid and solid phases when the adsorption process has reached equilibrium. The well-known isotherm models are those of Langmuir and of Freundlich, these explain systematically and scientifically the adsorption efficiency of a pollutant (34, 50-52).

Adsorption is a widely known equilibrium separation process which receives a great deal of attention because of the high efficiency, flexibility, ease of operation, simple design, cost-effectiveness (depending on the type of adsorbent), less requiring modification before application, minimization of biological and/or chemical sludge volumes and high efficiency of detoxifying effluents. Moreover, from health-related and environmental points of view, the benefits of regeneration, recovery and recycling potential as well as not producing harmful substances such as toxic by-products with detrimental impacts makes this method as a prominent technique to remove dyes from aqueous systems (4, 6, 9, 50, 52).

Liquid-phase adsorption (adhesion of atoms, ions or molecules from a liquid to a surface) is one of the most common methods for the removal of pollutants from the wastewater as it can yield a high-quality treated effluent. This method offers an efficient solution for the treatment of contaminated waters, specifically if the sorbent is cost-effective and an additional pretreatment phase is not necessary prior to its application. Adsorption has been proved to be

an efficient and inexpensive physical-chemical treatment method and as an on-site refining system to remove dyes from colored effluents (4, 30, 40, 50, 52).

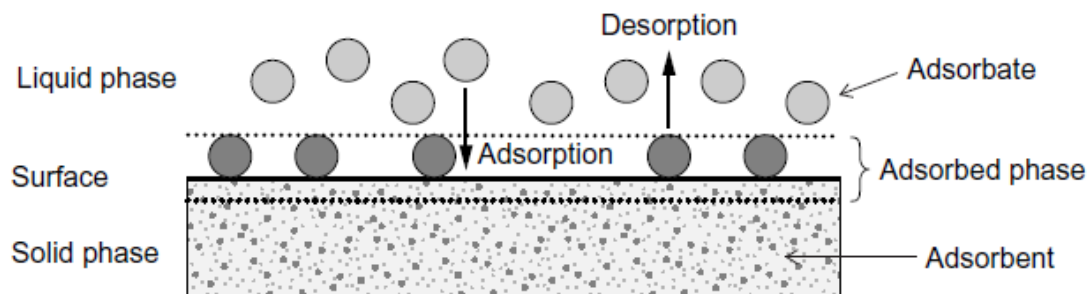


Fig. 18 Basic terms of adsorption

(Source: Ref (50) Worch. (2012))

Adsorption can be classified as chemical adsorption (chemisorption) or physical adsorption (physisorption) based on the adsorption process and the value of the adsorption enthalpy. Physical adsorption originates from Van-der-Waals forces (induction forces, dipole-dipole interactions, dispersion forces), which are quite weak interactions. In the case of physisorption, the adsorption enthalpy is usually less than 50 kJ mol^{-1} . The basis of chemisorption is chemical reactions between the adsorbate and the surface sites of the adsorbent, and the interaction energies, thereby having the magnitude of reaction enthalpies ($> 50 \text{ kJ mol}^{-1}$). It is worth mentioning that the distinction between chemisorption and physisorption is extensively subjective and the boundaries are fluid. A plethora of research has been conducted proving that among all physical-chemical methods adsorption belongs to the more effective methods for dye removal from aqueous effluents (4, 6, 33, 50, 53, 54)

Most of the conventional treatment methods such as chemical precipitation can be effectively and economically applied only if the solute concentrations are relatively high, in contrast, the adsorption technique is cost-effective for low concentrations (55).

It is worth mentioning that the feasibility of using adsorption for the removal of dyes obviates the need to use other expensive conventional treatment methods (6, 8, 56).

1.4.3.2 Natural adsorbents

Vermicompost

Dolomite/Charred dolomite

Bentonite

At present, the combination of biological treatment and adsorption on activated carbon becomes increasingly prevalent for the removal of dyes from colored wastewater. Using activated carbon for the adsorption of dyes is the most well-known technique if it is characterized by a large adsorption capacity, high removal efficiency and high surface area due to its microporous structure; nevertheless, its application as well as that of ion exchange for decolorization is limited as both are expensive and their regeneration is difficult (4).

Recently, there has been an increasing interest in identifying alternatives for activated carbon due to its inefficient removal for vat and disperse dyes and its costly regeneration as well as 10-15% loss of the adsorbent in the regeneration process which limits it for further applications. In fact, the production of char and activated carbon requires high temperatures with high energy consumption and a larger activation process (3, 4).

Several researchers have suggested a variety of non-conventional low-cost adsorbents, including natural materials, industrial wastes/by-products and agricultural wastes/by-products with these materials it was possible to remove dyes from water and/or wastewater. Some natural sorbents such as clay minerals or mineral mixtures such as fuller's earth (attapulgitic and montmorillonite varieties), bentonite (main component: montmorillonite), zeolites, biosorbents (chitosan, peat, biomass), siliceous material (silica beads, alunite, perlite), agricultural wastes namely rice husk, maize cob, corncob, wheat straw, coconut shell, barley husk, wood chips, date pits and orange peel, and industrial waste products, including metal hydroxide sludge, fly ash, red mud, palm oil ash, waste carbon slurries and the like have been reported over the past few years (3, 4, 50, 57).

Recently, growing interest has been shown in the application of clay minerals such as bentonite, kaolinite, diatomite and fuller's earth as adsorbents owing to their considerable adsorption capacity to remove both organic and inorganic compounds. Natural clay minerals have been considered viable candidates due to their high sorption capacity, low-cost and abundance in many regions worldwide. Interactions between clay materials and dyes have been widely studied. The net negative charge of the mineral structure of clays provides them with an ability to adsorb species with a positive charge such as heavy metals cations Cu^{2+} , Zn^{2+} or Cd^{2+} and cationic dyes. Their sorption capacity arises from their high porosity and high surface area. Montmorillonite clay has proved to have one of the highest surface areas and the greatest cation exchange capacity compared to other mineral materials. To specify, high-grade clays such as sepiolite, montmorillonite, kaolin and stevensite demonstrated high adsorption capacities for

basic dyes. Additionally, relatively high adsorption capacities have also been proven for organic dyes in textile wastewater treatment. The inclusion of non-pure clay with enough adsorption capacity and no or little required processing in the water and wastewater treatment technology results in a cleaner textile fabrics production and provides more efficient use of energy and resources (3, 50).

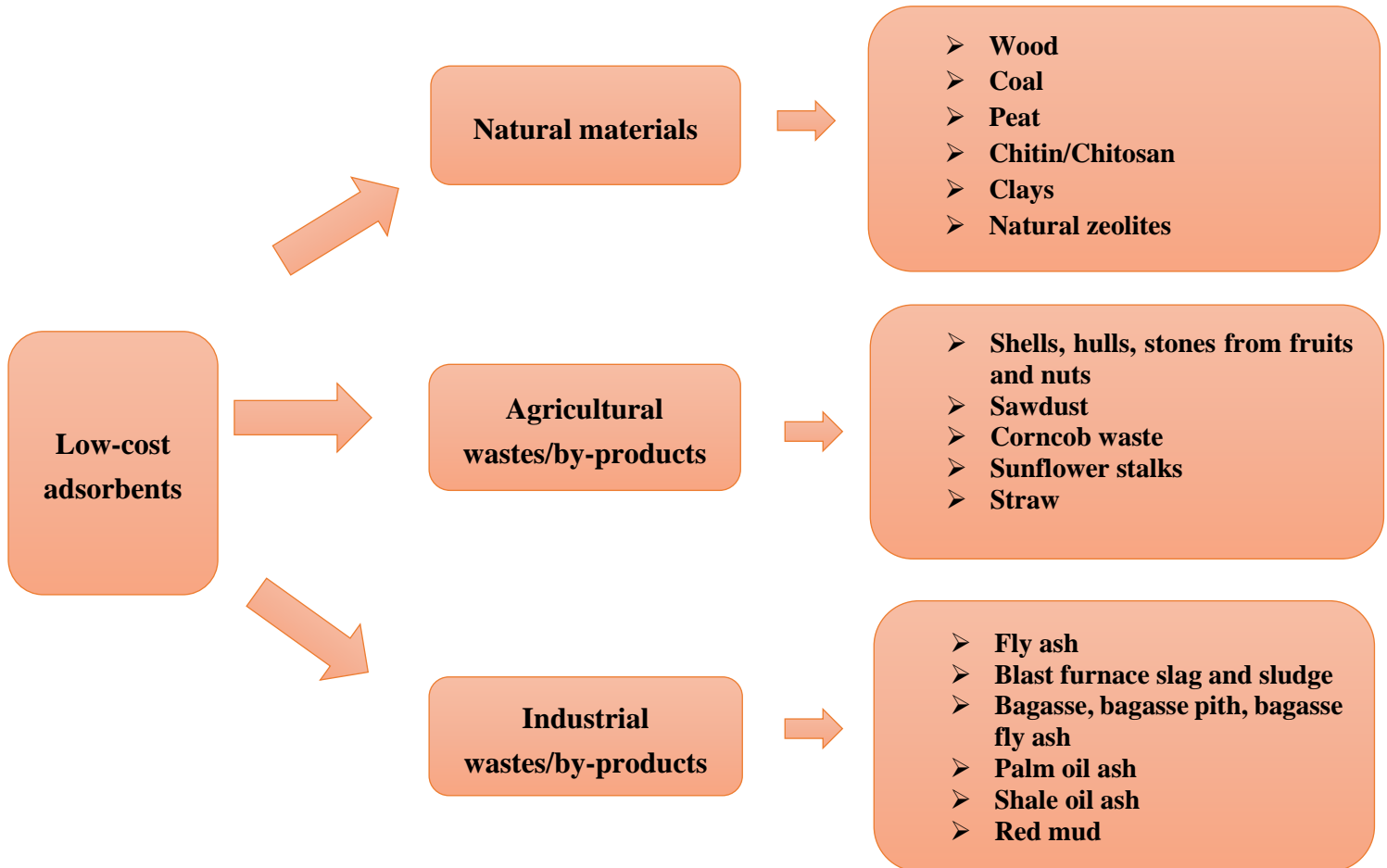


Fig. 19 Selected low-cost adsorbents
(Source: Ref (50) Worch. (2012)).

Vermicompost

In general, humic materials are of high porosity and carry a great number of negative charges resulting in a considerable cationic exchange capacity (CEC). Vermicompost, one of the most prominent humified materials that is used as a biosorbent, has these advantages of high porosity, a high number of negative charges and a remarkable cationic exchange capacity. Its water content is high, next to the organic fraction there are numerous mineral structures, and it is characterized by a wide particle size distribution. The metabolism of soil and organic matter results in the excretion of vermicompost by earthworms. Microorganisms speed up the

humification process in the digestive system of the worms which leads to the production of a highly stable material known as ‘vermicompost’ (58, 59).

Dolomite/Charred dolomite

Dolomite is a prevailing sedimentary mineral that forms rocks with alternate layers of calcite and magnesite which make up its structure. It has the general formula of $AB(CO_3)_2$ where A can be calcium, strontium and/or barium and B can be iron, magnesium, manganese and/or zinc.

The partial calcination (charring) process of dolomite gives a solid product consisting of rigid porous calcite and fine powdered magnesium oxide:



The resultant product is used in the majority of dolomite applications (8, 60-63).

Bentonite

Bentonite is the most prevailing 2:1 clay mineral within the smectite group consisting primarily of montmorillonite (31, 65). Bentonite consists of one Al octahedral sheet placed between two Si tetrahedral sheets. Isomorphous substitution of Al^{3+} for Si^{4+} in the tetrahedral layer and Mg^{2+} for Al^{3+} in the octahedral layer in bentonite translates into permanent negative charges. At the bentonite surface and in the layer between the sheets, the exchangeable cations (Na^+ , Ca^{2+} and the like) counteract the charge imbalance (54, 64, 65).

Regarding using natural mineral materials for treatment of textile wastewater, Titchou et al. (2017) conducted an experiment in a batch system, they applied Moroccan pozzolana for the removal of methylene blue from both a synthetic wastewater and from real textile wastewater (COD = 603 mg L⁻¹) which mainly contained methylene blue. They observed that the maximum adsorption capacity of the adsorbent for methylene blue was 43.86 mg g⁻¹. The removal efficiency for COD was concluded 95%. The treated effluent was colorless and was suitable to be discharged to the environment. However, the high conductivity of the treated effluent required further treatment since it was beyond the specific limit values of discharging into the environment in Morocco. 20 g L⁻¹ adsorbent was used to treat 60 ml of the real textile wastewater (66).

Xia et al. (2020) developed and used a novel *Juncus effusus* (JE)-based adsorbent (*Juncus effusus*: a naturally occurring cellulosic fiber that is prevalent in swamps and marshes) with interconnected channels and a three-dimensional network structure to remove dyes from wastewater. The biodegradable chitosan (CS) was used to chemically modify the JE fiber in

order to increase its capacity to absorb textile dyes. They concluded that the CS-JE fibers demonstrated a high adsorption capacity for three different anionic dyes at a temperature of 296 K: 255.1 mg g⁻¹ for C.I. direct blue 15 (DB₁₅), 452.5 mg g⁻¹ for C.I. reactive red 195 (RR₁₉₅) and 526.3 mg g⁻¹ for C.I. acid yellow 11 (AY₁₁), which are better results than obtained for most of other reported CS-modified adsorbents. Additionally, the results of the continuous filtration experiment showed that the CS-JE cake would be a viable adsorbent with a high flow flux (67).

A study was carried out using alkali-activated local sand for the removal of residual dyes from the actual textile wastewater in India with a COD of 670 mg L⁻¹ and pH 8.3 after receiving coagulation-flocculation treatment. When compared to non-modified sand, which could only remove 40% of the dye molecules even after 20 minutes of adsorption, the color removal efficiency with modified sand was found to be 70% in the first 3 min (2).

A study was carried out on the application of a hybrid process, including adsorption (walnut shell and corncob agricultural wastes were used for the preparation of the activated carbon), electrocoagulation and photo Fenton-like oxidation for the treatment of the pretreated real textile wastewater and to evaluate its further reuse as irrigation water. At the end of the hybrid process, 49% of COD (8-10% by adsorption, 18-20% by electrocoagulation and 24% by photo Fenton-like oxidation), 87% of the TOC removal (40-45% by adsorption, nearly 35% by electrocoagulation and 8% by photo Fenton-like oxidation), around 90% of color (35-40% by adsorption, nearly 50-55% by electrocoagulation and nearly 2% by photo Fenton-like oxidation), 96-98% of turbidity (nearly 5-7% by adsorption, more than 90% by electrocoagulation and 1-2% by photo Fenton-like oxidation) and around 95-97% of suspended solids removal (nearly 20-25% by adsorption, 70% by electrocoagulation and 2-5% by photo Fenton-like) were achieved. Therefore, the methods used were efficient to achieve the irrigation water standards of wastewater with the exception of chemical oxygen demand and salinity (68).

In 2020, Gilpavas et al. conducted an experiment concerning the treatment of real wastewater from a local jeans manufacturing plant in Colombia with a COD of 840 mg L⁻¹, using electrocoagulation and adsorption with activated carbon. The whole EC/AC process resulted in reductions of 96% for color, 60% for TOC (215 to 85 mg L⁻¹), 72% for COD (from 840 to 235 mg L⁻¹) and toxicity was null. Moreover, the biodegradability index (BOD₅/COD) improved from 0.13 to 0.29, indicating that the effluent is suitable for discharge (35).

In another study, two kinds of wastewaters, from dyeing linen and from the residual effluent pool (REP), were subjected to electrocoagulation with the aim to reuse it in the dyeing process. Treatment of dyeing linen wastewater led to a maximum reduction of 24%, 65% and 80% for the COD, turbidity and color, respectively. After the treatment of the residual effluent pool (REP), at pH 7.1 which was within the range of optimum values, the water demonstrated visible changes, reaching removal efficiencies of 86% (56.1 Pt-Co mg L⁻¹), 82% (2.3 NTU) and 59%

(196.3 mg L⁻¹), respectively. The authors drew the conclusion that the treated REP wastewater can be reused in the linen dyeing process. They claimed that using treated water has no impact on the dyed fabric color or quality (69).

1.5 Fixed-bed adsorber design

With respect to the operation mode, adsorption can be usually categorized into static or batch adsorption, and dynamic adsorption. Batch adsorption operates in a system containing a certain amount of adsorbent and a determined volume of adsorbate; whereas, a dynamic system is normally conducted in an open system where the adsorbate solution continuously moves through a column which is filled with the adsorbent.

The column adsorption is the most common alternative for the practical application of the adsorption process. In fact, for the practical application of the adsorption system, fixed-bed column investigations are necessarily required (22, 70, 71). The use of adsorption methods for large-scale wastewater treatment typically requires continuous operations, such as fixed-bed systems, as it enables high volumes of contaminated water to be treated within a shorter period of time. Such units might be simply scaled up from laboratory or pilot units, and the process can be easily monitored and operated. Continuous adsorption techniques using fixed-bed columns are efficient systems for a cyclic adsorption/desorption process as they are related to the concentration gradient. This allows the effective use of the sorbent capacity, and it increases the quality of the effluent.

For preliminary studies, batch adsorption isotherms have commonly been applied. Nonetheless, technical systems usually apply column type processes in practice. In this technique, the behavior of the adsorbent in a fixed-bed column at a constant room temperature is investigated in order to determine the breakthrough point which is required for the column scale-up approach (9, 72).

Adsorption by a granular adsorbent can be carried out by batch, column or fluidized-bed operation. The typical contacting systems are fixed-beds or counter-current moving beds due to their lower labor costs and high usage of the adsorbent adsorption capacity. Fixed beds may use downflow or upflow of the liquid; nevertheless, downflow is more common as the granular adsorbent bed may also act as a filter for suspended solids in addition to the adsorption of organic materials (73).

For any fixed-bed adsorber design, to know about the breakthrough behavior of the compounds to be removed is an important prerequisite. Various mathematical methods are available to predict the breakthrough behavior of adsorbates in a fixed-bed adsorber. The methods can be

categorized into two major groups, the breakthrough curve (BTC) and the scale-up models (50).

1.6 Scale-up approach

Fornwalt and Hutchins (1966) developed a scale-up method for the design of carbon adsorption columns. In this approach, a breakthrough curve from a test column, either laboratory or pilot scale, is required as the primary experimental data (73).

In order to predict the breakthrough behavior in full-scale adsorbers using scale-up techniques, BTCs must first be determined in lab-scale or pilot-scale tests (50).

1.7 Iran water situation

There is a general recognition that Iran is plagued by many environmental problems that have been locally and internationally discussed during the past four decades. Unfortunately, environmental sustainability receives very little heed in Iran. The government of Iran puts its focus on earning money from industries such as oil, car, refinery plants and the mining industry. Regarding the agricultural section, the government has continued to stand firmly in traditional methods of water management and very few changes have been made.

This section provides an overview of the general information about Iran and the current status of water. The following data was extracted word for word from a paper published by Professor Kaveh Madani, an Iranian environmental scientist, educator, and activist, working at the interface of science, policy and society, under the title of “Water management in Iran: what is causing the looming crisis?” (74).

“Iran is located in West Asia, bordering the Caspian Sea in the north, and the Persian Gulf and Sea of Oman in the south. Iran is the second-largest country in the Middle East (after Saudi Arabia) and the 18th largest country in the world with an area of 1,648,195 km². With an estimated population of over 77 million, Iran is the second most populated country in the Middle East (after Egypt) and the 17th most populated country in the world. Iran has a diverse topography. About 90% of Iran’s land area falls within the Iranian Plateau. One-fourth of the country comprises deserts and almost one-fourth of it is arable. The rest is worn to mountains and highlands. Iran enjoys a large climatic variability, mainly affected by the subtropical high-pressure belt. Temperatures can vary significantly (from -20 to +50 °C) throughout the country and during the year. January, with an average temperature range of - 6 to 21 °C, and July, with

an average temperature range of 19 to 39 °C, respectively, are the coldest and hottest months of the year in most parts of the country.

The annual precipitation in total is 413 billion cubic meters (bcm), but it varies greatly across the country, ranging from less than 50 mm in central Iran to about 1,000 mm at the Caspian coast. Average precipitation is about 250 mm per year, less than one-third of the average annual precipitation at the global level. Most of the country receives less than 100 mm of precipitation per year, and 75% of the precipitation of the country falls over only 25% of its area. Also, 75% of the precipitation is offseason, i.e. it falls when not needed by the agricultural sector. Winter is the season with the heaviest precipitation and only a few parts of the country (Caspian Sea coast, northwest and southeast) receive rainfall in summer. The considerable spatial and temporal precipitation variability in Iran has been the main motivation to construct numerous dams and large reservoirs to regulate water flows. Most (65%) of the country is considered to be arid, 20% is semi-arid and the rest has a humid or semi-humid climate. The total renewable freshwater of the country annually and the total returned water from consumption are estimated at 130 and 29 bcm, respectively. The annual renewable water per capita in Iran is estimated to be less than 1,700 m³, well below the global level (7,000 m³) and slightly above the MENA (Middle-East and North Africa) level (1,300 m³).

It is argued that Iran is experiencing significant water challenges that have turned water security to a national priority at the moment. Despite having a more advanced water management system than most Middle Eastern countries, similar to the other countries in the region, Iran is experiencing a serious water crisis. The country is faced with serious challenges in the water sector, including but not limited to rising water demand and shortage, declining groundwater levels, deteriorating water quality, and increasing ecosystem losses. If immediate actions are not taken to address these issues, the situation could become more tragic shortly.

Drying lakes and rivers, declining groundwater resources, land subsidence, water contamination and such like are the modern water-related issues of a nation that was once recognized as the pioneer of sustainable water management for thousands of years. The Iranian water tragedy is not limited to surface waters. Iran is currently among the top groundwater miners in the world. It is estimated that the Iranians have already used most of their groundwater reserves. Declining groundwater tables have also caused significant land subsidence throughout the country. The excess groundwater withdrawal is hard to estimate, but the dramatic drop of the groundwater table (2 m per year in some parts of the country) reflects the extent of the consumption of the non-renewable portion of groundwater. As a result, 277 of the 609 plains in the country are in a critical condition and the declining groundwater table has caused significant land subsidence in many plains throughout the country.

The population in the metropolitan Tehran has surpassed 14 million (18% of the country's population), despite its limited access to water resources. Iran has always suffered from

seriously inefficient agriculture that heavily relies on irrigation and consumes most of the country’s limited water resources. While only 15% of the country’s area is cultivated, this sector is responsible for 92% of the water consumption in Iran (compared to the 7% domestic water use and 1% industrial water use).

The dramatic increase in population of Iran has reduced the per capita renewable freshwater availability. Nevertheless, Iranians continue to use more than 250 L of water per day per person and their daily consumption can exceed 400 L per person in some urban areas like Tehran. This means that Iran’s water usage is twice the world’s standard despite its limited water availability. To satisfy their high-water demand, Iranians are currently using more than 70% of their renewable freshwater resources. This is insufficient to tackle the very high-water stress situation (75)”.

1.8 Textile industry in Iran

Iran's textile industry is one of the country's oldest and largest industries. It employs more than 10% of Iran's manufacturing workforce. In 2003, the textile industry accounted for roughly 6% of the country's overall industrial output (76).

Considering the population growth in Tehran, the volume of industrial wastewater produced is estimated at 15 liters per capita per day in 2021. The total amount of wastewater from textile industries in Tehran has been calculated 18,565 m³ per day. Although many studies seek to reduce the amount of water used in the dyeing process or to use sustainable and environmentally friendly dyeing materials, water resources shortage and environmental pollution remain crucial problems in this dry climate region (77). The most commonly used dyes in the textile industry of Iran are listed in Table 8.

Table 8 Most commonly used dyes in the textile industry of Iran

Cationic dyes	Anionic dyes
Yellow 28	Yellow 160
Yellow 13	Yellow 145
Flavine (Yellow 40)	Yellow 42
Red 18	Red 195
Red 46	Red 198
Violet 16	Orange 122
Blue 41	Orange 16

Cationic dyes	Anionic dyes
Blue 162	Turquoise (Blue 21)
Turquoise (Blue 3)	Blue 19
Navy Blue -	Violet 5
Black -	Black b 5
	Navy (Blue 222)
	Black RL 31

Currently, combined treatment of textile wastewater by biological and physical-chemical processes such as coagulation-flocculation is the most prevailing approach (31, 78). In Iran, many industries use the coagulation-flocculation process as the main method in the treatment of acrylic fiber dyeing effluents. The main drawback of this treatment method is related to producing a large amount of toxic sludge requiring combustion or disposal on lands for a long time. In other words, with respect to coagulation-flocculation processes, the contaminants are merely moved from wastewater to the sludge, which then requires careful disposal. Due to ineffective color removal with using this treatment process, industries need physical-chemical post-treatment technologies to treat their colored effluents. At present some of them still produce wastewater with a high amount of color (5, 30).

1.9 Reuse of the treated wastewater in the textile industry

Most of the studies have investigated the treatment of textile wastewater to comply with the discharge requirements. However, there has been a growing interest in studying on-site reuse of treated textile wastewater in the textile industry to substantially reduce water consumption by reducing the use of fresh and high-quality water (47).

The average consumption of freshwater in the textile industry amounts to 500,000 m³ per year in Europa which is mainly used in textile pre-treatment, dyeing, printing and final finishing. On average, rinsing purposes use 60-90% of the total amount of water consumed. They clearly require many rinsing sequences after each step.

Water reuse, in fact, is not a common practice in the textile industry. Contrarily, water reuse close to the processes has already been used for decades in several industries such as the paper industry, galvanic industry, cooling towers, etc. Besides, the big picture about industrial water reuse is that although there is sufficient legislation at the European level to justify reuse programs and the primary areas of application for municipal wastewater reuse in the European region are agriculture and urban areas, industrial water reuse has a different situation. The extent of water reuse used in the industry varies considerably between different industrial

sectors and is highly dependent on particular situations such as types of processes, the applications of the water, local circumstances such as water availability, the scales and places where water is used (79).

Table 9 shows the general requirements for the recycled wastewater which is necessary to be applied in the textile wet processing and the requirements for high, moderate and low-quality water suggested by the European AquaFit4Use project. This is more detailed than indications telling only one type of process water quality which is the highest needed, i.e. this high standard must be complied with for very sensitive purposes such as for the preparation of dyeing liquors (80, 81).

The European AquaFit4Use project (within the 7th framework program of the European Commission), which presented the important and useful water reuse know-how technologies for most water-consuming sectors in Europe such as chemicals, food, paper and textiles was used as a reference for water reuse requirements.

The feasibility of reusing the treated effluent in the textile industry was assessed considering the respective requirements (see Table 9). Generally, water required for textile processing has to be of better water quality than water which is allowed to be discharged into the environment. High-quality water should be used for dyeing, printing and final rinse baths. Water of moderate quality should be applied for mercerization, desizing, washing-off stages after scouring, dyeing/printing and finishing, and bleaching. For screen washing in print works, washing-down the equipment, paste containers and floors, low-quality water can be used (80).

Table 9 Main requirements in reuse purposes in the textile industry

(Source: Ref (26) Integrated Pollution Prevention and Control, 2003)

Parameter (units)	High quality water ^a	Moderate quality water ^a	Low quality water ^a	General water quality ^b
Color	Non-visible	Non-visible	Non-visible	-
Absorbance at each wavelength (AU)	-	-	-	<0.01
Chemical oxygen demand – COD (mg O ₂ L ⁻¹)	20-50	200	500-2000	60
pH	6.5-7.5	7.0-8.0	6.5-8.0	6.5-8.0
Total hardness (mg CaCO ₃ L ⁻¹)	90	100	100	-
Chloride – Cl ⁻ (mg L ⁻¹)	500	500-2000	3000-4000	-
Total iron – Fe (mg L ⁻¹)	0.1	0.1	0.1	0.1
Total copper – Cu (mg L ⁻¹)	0.005	0.05	0.05	0.05
Total chromium – Cr (mg L ⁻¹)	0.01	0.1	0.1	-
Total aluminum – Al (mg L ⁻¹)	0.01	-	-	-
Total manganese – Mn (mg L ⁻¹)	0.02	-	-	0.05
Total suspended solids (mg L ⁻¹)	-	-	-	10
Turbidity (NTU)	-	-	-	1.0
Conductivity (μS m ⁻¹)	-	-	-	1500

^a Requirements presented in the AquaFit4Use project (AquaFit4Use, 2010) according to water quality for recycled textile wastewater;

^b Requirements proposed by the AquaFit4Use project (AquaFit4Use, 2010) for recycled textile wastewater.

Based on the AquaFit4Use project, the color parameters of the treated water with high, moderate and low quality should comply with reuse requirements for textile wet processing, i.e. non-visible color. Besides, COD of the treated water should be in between 20 and 50 mg L⁻¹ for high-quality water, 200 mg L⁻¹ for medium-quality water and between 500 and 2000 mg L⁻¹ for low-quality water (see Table 9) (47, 79, 80).

After all, one of the key conclusions of the AquaFit4Use project is that water reuse in small and medium textile enterprise requires the development of small-scale, tailor-made and very specific solutions with a combination of techniques (which can also be adopted from the conventional technologies) to produce “fit-for-use” water (79).

Furthermore, German legislation was contemplated as it has specific color limits (spectral absorption coefficient (SAC)) for direct discharge of textile wastewater. Accordingly, the color parameters of the treated water should comply with German discharge limits into water bodies for textile wastewaters, i.e.: 7 m⁻¹ for SAC₄₃₆ nm, 5 m⁻¹ for SAC₅₂₅ nm and 3 m⁻¹ for SAC₆₂₀ nm (78).

1.10 Reuse of the spent adsorbent in the production of LWAs

As the economy grows, the demand for raw materials is gradually rising (82). Therefore, the effective use of raw materials and resources is an important issue facing our societies. On the other hand, the "take-make-use-dispose" linear economy is not a sustainable model and is currently experiencing difficulties. Consequently, the circular economy with the aim of reducing the extraction of raw materials and taking an approach to decrease the generation of waste has been implemented. Subsequently, various industries, including the building industry must adapt to new technologies and materials allowing environmentally sustainable construction. Recently, incorporating waste into building materials such as agricultural residues, wood, paper, ash or slag, plastic, cutting minerals powder or dry sludge from wastewater treatment plants and the like have been investigated by different researchers (83). As the adsorption technology in water treatment has to consider the adsorbent regeneration costs and/or disposal of the concentrate stream, finding a proper waste management method is an outstanding issue that needs addressing (1). The incorporation of the spent adsorbent in materials for construction can be promising to reduce the environmental impacts of the disposal of the generated spent adsorbents.

1.10.1 Lightweight aggregates (LWAs)

After water, aggregate is the second most common consumed raw material. Aggregate industry is considered the leading supplier of raw materials for the construction of buildings, infrastructures, for industry and environmental protection, which gives it a specifically strategic character. Nowadays, LWAs constitute a large part of the total quantity of aggregates planned for use in construction (84). A porous granular material with a loose bulk density qualifies as a lightweight aggregate (85).



Fig. 20 Lightweight aggregate
(Source: <http://leca.asia>).

Raw materials for LWAs can have a natural or artificial origin. LWAs can be generated from natural resources (e.g. pumice, volcanic aggregates), requiring only mechanical treatment or produced through thermal processes in kilns. Igneous materials such as pumice and tuffs, sedimentary materials namely claystone or shale, or very low-grade metamorphic rocks are the most widely used natural materials mostly used for LWAs production (86).

Typically, clay, perlite and vermiculite are appropriate starting materials for the generation of LWAs.

Synthetic aggregates can be defined as ceramic materials produced by thermal treatment of materials with expansive properties such as (i) clay, vermiculite, perlite and shale and (ii) industrial by-products (e.g. slags, sludge, fly ash) (84).

One of the most extensively used types of lightweight aggregates is LWAs generated from expanded clay which is commercially known as “LECA” (lightweight expanded clay aggregate) or generated from coal fly ash referring to as “Lytag”. Pyroplasticity and formation of gas occur at the same time where bloating (expansion) takes place by heating materials to fusion temperature. The technical applications of LWAs are mainly related to high compressive strength and low density (18).

In fact, artificial LWAs are produced by the rapid heating of materials capable of expanding at remarkably high temperatures. The sintering process is aimed at forming a mechanically durable and highly porous structure to satisfy the required standards of the final product (86). In the sintering process, the foaming or bloating phase is of crucial importance. Upon firing,

the bloating phase occurs through the creation of a liquid phase which results in the formation of porosity in the obtained granules. In the absence of the liquid phase, the resulting gases from decomposition of different materials can escape. Normally, industries add some additives which cause foaming or bloating the materials and increase the porosity. In addition to raw material constituents, additives degas (i.e. the foaming or bloating agent degasses results in an increase in porosity) at temperatures between the softening point and the maximum firing temperature, and the resultant gases remain trapped within the glassy structure (84).

The expansion behavior comprises three prerequisites for bloating at a given firing temperature: (1) adequate amount of liquid phase to transform the material body into a viscous (pyroplastic) state; (2) a gaseous emission along with the development of gas bubbles; (3) a liquid phase viscosity appropriate for the gas bubbles entrapment and growth that results in bloating (18). Hydrocarbons, coal and waxes are extensively used as artificial gas-producing materials in the manufacturing process of industrial LWAs (81).

The consumption of artificial LWAs is considerably low compared to that of natural aggregates; however, the properties such as low density, high porosity, acceptable mechanical strength and inert character of LWAs extends its applications in a variety of sectors (87).

In recent years, there has been an increasing interest in utilizing LWAs in different applications due to their various advantages, including higher thermal and acoustic insulation, reduction of dead load, and sound and fire resistance properties. Depending on the chemical and physical properties of LWAs which hinges upon the raw material composition and sintering process, they can be applied in the building industry e.g., manufacturing of lightweight concrete and precast structural units, marine and floating structures, road construction, gardening, insulating and geotechnical applications such as embankments on soft grounds and backfills behind retaining structure, in horticulture applications such as green roofs, and use as a reservoir for fertilizers and irrigating water. Nonetheless, LWAs are widely used in the production of building materials such as concrete blocks, lightweight concrete structures and road construction insulators. The application of LWAs in concrete has the following advantages: (a) reducing the dead load of the concrete due to the lower density of aggregates leading to a lower footing size (b) reducing the beam dimensions and column sizes which leads to the greater space availability (c) obtaining higher thermal insulation due to the porous and sintered core in aggregates (d) improving fire resistance caused by the existence of pores and (e) strengthening the concrete properties as a consequence of the spherical shape of the aggregates (88, 89).

LWAs to be used in concrete must have low water absorption capacity, they should be roughly spherical, hard, porous, with a sintered core and should have an impermeable rough surface to increase the cement-aggregate bond. Enhancement of the properties through thermal insulation and decreases the structural dead load and possibility of the construction of larger buildings with the same foundation size can reduce the CO₂ emissions (87).

At present, the concrete industry is faced with a decreasing supply of natural resources used as raw and construction materials, i.e. aggregates and cement. Therefore, the market for LWAs is expected to grow as the demand for lightweight and thermally insulating concrete rises (85, 88, 89).

A great deal of attention has been paid to develop several types of artificial LWAs and geopolymer binders from various waste streams to resolve the problems. The application of these LWAs in concrete has many other benefits such as management of the depletion of natural resources.

Recently, a great deal of effort has been made to find the best way to use various types of waste materials for the manufacture of LWAs. The main reasons behind these efforts stem from the following points: (i) to minimize the production expenses by replacing natural raw materials by waste materials, and (ii) to re-use waste materials in possible applications instead of bringing them to landfills and paying fees for that. The applicability of various types of waste materials for the production of LWAs has been shown namely for organic (non-toxic) waste, sewage sludge ash, polishing residue, glazing waste, fly ash and waste glass (84, 88-90).

1.10.2 Life cycle assessment and Monte Carlo analysis

Life cycle assessment (LCA) has been known as one of the most extensively used sustainability tools to assess the environmental impacts related to WWTPs, water supply and wastewater management systems (91, 92). Furthermore, LCA methodologies are usually applied to assess waste treatment options to determine a technology with the lowest environmental impact (93). LCA is a standardized and comprehensive procedure using the cradle to grave approach to evaluate the potential environmental impacts of a process, product or activity and it is seen as a useful tool for decision makers. Moreover, LCA can be used to compare, contrast and choose between products, processes or technologies regarding the potential environmental impacts over the course of their life cycle. A comparative LCA requires the same functional unit as the functional unit gives a reference to the level of process performance and time (92, 93).

With reference to ISO 14040 standards, the LCA has four phases including definition of the goal and scope, inventory analysis, impact assessment and interpretation (94). Based on ISO 14040, life cycle inventory (LCI) phase involves the compilation and quantification of inputs and outputs for a product in its life cycle (95). For the life cycle inventory, all the inputs including material and energy and outputs of the system including emissions and waste are listed for the various phases of the life cycle (96). According to ISO 14040, the aim of the life cycle impact assessment (LCIA) phase is to evaluate and understand the significance and

magnitude of the potential environmental impacts for a product system in the life cycle of the product (95).

Different damage categories for studying impact assessment are defined as human health, ecosystems and resources. Different environmental impact categories are included in the LCA such as ozone depletion, global warming, human toxicity, photochemical ozone formation, freshwater aquatic toxicity, eutrophication, acidification, land use and energy consumption (96).

With reference to ISO 14040, in order to conclude and make recommendations based on the evaluations on the findings of either the impact assessment or inventory analysis, life cycle interpretation phase is carried out related to the defined goal and scope (95).

The well-known statistical simulation method of Monte Carlo can be applied to determine the overall uncertainty of the final results; accordingly, to define the significance of the difference between various scenarios with running repeated analysis with random input values to make a probability distribution (96, 97).

Summary of chapter 1

The textile industry uses various sources/raw materials, including fabrics, chemicals such as dyestuffs/pigments and auxiliaries. Dyes can be categorized into different groups depending on the chemical structure and chemical nature. Mainly two types of fibers, including natural and man-made are used in the textile industry. Acrylic (PAC) fibers are synthetic polymer fibers in which the polymer is formed by radical polymerization of acrylonitrile in a solvent or aqueous emulsion. The acrylic (PAC) fibers can be dyed with both cationic and disperse dyes since they comprise anionic groups in their structure. The wet fabric manufacturing industry involves processing operations such as desizing, scouring, mercerizing, bleaching, dyeing, finishing and printing.

In the dyeing process, the color is imparted to fabric or yarn with a dye that can be carried out in a batch or in a continuous/semi-continuous system. Both types of dyeing processes consist of different phases, including preparation of the dye, dyeing, fixation, washing and drying.

The textile industry is one of the main industries that uses water, dyestuffs and other chemicals leading to the generation of a large volume of polluted wastewater which can render the water resources contaminated. The water-polluting substances can increase total dissolved solids (TDS) and COD/BOD₅ of textile wastewater and some of them are carcinogenic, mutagenic and toxic.

The main conventional treatment methods for the removal of pollutants from the textile effluents can be categorized into physical, chemical and biological methods. Different treatment techniques are adsorption, membrane filtration, anodic oxidation (AO), electrochemical and chemical advanced oxidation processes (AOPs/EAOPs), coagulation-flocculation and the application of pure and mixed microbial cultures under anaerobic and/or aerobic conditions.

The adsorption process is an enrichment of chemical species dissolved in a fluid phase on the surface of a solid or a liquid. There has been a growing interest in the application of non-conventional low-cost adsorbents, including natural materials, industrial wastes/by-products, agricultural wastes/by-products in water/wastewater treatment due to high cost of activated carbon production and difficulties in the regeneration process. Using natural clay minerals for water treatment may provide an applicable alternative to adsorbents owing to their abundance in many regions worldwide, high adsorption capacity and low-cost. Fixed-bed column adsorption is widely used for the practical application of the adsorption process. For large-scale wastewater treatment, the adsorption process in continuous operations is used such as fixed-bed systems to determine the breakthrough point which will result in the column scale-up approach.

The Acryl Tab company exclusively dyes polyacrylonitrile fibers (PAN) with cationic dyes for carpet and knitwear production. Like many other textile industries in Iran, they treat the produced wastewater only with coagulation-flocculation as the main treatment process. Thus, due to inefficient color removal a necessary further treatment step is required. As textile industries in Iran have economic problems and cannot afford wastewater treatment with costly activated carbon or AOPs, low-cost adsorbents can be used alternatively.

Different processes in the textile industry use a high volume of water. Thus, the on-site reuse of treated textile wastewater is of interest to many industries. The general requirements for the recycled wastewater which is necessary to be applied in the textile industry and the requirements for high, moderate and low-quality water which was suggested by the European AquaFit4Use project can be used as a reference to assess the quality of the treated water for reuse purposes.

As the adsorption process has to consider regeneration costs and/or disposal of the produced waste, a focus on a proper waste management method is highly important. This can be the incorporation of the generated waste into building materials, including LWAs. The LWAs are produced by the rapid sintering of materials capable of expanding at high temperatures. The sintering process results in forming a highly porous and mechanically durable structure to meet the required standards of the final product.

Life cycle assessment method has been known as one of the most effective sustainability tools for waste and wastewater treatment technologies. It has four different steps including goal and scope, inventory analysis, impact assessment and interpretation. All the stages have been defined in ISO 14040. Monte Carlo simulation method is used for the determination of uncertainty on results.

References (Published papers):

Khalilzadeh Shirazi E, Metzger J.W, Fischer K, Hassani A.H, Design and cost analysis of batch adsorber systems for removal of dyes from contaminated groundwater using natural low-cost adsorbents, *International Journal of Industrial Chemistry*, Vol. 11, 101–110, 2020.

Khalilzadeh Shirazi E, Metzger J.W, Fischer K, Hassani A.H, Simultaneous removal of a cationic and an anionic textile dye from water by a mixed sorbent of vermicompost and Persian charred dolomite, *Chemosphere*, Vol. 234, 618-629, 2019.

Khalilzadeh Shirazi E, Metzger J.W, Fischer K, Hassani A.H, Removal of cationic and anionic dyes from single and binary dye systems with Persian charred dolomite using first-order

derivative spectrophotometer analysis method, *International Journal of Advances in Science Engineering and Technology*, Vol. 6 (4), 2018.

Khalilzadeh Shirazi E, Metzger J.W, Fischer K, Hassani A.H, Removal of textile dyes from single and binary component systems by Persian bentonite and a mixed adsorbent of bentonite/charred dolomite, *Colloids and Surfaces A: Physicochemical and Engineering Aspects*, Vol. 598, 124807, 2020.

2. Materials and Methods

2.1 Material characterization

2.1.1 Adsorbents

Different natural adsorbents, including the local mineral adsorbents Persian charred dolomite and Persian natural bentonite, and biosorbent vermicompost were chosen and studied for their capability to eliminate dyes from dye-contaminated groundwater. Experiments were performed with solutions of individual dyes (single dye solutions), a cationic or an anionic dye, or solutions containing mixtures of both dyes (binary dye solutions).

Vermicompost was obtained from Golbang Yas CO., Tehran, Iran (Fig. 21 a). It was made from dung (bovine manure), sawdust and forest waste. It was sieved (particle size < 2 mm) and the obtained material was dried in a conventional oven at 60 °C for 24 h (Fig. 21 b) (6, 8).



Fig. 21 (a), Vermicompost farm (Golbang Yas CO.) (b), dried vermicompost

Charred, i.e. thermally processed (treated at ca. 800 °C) dolomite (Fig. 22 a, b) was acquired from Iranian Refractories Procurement & Production CO., Tehran, Iran (8). The charring process includes calcination of the raw dolomite in a muffle furnace at a temperature of ca. 800 °C for ca. 4 hours and leads to a porous calcite magnesium oxide structure. Typically, with thermal processing or calcining the dolomite sample at ca. 800 C°, the magnesium carbonate component of the dolomite decomposes completely to magnesium oxide; however, calcium carbonate (calcite) remains unchanged in the sample. This partial decomposition results in changes in the chemical composition and porosity of the sample, particularly, in an increase in specific surface area and pore volume of the dolomite (8, 27, 63).

The product was sieved to a fine powder (particle size 0.074 to 0.149 mm) (8).



Fig. 22 Charred dolomite from Iranian Refractories Procurement & Production CO.

Persian raw bentonite was supplied by Iran Barite Falat CO., Tehran, Iran. 'Standard' clay (Nanoclay, hydrophilic bentonite) was obtained from Sigma-Aldrich Chemie GmbH, Steinheim, Germany (Fig. 23). Natural bentonite was sieved to a fine powder (particle size < 0.044 mm) and was used directly without any further purification. The particle size of the commercial 'standard' bentonite was $\leq 25 \mu\text{m}$ (65).



Fig. 23 Persian natural bentonite and standard bentonite from the Iran Barite Falat CO.

Natural granular bentonite was supplied by Iran mineral products CO. in Iran (Fig. 24). The natural granular bentonite was sieved to a size of 1.7-2.3 mm (8-12 mesh) and was used directly without any further treatment (65).



Fig. 24 Natural granular bentonite from Iran mineral products CO.

2.1.2 Fabric dyes and stock solutions

Basic violet 16 (BV₁₆, C₂₃H₂₉ClN₂, 368.9 g mol⁻¹) and reactive red 195 (RR₁₉₅, C₃₁H₁₉ClN₇Na₅O₁₉S₆, 1168.2 g mol⁻¹) were purchased from Jin-Jiang Chemical Dyestuff CO. Ltd, Hangzhou, China, and Atul CO. Ltd, Gujarat, India, respectively (structural formulae see Fig. 25 a, b). All other chemicals and solvents used were supplied by Merck (Darmstadt, Germany). Dye stock solutions were prepared by dissolving known amounts of BV₁₆ and RR₁₉₅ in groundwater (from Tehran, Hesarak area) and different initial concentrations were obtained from the stock solutions by dilution (dilution range 10-100 mg L⁻¹ for calibration curves, and dilution chosen for the experiments 5-50 mg L⁻¹) (8).

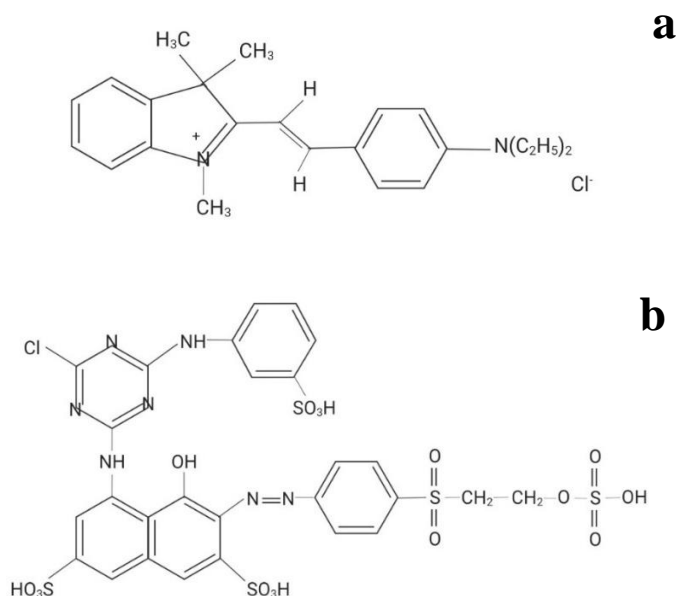


Fig. 25 Structural formulae of (a) basic violet 16 (BV₁₆) and (b) reactive red 195 (RR₁₉₅) (Source: Ref (8, 98, 99) Khalilzadeh Shirazi E et al. (2019))

Table 10 Characteristics of the two fabric dyes basic violet 16, reactive red 195

(Source: Ref (22, 98, 99) Díaz Gómez-Treviño et al. (2007))

Parameters	Basic violet 16	Reactive red 195
Molecular weight (g mol ⁻¹)	368.9 g mol ⁻¹	1168.3 g mol ⁻¹
Class of dye	Methine dye	Single azo dye
Absorption maxima (nm)	548 nm	540 nm
Molecular formula	C ₂₃ H ₂₉ ClN ₂	C ₃₁ H ₁₉ ClN ₇ Na ₅ O ₂₁ S ₆
Industrial application	Textile, leather, preparing carbon paper, stamp pad inks, paints, water tracer fluorescent, as a component of navy blue and black inks for printing, ball-point pens and ink-jet printers, fertilizers, anti-freezes, detergents and leather jackets	Textile industries, cellulose fabric dyeing, also can be used for cotton and viscose fiber printing

The dyes studied were selected among the most commonly used dyes in the textile industry of Iran (see Table 8). The removal of the two selected dyes from single and binary solutions using single and binary adsorbents (mixed sorbents) which are mentioned above has not been studied before (65).

Structural formulae of basic violet 16 (BV₁₆; a) and reactive red 195 (RR₁₉₅; b) (8) are shown in Fig. 25. Characteristics of the two fabric dyes basic violet 16 and reactive red 195 are given in Table 10. RR₁₉₅ has been chosen in this work as an anionic dye surrogate indicator due to its chemical composition and environmental relevance. RR₁₉₅ is a highly water-soluble anionic dye due to the five substituted sulfonic acid functional groups in its structure. The sulfonic groups occupy five separate benzene rings in RR₁₉₅.

BV₁₆ is a cationic dye commonly used for the dyeing of acrylic fibers. It was chosen as a representative of cationic dyes considering its carcinogenicity, neurotoxicity and chronic toxicity towards humans and animals which has been studied before (6, 46, 98, 100).

2.1.3 Textile wastewater from Acryl Tab textile company

The textile wastewater was collected from a wastewater treatment plant (WWTP) at the Acryl Tab company located in Behshahr, in Mazandaran province in the north of Iran.

The WWTP is composed of the following main units: (i) equalization tank (ii) coagulation and flocculation tanks (lime $\text{Ca}(\text{OH})_2$ and FeCl_3 addition) (iii) sedimentation tanks (see Fig. 26). Textile wastewater applied in this study was collected from the sedimentation tank before adding chlorine (see Fig. 27). In the last basin, they usually add chlorine before discharging the treated wastewater into the environment (see Fig. 28).

Characteristics of the raw textile wastewater used for this study are presented in Table 16.



Fig. 26 Wastewater treatment plant in the Acryl Tab company
(photo: E. Khalilzadeh Shirazi)



Fig. 27 Sedimentation basin before adding chlorine in the Acryl Tab company
(photo: E. Khalilzadeh Shirazi)

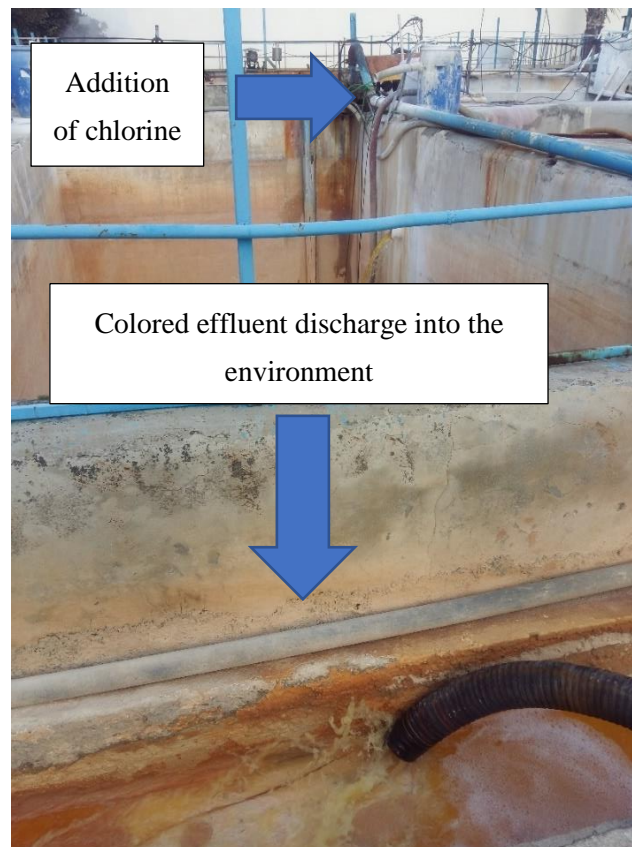


Fig. 28 Addition of chlorine to the treated wastewater in the last basin in the Acryl Tab industry
(photo: E. Khalilzadeh Shirazi)

2.1.4 Characterization of the wastewaters from different baths (dark, medium and pale shade) in cationic exhaust dyeing

In order to characterize wastewaters of different baths (dark, medium and pale shade) in the exhaust dyeing process the parameters pH, temperature, COD, conductivity and color of each wastewater were measured.

2.2 Analytical and experimental methods

An UV-Vis spectrophotometer model HACH LANGE DR-6000, Germany, was used for the absorption measurements. During the adsorption processes, the color was determined by measuring the absorbance at 436, 525 and 620 nm. To specify, two different approaches were used for the color measurement. Firstly, the absorbance at three wavelengths (436, 525 and 620 nm) was determined and then, the spectral absorption coefficient (SAC) or values of indexes of transparency DFZ (Durchsichtfarbzahl) were measured based on Eq. (7) (see chapter 3), with reference to method DIN EN ISO:7887 (100-103). Secondly, the Platinum-Cobalt (Pt-Co) technique was used at a wavelength of 400 nm. The ASTM Designation D1209, "Standard Test Method for Color of Clear Liquids (Platinum-Cobalt Scale)" was used to determine the Platinum-Cobalt color scale (KPt-Co). The Pt-Co method is not comparable to SAC (spectral adsorption coefficient). In 1892, the platinum-cobalt color number (Pt/Co) was developed for the analysis of wastewater. This method is also known as the APHA-Hazen color number. The samples are calorimetrically compared to an acidic solution of potassium hexachloroplatinate (IV) and cobalt (II) chloride, which are given a color number based on their platinum content, which varies from 0 to 500 (mg L^{-1}). Only yellowish coloring is employed with this approach (102, 104). Thus, the results of this method are not really reliable for characterising the color of wastewater.

Derivative spectrophotometry was applied for the simultaneous analysis of BV₁₆ and RR₁₉₅ in binary dye mixtures using a UV-Vis spectrophotometer model HACH DR-5000, Germany, with software Spectragryph version 1.1.2. A shaker model Unimax 1010, Heidolph CO., Germany, and a WiseStir JT-M6 Digital Jar Tester, Daihan CO., China, were used for the batch adsorption experiments. The morphology of the adsorbents was studied with field emission scanning electron microscopy (FESEM) using a model Sigma VP, Zeiss CO., Germany, and a model MIRA3, TESCAN CO., Czech Republic. X-ray diffractograms (XRD) of the adsorbents were determined with Cu K α radiation using a X' Pert Pro, Panalytical CO., England. The chemical composition of the adsorbents was determined with X-ray fluorescence (XRF) using an ED 2000, Oxford CO., England. The specific surface areas, pore volumes and mean pore

diameters of the adsorbents were measured with the Brunauer-Emmett-Teller N₂-BET model BELSORP Mini, Microtrac Bel Corp., Japan. A centrifuge model 3-18KS, Sigma CO., Germany, was used. A peristaltic pump model Pump Drive 5006, Heidolph CO., Germany, was applied for continuous adsorption experiments. TDS (total dissolved solids), pH and conductivity were measured with a portable multimeter model HQ40D, HACH CO., Germany. To measure COD (chemical oxygen demand) and TOC (total organic carbon), a UV-Vis spectrophotometer model HACH LANGE DR-6000, Germany, and for the digestion of the samples, a digestion reactor model DRB200, HACH CO., Germany, were used. Spectroscopic studies were done with a Fourier transform infrared spectrometer (FTIR) model Spectrum Two, Perkin Elmer CO., USA. To analyze heavy metals of the samples, an Inductively Coupled Plasma-atomic emission spectrometer (ICP) AES model Optima 7300DV, PerkinElmer CO., USA, was used. The loss on ignition (LOI) was determined after heating the dry samples at 1000 °C for 1 h in a muffle furnace (12, 69).

The German textile wastewater discharge standard was used for the technical evaluation of the present study. Due to two major reasons: (i) a simple and effective procedure for color measurement based on DIN EN ISO:7887 has been adopted; and (ii) for the actual textile wastewater used in this study, the German legislation determined 7 m⁻¹ for SAC_{436 nm}, 5 m⁻¹ for SAC_{525 nm} and 3 m⁻¹ for SAC_{620 nm} which follows Iranian regulations (75 mg Pt-Co L⁻¹) (78).

2.3 Dye analysis

To analyze dyes in single and binary dye solutions, zero-order spectrophotometry and first-order derivative spectrophotometry were applied, respectively, using a UV-Vis spectrophotometer. For the analysis of single dye solutions (10 mg L⁻¹), zero-order absorption spectra of BV₁₆ and RR₁₉₅ were recorded in the wavelength range between 300 and 700 nm. The pronounced overlap of absorption bands in the spectra of binary dye solutions made it necessary to use derivative spectrophotometry as a viable alternative method to determine the concentrations of BV₁₆ and RR₁₉₅ in parallel (8, 105, 106).

2.3.1 Analysis of BV₁₆ and RR₁₉₅ in single and binary dye solutions using zero-order spectrophotometry

λ_{max} value of BV₁₆ and RR₁₉₅ were 548 nm and 540 nm, respectively. In the VIS spectra of binary solutions containing 10 mg L⁻¹ of each dye, the strong overlapping of the individual dye

absorptions impedes the direct determination of the individual concentrations from the total absorbance of the dye mixture (see Fig. 29) (8).

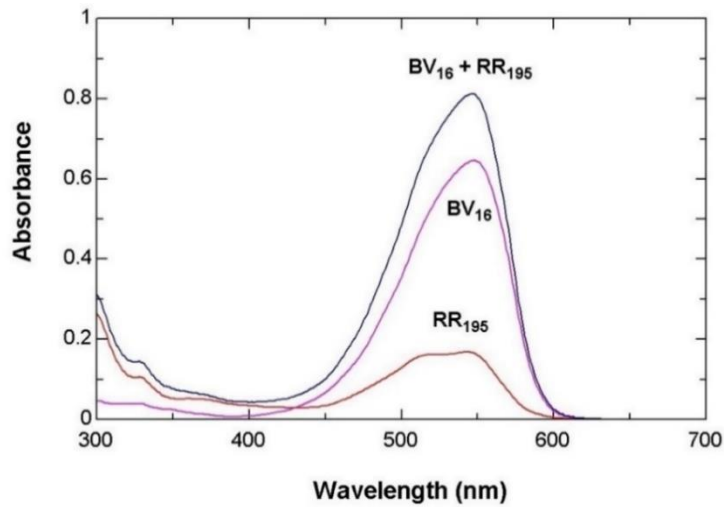


Fig. 29 Zero-order absorption spectra of BV₁₆ (10 mg L⁻¹, λ_{\max} = 548 nm), RR₁₉₅ (10 mg L⁻¹, λ_{\max} = 540 nm), and a 1:1 mixture of both (10 mg L⁻¹ each) (Source: Ref (8) Khalilzadeh Shirazi E et al. (2019))

2.3.2 Simultaneous analysis of BV₁₆ and RR₁₉₅ in binary mixtures using first-order derivative spectrophotometry

A series of measurements of the first-order derivative absorption spectra of BV₁₆ and RR₁₉₅ in binary mixtures led to the result that BV₁₆ can be quantified in the presence of RR₁₉₅ at 580 nm, at which $dA/d\lambda$ of the RR₁₉₅ curve is zero; on the other hand, RR₁₉₅ can be determined in the presence of BV₁₆ at 308 nm, at which the $dA/d\lambda$ of the BV₁₆ curve is zero (see Fig. 30) (8).

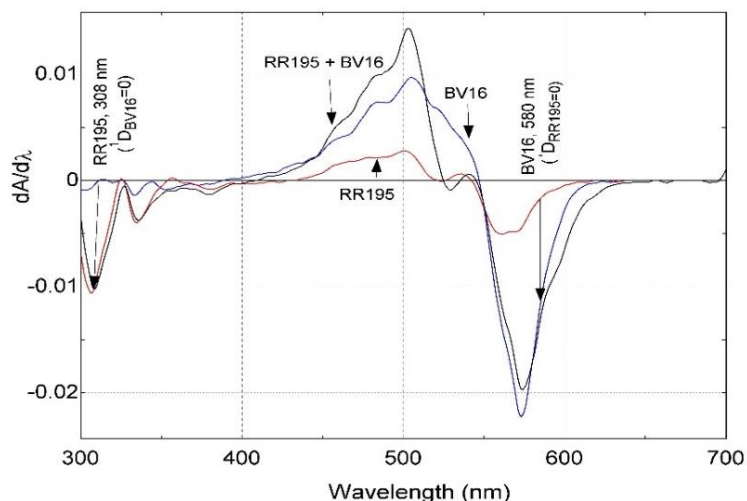


Fig. 30 First-order absorption spectra of BV₁₆ (10 mg L⁻¹), RR₁₉₅ (10 mg L⁻¹), and a 1:1 mixture of both (10 mg L⁻¹ each) (Source: Ref (8) Khalilzadeh Shirazi E et al. (2019))

Calibration curves of the first-order derivative spectra of BV₁₆ and RR₁₉₅ with different proportions were recorded. Fig. 31 provides an example for identical concentrations (1:1; w/w) of dyes in binary solutions using first-order derivative spectrophotometry. Fig. 32 shows a calibration curve with a fixed concentration of BV₁₆ (20 mg L⁻¹) mixed with varying concentrations of RR₁₉₅ (2-10 mg L⁻¹). By contrast, Fig. 33 provides information of a calibration curve with a fixed concentration of RR₁₉₅ (20 mg L⁻¹) mixed with varying concentrations of BV₁₆ (2-10 mg L⁻¹) (8).

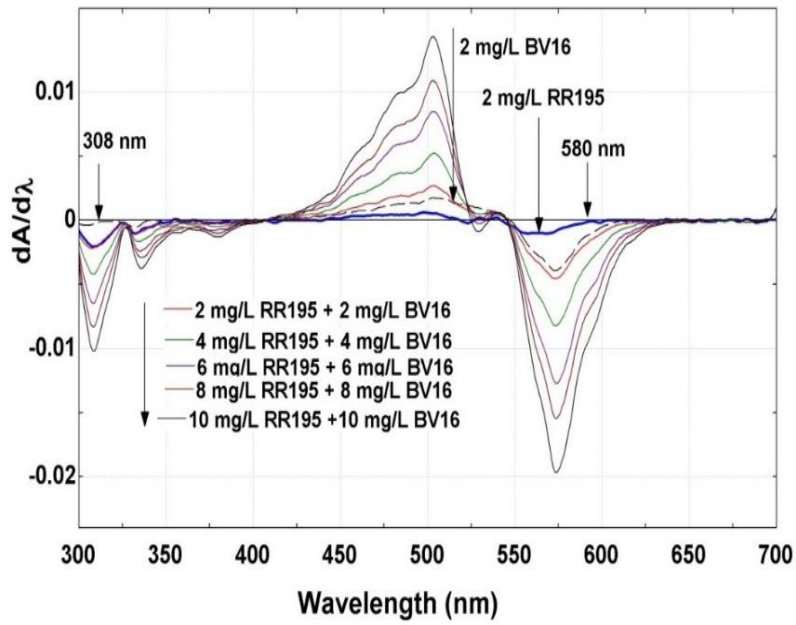


Fig. 31 First-order derivative spectra of 1:1 mixture of BV₁₆ and RR₁₉₅ (each in concentrations of 2, 4, 6, 8 or 10 mg L⁻¹) (Source: Ref (8) Khalilzadeh Shirazi E et al. (2019))

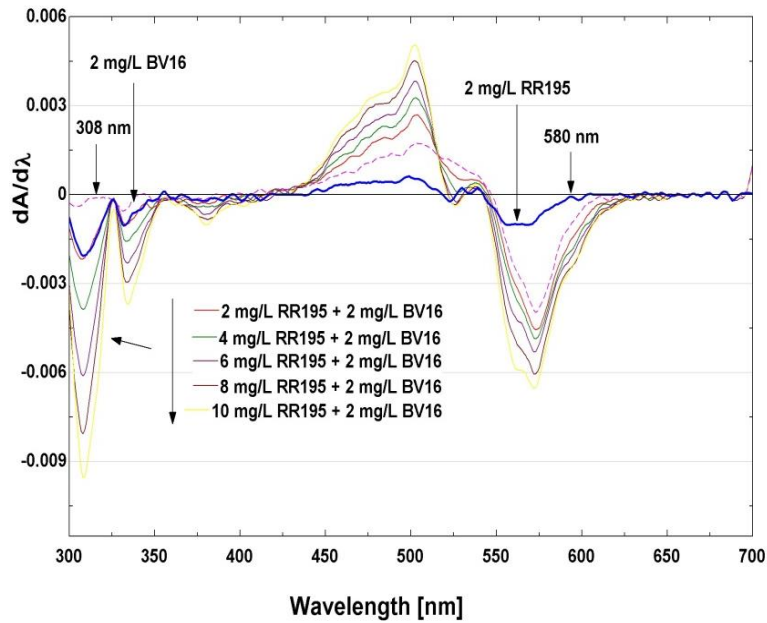


Fig. 32 First-order derivative spectra of mixture of BV₁₆ and RR₁₉₅ (fixed concentration of 2 mg L⁻¹ BV₁₆ and varying concentrations of 2, 4, 6, 8 or 10 mg L⁻¹ RR₁₉₅) (Source: Ref (8) Khalilzadeh Shirazi E et al. (2019))

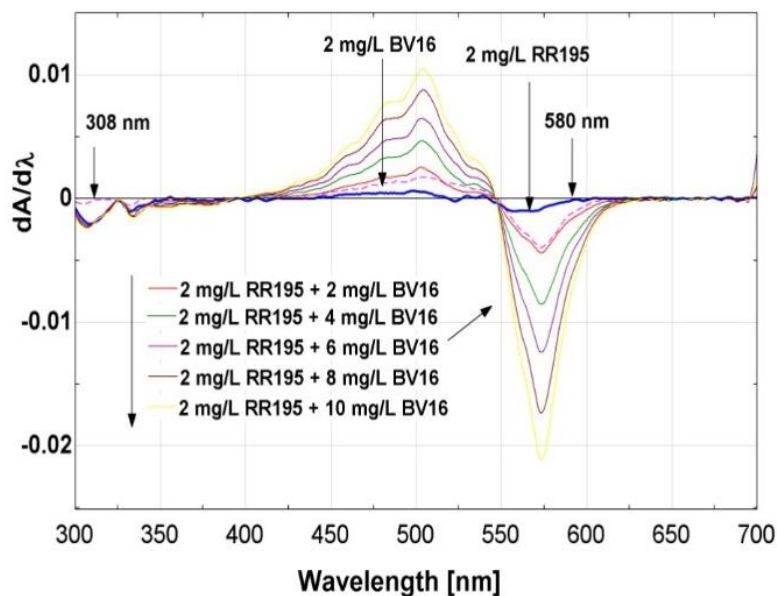


Fig. 33 First-order derivative spectra of mixture of BV₁₆ and RR₁₉₅ (fixed concentration of 2 mg L⁻¹ RR₁₉₅ and varying concentrations of 2, 4, 6, 8, or 10 mg L⁻¹ BV₁₆)

(Source: Ref (8) Khalilzadeh Shirazi E et al. (2019))

2.4 Adsorption in batch experiments

The optimization of the adsorption parameters in single dye experiments is an initial and necessary step to proceed to the next steps of dye adsorption in binary dye experiments and the adsorption of dyes from single and binary solutions using mixed adsorbents.

To study the effect of the mass/volume ratio on the adsorption efficiency, the mass of vermicompost, charred dolomite, natural bentonite and standard bentonite used ranged from 0.3-1.8 g, 0.25-2 g, 0.01-0.035 g and 0.01-0.04 g, respectively, in 0.5 L of solution (at a constant dye concentration of 20 mg L⁻¹, constant impeller speed of 200 rpm, at ambient temperature, at the pH of the dye solution without further pH adjustment). To study the effect of the concentration, the initial concentrations of dye solution lay between 10 and 50 mg L⁻¹ (at a constant mass/volume ratio of 1.5 g vermicompost/0.5 L, at constant mass/volume ratio of 1.5 g charred dolomite/0.5 L, at constant mass/volume ratio of 0.025 g natural bentonite/0.5 L, at constant mass/volume ratio of 0.03 g standard bentonite/0.5 L, a constant impeller speed of 200 rpm, at ambient temperature). To study the effect of the agitation rate, a variable speed motor was used at 100 to 300 rpm (at constant mass/volume ratio of 1.5 g vermicompost/0.5 L, at constant mass/volume ratio of 1.5 g charred dolomite/0.5 L, at constant mass/volume ratio of 0.025 g natural bentonite/0.5 L, at constant mass/volume ratio of 0.03 g standard bentonite/0.5 L, a constant dye concentration of 20 mg L⁻¹, at ambient temperature) (8, 65).

Table 11 Adsorption of dyes on different adsorbents in single dye experiments

(Source: Ref (8, 65) Khalilzadeh Shirazi E et al. (2019), Khalilzadeh Shirazi E et al. (2020))

Adsorbent	Dye	Concentration of adsorbents (in g L ⁻¹)	Contact time (in min)	Stirring speed (rpm)	Capacity (mg g ⁻¹)
CD	RR ₁₉₅	3	80	200	7.3
VC	BV ₁₆	3	40	200	16
NB	BV ₁₆	0.05	10	200	434.8
SB	BV ₁₆	0.06	10	200	500

From an environmental point of view, it is desirable that the water after treatment has a pH close to neutral. Thus, there was no pH adjustment in all experiments. The spectroscopic measurements were performed at $\lambda_{\text{max}} = 540$ nm for RR₁₉₅ and at $\lambda_{\text{max}} = 548$ nm for BV₁₆. At the end of the adsorption experiments, the supernatant was centrifuged for 10 min at 8000 min⁻¹.

For binary dye experiments, solutions of dyes (500 mL) were prepared with one dye at a fixed concentration and the other dye at varying concentrations. For vermicompost, natural bentonite and standard bentonite, one set of tests was carried out at a fixed RR₁₉₅ concentration (20 mg L⁻¹) and varying concentrations (10-50 mg L⁻¹) of BV₁₆. The other set of tests was conducted at a fixed BV₁₆ concentration (20 mg L⁻¹) while selecting various RR₁₉₅ concentrations (5-30 mg L⁻¹). In the case of charred dolomite, the RR₁₉₅ concentration varied in the range of 10-50 mg L⁻¹ at a fixed concentration of BV₁₆ (20 mg L⁻¹) and at a fixed concentration of RR₁₉₅ (20 mg L⁻¹) the concentrations of BV₁₆ were 5-30 mg L⁻¹. For mixed adsorbent experiments, optimized amounts of natural or standard bentonite and charred dolomite were mixed to simultaneously remove the two dyes from binary solutions. Furthermore, different sets of experiments were performed with a mixture of vermicompost and charred dolomite (1:1; w/w) studying binary dye solutions. All experiments were performed at a temperature of 20±1°C under constant stirring (200 rpm) and without pH adjustment.

To evaluate the efficiency of the granular bentonite for the removal of color and COD from the real textile effluent, batch experiments were conducted. The influence of the experimental parameters of mass/volume ratio and contact time on the removal efficiency of granular bentonite for color and COD was studied. To study the color removal of the wastewater, SAC_{436 nm}, SAC_{525 nm} and SAC_{620 nm} were measured.

To study the effect of the mass/volume ratio on the removal of color at different wavelengths of 436, 525 and 620 nm, the mass of granular bentonite used ranged from 0.3-1 g, in 0.1 L of wastewater in 250 mL glass flasks. Samples were taken from the solutions at predetermined time intervals in order to study the isotherm and kinetics of the adsorption process. At the end of the adsorption experiments, the supernatants were centrifuged for 10 min at 8000 min⁻¹. All

the experiments were performed at an ambient temperature of $20\pm 1^\circ\text{C}$ on a shaker under constant stirring at 250 rpm and at the original pH of the wastewater, without further pH adjustment (8, 65).



Fig. 34 Batch experiments using granular bentonite for the treatment of real textile wastewater (Laboratory of Water and Wastewater Treatment at Azad University in Iran)

2.4.1 Equilibrium isotherms

The adsorption isotherms which are used to describe the equilibrium relationship between the adsorbent and adsorbate are of crucial importance in designing the adsorption systems. The Langmuir and Freundlich isotherms are widely used to describe the adsorption of dissolved pollutants. The isotherm models of Langmuir and Freundlich describe the non-linear equilibrium between a compound adsorbed and in solution at a constant temperature. The Langmuir model explains the monolayer adsorption on homogenous surfaces (8, 65).

The non-linearized form of the Langmuir isotherm equation is given by Eq. (1):

$$q_e = \frac{q_{\max} K_L C_e}{1 + K_L C_e} \quad (1)$$

where q_e (in mg g^{-1}) is the amount of adsorbate on the adsorbent at equilibrium, q_{\max} (in mg g^{-1}) is the monolayer maximum adsorption capacity, K_L (L mg^{-1}) is the Langmuir constant related to the adsorption energy and C_e (in mg L^{-1}) is the concentration of the sorbate in solution at equilibrium (65, 106).

The Freundlich adsorption isotherm yields essential information regarding the adsorption on heterogeneous surfaces through a multilayer adsorption mechanism.

The Freundlich isotherm is described by Eq. (2):

$$q_e = K_F C_e^{1/n} \quad (2)$$

where q_e (in mg g^{-1}) is the amount of dye adsorbed per unit mass of adsorbent, C_e (in mg L^{-1}) is the equilibrium concentration of the dye in the solution, K_F (in $(\text{mg/g})(\text{L/mg})^{1/n}$) is the equilibrium constant indicative of the adsorption capacity and n is the adsorption equilibrium constant which is a measure of the intensity of the adsorption (22, 61, 65, 106).

The concentrations of the unadsorbed dye in all tests were calculated from the Beer Lambert plot with the percentage of the dye adsorbed, using Eq. (3):

$$R (\%) = \frac{C_0 - C_t}{C_0} \times 100 \quad (3)$$

where R is the percentage of dye adsorbed by adsorbent, C_0 (in mg L^{-1}) is the initial concentration of dye molecules and C_t (in mg L^{-1}) is the concentration of dye molecules at time t . At equilibrium, dye uptake by adsorbents is determined according to Eq. (4) (8, 23, 65, 107-109).

$$q = \frac{V(C_i - C_e)}{M} \quad (4)$$

2.4.2 Adsorption kinetics

The changes of the adsorbate adsorption versus time are normally assessed to study the rate of removal using a pseudo-first-order kinetic and pseudo-second-order model as described in Eq. (5) and (6), respectively (8, 22).

Physical and/or chemical characteristics of the adsorbents play a pivotal role in the kinetics of the adsorption. Furthermore, the adsorbates effect on the adsorption mechanism (65, 110).

The equation for the pseudo-first-order kinetics (Lagergren) is given by:

$$q_t = q_e (1 - e^{-k_1 t}) \quad (5)$$

where q_e and q_t (in mg g^{-1}) are the amounts of dye adsorbed at equilibrium and at time t (in min), respectively, and k_1 (in g mg min^{-1}) is the rate constant.

This model equation for pseudo-second-order kinetics can be written as follows:

$$q_t = \frac{q_e^2 k_2 t}{1 + q_e k_2 t} \quad (6)$$

where k_2 (in g mg min^{-1}) is the pseudo-second-order rate constant and q_e (in mg g^{-1}) is the adsorption capacity at equilibrium and q_t (in mg g^{-1}) is the adsorption capacity at any time t (in min) (8, 106-111).

2.5 Fixed-bed column adsorption experiments

The pilot-scale experimental set-up consisted of a granular bentonite fixed-bed column, a tank containing real textile wastewater and a peristaltic pump. The cylindrical plexiglass column had a diameter of 5 cm, and a height of 100 cm. The particle size of the granular bentonite was 1.7 - 2.3 mm (8-12 mesh), the bed heights were 5, 10 and 20 cm. The colored real textile wastewater was pumped to the top of the column (down-flow stream) at flow rates of 5, 10 and 20 ml min^{-1} with a peristaltic pump (Heidolph pump drive 5006). A layer of glass beads (2 cm) was placed at the end of the column to prevent the adsorbent particles from exiting the column. The samples of the treated effluent were collected at different intervals (every 30 min in the first two hours, and then, at 60 min intervals for the rest of the experiment) and were analyzed for the residual color concentration in the effluents. The color was measured by a UV-Vis spectrophotometer (HACH-LANGE DR6000) at three peak absorption wavelengths of 436, 525 and 620 nm. Before the analysis, samples were filtered through 45 μm filters to remove the fibers and suspended matter (112).



Fig. 35 Treatment of acrylic fiber dyeing wastewater using natural granular bentonite in a fixed-bed continuous system (Laboratory of Water and Wastewater Treatment at Azad University in Iran)

Measurement of color was carried out based on the single-wavelength method with a HACH-LANGE DR6000. The color intensity was then presented as a spectral absorption coefficient (SAC), which is defined by the Eq. (7).

$$\text{SAC}(\lambda) = \frac{A(\lambda) \times 1000}{D} \quad (7)$$

where $A(\lambda)$ is spectral absorbance at a given wavelength λ and D is the cell depth in mm (10 mm or 1 cm) (102, 112).

The effectiveness of the adsorbent granular bentonite was tested via the ability to remove color and COD in the fixed-bed reactor.

The normalized effluent color intensity C_t/C_0 (in mg L^{-1}) of the effluent versus time (t , in min) and/or throughput volume (in L) was plotted to create breakthrough curves where C_t (in mg L^{-1}) is the effluent color concentration, C_0 (in mg L^{-1}) is the influent color concentration and t is the time (in min). All the tests were conducted at room temperature ($25 \pm 2^\circ\text{C}$).

The bed volumes were obtained as follows:

$$BV = \frac{V_F}{V_R} = \frac{Q_F t}{V_R} \quad (8)$$

where V_F (in L) is the total water volume passing through the column during the adsorption process, V_R (in L) is the fixed-bed volume of the adsorbent, Q_F (in $L \text{ min}^{-1}$) is the feed flow rate in the fixed-bed and t (in min) is the service time (9, 113).

2.5.1 Effect of various operating parameters

The influence of the various operating parameters such as bed height and volumetric flow rate on the removal of color in a fixed-bed adsorption by the natural granular bentonite was studied and the breakthrough curves are shown in Figs. 70-75.

2.5.1.1 Effect of feed flow rate

Since the flow rate controls the contact time between the solute and the adsorbent surface, is of crucial importance for an optimized operation of the column.

The effect of the flow rate on the breakthrough curves was studied using flow rates of 5, 10 and 20 mL min^{-1} . In all the experiments, the wastewater passed a column with 100 cm in height.

2.5.1.2 Effect of bed height

To study the effect of bed height on the removal efficiency of the color using a fixed-bed adsorption column, different bed heights of 5, 10 and 20 cm were studied (9, 114).

2.5.1.3 Analysis of fixed-bed adsorption

The treated effluent volume V_t (in mL) was determined using the following equation:

$$V_t = Q t_e \quad (9)$$

where Q (in mL min^{-1}) is the volumetric flow rate and t_e (in min) is the time at exhaustion.

For a given inlet concentration of feed flow rate, the maximum column capacity q_c (in mg) can be calculated from the area above the breakthrough curve. Thus, the maximum column capacity will be obtained from the area under the curve of the concentration adsorbed versus time, which was measured by integrating the C_{ad} (in mg L^{-1}) versus t (in min) plot using the following equation:

$$q_c = \frac{QA}{1000} = \frac{Q}{1000} \int_{t=0}^{t=t_{\text{total}}} C_{\text{ads}} dt \quad (10)$$

C_{ad} used in the above equation can be calculated from the difference between influent and effluent dye concentrations as shown below in the following equation:

$$C_{\text{ads}} = C_i - C_e \quad (11)$$

where C_{ad} , C_i , C_e and Q are the concentrations (in mg L^{-1}) of the adsorbed dye, of the influent dye, and the effluent dye, respectively, t_{total} is the total flow time (in min), and Q is the volumetric flow rate (in L min^{-1}).

2.6 Scale-up approach

The bed volume (BV) of the design column can be calculated from the equation below:

$$BV = \frac{Q}{Q_b} \quad (12)$$

where Q (in $\text{m}^3 \text{d}^{-1}$) or (in L h^{-1}) is the design liquid flow rate, Q_b (in BV h^{-1}) is obtained from the breakthrough curve from an experimental pilot column and BV is the bed volume of the design column.

For the design column, the mass or weight of the adsorbent, M (in kg), is calculated by:

$$M = (BV)(\rho_s) \quad (13)$$

where ρ_s (in kg m^3) is the bulk density of the adsorbent and BV is the bed volume of the design column.

The breakthrough volume, V_B (in L) (for the allowable effluent solute concentration), can be determined from the breakthrough curve for the laboratory - or pilot-scale column. Then, the volume of the liquid treated per unit mass of adsorbent V'_B (in L kg^{-1}) is calculated by:

$$V'_B = \frac{V_B}{M} \quad (14)$$

where M (in kg) is the mass of the adsorbent and V_B (in L) is the breakthrough volume in the design column.

For the design column, the mass of the adsorbent exhausted per hour, M_t (in kg h^{-1}), is calculated from:

$$M_t = \frac{Q}{V'_B} \quad (15)$$

where Q (in $\text{m}^3 \text{L}^{-1}$) is the design liquid flow rate and V'_B (in L kg^{-1}) is the volume of the liquid treated per unit mass of adsorbent.

The breakthrough time T (in h or d) in the design column is as follows:

$$T = \frac{M}{M_t} \quad (16)$$

where M (in kg) is the mass of the adsorbent in the design column and M_t (in kg h^{-1}) is the mass of the adsorbent exhausted per hour in the design column.

For the design column, the breakthrough volume, V_B (in m^3) is computed from the equation below:

$$V_B = QT \quad (17)$$

where Q (in $\text{m}^3 \text{L}^{-1}$) is the design liquid flow rate and T (in d or h) is the breakthrough time in the design column (73).

2.7 Reuse of the spent adsorbent in the production of LWAs

2.7.1 Production process in the LECA company

The LECA company uses natural clay (Fig. 36) as a raw material to produce lightweight expanded clay aggregate (LECA).



Fig. 36 Natural clay deposit in the LECA CO. in Iran
(photo: E. Khalilzadeh Shirazi)

The production process used to obtain LWAs as LECA is composed of three steps: mixing process, thermal treatment and expansion process.

The raw clay soil is finely ground in the manufacturing process. The unfired “green” granules are formed by extrusion or granulation by adding sufficient water (Fig. 37). The material burns and expands with the aid of an additive called “Mazut” (expansion process). In other words, after agglomeration, the ‘green’ granules are dried and then sintered in which the sintering temperatures in the factory are normally between 1100 °C and 1250 °C (Fig. 38). In the sintering process, gas generation and gas retention occur simultaneously for the clay-derived LWAs within the temperature profile.



Fig. 37 Green granules made of the spent adsorbent, water and additive (quality control laboratory at LECA CO.) (photo: E. Khalilzadeh Shirazi)



Fig. 38 (a, b) Thermal treatment of green granules in a muffle furnace (quality control laboratory at LECA CO.) (photo: E. Khalilzadeh Shirazi)

The manufacturing processing steps of the LECA product include:

- 1- Extraction
- 2- Transportation
- 3- Box feeder
- 4- Separation of iron
- 5- Edge mill
- 6- Adding water in edge mill
- 7- Pugmill (mixing/homogenization, and in some cases adding water and special additives)
- 8- Roller
- 9- Drying and nodulation in drying furnace
10. Burning
11. Satellite (Rotating cooler)

The thermal treatment during LECA production at LECA CO. (temperature profile see Fig. 39) includes:

- 1- Drying: 0 to 120 °C and afterwards 120 to 600 °C
- 2- Burning: 600 to 1100-1250 °C = clay sintering
- 3- Cooling: 1250 °C to 100-105 °C

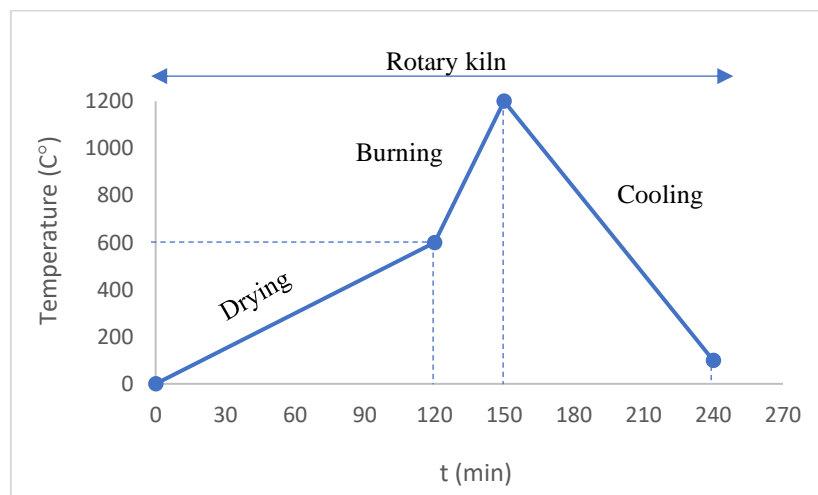


Fig. 39 The temperature profile of the LECA production process at LECA CO.



Fig. 40 Installations for heat treatment of the green granules in different phases of drying, burning and cooling at the LECA CO. (photo: E. Khalilzadeh Shirazi)

2.7.2 Preparation and characterization of LWAs

The methodological framework followed in this work to prepare and sinter the LWAs was based on the quality control method of the laboratory of the LECA industrial plant that manufactures commercial LWAs from natural clay.

The “control” LWAs from expanded clay were made with natural raw clay based on the procedure described below. A series of samples were produced by incorporating a certain percentage of the spent bentonite, and another series of LWAs were manufactured solely with the spent bentonite.

The raw granular bentonite and the spent granular bentonite were ground in a ball mill separately to make them ready for producing LWAs. Also, the raw material (natural clay) of the LECA CO. was blended with different proportions of the raw granular bentonite and of the spent granular bentonite (10, 20, 30 and 40 wt.%). After adding water (to obtain enough plasticity, consistency and workability) and an expanding agent (1% Mazut), the mixtures were carefully homogenized, granules with a diameter of about 16 mm were formed and dried in an oven for one hour at a temperature of 150 °C. Afterward, the generated granules were heated to a temperature of 1140 °C (sintering) in a muffle furnace for 4 minutes to obtain a glassy material, which then was cooled.

Compressive strength, water absorption and density of the generated expanded granules were determined.

In order to determine and assess the suitability of a material for bloating, the percentages of SiO_2 and the fluxing elements ($\Sigma\text{Flux} = \text{K}_2\text{O} + \text{Na}_2\text{O} + \text{CaO} + \text{MgO} + \text{FeO} + \text{Fe}_2\text{O}_3$) were calculated. The $\text{SiO}_2/\Sigma\text{Flux}$ ratio has to be ≥ 2 . This is essential for the generation of a proper viscosity during the aggregate firing, an indication of the proper chemical characteristics to expand if gases are developed during firing (20).

2.7.3 Life cycle assessment (LCA) and Monte Carlo analysis for comparing textile wastewater treatment with bentonite and activated carbon

In this study, LCA and Monte Carlo simulation methods were performed to evaluate and compare which material, which included the natural granular Persian bentonite and activated carbon as the reference adsorbent, is preferable from the environmental and economic point of view for the decolorization of the pretreated acrylic fiber dyeing wastewater at the case study company in Iran.

The inventory and the impact calculations were performed on SimaPro developer 9.0.0.48 software, and the database Ecoinvent 3 was used. For the life cycle inventory analysis, the experimental data was obtained directly from the company, the laboratory and SimaPro to ensure the high accuracy and sensitivity of the obtained results. Impact evaluations were made using the ReCiPe 1.10 calculation method for 3 endpoint damage categories. The endpoint damage categories were considered human health, resources and ecosystem. The functional unit selected 1 m^3 of the textile wastewater.

Due to the high variety of specific surface areas of activated carbon products which can be ascribed to their different chemical and physical characterization, uncertainty analysis by Monte Carlo was used to predict the required amount of activated carbon for the treatment of a certain volume of textile wastewater (1 m^3) at the studied industry. The estimation of required activated carbon was carried out in relation to the obtained amount of bentonite for the treatment of the colored wastewater from the pilot-scale experiments.

First, a certain range of specific surface area values related to different activated carbon products investigated in the literature was analyzed in oracle crystal ball to build a distribution model and to run Monte Carlo simulations.

Regarding the scope of LCA for textile wastewater treatment in this investigation, only different disposal scenarios were assessed from an environmental perspective for the reason that the beforehand pretreatment processes at WWTP of the studied company were the same. The boundary definition of this LCA for wastewater treatment involves the following scenarios:

- 1) spent bentonite landfilling,

- 2) spent activated carbon landfilling,
- 3) regeneration of the spent activated carbon,
- 4) reusing the spent bentonite in lightweight aggregate (LWAs) at LECA company.

In the scenario of "spent activated carbon landfilling", the required amount of granular activated carbon for the treatment of 1 m³ colored pretreated wastewater was considered.

The scenario of "spent bentonite landfilling" includes the extraction of a specific amount of granular bentonite from the mine which was concluded for the treatment of 1 m³ colored wastewater.

In the scenario of "regeneration of the spent activated carbon", heat and electricity needed for the regeneration of the spent activated carbon were considered. According to the literature, the heat (800-900 °C) required for the regeneration of AC is the same as the temperature needed to produce AC (115-119).

Therefore, the relevant heat, electricity and industrial furnace production processes were added to this scenario which was extracted from the original AC production process in SimaPro. All the values related to heat and electricity were analysed in crystal ball with Monte Carlo analysis method and the concluded mean values were added to this scenario for conducting the uncertainty analysis with their related standard deviation. The material and energy requirements of producing and regenerating GAC and the environmental burdens of those material and energy inputs (coal, electricity, steam, etc.) have been obtained from the Ecoinvent database.

In the scenario of "reusing the spent bentonite in LECA", transportation of the spent bentonite from Acryl Tab CO. (wastewater treatment plant) to the LECA company should be added. LCA of the spent bentonite can be explained in this way that LECA CO. provides bentonite from the mine, on the way to the LECA factory, bentonite will be delivered to Acryl Tab for wastewater decolorization and then the spent adsorbent will be transported to the LECA factory for lightweight aggregate (LWAs) production. The cost and environmental burden related to the transportation of the waste material will be paid by the LECA Co.

Summary of chapter 2

Different natural materials, including local mineral adsorbents of Persian charred (i.e. treated at 800 °C) dolomite, Persian natural bentonite and a biosorbent of vermicompost were studied for their adsorption capacity for dye removal from dye-contaminated groundwater containing a cationic and an anionic dye in single and binary dye solutions. The dyes studied were selected among the most widely used dyes in the textile industry of Iran, including basic violet 16 and reactive red 195. Specifically, BV₁₆ is commonly used for the dyeing of acrylic fibers. Granular bentonite, a natural local mineral material from a mine in Iran, was used to study the decolorization of real acrylic fiber dyeing wastewater collected from the wastewater treatment plant (WWTP) at the Acryl Tab company located in Behshahr. Characterization of the wastewaters from different baths (dark, medium and pale shade) in cationic exhaust dyeing was carried out in terms of pH, temperature, COD, conductivity and color.

Different analytical instruments and experimental methods were used for the characterization of adsorbents, the raw and treated wastewater and for the absorption measurements in batch and fixed-bed column adsorption studies.

The optimization of the adsorption parameters in single-dye experiments, including the mass/volume ratio, the effect of the dye concentration, the agitation rate and the contact time was carried out to proceed to the next steps of dyes adsorption in binary dye experiments and the adsorption of dyes from single and binary solutions using mixed adsorbents.

In the absorption spectra of the two dyes studied the absorption bands severely overlap. To determine the concentration of the individual dyes in the binary dye experiments, a method based on first-order derivative spectrophotometry was developed and applied. The results showed that the concentration of each dye can be precisely and effectively quantified by using this method.

For experiments with a mixture of two adsorbents, different sets of experiments were conducted. A mixture of vermicompost and charred dolomite (1:1; w/w) was used in experiments with binary dye solutions. A mixture with optimized amounts of natural or standard bentonite and charred dolomite was used to remove two dyes from the binary solutions simultaneously.

For the removal of color and COD from “real” textile effluent, batch experiments with granular bentonite were performed. The influence of the experimental parameters of mass/volume ratio and contact time on the removal efficiency of granular bentonite for color using the parameters SAC_{436 nm}, SAC_{525 nm} and SAC_{620 nm}, and for COD was studied.

The adsorption isotherm models of Langmuir and Freundlich were used to describe the equilibrium relationship between the adsorbents and adsorbates to describe the adsorption of pollutants. Pseudo-first- and pseudo-second-order kinetic models were used to study the rate of dye removal.

For fixed-bed adsorption studies, several column tests were carried out and the effect of various operating parameters such as bed height and volumetric flow rate on the fixed-bed adsorption of color by the natural granular bentonite was studied. The breakthrough curves from the pilot-scale experiments (the set-up consisted of a granular bentonite fixed-bed column with a diameter of 5 cm and a height of 100 cm, a tank containing real textile wastewater and a peristaltic pump) were studied to provide the principal information for the scale-up approach.

As a solution for what to do with the spent adsorbent, green granules made of the spent adsorbent, water and additive were made, dried and sintered in a muffle furnace. Compressive strength, water absorption and density of the generated expanded granules were measured.

To assess the suitability of the spent material for bloating the percentages of SiO_2 and the fluxing elements ($\Sigma\text{Flux} = \text{K}_2\text{O} + \text{Na}_2\text{O} + \text{CaO} + \text{MgO} + \text{FeO} + \text{Fe}_2\text{O}_3$) were calculated. The $\text{SiO}_2/\Sigma\text{Flux}$ ratio necessary should be ≥ 2 .

The Monte Carlo analysis method was used to estimate the required amount of activated carbon for the decolorization of the pretreated acrylic fiber dyeing wastewater in the Acryl Tab company in relation to the obtained amount of bentonite at pilot-scale experiments. Different disposal scenarios for textile wastewater treatment using activated carbon and bentonite were defined and compared from the economic and environmental points of view with using LCA and Monte Carlo analysis method.

References (Published papers):

Khalilzadeh Shirazi E, Metzger J.W, Fischer K, Hassani A.H, Design and cost analysis of batch adsorber systems for removal of dyes from contaminated groundwater using natural low-cost adsorbents, *International Journal of Industrial Chemistry*, Vol. 11, 101–110, 2020.

Khalilzadeh Shirazi E, Metzger J.W, Fischer K, Hassani A.H, Simultaneous removal of a cationic and an anionic textile dye from water by a mixed sorbent of vermicompost and Persian charred dolomite, *Chemosphere*, Vol. 234, 618-629, 2019.

Khalilzadeh Shirazi E, Metzger J.W, Fischer K, Hassani A.H, Removal of cationic and anionic dyes from single and binary dye systems with Persian charred dolomite using first-order derivative spectrophotometer analysis method, International Journal of Advances in Science Engineering and Technology, Vol. 6 (4), 2018.

Khalilzadeh Shirazi E, Metzger J.W, Fischer K, Hassani A.H, Removal of textile dyes from single and binary component systems by Persian bentonite and a mixed adsorbent of bentonite/charred dolomite, Colloids and Surfaces A: Physicochemical and Engineering Aspects, Vol. 598, 124807, 2020.

3. Results and Discussion

This study comprises several parts as follows:

- selection and characterization of natural adsorbents (vermicompost, natural and standard bentonite, charred dolomite and natural granular bentonite),
- studies on the adsorption efficiency of vermicompost, natural and standard bentonite for the cationic dye basic violet 16 and charred dolomite for the anionic dye reactive red 195 in single dye solutions (8, 65),
- the development of an analytical method for the simultaneous analysis of the two fabric dyes BV₁₆ and RR₁₉₅ in binary dye mixtures,
- studies on the adsorption of the two dyes in binary mixtures on vermicompost, charred dolomite, natural bentonite and standard bentonite (65),
- studies on the mutual interactions of the dyes with single adsorbents in binary solutions (8),
- the investigation of the adsorption of dyes on the mixed adsorbents in binary dye solutions,
- characterization of the real pretreated acrylic fiber dyeing wastewater from the WWTP in Acryl Tab company,
- studies on the characterization of the wastewaters from different baths (dark, medium and pale shade) in cationic exhaust dyeing,
- studies on the removal efficiency of color and COD using natural granular bentonite in a continuous fixed-bed column,
- determination of breakthrough curves for fixed-bed columns with different bed heights operated at different flow rates,
- studies on the adsorption efficiency of granular bentonite for batch treatment of “real” textile effluent,
- equilibrium and kinetic studies for the adsorption of dyes from real textile effluent on granular bentonite,
- studies on the possibility of reusing the textile effluent treated with granular bentonite in the textile industry,
- studies on the design of a fixed-bed column by a scale-up approach,
- studies on waste management, i.e. study on the possibility of using the spent granular bentonite in the production of LWAs.

3.1 Characterization of the adsorbents

Table 12 Characterization of vermicompost; chemical constituents as determined with XRF and elemental analysis (in ppm)

Chemical constituents	Concentration in ppm
Zn	20.67
Cu	38.9
Fe	11.05
Ca	44.96
Si	28.59
Al	3.77
Mg	1.89
S	5.95
Parameters	Values
TOM	48.13 %
Humidity	63 %
Specific surface area (m ² g ⁻¹) *	2.91
EC (dS m ⁻¹)	2.78
C/N	9.97

* determined by Brunauer-Emmett-Teller N₂-BET

The high concentration of total organic matter (TOM) (see Table 12) in vermicompost originates from the raw matter source of forestry waste and animal manure such as cow dung as well as sawdust. The high humidity level of vermicompost (see Table 12) can be attributed to high amounts of hydrophilic groups (–OH, –COOH, –SH) which interact with water. The low surface area of vermicompost (2.91 m² g⁻¹) is in accordance with the characteristics of an agro-waste (8, 58, 120).

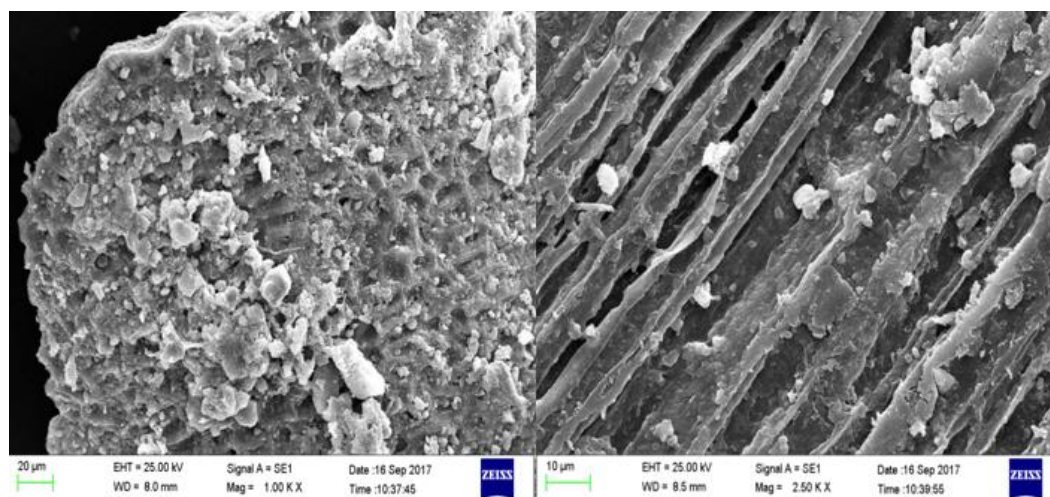


Fig. 41 Field emission scanning electron microscopic (FESEM) images of the pristine *vermicompost*

The FESEM image of the pristine vermicompost shows a porous nature, a rough surface with a fiber-like structure and an irregular morphology (Fig. 41) which is a characteristic of an agro-waste (58, 122-124).

In general, humic materials such as vermicompost have a great number of negative charges, which are responsible for the adsorption of the cationic dyes (125, 126).

Table 13 Characterization of Persian charred dolomite, natural bentonite and standard bentonite; chemical constituents as determined with XRF and elemental analysis (in weight %) (Source: Ref (8, 65) Khalilzadeh Shirazi E et al. (2019), Khalilzadeh Shirazi E et al. (2020))

Chemical constituents	Values in weight %		
	Natural bentonite	Standard bentonite	Charred dolomite
Al ₂ O ₃	10.10	12.72	0.84
SiO ₂	77.17	75.35	2.37
Na ₂ O	1.11	-	-
MgO	1.50	1.81	12.61
P ₂ O ₅	0.67	0.30	-
SO ₃	0.97	0.59	0.51

Results and Discussion

Chemical constituents	Values in weight %		
Cl	0.13	-	-
K ₂ O	0.53	0.11	-
CaO	2.77	2.13	78.36
Parameters			
Specific surface area (m ² g ⁻¹)*	238.34	1205.3	11.88

* determined by Brunauer-Emmett-Teller N₂-BET

The main constituents of charred dolomite are MgO and CaO which are supposed to be primarily responsible for the adsorption of the dyes from the solution (Table 13). Other oxides are present only in trace amounts.

From the analysis, it can be concluded that the main constituents of natural bentonite and standard bentonite are Al₂O₃ and SiO₂ which are supposed to be principally responsible for the adsorption of the dyes from the solution, whereas other oxides are present only in trace amounts (Table 13). The contents of CaO, Na₂O and K₂O reflect the interlayer cations in natural bentonite. The presence of Na₂O and K₂O shows that high-silica bentonite is enriched with sodium and potassium (65, 113).

The total pore volume and mean pore diameter of charred dolomite measured were 0.09 cm³ g⁻¹ and 32.46 nm, respectively.

Table 14 shows product specification of standard bentonite which was provided from Sigma-Aldrich (Merck).

Table 14 Product specification of standard bentonite (Sigma-Aldrich (Merck))

Product name	Nanoclay, hydrophilic bentonite
Product number	682659
Formula	$H_2Al_2O_6Si$
Formula weight	180.1 g mol ⁻¹
Appearance (Color)	Light tan to brown
Appearance (Form)	Powder
Loss on drying	< 18.0 %
Bulk density	600 - 1100 kg/m ³
Average particle size	≤ 25 microns

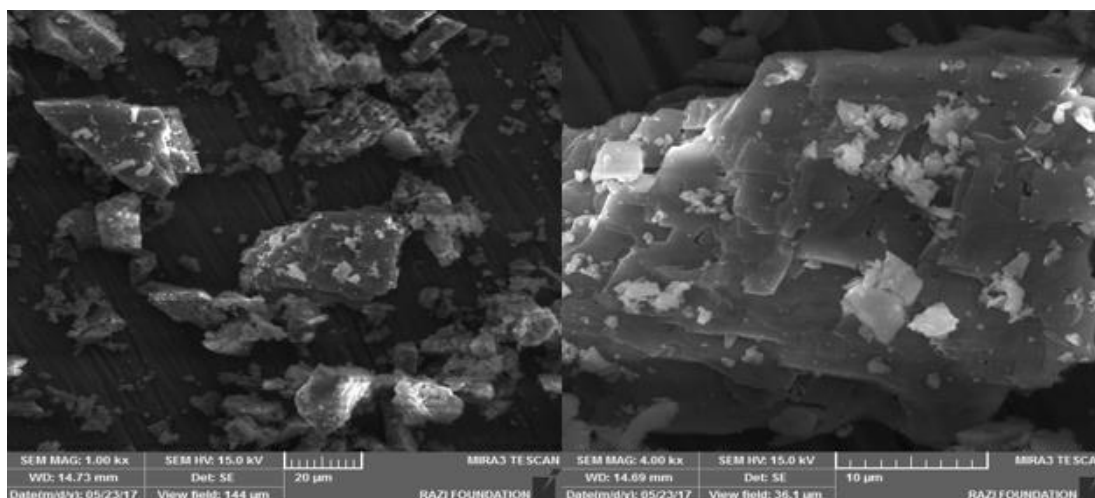


Fig. 42 Field emission scanning electron microscopic (FESEM) images of the pristine *charred dolomite*

The typical morphology of charred dolomite with a plain and approximately compact stratified surface with sharp edges and crumbly nature can be seen in Fig. 42 (8, 27).

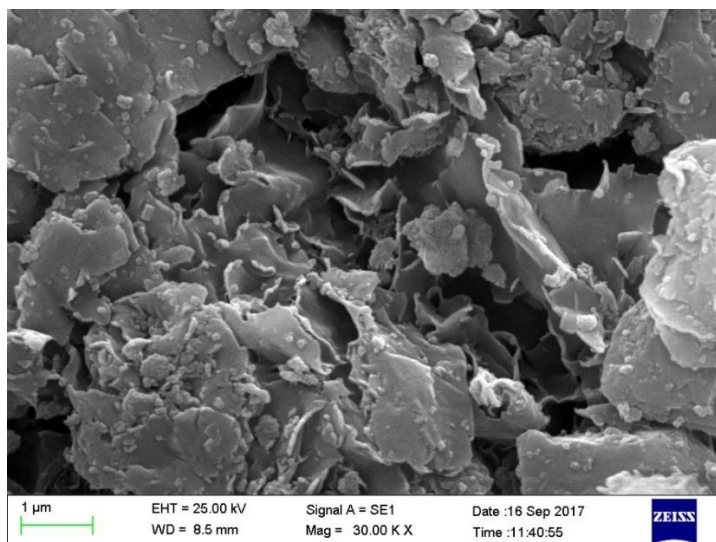


Fig. 43 Field emission scanning electron microscopic (FESEM) images of the pristine *natural bentonite*

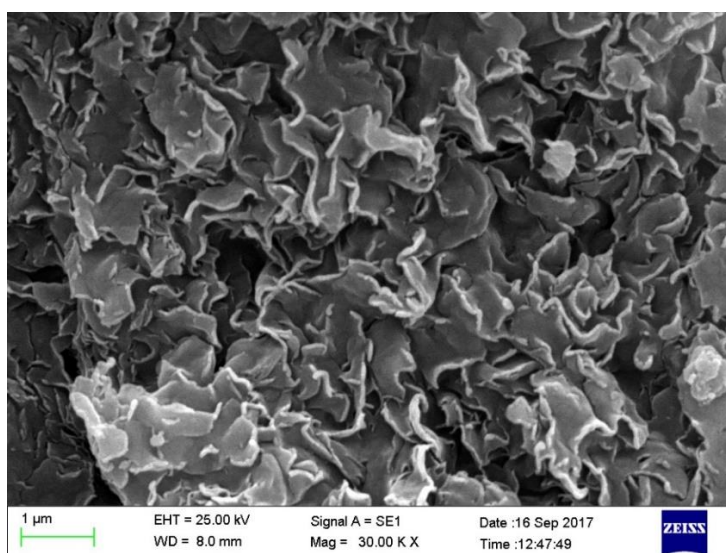


Fig. 44 Field emission scanning electron microscopic (FESEM) images of the pristine *standard bentonite*

Fig. 43 and Fig. 44 are the FESEM images of the respective pristine natural and standard bentonite depicting an irregular morphology and sheet-like structure containing various size particles (65).

3.1.1 Characterization of natural granular bentonite as the adsorbent used for the treatment of textile wastewater

Individual physical-chemical properties of the natural granular bentonite from the Garmsar deposit in the region of Semnan, Iran, are shown in Table 15.

Table 15 Characterization of natural granular bentonite; chemical constituents as determined with XRF and elemental analysis (in weight %)

Chemical constituents in weight %	Values
SiO ₂	59.87
Al ₂ O ₃	11.01
Fe ₂ O ₃	5.48
CaO	6.25
Na ₂ O	0.87
K ₂ O	3.61
MgO	2.81
TiO ₂	0.69
MnO	0.18
P ₂ O ₅	0.13
SO ₃	0.08
Parameters	Values
Purity (in %)	92-96
Humidity (in %)	2.91

Results and Discussion

Parameters	Values
pH	9.77
Loss on ignition, LOI (in %)	8.86
Total Organic Carbon (TOC) (in mg kg ⁻¹)	548
Particle density (apparent density, in g cm ⁻³)	2.62
Bulk density in g cm ⁻³	1.12
Specific surface area (m ² g ⁻¹) *	41.83
Total pore volume (cm ³ g ⁻¹) *	0.089
Average pore diameter (nm) *	8.55

* determined by Brunauer-Emmett-Teller N₂-BET

From XRF and elemental analysis, it can be concluded that the main constituents (~ 70%) of the natural granular bentonite are SiO₂ and Al₂O₃ which are supposed to be mainly responsible for the adsorption of the dyes from the colored wastewater, whereas other oxides are present only in trace amounts (Table 15). Principally, the oxides SiO₂ and Al₂O₃ can originate from quartz, phyllosilicates and feldspars (20, 65).

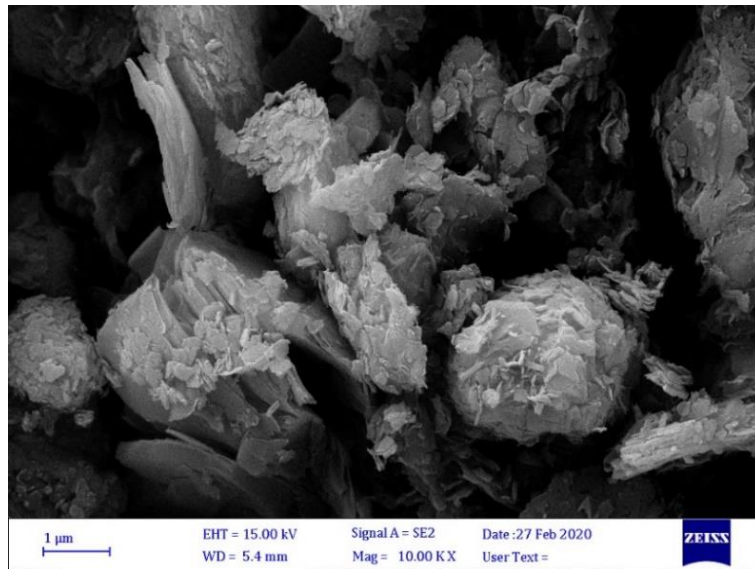


Fig. 45 Field emission scanning electron microscopic (FESEM) images of the pristine *granular bentonite* (before adsorption)

A field emission scanning electron microscope was used to analyze the morphology and microstructure of the pristine adsorbent. The FESEM image of the pristine granular bentonite (before adsorption) depicting an irregular morphology, a porous nature and almost a sheet-like structure containing particles with various sizes is shown in Fig. 45 (65, 127, 128).

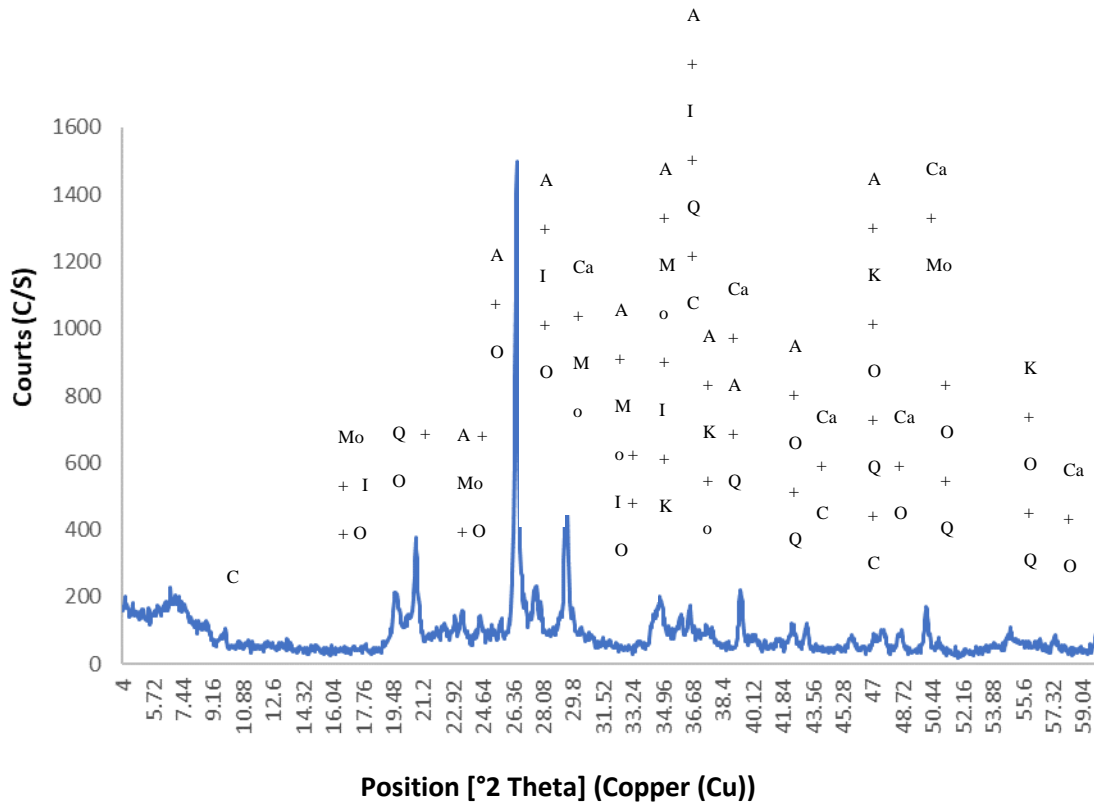


Fig. 46 X-ray diffractograms of natural granular bentonite (Position °2 Theta, Cu K α radiation);

A Albite, C Clinoptilolite, Ca Calcite, I Illite, K Kaolinite, Mo Montmorillonite, Mu Muscovite, O Orthoclase, Q quartz

A natural granular bentonite sample was characterized using an X-ray diffractometer (XRD) to determine the phase composition of the sample. With reference to Fig. 46, in the granular bentonite sample identified different phases namely montmorillonite, clinoptilolite, kaolinite and muscovite-illite. Some non-clay components such as quartz, feldspar (albite, orthoclase) and calcite can also be identified. The main phase as determined by mineral analysis of the raw natural material is primarily composed of montmorillonite (31%). The other peaks in the diffractograms of natural granular bentonite originate from impurities relating to quartz and feldspar. The presence of montmorillonite was confirmed by the high content of silica (59.87% w/w) and alumina (11.01% w/w).

The natural raw sample studied here is similar to other common natural clay deposits which typically contain smectite, illite and kaolinite in addition to some non-clay components such

as feldspars, calcite and quartz. Other phases related to clay minerals such as muscovite have also been identified (18, 65).

3.2 Characterization of the raw textile wastewater from Acryl Tab CO.

The raw wastewater having been treated by coagulation, flocculation and sedimentation (clarification) had an alkaline pH of 11.6 and a COD value of 890 mg L⁻¹ (values of a grab sample which cannot be considered to be representative).

In the dye house of the Acryl Tab company, various cationic dyes and different auxiliary chemicals are used in the dyeing process in five different vessels (see Fig. 47). The textile wastewater had a yellowish-orange color characterized by a Pt-Co scale value of 456 mg L⁻¹, and SAC numbers of 20.2 m⁻¹ (436 nm), 6.4 m⁻¹ (525 nm) and 3.9 m⁻¹ (620 nm), respectively (see Table 16). These color parameters of the raw wastewater comply neither with Iranian nor with German discharge limits into water bodies for textile wastewaters (in Iran: 75 mg Pt-Co L⁻¹, in Germany: 7 m⁻¹ for SAC_{436 nm}, 5 m⁻¹ for SAC_{525 nm} and 3 m⁻¹ for SAC_{620 nm}), nor with reuse requirements for textile processing, demanding non-visible color (see Table 9).

The sampling of the wastewater was carried out based on a 2-hour composite sampling. The samples were taken from the basin without the chlorine addition. Within 2 hours, 200 ml of the influent and 200 ml of the effluent of the basin were taken every 10 minutes and added into a container. This process was repeated every 10 minutes. After 2 hours, the container containing the samples were shaken strongly to obtain a homogeneous mixture.

Table 16 Characterization of the raw textile wastewater from the Acryl Tab CO.

Parameter	Value
Color	Yellowish orange
Color: DFZ * number/ SAC ** at	
436 nm	20.2
525 nm	6.4
620 nm	3.9
Conductivity in $\mu\text{S m}^{-1}$	2113

Results and Discussion

Parameter	Value
pH	11.69
Color: Platinum - Cobalt (Pt-Co) scale ***	456
COD in mg L ⁻¹	890
TDS in mg L ⁻¹	1193

* DFZ = "Durchsichtfarbzahl"; DIN ISO 7887:2012-04

** SAC = Spectral absorption coefficient

*** also called APHA color or Hazen scale, ranges from 0 (distilled water) to 500 ppm

The raw textile wastewater exceeded limits for the presence of color for high, for moderate and as well for low-quality reuse waters according to the reuse requirements in the textile industry (Table 9). In addition to color, the COD should also be lowered from 890 mg L⁻¹ to a range listed in Table 9. Regarding conductivity, there are no determined water quality requirements for recycled textile wastewater presented in the AquaFit4Use project. However, based on general reuse water requirements for recycled textile wastewater proposed there and taking into account various publications and textile companies, the conductivity should be lowered from 2113 to 1500 $\mu\text{S m}^{-1}$. However, demands depend on the purpose of water reuse.



Fig. 47 Different vessels in the dye house of the Acryl Tab company in Iran
(photo: E. Khalilzadeh Shirazi)

3.3 Characterization of the wastewaters from different baths (dark, medium and pale shade) in cationic exhaust dyeing

Analysis of different parameters such as COD, color, conductivity, temperature and pH from textile effluents from textile pretreatment bath, exhausted dye bath and rinsing bath for light, medium and dark shades was carried out (each sampling was done at 3 different times, i.e. 9 dyeing procedures were investigated) (see Table 17, Fig. 48).

Results and Discussion

Table 17 Characterization of different baths (dark, medium and light shade) in cationic exhaust dyeing

Dark shade	pH	Temperature C°	COD mg L ⁻¹	Conductivity μS m ⁻¹	Color
First rinsing (Pretreatment bath)	7.46	45	1010	844	SAC _{436 nm} : 16.9 SAC _{525 nm} : 12.0 SAC _{620 nm} : 8.5
Chemicals (Acetic acid, retarder)	4.50	41	10521	1075	SAC _{436 nm} : 7.6 SAC _{525 nm} : 5.5 SAC _{620 nm} : 4.7
Dyeing (Exhausted dye bath)	4.23	70	5210	1994	SAC _{436 nm} : 25.5 SAC _{525 nm} : 41.3 SAC _{620 nm} : 36.8
Last rinsing (Rinsing bath)	6.33	28	284	1142	SAC _{436 nm} : 11.8 SAC _{525 nm} : 13.0 SAC _{620 nm} : 14.0

Medium shade	pH	Temperature C°	COD mg L ⁻¹	Conductivity μS m ⁻¹	Color
First rinsing (Pretreatment bath)	7.77	43	1425	851	SAC _{436 nm} : 12.4 SAC _{525 nm} : 10.9 SAC _{620 nm} : 9.1
Chemicals (Acetic acid, retarder)	4.25	43	10430	1268	SAC _{436 nm} : 12.6 SAC _{525 nm} : 11.2 SAC _{620 nm} : 9.6
Dyeing (Exhausted dye bath)	4.09	72	4620	1953	SAC _{436 nm} : 75.7 SAC _{525 nm} : 107.9 SAC _{620 nm} : 14.3
Last rinsing (Rinsing bath)	6.65	25	280	873	SAC _{436 nm} : 4.2 SAC _{525 nm} : 4.6 SAC _{620 nm} : 0.9

Results and Discussion

Pale shade	pH	Temperature C°	COD mg L ⁻¹	Conductivity μS m ⁻¹	Color
First rinsing (Pretreatment bath)	7.59	46	1710	797	SAC _{436 nm} : 29.7 SAC _{525 nm} : 22.9 SAC _{620 nm} : 17.3
Chemicals (Acetic acid, retarder)	4.31	46	10010	1332	SAC _{436 nm} : 12.2 SAC _{525 nm} : 10.7 SAC _{620 nm} : 9
Dyeing (Exhausted dye bath)	4.04	72	3240	1966	SAC _{436 nm} : 17 SAC _{525 nm} : 12.3 SAC _{620 nm} : 8.9
Last rinsing (Rinsing bath)	6.73	23	360	881	SAC _{436 nm} : 4.5 SAC _{525 nm} : 3.8 SAC _{620 nm} : 3

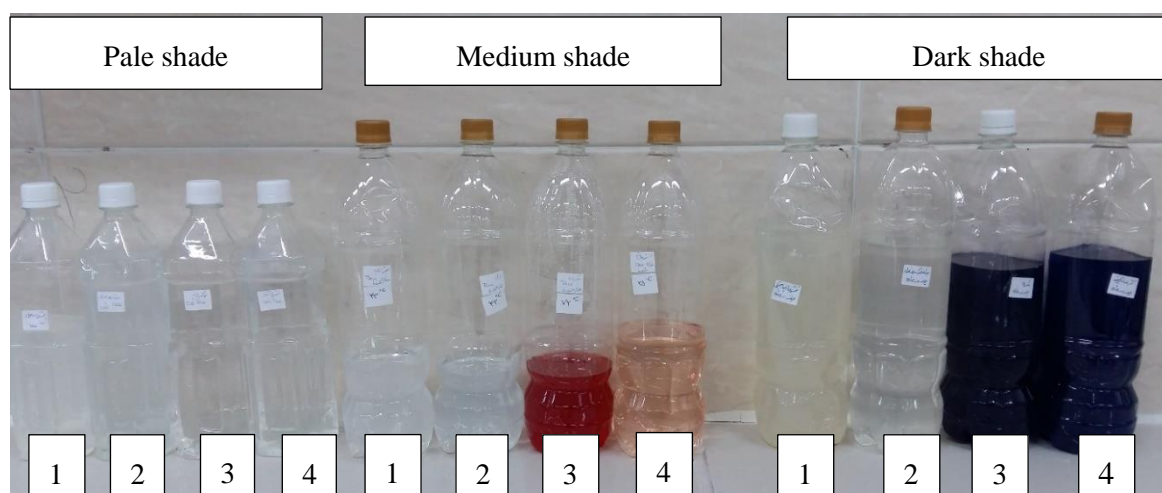


Fig. 48 Wastewater from different baths (dark, medium and pale shade) from cationic exhaust dyeing

1 Wastewater from pretreatment bath 2 Wastewater from the step of adding chemicals 3 Wastewater from exhausted dye bath 4 Wastewater from rinsing bath

3.4 Batch adsorption studies on real textile wastewater

Adsorption experiments were performed in batch mode. The influence of the different experimental parameters such as mass/volume ratio and contact time on the efficiency of the adsorbent to remove color and COD was studied.

3.4.1 Effect of the amount of granular bentonite on the removal of color as determined by measurement of the SAC number at different wavelengths

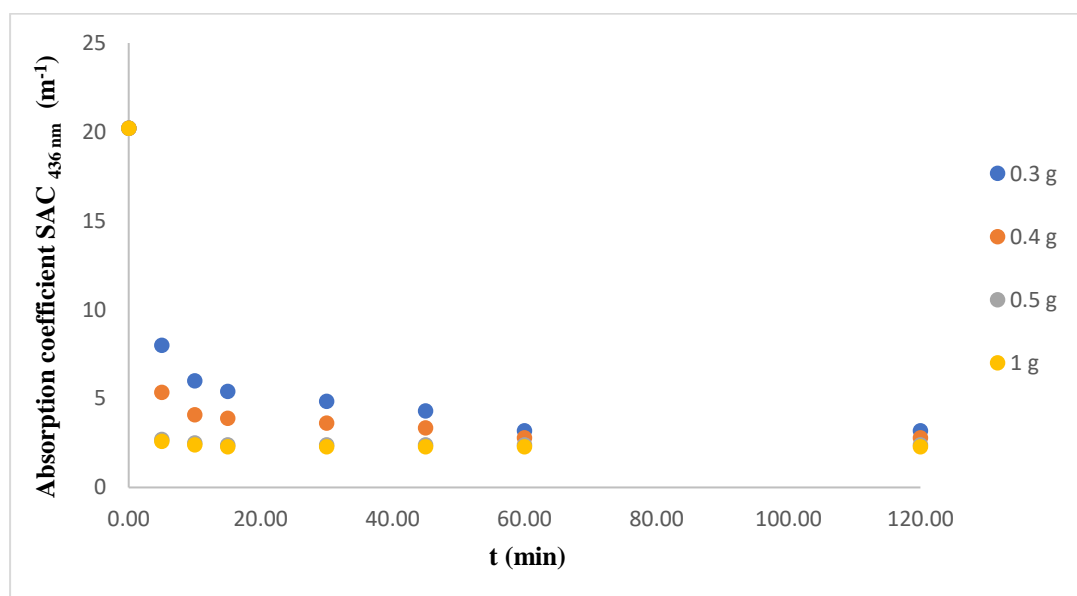


Fig. 49 Effect of the amount of granular bentonite on color removal, measured as spectral absorption coefficient (SAC) in m⁻¹ at a wavelength of 436 nm (experimental conditions: stirring speed of 250 rpm, no pH adjustment, ambient temperature, volume = 100 ml)

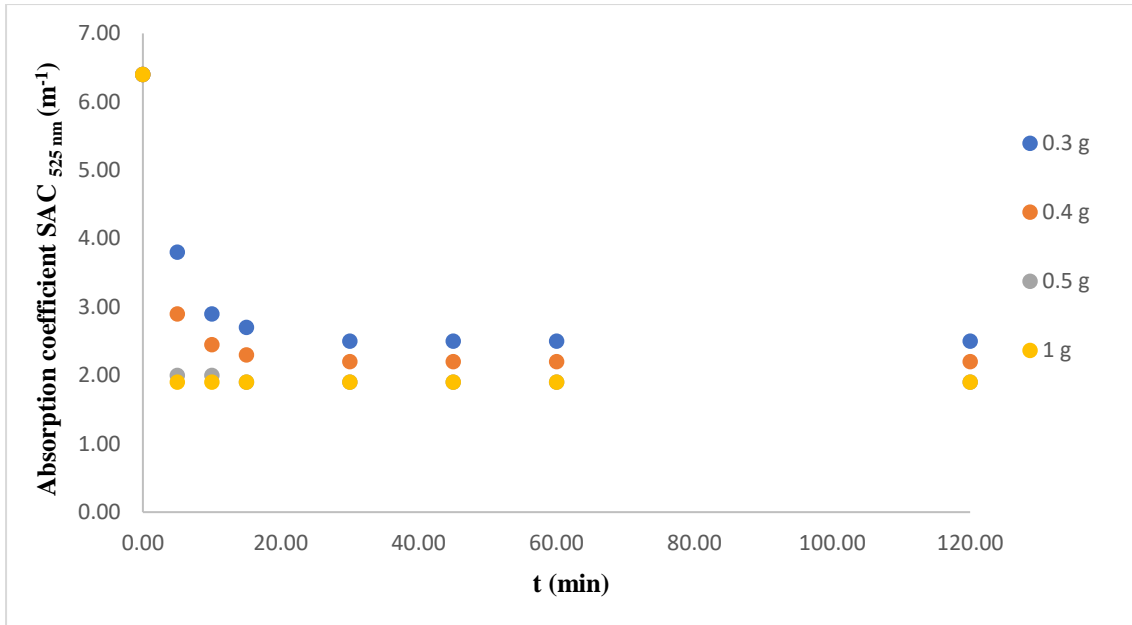


Fig. 50 Effect of the amount of granular bentonite on color removal, measured as spectral absorption coefficient (SAC) in m^{-1} at a wavelength of 525 nm (experimental conditions: stirring speed of 250 rpm, no pH adjustment, ambient temperature, volume = 100 ml)

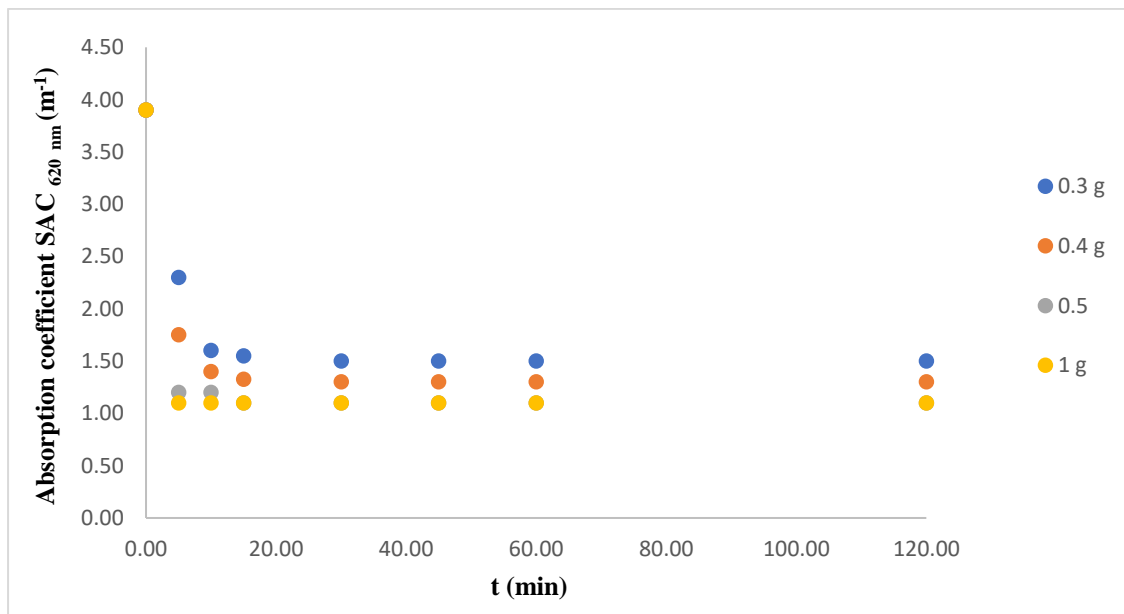


Fig. 51 Effect of the amount of granular bentonite on color removal, measured as spectral absorption coefficient (SAC) in m^{-1} at a wavelength of 620 nm (experimental conditions: stirring speed of 250 rpm, no pH adjustment, ambient temperature, volume = 100 ml)

To investigate the effect of the sorbent amount on the adsorption of dyes studied at different wavelengths (SAC 436, 525 and 620 nm), different amounts of the natural material were brought into contact with 100 ml of wastewater (see Fig. 49-51). As illustrated, an increase in the amount of the adsorbent increases the number of active sites for the adsorption resulting in a higher color removal. However, as the percentage of adsorbed dye molecules on 0.5 and 1 g of the adsorbent does not change much with time, 0.5 g granular bentonite was considered as the optimum amount for further experiments. In the beginning of the adsorption process, due to the presence of a large number of free active sites on the surface of granular bentonite and subsequently improvement of the dye diffusion flux to the adsorbent, the adsorption process accelerates. After approximately 5 min equilibration, the concentration of dye molecules keeps constant.

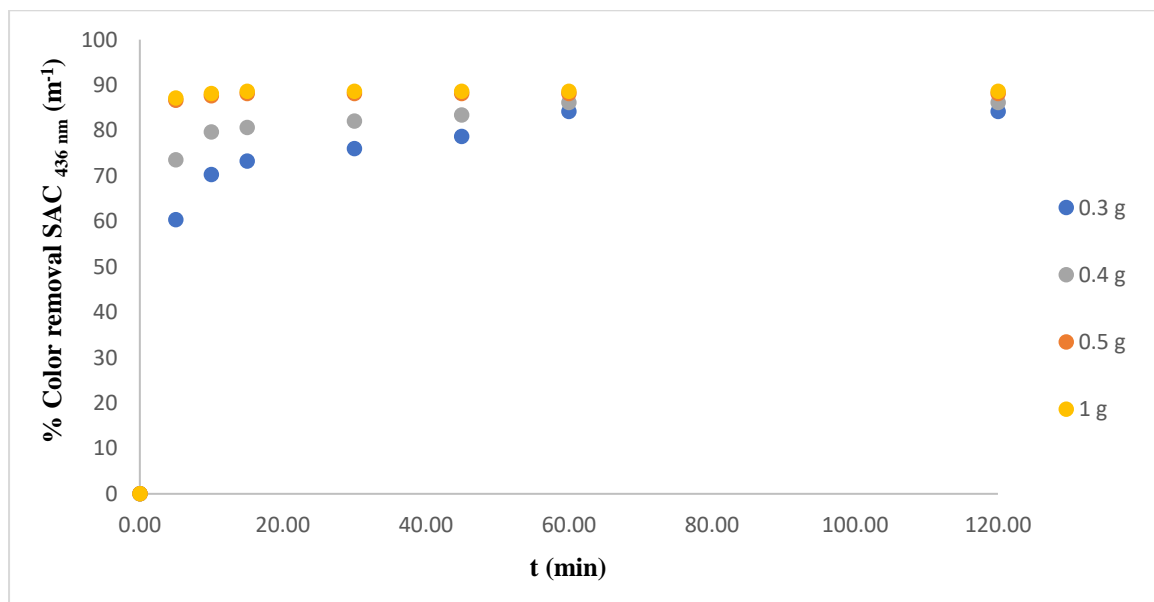


Fig. 52 Effect of the amount of granular bentonite on color removal efficiency, measured as spectral absorption coefficient (SAC) in m^{-1} at a wavelength of 436 nm (experimental conditions: stirring speed of 250 rpm, no pH adjustment, ambient temperature, volume = 100 ml)

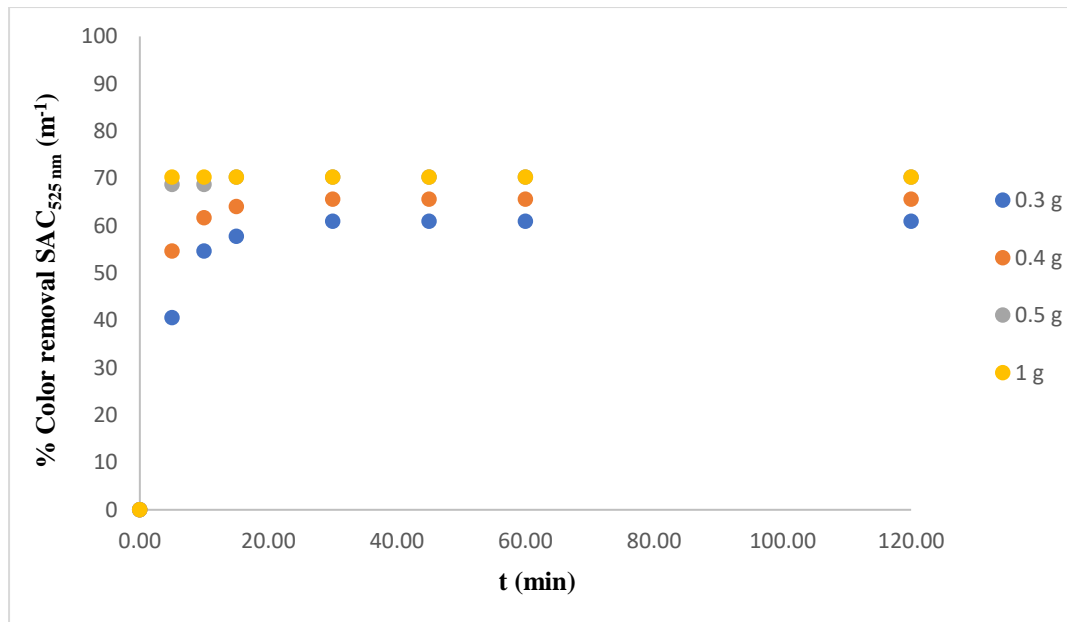


Fig. 53 Effect of the amount of granular bentonite on color removal efficiency, measured as spectral absorption coefficient (SAC) in m^{-1} at a wavelength of 525 nm (experimental conditions: stirring speed of 250 rpm, no pH adjustment, ambient temperature, volume = 100 ml)

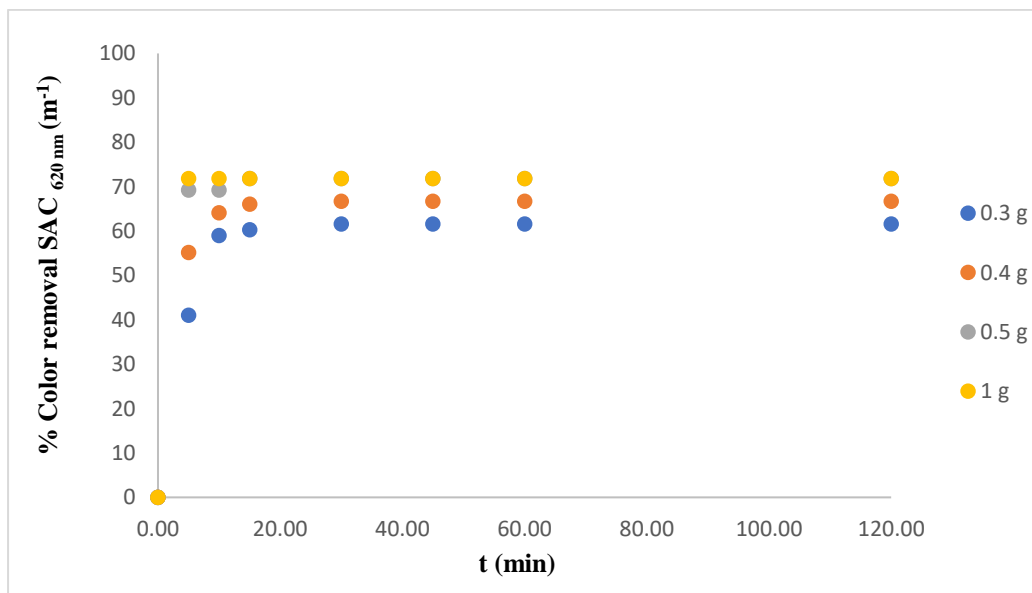


Fig. 54 Effect of the amount of granular bentonite on color removal efficiency, measured as spectral absorption coefficient (SAC) in m^{-1} at a wavelength of 620 nm (experimental conditions: stirring speed of 250 rpm, no pH adjustment, ambient temperature, volume = 100 ml)

The initial strong change at the beginning of the adsorption process observed for all four amounts of the adsorbent (see Figs. 52-54) indicates a high affinity of the dye molecules to

the adsorbent surface. Furthermore, the color removal increases with time from the beginning of the adsorption process to approximately between 20 to 30 min which can be seen for lower adsorbent amounts of 0.3 and 0.4 g. At first, there is a high number of free active sites on the surface of the adsorbent leading to a high dye diffusion flux to the adsorbent. A gradual increase in the adsorption rate occurs, and more and more active sites are occupied. This causes a decrease in the concentration gradient and a gradual decline in the adsorption rate leading finally to saturation, i.e. no more available adsorption sites at the adsorbent surface. In other words, with increasing time, saturation at the surface of the adsorbents translates into the reduction of the concentration gradient and the tapering off in the adsorption rate. After a specific time, a constant value is reached at which no more dye will be removed from the wastewater (8).

In the batch experiments the color reduction was observed 88.1% ($SAC_{436\text{ nm}}$), 70.3% ($SAC_{525\text{ nm}}$) and 71.8% ($SAC_{620\text{ nm}}$). Considering the wastewater color removal, using $SAC_{436\text{ nm}}$, $SAC_{525\text{ nm}}$ and $SAC_{620\text{ nm}}$ as indicators, the adsorption using the mineral adsorbent of granular bentonite suggested to be an effective decolorization method.

3.4.2 Effect of the amount of granular bentonite on COD removal

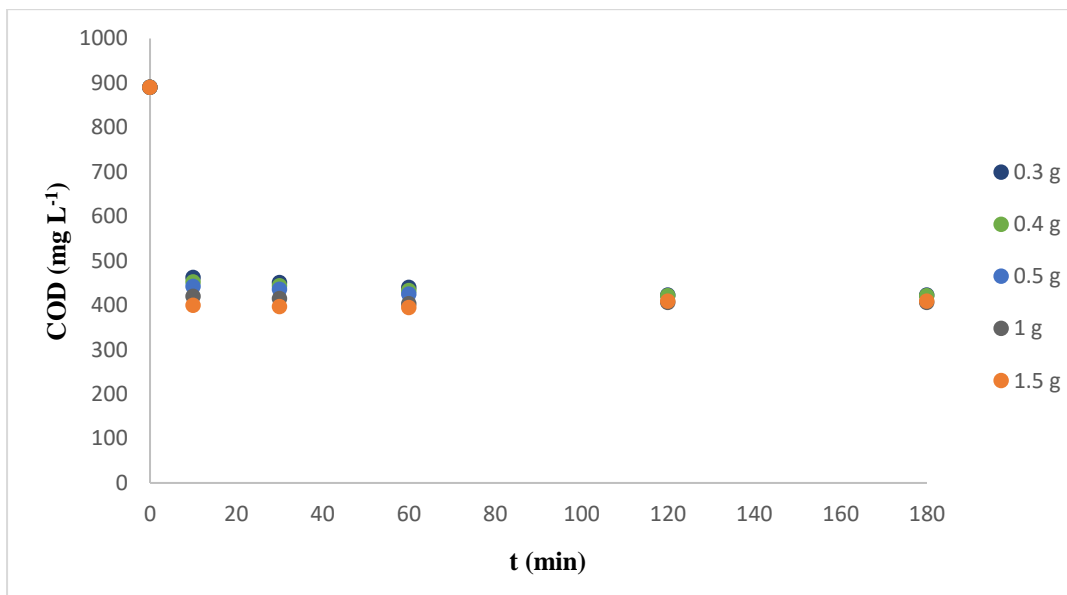


Fig. 55 Effect of the amount of granular bentonite on COD removal (experimental conditions: stirring speed of 250 rpm, no pH adjustment, ambient temperature, volume = 100 ml)

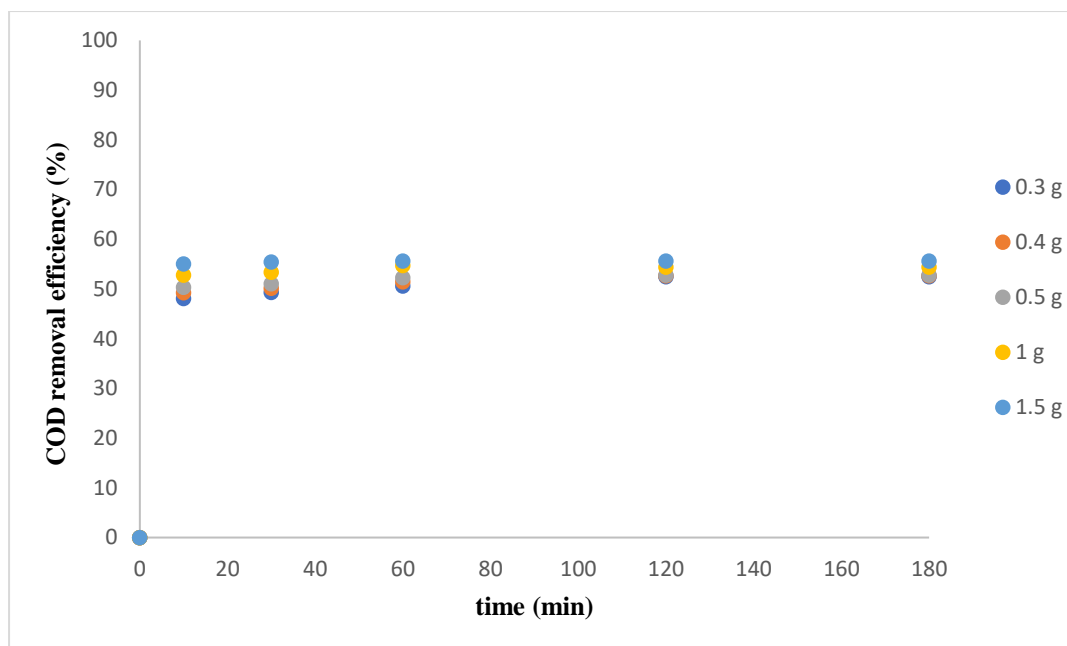


Fig. 56 Effect of the amount of granular bentonite on color removal efficiency (experimental conditions: stirring speed of 250 rpm, no pH adjustment, ambient temperature, volume = 100 ml)

The effect of the amount of adsorbent and the contact time on the removal of COD from real textile wastewater was also studied over a contact time of up to 180 min (see Figs. 55 and 56). Already after 10 min, the maximum of the removal of COD was reached, which later only slightly changed in the course of time. After 20 min no noticeable change in the reduction of COD was observed for neither amount of adsorbent indicating this to be a sufficiently long time to attain equilibrium. The most rapid reduction in COD occurred within the first 10 min of the adsorption process which might be attributed to the presence of a large number of binding sites on the surface of the adsorbent, due to the rapid attachment of solute to the adsorbent surface. Afterwards, the saturation of the available binding sites on the granular bentonite surface leads to a slowdown of the adsorption process.

In addition, the results show that by increasing the mass of the adsorbent from 0.3 g to 1.5 g, the dye removal efficiency at an equilibrium time of 20 min increased from 50% to 55% (Fig. 56). With the increase in the amount of adsorbent up to 0.5 g the COD removal efficiency increased, while higher amounts did not lead to further changes. Thus, an amount of 0.5 g granular bentonite was selected as the optimized amount.

3.4.3 Equilibrium isotherm studies

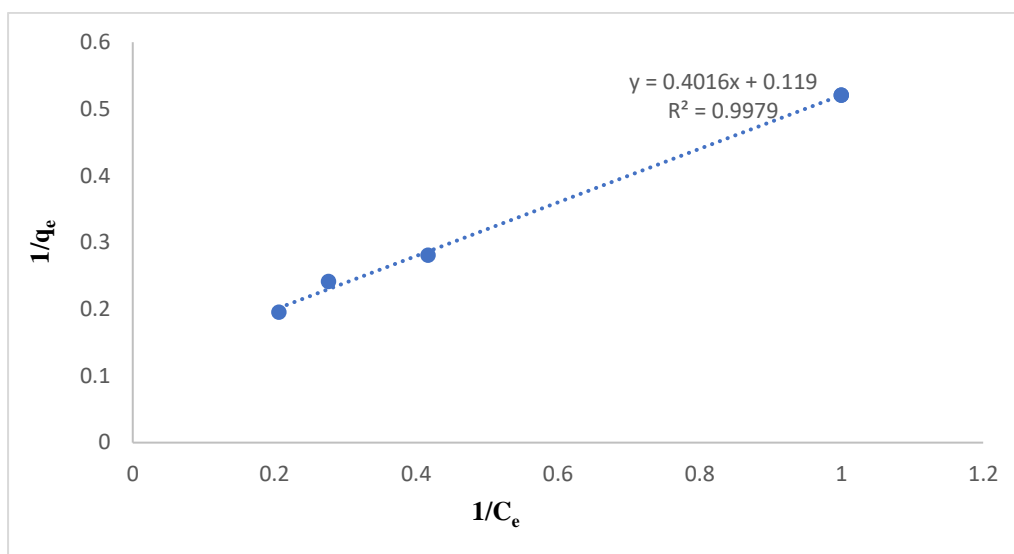


Fig. 57 Langmuir isotherm of the adsorption of color (determined as $SAC_{436\text{ nm}}$) on granular bentonite

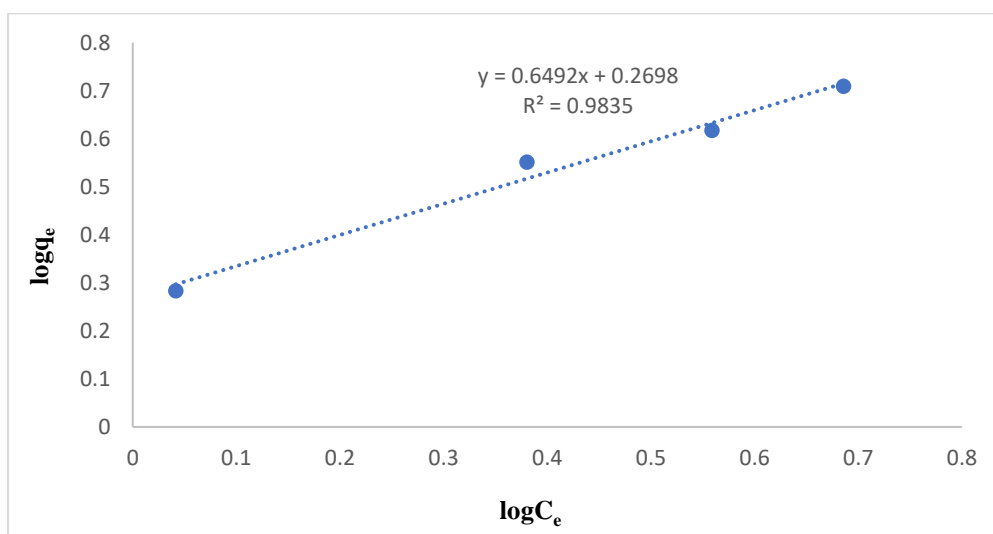


Fig. 58 Freundlich isotherm of the adsorption of color (determined as $SAC_{436\text{ nm}}$) on granular bentonite

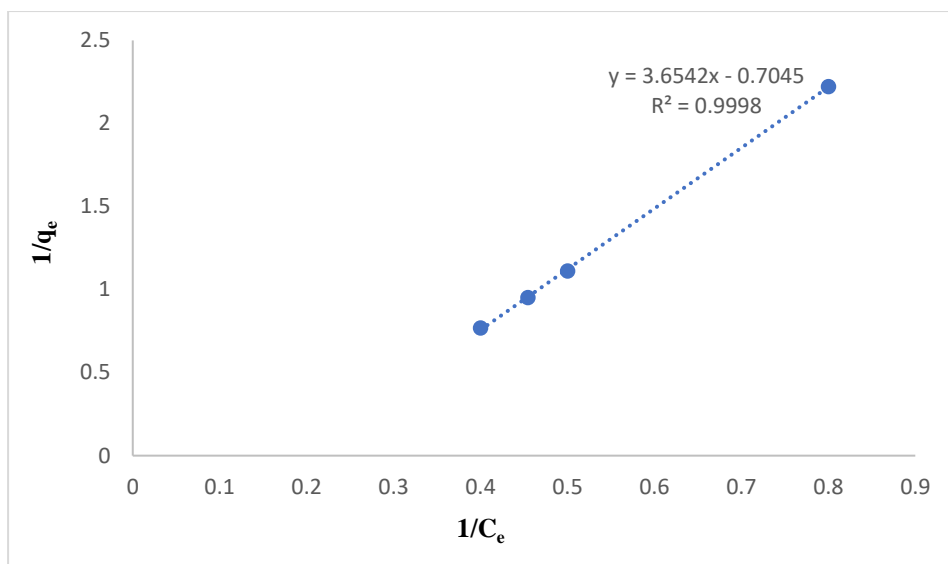


Fig. 59 Langmuir isotherm of the adsorption of color (determined as $SAC_{525\text{ nm}}$) on granular bentonite

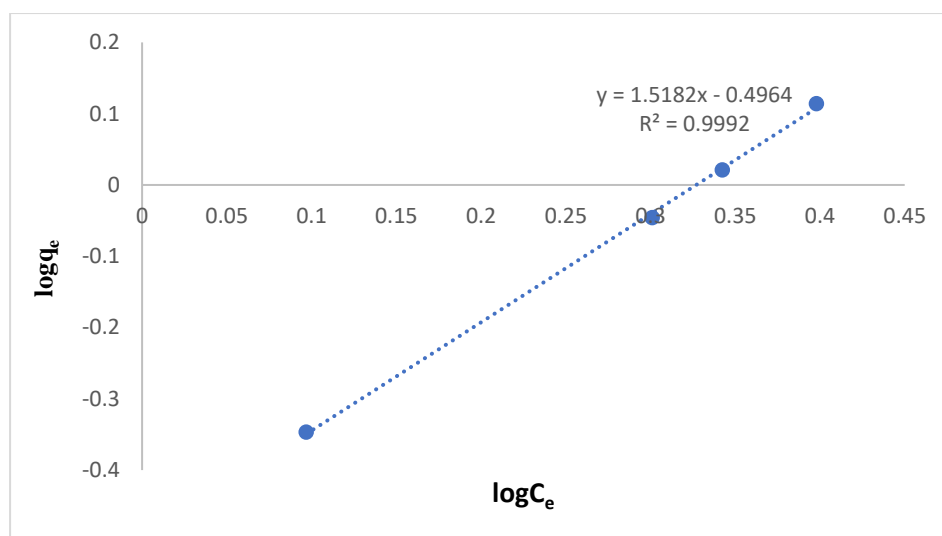


Fig. 60 Freundlich isotherm of the adsorption of color (determined as $SAC_{525\text{ nm}}$) on granular bentonite

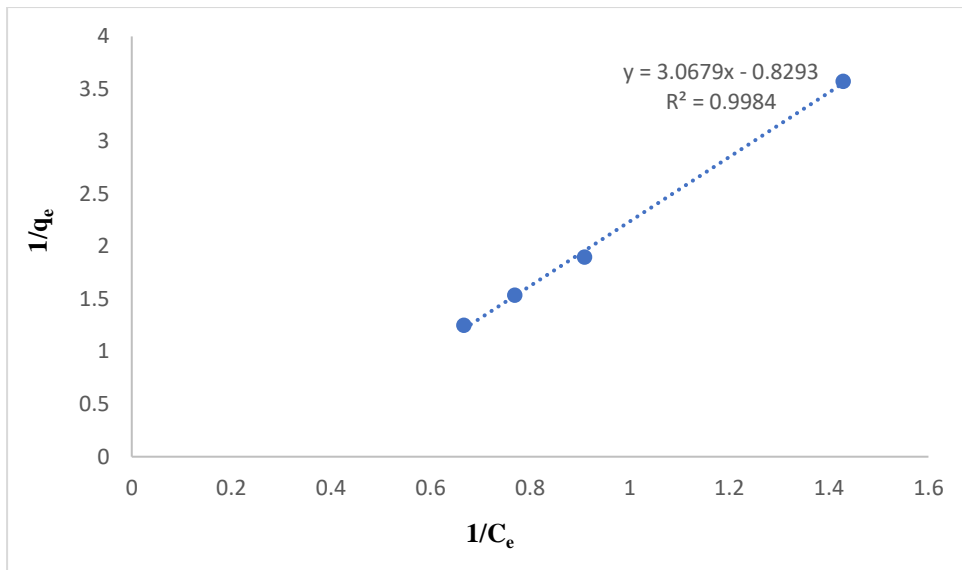


Fig. 61 Langmuir isotherm of the adsorption of color (determined as $SAC_{620\text{ nm}}$) on granular bentonite

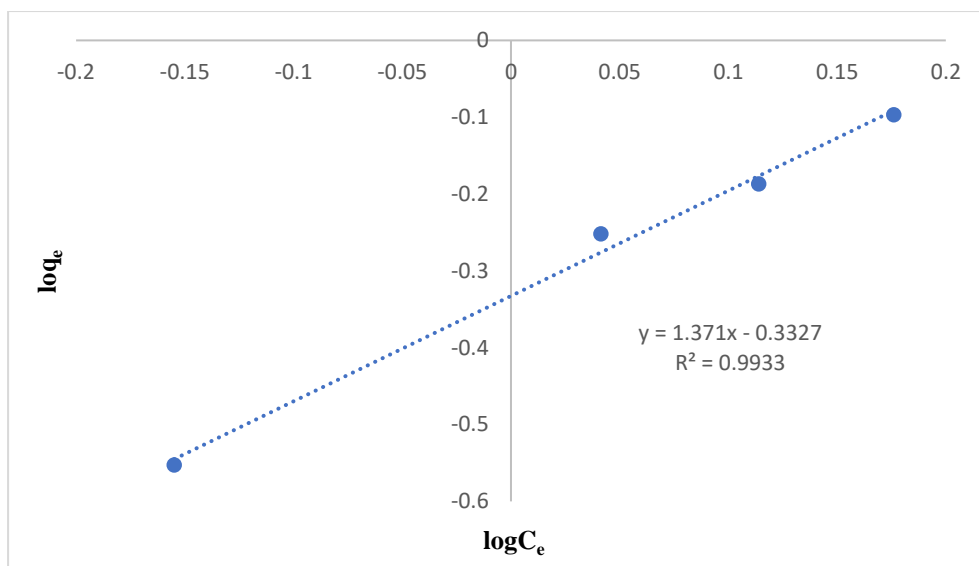


Fig. 62 Freundlich isotherm of the adsorption of color (determined as $SAC_{620\text{ nm}}$) on granular bentonite

Results and Discussion

Table 18 Isotherm parameters of the adsorption of color determined as SAC on granular bentonite

Isotherm	Parameter	Unit	Value	R ²
<i>SAC_{436 nm}</i>				
Langmuir	K _L	L mg ⁻¹	0.29	0.9979
	q _{max}	mg g ⁻¹	9	
Freundlich	K _F	mg g ⁻¹	0.26	0.9835
	1/n	mg L ⁻¹	0.64	
<i>SAC_{525 nm}</i>				
Langmuir	K _L	L mg ⁻¹	0.19	0.9998
	q _{max}	mg g ⁻¹	1.41	
Freundlich	K _F	mg g ⁻¹	0.49	0.9992
	1/n	mg L ⁻¹	1.51	
<i>SAC_{620 nm}</i>				
Langmuir	K _L	L mg ⁻¹	0.26	0.9984
	q _{max}	mg g ⁻¹	1.2	
Freundlich	K _F	mg g ⁻¹	0.33	0.9933
	1/n	mg L ⁻¹	1.37	

The graphs of the Langmuir and Freundlich equilibrium isotherms of the adsorption of color on granular bentonite are presented in Figs. 57-62. The correlation coefficients of the Langmuir isotherms were higher than those of the Freundlich isotherm; thus, the Langmuir model better describes the adsorption process of color on granular bentonite for all three wavelengths (SAC determined at 436, 525 and 620 nm). This indicates that the removal of color occurs via a monolayer adsorption process. The isotherm constants were calculated and are presented in Table 18. The higher value of K_L for SAC_{436 nm} compared to the SAC_{525 nm} and SAC_{620 nm} can be related to the physical-chemical properties of the cationic

dyestuffs applied for dyeing and subsequently present in the wastewater, which is explained in section 2.1.1.

Moreover, the Freundlich constant, n , was also calculated. The Freundlich constant n was found to be > 1 based on $SAC_{436 \text{ nm}}$ which indicates that the adsorption is more favorable for dyes absorbing at this wavelength compared to the other wavelengths studied. It can be associated to the structure and physical-chemical properties of the dyestuffs (8, 65).

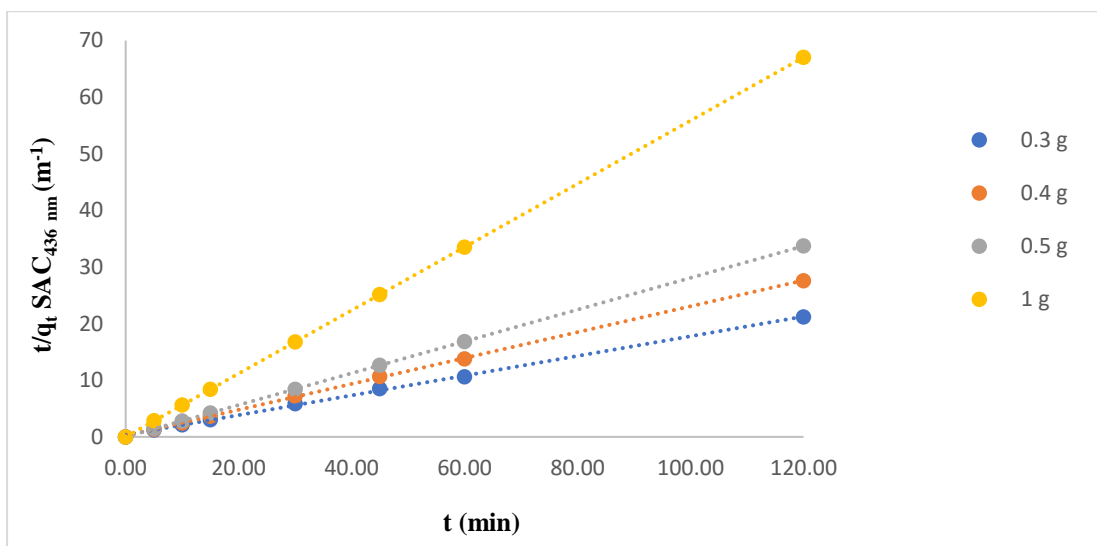


Fig. 63 Removal of color (determined via $SAC_{436 \text{ nm}}$) from textile wastewater applying granular bentonite, a pseudo-second-order equation was used

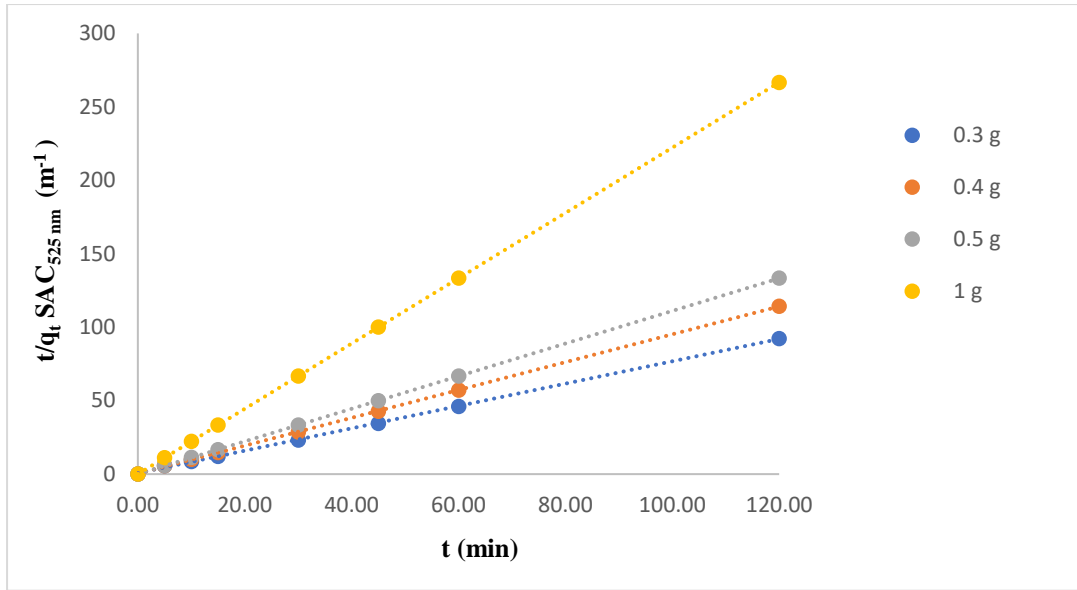


Fig. 64 Removal of color (determined via $SAC_{525\text{ nm}}$) from textile wastewater applying granular bentonite, a pseudo-second-order equation was used

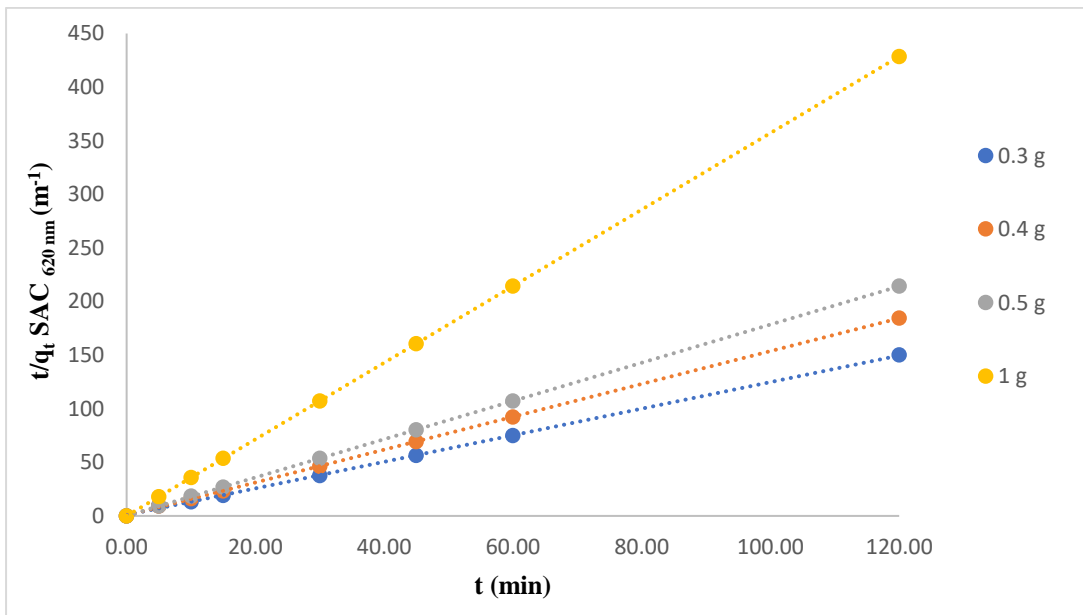


Fig. 65 Removal of color (determined via $SAC_{620\text{ nm}}$) from textile wastewater applying granular bentonite, a pseudo-second-order equation was used

Table 19 Parameters of the pseudo-second-order kinetics of dye adsorption on granular bentonite

SAC	Adsorbent dosage (g)	$q_{e,exp}$ (mg g ⁻¹)	k_2 (g/mg min)	$q_{e,cal}$ (mg g ⁻¹)	R^2
436	0.3	5.12	0.08	5.74	0.999
	0.4	4.14	0.25	4.37	0.9998
	0.5	3.56	9.06	3.56	1
	1	1.79	18.24	1.79	1
525	0.3	1.31	0.79	1.31	0.9996
	0.4	1.05	2.22	1.05	0.9999
	0.5	0.90	15.3	0.90	1.0000
	1	0.45	12.2	0.45	1.0000
620	0.3	0.80	1.73	0.80	0.9996
	0.4	0.65	4.43	0.65	0.9999
	0.5	0.56	15.09	0.56	1.0000
	1	0.26	12.75	0.28	1.0000

3.4.4 Kinetic analysis

Figs. 63-65 provide information on the results of the kinetic studies of color adsorption on the adsorbent studied at different wavelengths (SAC at 436, 525 and 620 nm, respectively). The results showed that the adsorption processes follow more satisfactorily a pseudo-second-order model (similar q_e for experiment and model as well as a high value of R^2) indicating that the adsorption process is most likely based on chemical adsorption. The type of the adsorption (chemisorption) can be related to the interaction of the cationic dyestuffs with the surface of the adsorbent (see the structure of the dyestuffs in section 2.1.1). With reference to literature, the adsorption on the raw (natural) montmorillonite (the main component of bentonite) is through both cation exchange and electrostatic attraction between cationic dyes and negatively charged surface of montmorillonite.

The overall charge of bentonite is neutral, and the lattice of this mineral material has an excess negative charge. Bentonite has three-layer structure with two tetrahedral silicate layers enveloping an octahedral aluminate layer. This derives from the partial substitution of tetravalent silica with trivalent aluminum that results in the replacement of trivalent aluminum with divalent calcium. The surface lattice of the bentonite clay with a negative charge allows an interaction with cationic dyes. In other words, owing to the isomorphous substitution (Al for Si), bentonite has excess negative charges, although natural bentonite has an overall neutral charge. Exchangeable cations between the layers from the external medium compensate for this kind of negative charge. The exchangeable cations like sodium ions diffuse away from the solid surface when water comes into contact with bentonite giving negative charges to the clay surface. Negative charges on the surface of clay layers attract dye cationic ions. Due to electrostatic attraction, the negatively charged sites of the bentonite favor the adsorption of cationic dyes.

A kind of the cation exchange is possibly the driving force for the adsorption of the cationic dye (12, 65, 128).

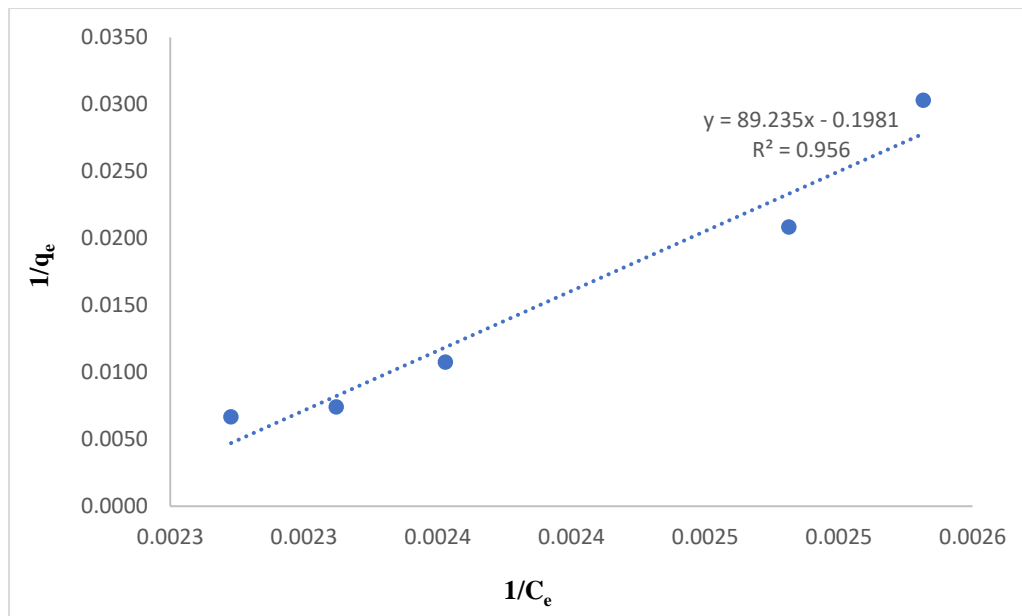


Fig. 66 Langmuir isotherm of the adsorption of COD on granular bentonite

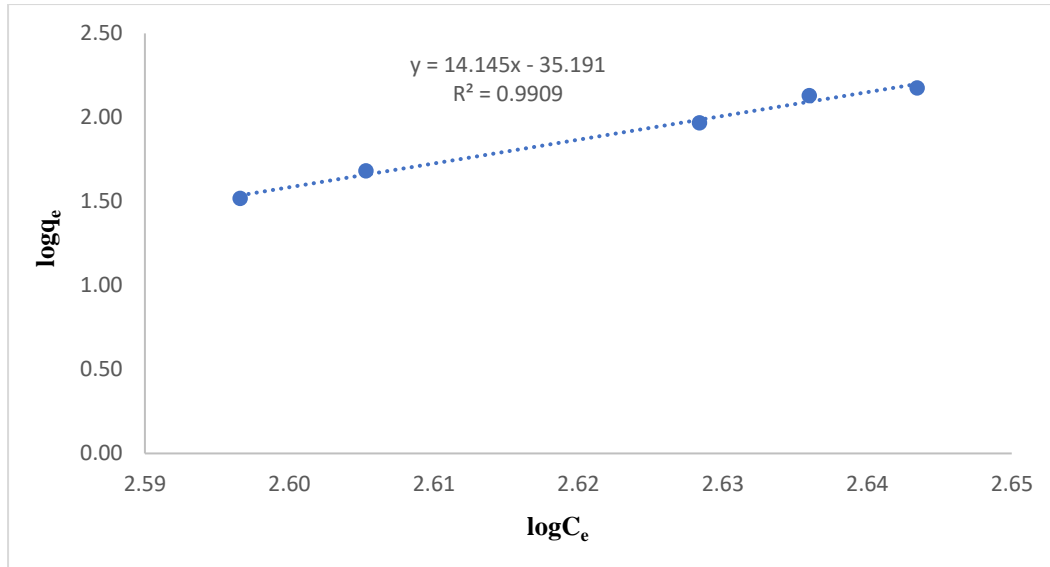


Fig. 67 Freundlich isotherm of the adsorption of COD on granular bentonite

Table 20 Isotherm parameters of the adsorption of COD on granular bentonite from textile wastewater

Isotherm	Parameter	Unit	Value	R ²
Langmuir	K _L	L mg ⁻¹	0.002	0.956
	q _{max}	mg g ⁻¹	5.04	
Freundlich	K _F	mg g ⁻¹	35.191	0.9909
	1/n	mg L ⁻¹	14.145	

The Langmuir and Freundlich equilibrium isotherms of COD on granular bentonite studied are presented in Figs. 66 and 67. The higher correlation of the Freundlich isotherm shows that the Freundlich model better describes the adsorption process of COD on granular bentonite. This indicates that the adsorption of COD occurs according to a multilayer model. The low value of K_L indicates a low removal efficiency of granular bentonite for COD. The Freundlich constant n was calculated to be < 1 which indicates that granular bentonite is unfavorable for COD removal (see Table 20).

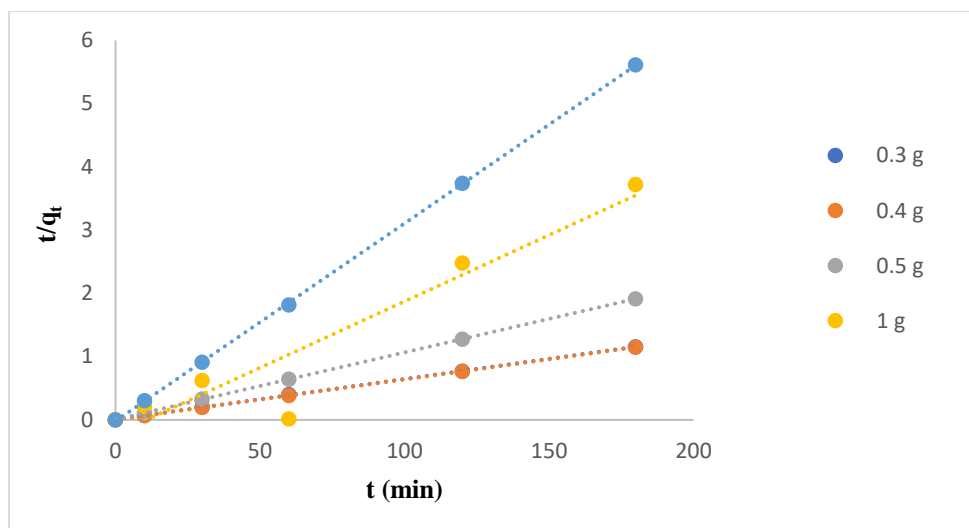


Fig. 68 Removal of COD from textile wastewater applying granular bentonite using a pseudo-second-order equation

Table 21 Kinetic constants of the adsorption of COD from textile wastewater onto granular bentonite

Adsorbent dosage (g)	$q_{e,exp}$ (mg g^{-1})	k_2 (g mg min^{-1})	$q_{e,cal}$ (mg g^{-1})	R^2
0.3	156.25	0.82	155.67	0.9998
0.4	156.25	1.77	156.67	1.0000
0.5	94	1.79	94.33	0.996
1	48	0.094	47.61	1.0000
1.5	32.07	1.77	32.05	0.9999

With reference to the correlation coefficient and similar q_e for experiment and model (Table 21) and according to Fig. 68 which shows removal of COD from textile wastewater applying different amounts of granular bentonite using a pseudo-second-order equation, COD adsorption on granular bentonite followed a pseudo-second-order kinetics. The kinetic constants (k_2 in Table 21) showed a faster COD uptake using less amount of the adsorbent. An explanation could be that the adsorbent particles might form aggregates when present at higher concentrations, changing the accessibility of binding sites on the surface of the individual particles.

All in all, it was found that the efficiency of natural granular bentonite to remove COD and color from the effluent after treatment with granular bentonite depended on the reaction time and the amount of the adsorbent. At best, under the optimum conditions, COD concentration could be lowered from an initial 890 mg L^{-1} to 403 mg L^{-1} , i.e. 54.7% of COD was removed. The batch results demonstrated that based on SAC measurements the color reduction was 88.1% ($\text{SAC}_{436 \text{ nm}}$), 70.3% ($\text{SAC}_{525 \text{ nm}}$) and 71.8% ($\text{SAC}_{620 \text{ nm}}$), respectively. This shows that the treatment by adsorption on granular bentonite can decrease the color of the wastewater to a higher degree than COD. This can be attributed to the fact that water-soluble compounds such as acetic acid or formic acid, maybe surfactants and so forth do not adsorb on the adsorbent whereas the physical-chemical properties of the cationic dyestuffs are much more favorable for adsorption.

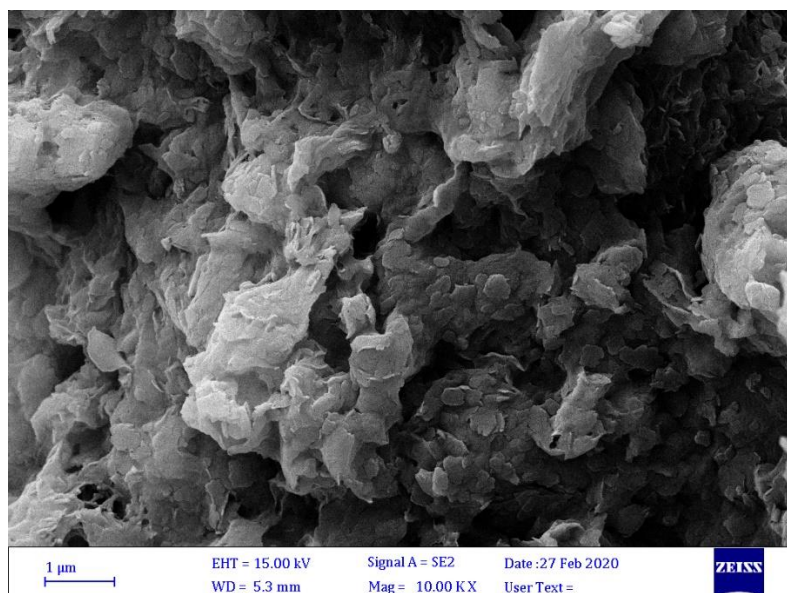


Fig. 69 Field emission scanning electron microscopic (FESEM) images of the spent *granular bentonite* (after adsorption)

The FESEM image of natural granular bentonite after the adsorption of dyes is shown in Fig. 69. The surface appears less porous and more homogeneous. This suggests that the dye molecules have penetrated into the pores and have “coated” the surface of granular bentonite, a prerequisite for an effective adsorption (127).

3.4.5 Fixed-bed column adsorption experiments

As a conclusion from the previous batch results, among the other investigated adsorbents of powdered bentonite, charred dolomite and vermicompost, the naturally occurring granular

bentonite was selected for the column tests. The reason for this selection was that the acrylic-textile dyeing wastewater to be decolorized only contains cationic (and no other) dyes. According to the previous experimental results conducted in this thesis, charred dolomite can merely adsorb the anionic dyes due to its positive surface charge. Regarding vermicompost, although it has a negative surface charge, its adsorption capacity achieved for cationic dyes was low. Powdered bentonite had a high adsorption capacity for cationic dyes due to its negative surface charge and high specific surface area.

The use of powdered clays in packed columns seemed to be not feasible since clays are made up of extremely fine particles, and their swelling capacity would likely result in substantial head losses and lead to clogging of the packed columns. Thus, to prevent the clogging effect in the column, the granular bentonite was selected to be used in the fixed-bed column tests rather than using the powdered bentonite.

As the breakthrough curves from the laboratory or the pilot-scale experiments are required to provide the principal information for the scale-up approach, several column tests were carried out to obtain the necessary data.

To study the ability of the natural mineral material “granular bentonite” to remove color from real textile wastewater tests were performed in a fixed-bed column reactor. The column was 1 m in height and had a diameter of 5 cm. The dependence of the flow rate and bed height on the removal efficiency of bentonite for color and COD was investigated.

The breakthrough curves for adsorption studies were constructed by plotting the normalized effluent color intensity C_1/C_0 (in mg L^{-1}); C_1 and C_0 are the effluent and influent dye concentrations, respectively, versus time t (in min) and throughput volume (in L).

Initially, different ranges of the flow rate with special focus on the head loss were analyzed with a column with a bed height of 5 cm, and finally, the flow rate range of 5 to 20 ml min^{-1} was selected for further experiments in order to determine the optimum flow rate.

3.4.5.1 Experimental breakthrough curves for different bed heights and flow rates

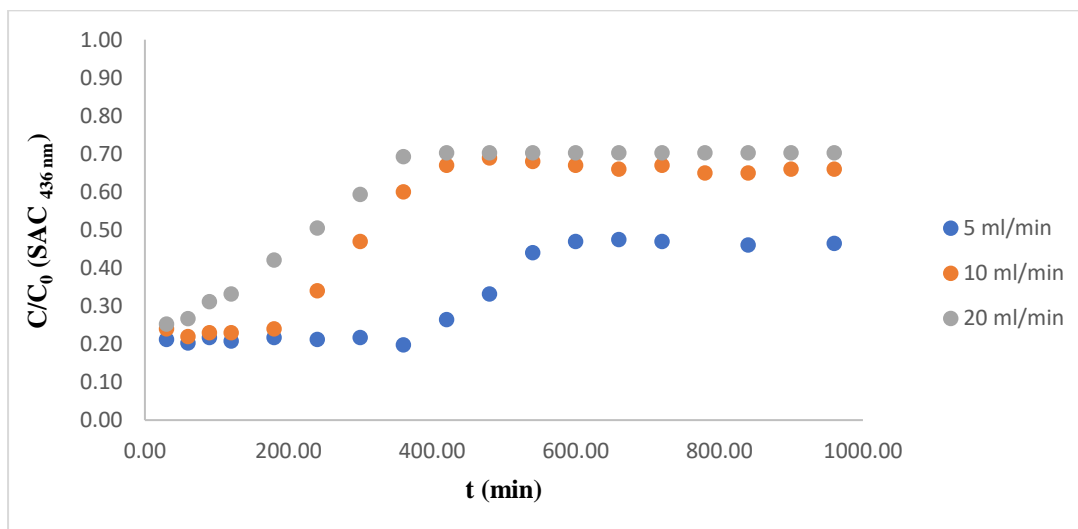


Fig. 70 Comparison of different breakthrough curves (C/C_0 versus time) at a constant bed height of 5 cm with different flow rates of 5, 10 and 20 ml min⁻¹, absorbance at SAC_{436 nm} (no pH adjustment, ambient temperature)

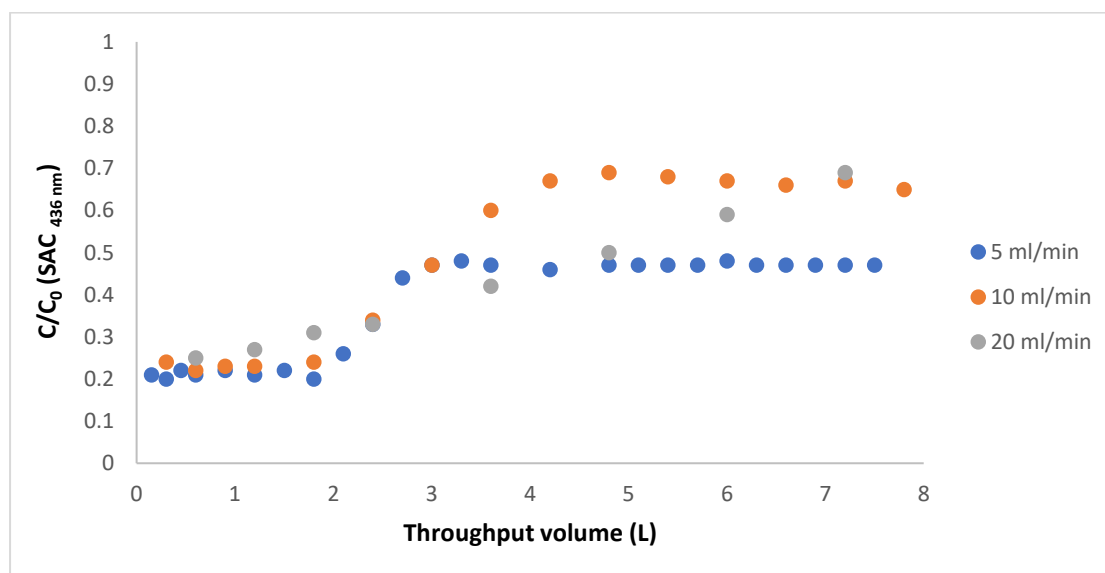


Fig. 71 Comparison of different breakthrough curves (C/C_0 versus throughput volume) at a constant bed height of 5 cm with different flow rates of 5, 10 and 20 ml min⁻¹, absorbance at SAC_{436 nm} (no pH adjustment, ambient temperature)

With reference to Fig. 70, breakthrough time and the exhaustion time of the color adsorption determined via SAC_{436 nm} with influent flow rate 5 ml min⁻¹ and a bed height 5 cm were 360 min and 600 min, respectively. Treated water volumes (V_b) at the breakthrough time and exhaustion time were found to be 1.8 L (see Fig. 71) and 3 L, respectively.

According to Fig. 70, breakthrough time and exhaustion time of the color adsorption determined via SAC_{436 nm} with influent flow rate 10 ml min⁻¹ and bed height 5 cm were 180 min and 420 min, respectively. Treated water volumes (V_b) at the breakthrough time and exhaustion time were found to be 1.8 L (see Fig. 71) and 4.2 L, respectively.

According to Fig. 70, breakthrough time and exhaustion time of the color adsorption determined via SAC_{436 nm} with influent flow rate 20 ml min⁻¹ and bed height 5 cm were 30 min and 360 min, respectively. Treated water volumes (V_b) at the breakthrough time and exhaustion time were found to be 0.6 L (see Fig. 71) and 7.2 L, respectively.

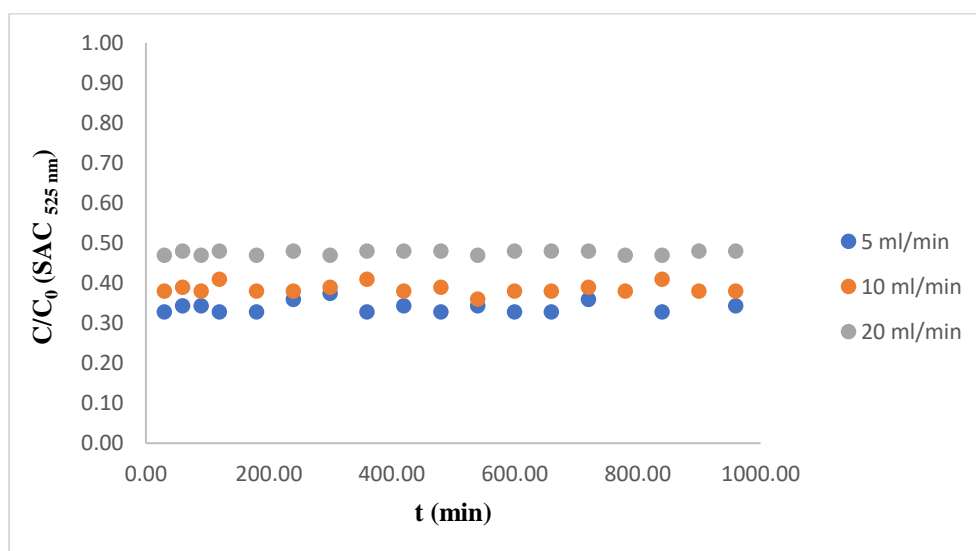


Fig. 72 Comparison of different breakthrough curves (C/C_0 versus time) at a constant bed height of 5 cm with different flow rates of 5, 10 and 20 ml min⁻¹, absorbance at SAC_{525 nm} (no pH adjustment, ambient temperature)

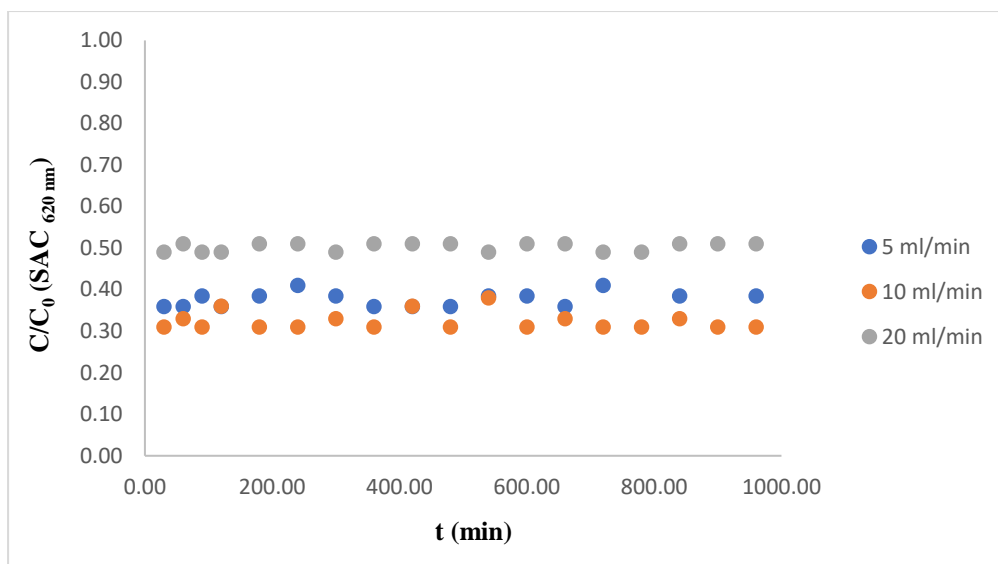


Fig. 73 Comparison of different breakthrough curves (C/C_0 versus time) at a constant bed height of 5 cm with different flow rates of 5, 10 and 20 ml min^{-1} , absorbance at $\text{SAC}_{620 \text{ nm}}$ (no pH adjustment, ambient temperature)

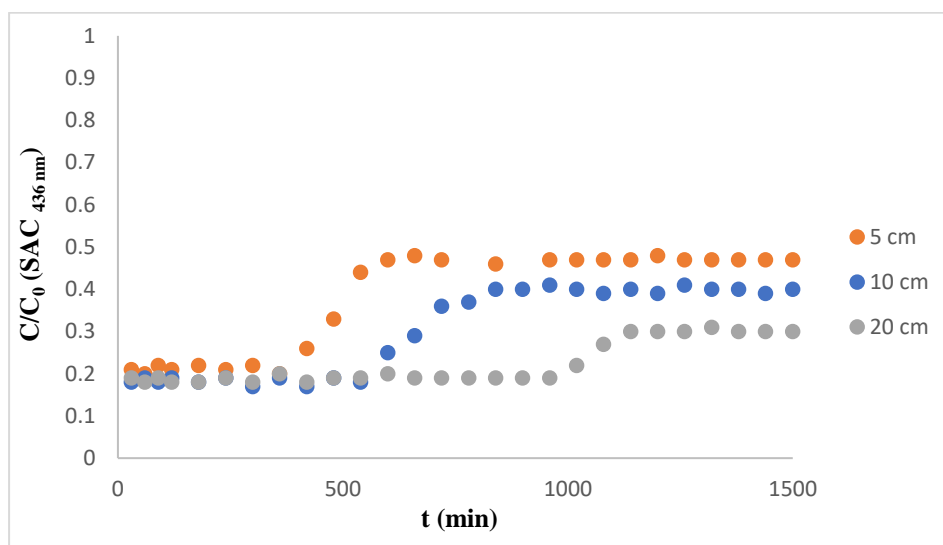


Fig. 74 Comparison of different breakthrough curves (C/C_0 versus time) at a constant flow rate of 5 ml min^{-1} with different bed heights of 5, 10 and 20 cm, absorbance at $\text{SAC}_{436 \text{ nm}}$ (no pH adjustment, ambient temperature)

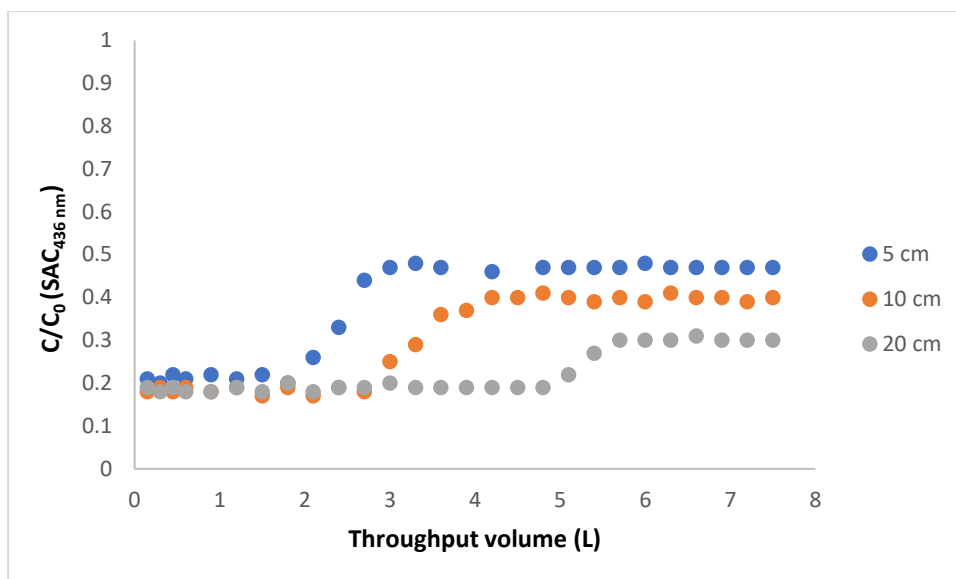


Fig. 75 Comparison of different breakthrough curves (C/C_0 versus throughput volume) at a constant flow rate of 5 ml min^{-1} with different bed heights of 5, 10 and 20 cm, absorbance at $SAC_{436\text{ nm}}$ (no pH adjustment, ambient temperature)

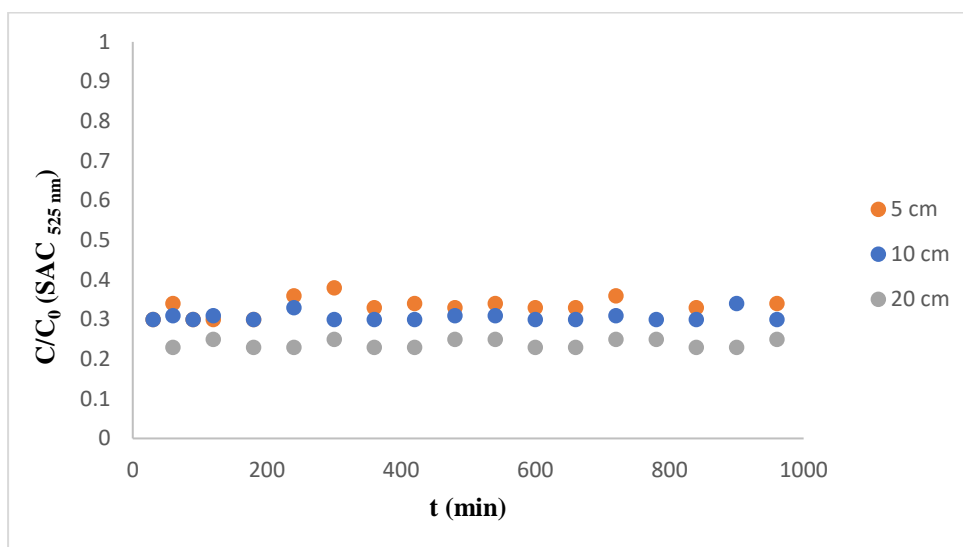


Fig. 76 Comparison of different breakthrough curves (C/C_0 versus time) at a constant flow rate of 5 ml min^{-1} with different bed heights of 5, 10 and 20 cm, absorbance at $SAC_{525\text{ nm}}$ (no pH adjustment, ambient temperature)

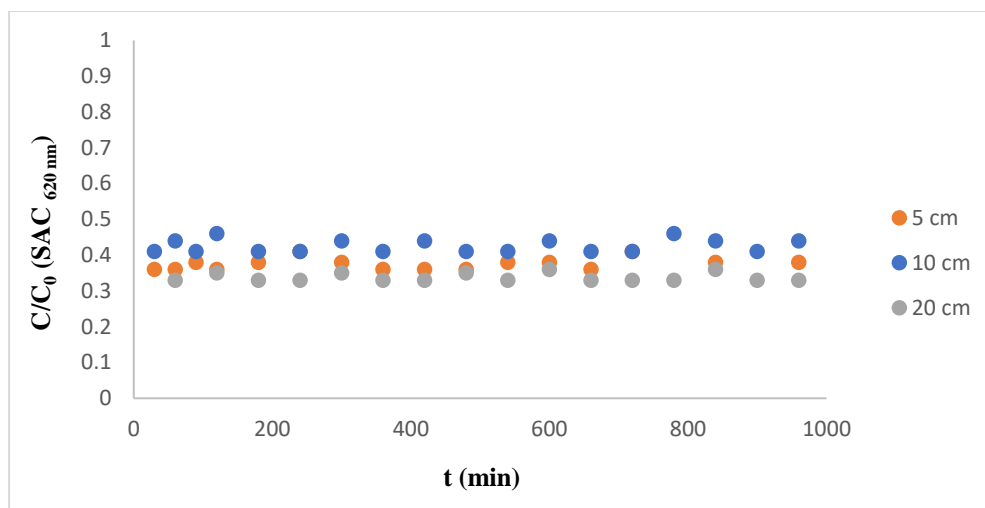


Fig. 77 Comparison of different breakthrough curves (C/C_0 versus time) at a constant flow rate of 5 ml min^{-1} with different bed heights of 5, 10, and 20 cm, absorbance at $\text{SAC}_{620 \text{ nm}}$ (no pH adjustment, ambient temperature)

Breakthrough times of the color removal using adsorbent bed heights of 5, 10 and 20 cm were 360, 540 and 960 min, for flow rate of 5 ml min^{-1} , respectively (See Fig. 74). The respective exhaustion times were 600, 840 and 1140 min. Treated water volumes (V_b) at the breakthrough time for adsorbent bed heights of 5, 10 and 20 cm were found to be 1.80 L, 2.70 L and 4.8 L for the flow rate of 5 ml min^{-1} , respectively (See Fig. 75). Furthermore, treated water volumes (V_e) at the exhausting time were 3 L, 4.2 L and 5.7 L for the flow rates of 5 ml min^{-1} , respectively.

3.4.5.2 Analysis of fixed-bed adsorption data

3.4.5.2.1 Dependence of adsorption efficiency on the flow rate

The column reactor with a filled with granular bentonite (bed heights: 5, 10 and 20 cm) was operated at three different flow rates of 5, 10 and 20 ml min^{-1} using the actual textile wastewater.

When wastewater is fed into the column, most of the mass transfer occurs near the bed inlet, where the fluid first contacts the material in column. The service time of the column, which can be defined as the time the adsorbed dye molecules break through the column bed and are detected in the effluent, is used to assess its overall performance for each bed volume of bentonite material. When the column is considered saturated, its operation can be terminated (129).

According to breakthrough curves, initially, there was no color in the effluent leaving the column samples until the breakthrough happened. After the breakthrough, an increasing

concentration of color was detected in the effluent. In other words, a relatively high removal of color was observed when the wastewater initially came in contact with the new porous adsorbent, this gradually changed with time until the breakthrough profile was developed. In fact, the breakthrough curves demonstrated an initial color removal followed by a gradual decrease with increasing time till saturation.

The colored wastewater as sorbate is continuously in contact with the given quantity of fresh granular bentonite as sorbent in the studied fixed-bed adsorption, providing the requisite concentration gradient between bentonite and cationic dyes for sorption. However, as the colored wastewater continuously enters and leaves the column, the equilibrium is never achieved at any stage (130).

The results of the experiments concerning the effect of different flow rates on the fixed-bed adsorption of color on granular bentonite showed that the parameter of flow rate affects the breakthrough curve (C/C_0 versus time or throughput volume). The breakthrough curves showed that at a lower flow rate of 5 ml min^{-1} the curves tended to be more gradual. In contrast, at relatively higher flow rates, i.e. 10 and 20 ml min^{-1} , the breakthrough curves were steeper. In conclusion, increasing the flow rate in the granular bentonite bed resulted in a decrease in color removal efficiency (see Fig. 70). This is due to the fact that at higher flow rates, the flow of the adsorption zone through the bed is faster which decreases the time for adsorption of dyes on the granular bentonite bed. Therefore, it can be concluded that a low contact time between the adsorbate and adsorbent leads to a reduction in the adsorption efficiency of the granular bentonite bed (113). In other words, the number of dyes adsorbed onto the adsorbent decreased with an increase in the flow rates, because the contact time between the solute in the fixed bed is directly related to the flow rate, and a large contact time will allow a higher amount of dye to be adsorbed. On the other hand, the concentration of color adsorbed onto the natural adsorbent increased with decreasing flow rates since the residence time of the solute in the fixed bed is directly proportional to the flow rate, and a longer residence time will allow a higher amount of dye to be adsorbed. In fact, the flow rate is an important parameter as it controls the contact time between the adsorbate and adsorbent surface. A decrease in the breakthrough time as well as the exhaustion time at a higher flow rate of 20 ml min^{-1} and at a lower bed length of 5 cm may be due to the rapid occupation the adsorption sites (9). In contrast, lower flow rate (5 ml min^{-1}) and higher bed height (20 cm) were found to improve the performance of the adsorption column due to the higher retention time facilitating sufficient contact time for efficient bonding of dye molecules to the active sites of the adsorbent and the diffusion processes of dye molecules into the pores; consequently, longer breakthrough and exhaustion times do result (Fig. 70 and Fig. 74).

In particular, the volumetric flow rate of the wastewater can affect the rate of change in bed capacity in two ways. The higher the volumetric flow rate of the liquid, the lower is the external film mass resistance on the surface of the adsorbent due to the additional velocity shear, thereby reducing the film thickness. At the same time, the residence time of wastewater in adsorbent bed decreases as the volumetric flow rate of the wastewater increases. This will reduce the time it takes for the adsorbed molecules to penetrate and diffuse into the center of the adsorbent.

Regarding the adsorption mechanism, cationic dyes carry positive charge which can enter into the precursor bentonite via cationic exchange reaction. In other words, cationic dyes are adsorbed on the clay via cationic exchange mechanism between cations and the exchangeable ions of bentonite. In conclusion, the uptake of cationic dyes on bentonite is carried out by both cation exchange and electrostatic attraction between the cation of dyes and negatively charged surface of bentonite (131).

3.4.5.2.2 Dependence of adsorption efficiency on the bed height

Figs. 70 and 71 suggest that a flow rate of 5 ml min^{-1} is an optimized flow rate for higher color removal efficiency.

Fig. 74 shows the breakthrough curves for columns with bed heights of 5, 10 and 20 cm operated at a constant flow rate of 5 ml min^{-1} . A higher adsorbent bed height means that due to the larger amount of the adsorbent being passed in sum a larger surface area for adsorption is available which should correlate also with an increased number of binding sites. Thus, the breakthrough point for lower bed heights can be reached - as expected - earlier than in the case of columns with larger ones. In other words, the breakthrough time and the saturation/exhaustion time both increased as the bed height from 5 to 20 cm was increased. This is due to the fact that the mass transfer zone had to travel farther from the bed's entry point to its exit point. At a longer bed height, the increase in the breakthrough time could be related to the moving time of the mass transfer zone and longer distance between two ends of the column (see Fig. 74). The mass transfer zone is the area where most of the concentration change happens. With increasing bed height, the slope of the breakthrough curve decreases, resulting in a broadened mass transfer zone. Due to the precedence of the axial dispersion over mass transfer when the bed height is reduced, the concentration of solute does not have enough time to diffuse into the entire bed of sorbent, decreasing solute diffusion (129).

The early exhaustion of the packed bed occurred with decreasing the bed height which caused the breakthrough curves to become steeper indicating faster saturation (600 min for the column with 5 cm bed height, 840 min for the one with 10 cm bed height and 1140 min

for the one with 20 cm bed height). The saturation time for the column with a higher mass of the adsorbent was greatly higher compared to the column with a lower amount of the adsorbent. The fact that more adsorption sites in a higher mass of the natural material are available results in the smaller gradient of its breakthrough curve.

The volume of the treated water at the breakthrough times and the exhausting times increased with an increase in bed height.

Concluding from the results of Fig. 74, the optimum conditions for the operation of the column with regard to the removal efficiency of color are: 20 cm bed height and a flow rate of 5 ml min⁻¹. At these parameters the breakthrough point was reached after 16 h and it lasted longest to reach the saturation point. At higher adsorbent bed height, a longer time was required for the available active sites of the adsorbent to be fully saturated resulting in a higher efficiency of adsorption. Therefore, breakthrough times and exhaustion times increased with the decrease of the flow rate and the increase of the adsorbent bed height.

The curves were similar to a classic “S-shaped” breakthrough curve at a lower flow rate (5 mL min⁻¹) suggesting a slower process and a higher color removal efficiency (9, 113).

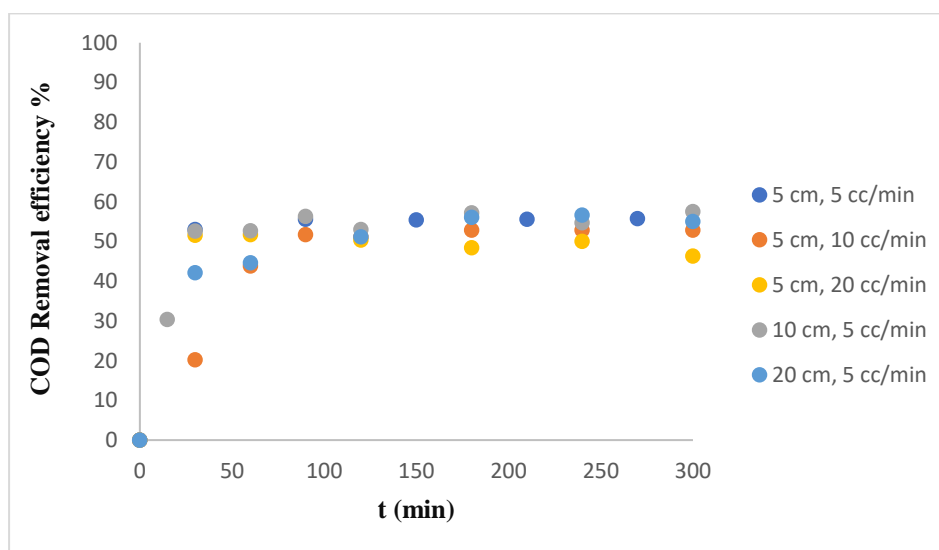


Fig. 78 Dependence of the COD removal efficiency of natural granular bentonite in columns of different bed heights (5, 10 and 20 cm) operated at various flow rates (5, 10 and 20 mL), (no pH adjustment, ambient temperature)

According to Fig. 78, for all bed heights the COD removal efficiencies were almost identical with slight differences at different flow rates. Thus, the amount of adsorbent did not have a major effect on the removal of the COD. At higher bed heights, COD removal is slightly

greater due to the longer residence time (higher contact time between the adsorbent and the adsorbate).

One of the advantages in using natural granular bentonite for the treatment of wastewater in a fixed-bed column is that due to the expansion (swelling) of the granular bentonite package observed in the column, the adsorbent gets more effectively packed, thereby decreasing the channeling along the walls of the column and between individual particles. This leads to better contact and interaction with the bulk solution, enhancing the mass transfer of the dye molecules which reduces the concentration of the dye in effluent (9).

3.4.6 Reuse of the treated textile wastewater in the studied textile industry

To comply with reuse requirements in the AquaFit4Use project mentioned in Table 9, the color of the treated effluent should be below certain detection limits ("non-visible") for all kinds of reuse waters (low- to high-quality water). According to the results, the effluent at the breakthrough point treated in the fixed-bed column (20 cm adsorbent height, 5 ml min⁻¹ flow rate) not only fulfils the requirement for reuse in textile processing (non-visible) (see Fig. 79) but it also meets German and Iranian legal requirements for discharge. To compare and comply with Iranian legislation for discharge, the color should be lowered from 456 to 75 mg Pt-Co L⁻¹. By treatment in the fixed-bed adsorption column, 32 mg Pt-Co L⁻¹ was reached which is below the determined limit demanded by Iranian standards. The color of the treated effluent reduced as determined via SAC went down from 20.2 to 3.9 for SAC_{436 nm}, from 6.4 to 1.5 for SAC_{525 nm} and from 3.9 to 1.4 for SAC_{620 nm}, this also fulfils German discharge limits.

The COD of the effluent after treatment in the fixed-bed column decreased from 890 mg L⁻¹ to 382 mg L⁻¹ which meets the allowed COD range for "low-quality water" mentioned in Table 9.

There is no limitation for the parameter "conductivity" in "low- to high-quality water" requirements determined by the AquaFit4Use project. Nevertheless, the conductivity of the effluent after treatment reached 1565 μS m⁻¹ (initial value: 2113 μS m⁻¹) and the pH reached 8.15 (initial value: 11.69). Thus, the parameter conductivity fulfils the "general water reuse" limitation and the pH meets the requirements for "medium- to low-quality water" (Table 9).

To comply with the heavy metal concentration limit of the "low-quality water", Fe, Cu and Cr should be below 0.1, 0.05 and 0.1 mg L⁻¹, respectively according to the reuse limitations in Table 9. The measurements of heavy metals by ICP AES for the treated wastewater after the fixed-bed adsorption showed that the Cu concentration (0.02 mg L⁻¹) is below the standard limit and the Cr concentration (0.12 mg L⁻¹) is almost equal to the suggested limit

value. However, Fe (1.97 mg L^{-1}) (this higher value might be ascribed to the addition of FeCl_3 to wastewater in coagulation-flocculation process) exceeded the reuse requirements for “low-quality water” suggested in the AquaFit4Use project. The concentration of heavy metals of the water for “fibers rinsing” (pretreatment step before dyeing) which is reused several times for washing the fibers, washing down the equipment, and for washing the floor in the Acryl Tab company were measured to be 0.005 mg L^{-1} for Cu, 0.05 mg L^{-1} for Cr and 0.937 mg L^{-1} for Fe. The results showed that the concentration of Fe in the treated water from the continuous fixed-bed adsorption system is close to the value measured in the water used for the pretreatment step. However, recycled water can only be used for very low-quality purposes. Besides, the total hardness of the treated water was measured to be $340 \text{ mg CaCO}_3 \text{ L}^{-1}$ which is higher than the required reuse standard limit suggested by the AquaFit4Use project ($100 \text{ mg CaCO}_3 \text{ L}^{-1}$). However, in the Acryl Tab company, the reused water (for washing the fibers in the pretreatment step) showed a higher value for the total hardness ($345 \text{ mg CaCO}_3 \text{ L}^{-1}$; the average value between 220 and $480 \text{ mg CaCO}_3 \text{ L}^{-1}$) than the standard limit. It should be noted that the COD of the reused water for the pretreatment bath measured was 6500 mg L^{-1} (average value between 5870 mg L^{-1} and 7650 mg L^{-1}) which not only is much higher than the proposed COD reuse limit in the AquaFit4Use project but also it is higher than the COD of the treated wastewater obtained from the adsorption process using granular bentonite. The chloride concentration of the treated wastewater from the adsorption process was 84.2 mg L^{-1} which is much less than that of the standard limit for high quality water (500 mg L^{-1}). The chloride amount in the reused water of the studied industry was 303.2 mg L^{-1} .

Therefore, the treated water obtained after the fixed-bed adsorption process can be recommended to be used in the studied industry for rinsing the fibers in the pretreatment step, washing down the equipment and washing the floors.



Fig. 79 Treated real acrylic fiber dyeing wastewater using fixed-bed column
(Laboratory of Water and Wastewater Treatment at Azad University in Iran)



Fig. 80 Pretreatment of the fibers in the Acryl Tab CO.

(photo: E. Khalilzadeh Shirazi)

3.4.7 Fixed-bed column design by the scale-up approach

The purpose of this part of the work was to suggest a design for an up-scaled packed-bed column based on the pilot-scale experimental data, i.e. the breakthrough curve parameters.

The data used in the following calculations were obtained from different experimental pilot-scale columns with different bed heights (5, 10 and 20 cm). The treated water at breakthrough points of all bed heights was concluded suitable to be used for reuse in washing purposes (as low-quality process water according to the Aquafit4use project) in the studied industry.

A breakthrough curve is shown in Fig. 74. The data used in the following calculations was obtained from an experimental pilot-scale column (5 cm bentonite bed height) operated at 3.06 BV/h. Other data related to the pilot-scale column are as follows: inside diameter: 5 cm, length: 1 m, mass of granular bentonite 0.11 kg and packed carbon density 1120 kg/m³. The scale-up approach was used to determine the design bed volume in m³, the design mass of granular bentonite required in kg, the breakthrough time (T) in hours and/or days and the breakthrough volume (V_B) in m³.

The wastewater flow rate in the Acryl Tab company is 150 m³ d⁻¹.

- 1) Bed volume of the design column:

$$\text{Bed volume (BV)} = Q/Q_b$$

Q = design liquid flow rate

Q_b = liquid flowrate in terms of bed volumes per unit time

$$= 150 \text{ m}^3/24 \text{ h}/3.06$$

$$= 2.04 \text{ m}^3$$

The liquid flowrate in terms of bed volumes per unit time (Q_b) was obtained 3.06 which the value of Q_b is usually from 0.2 and 3.0 bed volumes per unit time (68).

- 2) Mass or weight of the adsorbent for design column

$$M = (BV)(\rho_s)$$

Bulk density of the adsorbent: 1120 kg/m³

$$= 2.04 \text{ m}^3 * 1120 \text{ kg/m}^3$$

$$= 2287 \text{ kg}$$

- 3) Volume of liquid treated per unit mass of adsorbent

$$V^B = V_B/M$$

V_B = breakthrough volume (L)

M = adsorbent mass in pilot column (kg)

$$= 1.8 / 0.11 \text{ L/kg}$$

$$= 16.36 \text{ L/kg}$$

4) Mass of the adsorbent exhausted per hour for design column

$$M_t = Q/V^B$$

$$= 150 \text{ m}^3/24 \text{ h} * \text{kg}/16.36 \text{ L} * 1000 \text{ L/m}^3$$

$$= 381.25 \text{ kg/h}$$

5) Breakthrough time for design column

$$T = M/M_t$$

$$= 2287 \text{ kg}/381.25 \text{ (kg/h)}$$

$$= 6 \text{ h}$$

6) Breakthrough volume for design column

$$V_B = QT$$

$$= 150 \text{ m}^3/24 \text{ h} * 22.42 \text{ h}$$

$$= 37.5 \text{ m}^3$$

7) Adsorbent volume and height in the design column

$$\text{Volume} = (2287 \text{ kg}) (1 \text{ m}^3/1120 \text{ kg})$$

$$= 2 \text{ m}^3$$

$$\text{Adsorbent height} = (2 \text{ m}^3) (4/\pi) (1/2 \text{ m})^2$$

$$= 0.63 \text{ m}$$

According to the data obtained from the above calculations, the design column can treat 37.5 m^3 of wastewater in 6 hours using 2287 kg of bentonite which is required for the treatment of wastewater with a flow rate of $150 \text{ m}^3 \text{ d}^{-1}$. In total, 9148 kg of bentonite is required for wastewater treatment in 24 hours at the Acryl Tab company. As the company works mainly in 2 shifts (16 h), 6098 kg of bentonite is needed in practice.

The data used in the following calculations was obtained from an experimental pilot-scale column (10 cm bed height) operated at 1.53 BV/h. Other data related to the pilot-scale column are as follows: inside diameter: 5 cm, length: 1 m, mass of granular bentonite 0.22 kg and packed carbon density 1120 kg/m^3 .

1) Bed volume of the design column:

$$\text{Bed volume (BV)} = Q/Q_b$$

Q = design liquid flow rate

Q_b = liquid flowrate in terms of bed volumes per unit time

$$= 150 \text{ m}^3/24 \text{ h} / 1.53$$

$$= 4.08 \text{ m}^3$$

2) Mass or weight of the adsorbent for design column

$$M = (BV)(\rho_s)$$

Bulk density of the adsorbent: 1120 kg/m^3

$$= 4.08 \text{ m}^3 * 1120 \text{ kg/m}^3$$

$$= 4569.6 \text{ kg}$$

3) Volume of liquid treated per unit mass of adsorbent

$$V^B = V_B/M$$

V_B = breakthrough volume (L)

M = adsorbent mass in pilot column (kg)

$$= 2.7/0.22 \text{ L/kg}$$

$$= 12.27 \text{ L/kg}$$

4) Mass of the adsorbent exhausted per hour for design column

$$M_t = Q/V^B$$

$$= 150 \text{ m}^3/24 \text{ h} * \text{kg}/12.27 \text{ L} * 1000 \text{ L/m}^3$$

$$= 509.37 \text{ kg/h}$$

5) Breakthrough time for design column

$$T = M/M_t$$

$$= 4569.6 \text{ kg}/102 \text{ (kg/h)}$$

$$= 9 \text{ h}$$

6) Breakthrough volume for design column

$$V_B = QT$$

$$= 150 \text{ m}^3/24 \text{ h} * 9 \text{ h}$$

$$= 56.25 \text{ m}^3$$

7) Adsorbent volume and height in the design column

$$\text{Volume} = (4569.6 \text{ kg}) (1 \text{ m}^3/1120 \text{ kg})$$

$$= 4 \text{ m}^3$$

$$\begin{aligned} \text{Adsorbent height} &= (4 \text{ m}^3) (4/\pi) (1/2 \text{ m})^2 \\ &= 1.27 \text{ m} \end{aligned}$$

According to the data obtained from the above calculations, the design column can treat 56.25 m³ of wastewater in 9 hours using 4569.6 kg of bentonite which is required for the treatment of wastewater with a flow rate of 150 m³ d⁻¹. In total, 12185.6 kg of bentonite is required for wastewater treatment in 24 hours at the Acryl Tab company. As the company works mainly in 2 shifts (16 h), 8123.73 kg of bentonite is needed in practice. However, it can be a high quantity to handle and to process.

The data used in the following calculations was obtained from an experimental pilot-scale column (20 cm bed height) operated at 0.765 BV/h. Other data related to the pilot-scale column are as follows: inside diameter: 5 cm, height: 1 m, mass of granular bentonite 0.47 kg, packed bentonite density 1120 kg/m³.

- 1) Bed volume of the design column:

$$\text{Bed volume (BV)} = Q/Q_b$$

Q = design liquid flow rate

Q_b = liquid flowrate in terms of bed volumes per unit time

$$\begin{aligned} &= 150 \text{ m}^3/24 \text{ h} * 1/0.765 \\ &= 8.17 \text{ m}^3 \end{aligned}$$

The liquid flowrate in terms of bed volumes per unit time (Q_b) was obtained 0.765 which the value of Q_b is usually from 0.2 and 3.0 bed volumes per unit time (73).

- 2) Mass or weight of the adsorbent for design column

$$M = (\text{BV})(\rho_s)$$

Bulk density of the adsorbent: 1120 kg/m³

$$\begin{aligned} &= 8.17 \text{ m}^3 * 1120 \text{ kg/m}^3 \\ &= 9150.4 \text{ kg} \end{aligned}$$

- 3) Volume of liquid treated per unit mass of adsorbent

$$V^B = V_B/M$$

V_B = breakthrough volume (L)

M = adsorbent mass in pilot column (kg)

$$\begin{aligned} &= 5.1/0.47 \text{ L/kg} \\ &= 10.85 \text{ L/kg} \end{aligned}$$

- 4) Mass of the adsorbent exhausted per hour for design column

$$\begin{aligned}
 M_t &= Q/V^A B \\
 &= 150 \text{ m}^3/24 \text{ h} * \text{kg}/10.85 \text{ L} * 1000 \text{ L}/\text{m}^3 \\
 &= 575 \text{ kg/h}
 \end{aligned}$$

- 5) Breakthrough time for design column

$$\begin{aligned}
 T &= M/M_t \\
 &= 9150.4/575 \text{ (kg/kg)} \\
 &= 16 \text{ h}
 \end{aligned}$$

- 6) Breakthrough volume for design column

$$\begin{aligned}
 V_B &= QT \\
 &= 150 \text{ m}^3/24 \text{ h} * 16 \text{ h} \\
 &= 100 \text{ m}^3
 \end{aligned}$$

- 7) Adsorbent volume and height in the design column

$$\begin{aligned}
 \text{Volume} &= (9150.4 \text{ kg}) (1\text{m}^3/1120 \text{ kg}) \\
 &= 8.17 \text{ m}^3 \\
 \text{Adsorbent height} &= (8.17 \text{ m}^3) (4/\pi) (1/8.17 \text{ m})^2 \\
 &= 1.27 \text{ m}
 \end{aligned}$$

According to the data obtained from the above calculations, the design column can treat 100 m³ of wastewater in 16 hours using 9150.4 kg of bentonite which is required for the treatment of wastewater with a flow rate of 150 m³ d⁻¹. In total, 13725.6 kg of bentonite is required for wastewater treatment in 24 hours at the Acryl Tab company. As the company works mainly in 2 shifts (16 h), 9150.4 kg of bentonite is needed in practice.

Column diameter and column area, if the design column has a unit flow rate of 2.04 l/m²-s, are as follows:

$$\begin{aligned}
 D &= ((150 \text{ m}^3/\text{d}) (\text{d}/86400 \text{ s}) (\text{s}-\text{m}^2/2.04 \text{ l}) (1000 \text{ l}/\text{m}^3) (4/\pi))^{1/2} \\
 &= 1.04 \text{ m} \\
 &= \pi D^2/4 \\
 &= 0.84 \text{ m}^2
 \end{aligned}$$

The design column has an area A of 0.84 m² and diameter d of 1.04 m.

With respect to geometric considerations, a fixed-bed column is desirable to have a large height-to-diameter ratio (H/D). By increasing this ratio, the percent usage of the maximum

capacity of the adsorbent increases. Normally, H/D is between 3:1 to 5:1 and the unit liquid loading (hydraulic loading rate) is usually between 2.7 to 6.8 l/s-m².

As H/D of the column is usually between 3:1 to 5:1 (78), the height of the design column can be between 3.12 m and 5.2 m (73).

One of the aims of this thesis was to investigate the possibility of reusing the treated wastewater as process water in the studied industry. As the quality of the treated water at breakthrough points of all bentonite bed heights (5, 10 and 20 cm) fulfilled the requirements of water reuse (low-quality water for washing purposes based on the Aquafit4use project), the amount of bentonite scaled up from the pilot-scale column with 5 cm bed height will be reasonable to be considered for industry from the economic point of view.

With regard to the cost analysis, each kilogram of bentonite from the mine provided for this study costs 450 toman (1.34 cent). Supply of 6098 kilogram of bentonite per day which can treat wastewater generated from 2 working shifts of the textile company costs 82 euro (calculated for the design column based on the pilot-scale column with 5 cm bed height). Supply of 9148 kilogram of bentonite per day which can treat wastewater generated from 3 working shifts (sometimes the company produces in maximum working shifts, 24 hours) of the textile company costs 123 euro.

3.5 Reuse of the spent adsorbent in the production of LWAs

The chemical composition of the spent adsorbent determined by using XRF for the analysis of major elements is shown in Table 22.

Results and Discussion

Table 22 Characterization of the natural granular bentonite before and after adsorption; chemical constituents as determined with XRF and elemental analysis (in weight %)

Parameter	Before adsorption	After adsorption
Content of oxides*		
in % wt		
SiO ₂	59.87	59.03
Al ₂ O ₃	11.01	11.0
K ₂ O	3.61	3.71
CaO	6.25	6.53
MnO	0.18	0.19
Fe ₂ O ₃	5.48	20.78
Na ₂ O	0.87	0.83
MgO	2.81	2.71
LOI in %	8.86	10.86
TOC in mg kg ⁻¹	548	1807

* determined with XRF and elemental analysis

The SiO₂/ΣFlux ratio can be used to determine the ability of the green granules to bloat. If this ratio is ≥ 2 , sintering can produce a material with a favorably high viscosity. This ratio is an indicator of the suitable chemical characteristics for the expansion of a material when the gases evolve during the firing (18, 90, 115, 132).

According to the SiO₂/ΣFlux ratio, the percentages of SiO₂ and the fluxing agents (CaO + MgO + Na₂O + K₂O + Fe₂O₃ + FeO) related to the spent adsorbent (granular bentonite) and raw granular bentonite should be measured in order to evaluate their suitability for expansion in the production process of LWAs. In addition, real trials were carried out to verify the true propriety of the materials for bloating.

The flux content (defined as the weighted sum of Fe₂O₃, Na₂O, K₂O, CaO and MgO) for the raw and spent material was calculated. As the SiO₂/ΣFlux ratio for the raw adsorbent is ≥ 2 and the calculated ratio for the spent adsorbent is about 2, sufficient viscous phases are

therefore expected to be formed within the sintering of LWAs for the entrapment of a significant amount of the gaseous compounds released.

Furthermore, the granular bentonite adsorbent contains quartz, muscovite and feldspar (Fig. 46) which with reference to the literature, can promote the bloating process by forming a liquid phase when sintered and reduce the density of the granulates. In addition, the presence of these mineral phases improves the sintering process and the gas entrapment (93, 94).

Moreover, most clay minerals have shown bloating and can be utilized to make LWAs. It has been suggested that illitic clays are more effective than kaolinitic clay at trapping CO₂ from carbonate decomposition. With reference to the literature, the major minerals of expanding clays can be different in their quantities of smectite, illite, quartz, kaolinite and various related minerals which can be seen in XRD of the adsorbent (Fig. 46) (18).

Besides, as the organic materials present in the spent granular bentonite, carbon reacts with oxygen, CO₂ and other gases like CO, H₂O, H₂, O₂, SO₂ or Cl₂ can be formed in the process and remain captured in the granules assisting in more expansion of the granules (114).

Both granular bentonite samples, used and unused, contained a significant amount of SiO₂ (59%) (Table 22), which is responsible for the glassy phase of the ceramic products which directly affects the compressive strength of the LWAs. In addition, the spent adsorbent showed a higher degree of loss on ignition (LOI) (increased from ca. 8.8% in unused granular bentonite to 10.8% after color adsorption) which can be a consequence of the elevated content of organic matter, originating from the textile wastewater. It contributes to the formation of gases leading to pores inside the granules (133).

Based on these results it can be expected that the spent granular bentonite is suitable for the production of LWAs due to its feature of bloating and other physical-chemical properties.

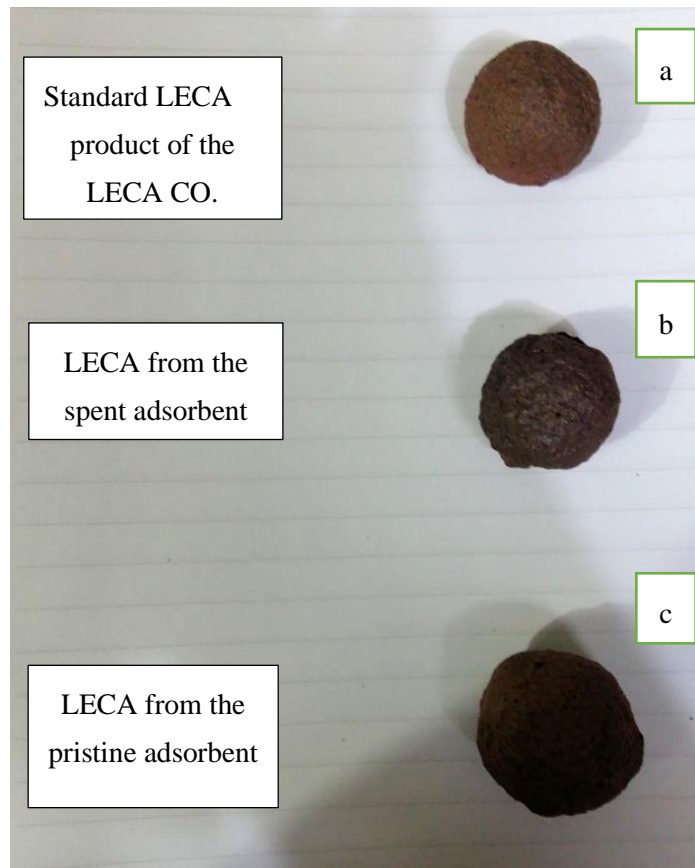


Fig. 81 (a) Produced LWAs from the natural clay (standard LECA), (b) from the spent adsorbent (granular bentonite), (c) from the pristine adsorbent (granular bentonite)

LWAs made from the spent granular bentonite had lower densities compared to the LWAs made from the "standard" clay from LECA CO. This can be attributed to the adsorbed organic substances in the spent material which decompose during the sintering process. The generation of porous beads and the development of a more porous structure of the aggregate are both influenced by further evolved gases, i.e. the porosity of the aggregates increases. This leads to the observed slight increase in water absorption.

In addition, LWAs when made with the spent granular bentonite showed a compressive strength (1.03 N/mm^2), water absorption (20%) and density 1.4 comparable with the standard LECA produced in the LECA CO. (1.3 N/mm^2 for compressive strength, 17% for water absorption and 1.8 g/cm^3 for density) which both were in the standard range at LECA CO.

In the LECA company, the standard range of compressive strength is between 1.4 to 1 N/mm^2 . The standard range of particle density is between 1.30 and 2.00 g/cm^3 . The standard range of water absorption is between 17 and 24%.

Results and Discussion

Comparing the standard LWAs and the lightweight aggregates produced with the mixtures of raw clay soil/spent materials, the addition of spent granular bentonite to clay soil can promote the development of pores and decrease the density of the produced LWAs; consequently, enhance the water absorption.

Table 23 Properties of lightweight aggregates produced with different percentages of natural clay (LECA CO; standard) and granular bentonite (granular bentonite; before and after usage for adsorption)

Clay used in the LWAs production process	Percentage of clay types used (%)	Density (g/cm ³)	Water absorption (%)	Compressive strength (N/mm ²)
Natural raw material	100% natural clay	1.80	17	1.3
	100% granular bentonite	2.04	21.33	0.93
Waste material (spent granular bentonite)	100% spent granular bentonite	1.40	20	1.03
	90% natural clay + 10% raw granular	1.67	22	0.9
Natural clay + raw granular bentonite	80% natural clay + 20% raw granular	1.55	21	0.9
	70% natural clay + 30% raw granular	1.50	18	0.8
	60% natural clay + 40% raw granular	1.47	18	1.2
	90 natural clay + 10% spent granular	1.78	21	1.0
Natural clay + waste material (spent granular bentonite)	80 natural clay + 20% spent granular	1.75	20	1.0
	70% natural clay + 30% spent granular	1.59	19	1.1
	60% natural clay + 40% spent granular	1.58	19	1.1
	90 natural clay + 10% spent granular	1.78	21	1.0

Results and Discussion

In general, the products (LWAs) made with the spent material are comparable to those made with the standard natural clay in terms of physical properties such as compressive strength, water absorption and density.

According to literature, at temperatures between 1100 °C and 1150 °C, organic matter is completely destroyed, and gases are formed which are responsible for the microstructure of LWAs with their high porosity.

With reference to the *Air Pollution Control Technology Fact Sheet* (EPA-452/F-03-022), between 590 °C and 650 °C, thermal destruction of most organic compounds already occurs. Moreover, it has been reported that most hazardous waste incinerators are operated at temperatures between 980 °C and 1200 °C to ensure almost complete destruction of the organics in the waste. Therefore, considering the temperature profile of the production process of LWAs at the LECA factory (see Fig. 39), almost all organic materials are destroyed in the generation process of expanded granules.

The outcome of the technical investigation proves the usefulness of the spent adsorbent to be applied in textile wastewater treatment for the production of relatively high-quality LWAs (84, 86, 134).

Table 24 Heavy metals in the produced sintered lightweight aggregate made of the spent adsorbent (determined by ICP-AES)

Heavy metals	wt. %
As	< 0.003
Ti	0.0285
Zr	0.0225
Ca	2.7518
Co	0.0048
Cr	0.0335
Cu	0.0051
Fe	7.9183
K	0.0707
Mg	2.4876

Results and Discussion

Heavy metals	wt. %
Na	0.7383
Ni	0.0024
Pb	0.0006
Zn	0.0097
Mn	0.0280
Sr	0.0341
Ba	0.0102

Within this context, considering specific applications for the produced LWAs from the spent adsorbent is of crucial importance. In the case of LWAs production in the LECA CO., the main application is in cement-bound products such as concrete blocks. The application of the spent adsorbent in LWAs which are used in agriculture should be avoided due to the direct contact of the LWAs with water.

It should be noted that the low leachability of contaminants/heavy metals typically observed is a significant advantage of incorporating polluted wastes into synthetic aggregates. It has been reported that the leaching of metals from cement-based materials is barely considered an issue. When LWAs are used as gravels in the production of concretes, the sensitivity of aggregates to external pH influences has no further consequences on the leaching behavior of LWAs. But when the aggregate is not used in bound form in different applications such as concrete, the influences of external pH is required to be considered, which may impose specific limitations on its application in acidic environments (18, 88, 135, 136).

In addition, from an environmental point of view, the sintering process at high temperatures (>1000 °C) leads to the destruction (organic compounds) or the immobilization (inorganic compounds like heavy metals) of hazardous components (21, 91, 137). During sintering at high temperatures, leachable heavy metals and other soluble substances present in the waste material is encapsulated in the silicate-based matrix or may replace other ions in the crystal structure or vitreous phases, rendering them non-leachable (90). In fact, in vitrified (glassy) phases formed by thermal treatment, chemical components are physically encapsulated and are usually not mobilized by leaching processes into the environment.

Some researchers observed a considerable immobilization of most of the studied contaminating rare-earth elements and metals in the body of LWAs.

Giro-Paloma et al. (2019) studied sintered granulates made of weathered bottom ash from a municipal solid waste incinerator and rice husk. They claimed that the permeability of contaminants in the large fraction (particle diameter > 8 mm) of the sintered granulates into water decreased due to the formation of the outer vitreous layer which waterproofs the inner layer, thereby reducing the release of contaminants (137).

Furthermore, Ju et al. (2017) drew the conclusion that the sintering process causes immobilization of potentially hazardous metals in LWAs produced from red mud and limestone, gold mine tailings, and thus, a lower risk for contamination of the environment exists when using these LWAs for construction (138).

Guoren Xu et al. (2013) who made an investigation on the stabilization of heavy metals in a lightweight aggregate made from river sediment and sewage sludge claimed that even when the broken LWAs with particle diameter like 2 mm were saturated with an acid solution, the solidification efficiency of heavy metals was greater than 95%. This means that strong chemical bonds within the silicate or aluminosilicate matrix in the sintered LWA were formed, making it difficult for heavy metals to leave the LWA and to cause harmful environmental effects (139).

3.6 Life cycle assessment (LCA) and Monte Carlo analysis for comparing textile wastewater treatment with bentonite and activated carbon

Based on the Monte Carlo analysis for determining an approximate amount of activated carbon in relation to the obtained amount of bentonite from pilot-scale experiments, a lognormal distribution and a mean specific surface area of 1080.5 g/m² (assumption cell) were concluded. To specify, in relation to 13 tons of granular bentonite (specific surface area of 40 g/m²) concluded from the scaled-up experimental results for the treatment of 150 m³ of the acrylic fiber-dyeing wastewater per day, Monte Carlo simulation was applied to estimate the relative required amount of activated carbon with mean specific area of 1080.5 g/m². The statistical analysis of Monte Carlo on the forecast cell resulted 3.81 as the mean kg of activated carbon with standard deviation of 6.32 for the treatment of 1 m³ wastewater after running repeated analyses with random input values (100000 iterations) based on the lognormal probability analysis. Although 6 tons of bentonite based on 5 cm bentonite bed height at pilot-scale experiments fulfilled the water reuse purposes in the studied company, for LCA studies the worst scenario with regard to the amount of bentonite (13 tons) was considered to increase the validity of the investigation.

In the scenario of "spent activated carbon landfilling", the production of 3.81 kg of granular activated carbon for the treatment of 1 m³ colored pretreated wastewater was considered.

The scenario of "spent bentonite landfilling" includes the extraction of 86.6 kg granular bentonite from the mine which was concluded for the treatment of 1 m³ colored wastewater.

Results of the comparison of 4 waste management scenarios related to the treatment of 150 m³ pretreated textile wastewater treatment are as follows:

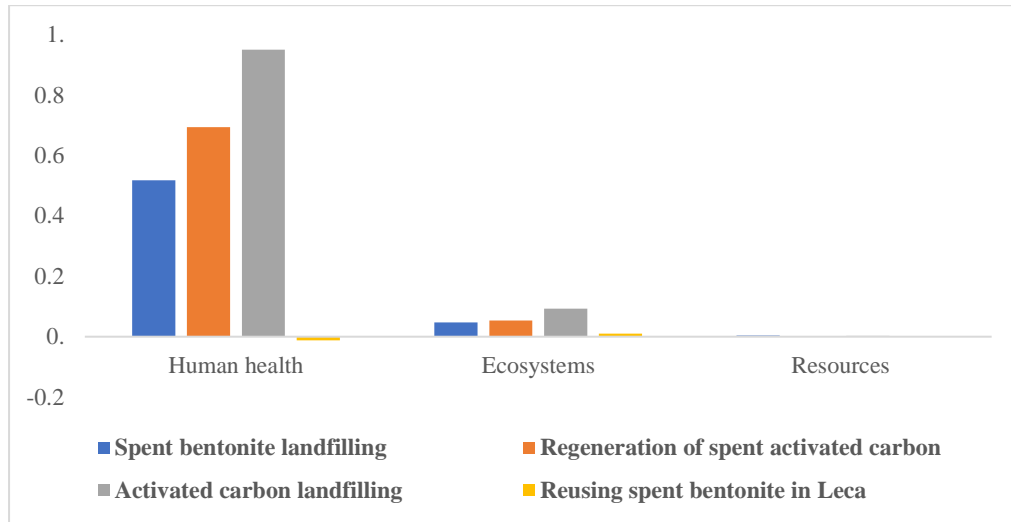


Fig. 82 Comparison of the scenarios - Impact characterization with ReCiPe 2016 v1.1 Endpoint (H).

According to the inventory data, single score results show environmental burden related to all compartments of emissions to air, soil, water and other parts such as raw material extraction and the like. Results (Fig. 82) indicated that the lowest environmental impact is pertaining to the scenario of reusing bentonite in LECA (single score: 1.81) but regeneration of activated carbon concluded 235 which it is about 130 times worse than reusing the spent bentonite in LECA production. On the other hand, to compare two landfilling scenarios, environmental burden of the spent bentonite landfilling with single score 180 is about half of the activated carbon landfilling with single score of 332.

The comparison between AC and bentonite revealed that the latter is a more environmentally friendly and cheaper alternative for the treatment of the acrylic fiber dyeing wastewater. The most affected environmental categories were human health and ecosystem.

In conclusion, the application of natural bentonite for the treatment of the pretreated textile wastewater to obtain a treated water suitable for water reuse as the process water in the studied industry concluded to be an economically and efficiently attractive option compared to activated carbon.

In order to study more precisely, two more scenarios were defined in SimaPro to compare the environmental impacts of the production of 3.81 kg granular activated carbon with production of 86.6 kg granular bentonite which both were already concluded for the treatment of 1 m³ textile wastewater.

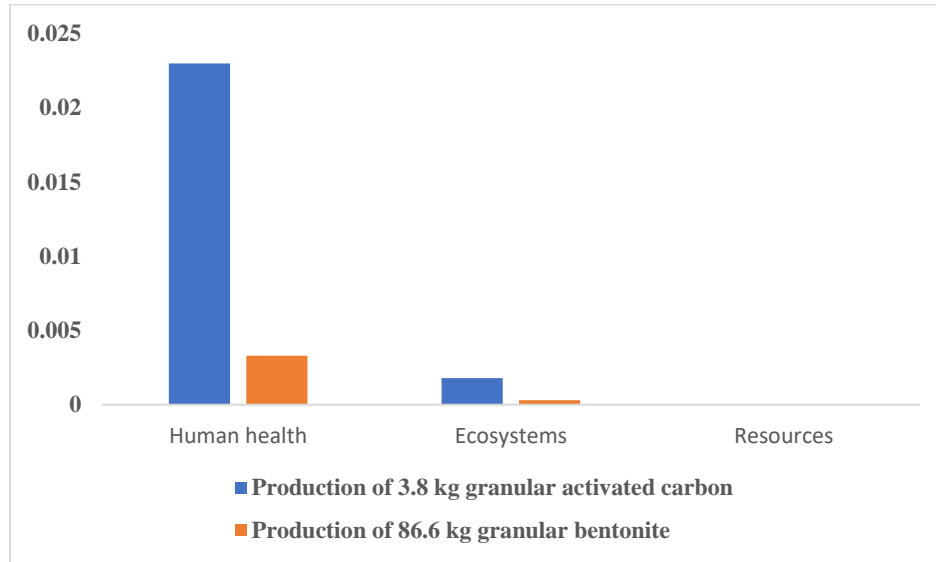


Fig. 83 Comparison of the scenarios - Impact characterization with ReCiPe 2016 v1.1 Endpoint (H).

According to the results, 86.6 kg of granular bentonite showed half of the environmental burden (single score of 1.68) compared to the environmental impacts of 3.81 kg granular activated carbon production (single score of 3.22).

From a weighted life cycle impact assessment (LCIA) results perspective (Fig. 83), natural bentonite appears as a much more environmentally friendly alternative compared to activated carbon for the pretreated textile wastewater treatment. The environmental impact of using activated carbon as an adsorbent in wastewater treatment is dominated by energy and heat in the production and reactivation processes.

In order to compare both adsorbents of granular bentonite and activated carbon from the economic perspective, the prices of different products were compiled from industries in Iran. In Iran market, the price for AC is from 100 000 to 1350000 toman (3 to 41 euro) per kilogram, and the price for bentonite is from 450 to 2000 toman (0.01 to 0.06 euro) per kilogram.

Probability distributions were determined on the range of products prices. Probability distribution of AC price range was concluded triangular with likeliest price of 500 000

toman (15 euro) per kilo, and the probability distribution of bentonite price range was concluded uniform.

The forecast cells in crystal ball were defined as: 1) the price of wastewater treatment with AC per hour, 2) the price of wastewater treatment with bentonite per hour and 3) the ratio of both defined forecasts cells. The Monte Carlo analysis was carried out with 10000 trials. 10000 runs means 10000 different AC or bentonite products were bought and the wastewater were treated 10000 times with using each product.

The ratio of both defined forecasts was concluded: 0.06 (the mean price of wastewater treatment with 86.6 kg bentonite per hour/the mean price of wastewater treatment with 3.8 kg AC per hour). The mean price of wastewater treatment with 3.8 kg AC per hour: 2 515 201 toman (76.21 euro). The mean price of wastewater treatment with 86.6 kg bentonite per hour: 106 131 toman (3.21 euro). The treatment cost with AC is about 24 times more than the treatment cost with bentonite. The reason is that the mean price of AC in Iran (500 000 toman) is 500 times more expensive than the mean price of bentonite in Iran (1000 toman).

It can be concluded that treatment of textile wastewater with GAC entail higher costs compared to natural bentonite, due to the highly intensive use of energy and heat in GAC production and regeneration phases as well as much more expensive price of AC compared to bentonite in Iran.

Additionally, the carbon footprint of both adsorbents of bentonite and activated carbon in the treatment of textile wastewater was assessed in this study.

Emitted carbon dioxide which is one of the main sources of the global warming potential burden are as follows for the studied scenarios (see Table 25):

Table 25 Emitted carbon dioxide in different scenarios of the spent adsorbents disposal

Scenarios	Spent bentonite landfilling	Spent activated carbon landfilling	Regeneration of spent activated carbon	Reusing spent bentonite in LECA
Emitted CO ₂	0.709	1.81	0.624	0.36

Based on the results (see Table 25), the highest amount of the emitted carbon dioxide is concluded in the scenario of "spent activated carbon landfilling" and the lowest amount is concluded in "reusing the spent bentonite in LECA". The amount of CO₂ emitted to

atmosphere in reusing spent bentonite in LECA is about half of the emitted carbon dioxide in regeneration process of spent activated carbon.

3.7 Batch adsorption studies on dye-spiked groundwater

3.7.1 Equilibrium isotherms in single and binary dye systems

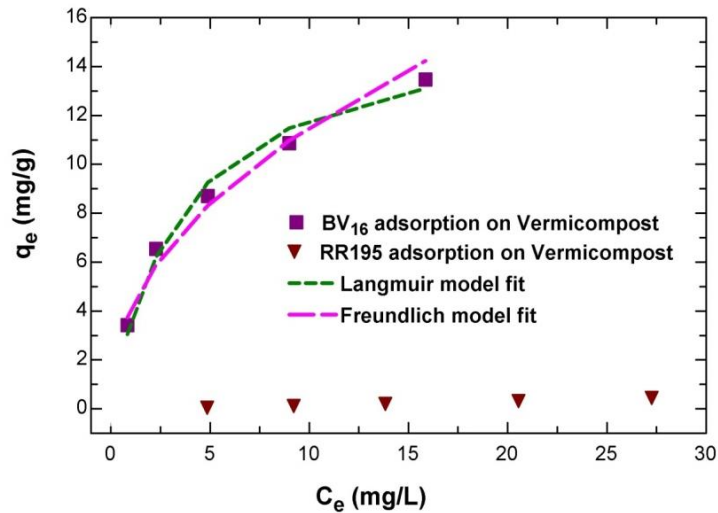


Fig. 84 Isotherms of the adsorption of BV₁₆ (10-50 mg L⁻¹) and RR₁₉₅ (5-30 mg L⁻¹) on *vermicompost* in single dye solution at 25 C° (Source: Ref (8) Khalilzadeh Shirazi E et al. (2019))

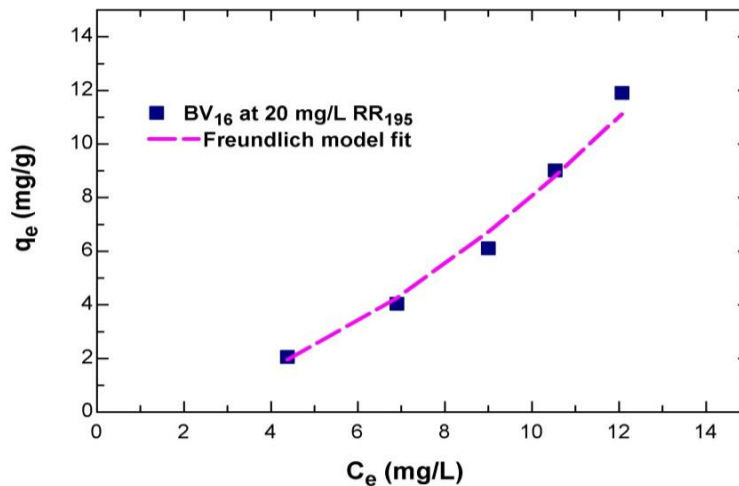


Fig. 85 Freundlich isotherm of the adsorption of BV₁₆ (10-50 mg L⁻¹) in the presence of a fixed RR₁₉₅ concentration (20 mg L⁻¹) on *vermicompost* at 25 C° (Source: Ref (8) Khalilzadeh Shirazi E et al. (2019))

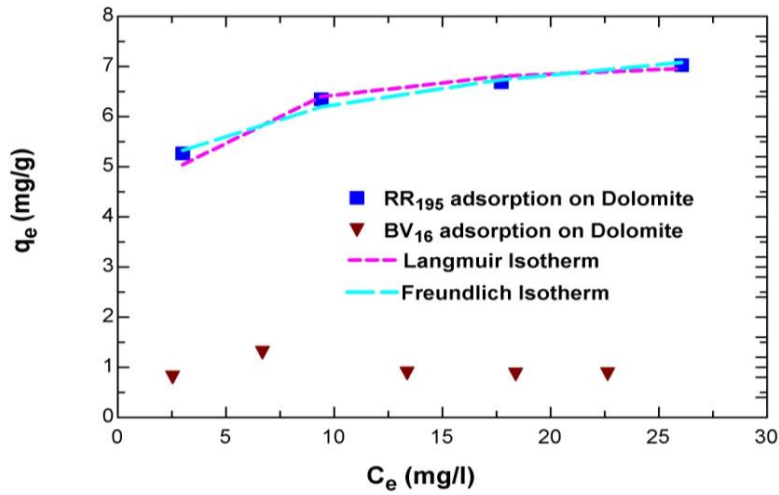


Fig. 86 Isotherms of the adsorption of BV₁₆ (5-30 mg L⁻¹) and RR₁₉₅ (10-40 mg L⁻¹) on *charred dolomite* in single dye solutions at 25 C°
 (Source: Ref (8) Khalilzadeh Shirazi E et al. (2019))

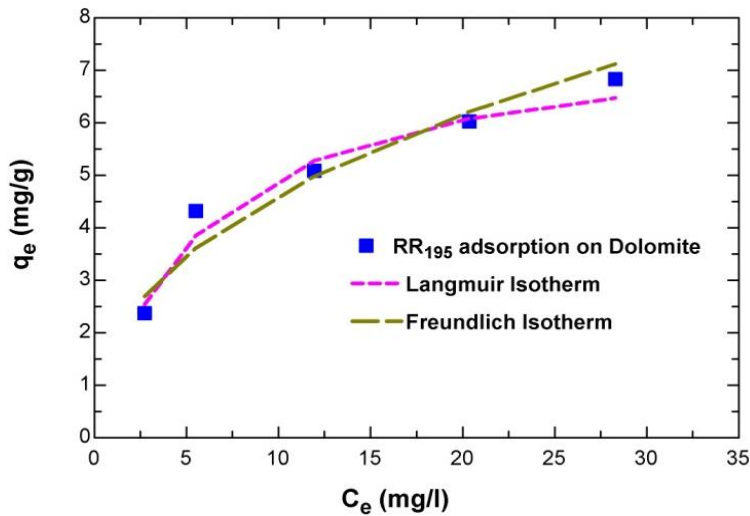


Fig. 87 Isotherms of the adsorption of RR₁₉₅ (10-50 mg L⁻¹) in the presence of a fixed BV₁₆ concentration (20 mg L⁻¹) on *charred dolomite* at 25 C°
 (Source: Ref (8) Khalilzadeh Shirazi E et al. (2019))

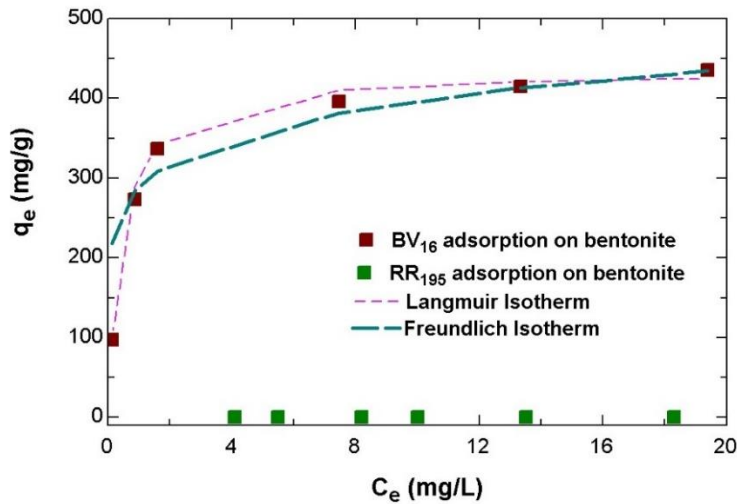


Fig. 88 Isotherms of the adsorption of BV₁₆ (10-40 mg L⁻¹) and RR₁₉₅ (5-30 mg L⁻¹) on *natural bentonite* in single dye solutions at 25 C°

(Source: Ref (65) Khalilzadeh Shirazi E et al. (2020))

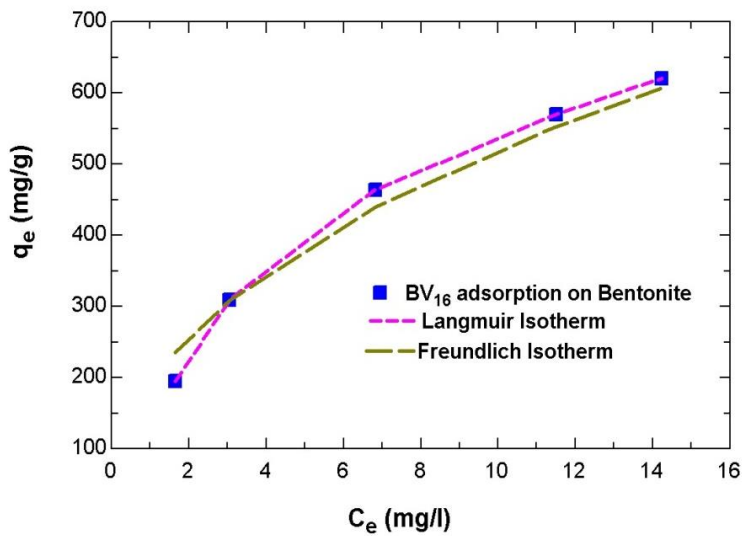


Fig. 89 Isotherms of the adsorption of BV₁₆ (10-50 mg L⁻¹) in the presence of a constant RR₁₉₅ concentration (20 mg L⁻¹) on *natural bentonite* at 25 C°

(Source: Ref (65) Khalilzadeh Shirazi E et al. (2020))

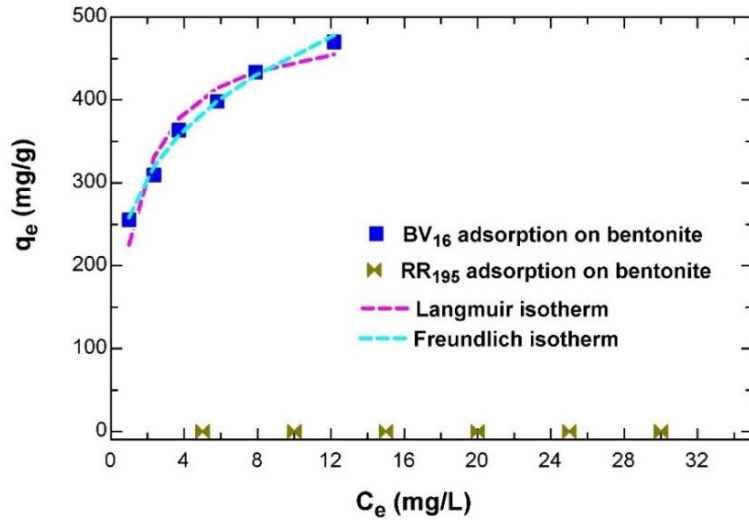


Fig. 90 Isotherms of the adsorption of BV₁₆ (10-40 mg L⁻¹) and RR₁₉₅ (5-30 mg L⁻¹) on *standard bentonite* in single dye solutions at 25 C° (Source: Ref (65) Khalilzadeh Shirazi E et al. (2020))

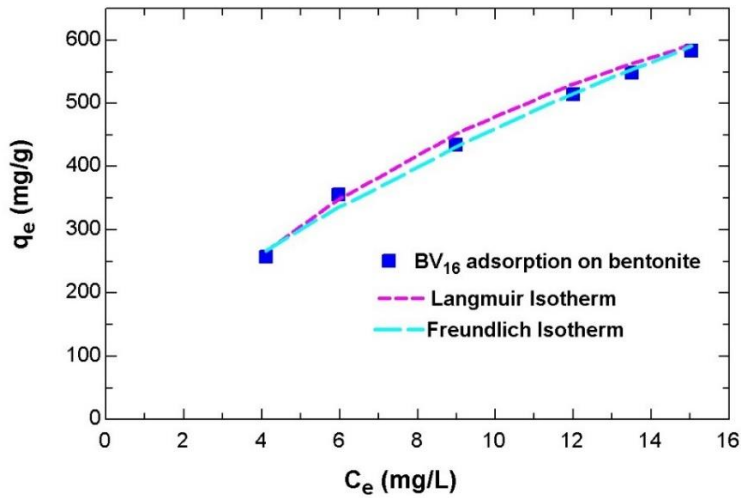


Fig. 91 Isotherms of the adsorption of BV₁₆ (10-50 mg L⁻¹) in the presence of a constant RR₁₉₅ concentration (20 mg L⁻¹) on *standard bentonite* at 25 C° (Source: Ref (65) Khalilzadeh Shirazi E et al. (2020))

Results and Discussion

Table 26 Isotherm parameters of the adsorption of BV₁₆ and RR₁₉₅ on charred dolomite (CD), vermicompost (VC), natural bentonite (NB) and standard bentonite (SB) in single and binary dye solution (* no data fit)

(Source: Ref (8, 65) Khalilzadeh Shirazi E et al. (2019), Khalilzadeh Shirazi E et al. (2020))

Dye/ adsorbent	Dye solution	Langmuir isotherm			Freundlich isotherm			
		q _{max} (mg g ⁻¹)	K _L (L mg ⁻¹)	R ²	R _L	K _F (mg g ⁻¹)	1/n	R ²
^a BV ₁₆ /VC ^b	Single	16.07	0.27	0.990	0.26-0.06 (10-50 mg L ⁻¹ C ₀ BV ₁₆)	4.03	0.456	0.978
BV ₁₆ /VC	Binary	*	*	*	*	0.15	1.668	0.989
^c RR ₁₉₅ /CD ^d	Single	7.32	0.73	0.999	0.12-0.02 (10-50 mg L ⁻¹ C ₀ RR ₁₉₅)	4.60	0.13	0.982
RR ₁₉₅ /CD	Binary	7.74	0.14	0.995	0.1-0.35 (10-50 mg L ⁻¹ RR ₁₉₅)	1.88	0.45	0.959
BV ₁₆ /NB ^e	Single	434.78	2.30	0.995	0.041-0.008 (10-50 mg L ⁻¹ C ₀ BV ₁₆)	289.13	0.13	0.962
BV ₁₆ /NB	Binary	833.33	0.18	0.998	0.1-0.35 (10-50 mg L ⁻¹ C ₀ BV ₁₆)	189.00	0.43	0.996
BV ₁₆ /SB	Single	500.00	0.83	0.997	0.1-0.02 (10-50 mg L ⁻¹ C ₀ BV ₁₆)	258.82	0.24	0.996
BV ₁₆ /SB	Binary	1111.111	0.08	0.991	0.5-0.2 (10-50 mg L ⁻¹ C ₀ BV ₁₆)	112.10	0.61	0.988

^a BV₁₆: Basic violet 16

^b VC: Vermicompost

^c RR₁₉₅: Reactive red 195

^d CD: Charred dolomite

^e NB: Natural bentonite

^f SB: Standard bentonite

The adsorption equilibrium isotherms of BV₁₆ on vermicompost and on the two kinds of bentonites studied, and the equilibrium isotherms of RR₁₉₅ on charred dolomite are presented in Figs. 84-91. With reference to the correlation coefficients determined, the Langmuir model can efficiently describe the adsorption process of BV₁₆ on vermicompost and the adsorption process of RR₁₉₅ on charred dolomite in single dye solutions. In binary dye solutions, the adsorption of the cationic dye on vermicompost was in agreement with the Freundlich model, while the Langmuir model better explains the results of the adsorption

of the anionic dye on charred dolomite. The results related to the adsorption of the cationic dye on vermicompost in binary solution only poorly fitted to the Langmuir isotherm model (data not shown). With respect to the two kinds of bentonites studied, the correlation coefficients of the Langmuir isotherms were higher than that of the Freundlich isotherm; thus, the Langmuir model better describes the adsorption process of the dyes on the adsorbents in single and binary dye solutions. Other researchers have subscribed to the view that the Langmuir isotherm model can well define multi-solute adsorption systems (8, 65, 140, 141).

The initial sharp rise of the curves observed in Figs. 88 and 90 suggests a high affinity between the dye and the adsorbent surface. For natural and standard bentonite high adsorption capacities of 435 mg g^{-1} and 500 mg g^{-1} for BV₁₆ were determined, respectively. Abidi et al. proved that the high adsorption capacity of bentonite for the cationic dye roots in the colloidal properties and negatively charged layers of bentonite. The adsorption capacity of natural bentonite for BV₁₆ (833 mg g^{-1}) and of standard bentonite for BV₁₆ (1111 mg g^{-1}) doubled in the presence of the anionic dye (11, 65).

The isotherm constants were calculated (see Table 26). For single dye solutions, the high values of K_L indicate a strong bonding of the dyes to the adsorbents. However, the K_L values of the adsorbate/adsorbent systems RR₁₉₅/CD, BV₁₆/NB, and BV₁₆/SB for binary solutions were found to be lower than those found for single solutions. This can be ascribed to the fact that the adsorption affinity of BV₁₆ to both kinds of bentonites, and RR₁₉₅ to charred dolomite is greater in the single solution than in binary mixtures. Obviously, the adsorption affinity of the adsorbents is affected by the presence of the oppositely-charged dye (65).

Moreover, the Freundlich constants, K_F and n , were also calculated for the adsorption of the dyes in single and binary mixtures. With regard to the adsorption of the cationic BV₁₆ on vermicompost and two bentonites, and to the adsorption of the anionic RR₁₉₅ on charred dolomite, the Freundlich constant n was found to be > 1 in the single dye solution and in binary solution in the presence of the oppositely-charged dye which indicates that the adsorption is favorable in both cases. In contrast, in binary solution a value $n < 1$ obtained for the adsorption of the cationic dye on vermicompost reflects an unfavorable adsorption process attesting a negative impact of the presence of the anionic dye on BV₁₆ adsorption. The high value of K_F proves a relatively easy uptake of the cationic dye BV₁₆ to vermicompost and both natural and standard bentonite, and of the anionic dye RR₁₉₅ to charred dolomite in both single and binary dye solutions. The decrease in the constant K_F in binary solutions affirms the interfering role of the other dye (8, 65).

Furthermore, the adsorption capacity of the natural bentonite used in this study is roughly comparable to that of the standard clay investigated. The approximate similarity of the adsorption capacities and the adsorption behaviour between the two kinds of bentonite in

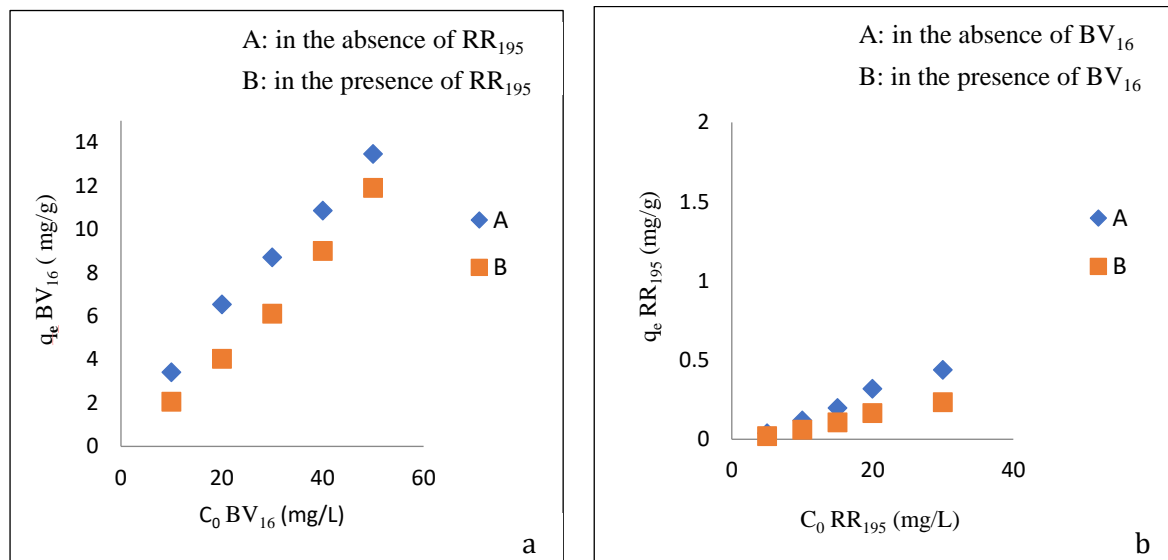
the dye systems might thus be attributed to their similar surface characteristics and chemical nature (65, 110).

Moreover, the R_L values lying between 0 and 1 indicate the favourable adsorption of BV_{16} onto vermicompost (in single dye solution), and of BV_{16} onto both bentonites, and of RR_{195} on charred dolomite in single and binary dye experiments.

The maximum adsorption capacity of both bentonites is highly greater than that of vermicompost and charred dolomite. It shows that natural bentonite can provide more adsorption sites than charred dolomite and to vermicompost due to the higher specific surface area (8).

3.7.2 Dye interactions in binary dye experiments

The effect of the initial concentration of one dye on the adsorption of the second dye onto the adsorbents in binary solutions was studied and compared to the respective results of single-dye experiments (65).



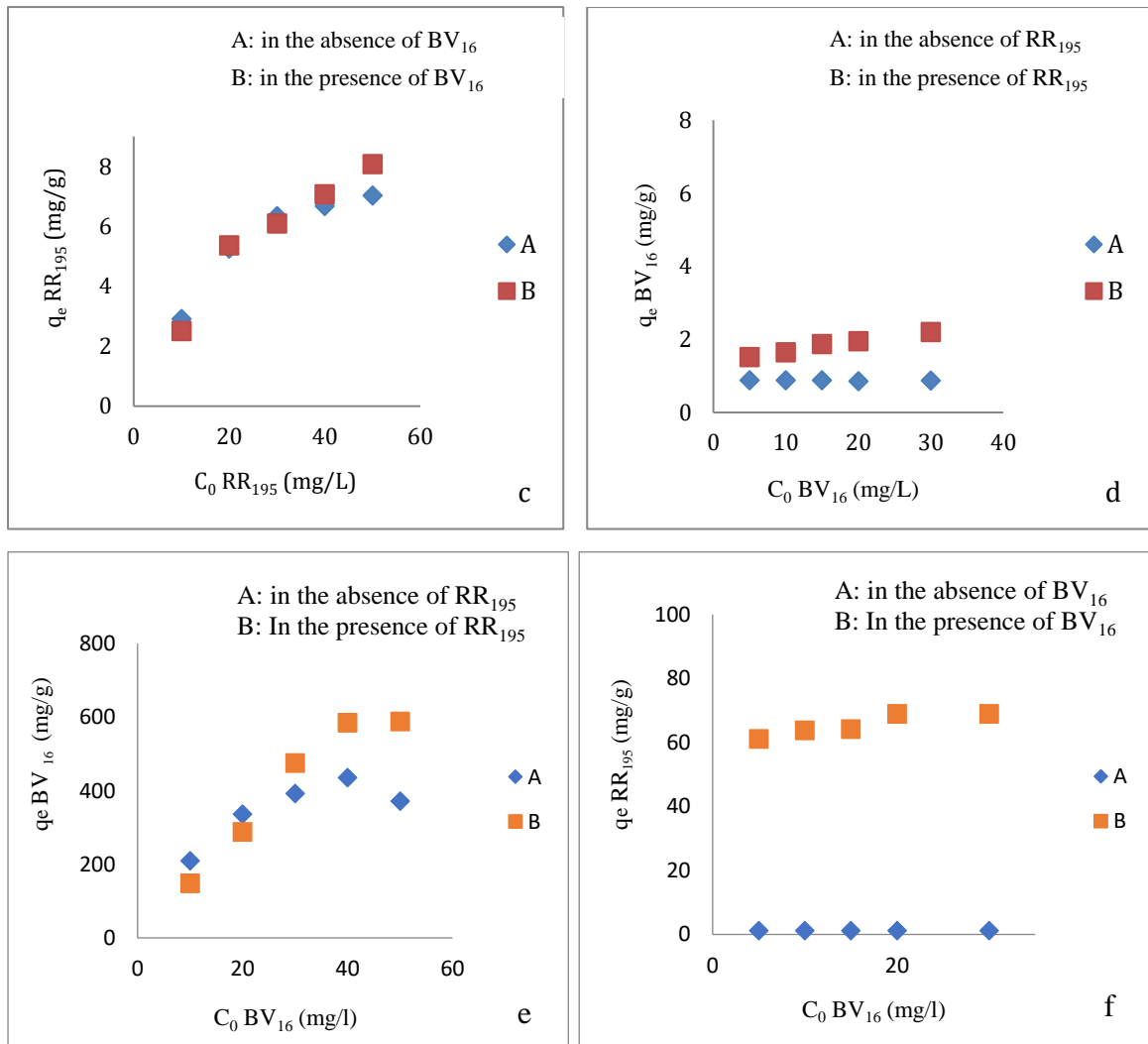


Fig. 92 Adsorption capacities of the different adsorbents for dyes:

- (a) vermicompost toward BV_{16} in the absence and presence of RR_{195}
- (b) vermicompost toward RR_{195} in the absence and presence of BV_{16}
- (c) charred dolomite toward RR_{195} in the absence and presence of BV_{16}
- (d) charred dolomite toward BV_{16} in the absence and presence of RR_{195}
- (e) natural bentonite toward BV_{16} in the absence and presence of RR_{195}
- (f) natural bentonite toward RR_{195} in the absence and presence of BV_{16}

(Source: Ref (8, 65) Khalilzadeh Shirazi E et al. (2019), Khalilzadeh Shirazi E et al. (2020))

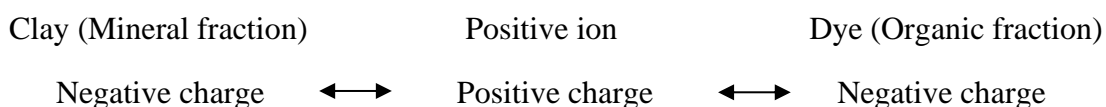
Principally, when a mixture of dyes is present in a water sample there might be three different possible types of interactions between the components leading to increasing or decreasing removal efficiencies/adsorption capacities: synergism, antagonism and non-interaction (65, 105, 142).

Fig. 92 a shows the effect of the anionic dye on the adsorption of the cationic dye on vermicompost. Apparently, antagonistic effects were observed for the adsorption of BV_{16} on vermicompost in the presence of fixed concentrations of RR_{195} (20 mg L^{-1}). Although, the adsorption of negatively charged RR_{195} on negatively charged vermicompost is very

low, it is even less in binary compared to a single dye solution presumably due to a strong electrostatic attraction between positively charged BV₁₆ and negatively charged vermicompost (Fig. 90 b) (8).

Fig. 92 c shows the effects of initial concentrations of BV₁₆ on the adsorption of RR₁₉₅ on charred dolomite. Similar adsorption capacities for both single and binary dye solutions proved that the presence of BV₁₆ roughly had no competitive effect on the adsorption of RR₁₉₅ on charred dolomite. Fig. 92 d shows the effects of initial concentrations of RR₁₉₅ on the adsorption of BV₁₆ on charred dolomite. The adsorption capacity of charred dolomite for BV₁₆ increased with an increasing concentration of BV₁₆ at a constant concentration of RR₁₉₅ (synergistic effect). The presence of RR₁₉₅ promoted the adsorption of BV₁₆ in the binary solution. This synergistic effect presumably resides in the structure of the RR₁₉₅ molecule. There are four SO₃⁻ (sulfonate) groups per RR₁₉₅ molecule (and one sulphate group SO₄²⁻). Some of these groups can interact with the functional groups on the surface of charred dolomite, the other free groups can provide negatively charged active sites for adsorption of the cationic dye. RR₁₉₅ serves as a bridge between BV₁₆ and charred dolomite. Similar results were reported by Jun-xia Yu et al. (2015) and Wang et al. (2012) (8, 33, 106).

The anionic dye RR₁₉₅ (20 mg L⁻¹) had an inhibitory (antagonistic) effect on the adsorption of cationic BV₁₆ on natural bentonite in low concentrations (10-20 mg L⁻¹; Fig 92 a). By contrast, at higher concentrations of BV₁₆ (30-50 mg L⁻¹), the maximum adsorption capacity for BV₁₆ increased considerably (from 435 mg g⁻¹ to 833 mg g⁻¹; see Table 26) in the presence of anionic RR₁₉₅, which proves its promoting effect. This enhancing effect on the removal efficiency of the cationic BV₁₆ can be seen in Fig. 92 a as well. Fig. 92 b shows the influence of a given initial concentrations of the cationic dye on the adsorption of anionic RR₁₉₅ on natural bentonite. The adsorption capacity of RR₁₉₅ was much higher in the presence than in the absence of BV₁₆. It was observed that the adsorption of both BV₁₆ and RR₁₉₅ increased in the experiments with binary dye solutions which affirmed the synergistic effect. This might be ascribed to the contribution of the permanently positively charged quaternized nitrogen atoms of BV₁₆ resulting in a positive net surface charge with which RR₁₉₅ molecules can interact. It can be concluded that the cationic dye supports the bonding of the anionic dye to bentonite in binary mixtures (65).



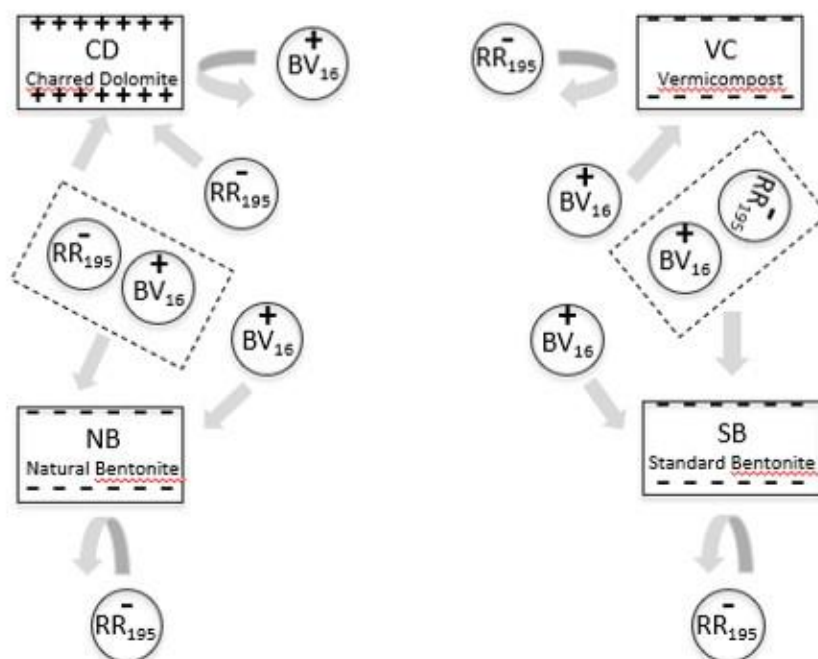


Fig. 93 Interaction of dyes in binary dye experiments

3.7.3 Kinetic analysis

Figs. 94-97 provide information on the results of kinetic studies of BV_{16} and RR_{195} on the adsorbents studied, in both single- and binary-dye solution with identical initial concentrations (20 mg L^{-1}) at different time intervals. The results show that the adsorption processes in both single and binary dye solutions follow more satisfactorily a pseudo-second-order model (similar q_e for experiment and model as well as a high value of R^2) indicating that the adsorption process is chemical sorption (8, 143).

Moreover, a similar pseudo-order kinetics in both individual dye solutions highlight that the dye adsorption kinetics on the adsorbents is not changed compared to the binary dye solution. However, the kinetic constants (k_2 in Table 27) indicate faster adsorption of dyes on the adsorbents in single dye solutions compared to the binary dye solution (8, 65).

Results and Discussion

Table 27 Parameters of the pseudo-second-order kinetics of dye adsorption on vermicompost (VC), charred dolomite (CD), natural bentonite (NB) and standard bentonite (SB) (Source: Ref (8, 65) Khalilzadeh Shirazi E et al. (2019), Khalilzadeh Shirazi E et al. (2020))

Dye/Adsorbent	Dye solution	$q_{e,exp}$ (mg/g)	k_2 (g/mg min)	$q_{e,cal}$ (mg/g)	R^2
BV ₁₆ /VC	Single	6.54	0.01	6.79	0.999
BV ₁₆ /VC	Binary	4.038	0.03	4.74	0.999
RR ₁₉₅ /CD	Single	5.26	0.009	6.41	0.996
RR ₁₉₅ /CD	Binary	4.68	0.012	5.55	0.999
BV ₁₆ /NB	Single	336.45	0.014	344.82	0.999
BV ₁₆ /NB	Binary	288.31	0.15	285.71	0.999
BV ₁₆ /SB	Single	255.24	0.006	263.15	0.999
BV ₁₆ /SB	Binary	249.48	0.005	256.41	0.999

In both single and binary dye solutions, BV₁₆ and RR₁₉₅ adsorption increased with time (Figs. 94-97). However, the lesser degree of adsorption of BV₁₆ and RR₁₉₅ in the binary-dye solution revealed the interference of the second dye on the rate of the adsorption process of the first one. Initially, the high number of active sites on the surface of the adsorbents promotes the adsorption process due to the improvement of dye diffusion flux to the adsorbent. Later on, a gradual increase in the adsorption rate takes place followed by a decrease in the concentration gradient and gradual decline in the adsorption rate due to saturation, i.e. less adsorption sites at the adsorbent surface are available (8, 63).

In other words, with increasing time, gradual saturation of the surface of the adsorbents translates into the reduction of the concentration gradient and the tapering off in the adsorption rate. At some specific time (equilibrium), a constant value is reached at which the dye concentration in solution will be constant (8, 144).

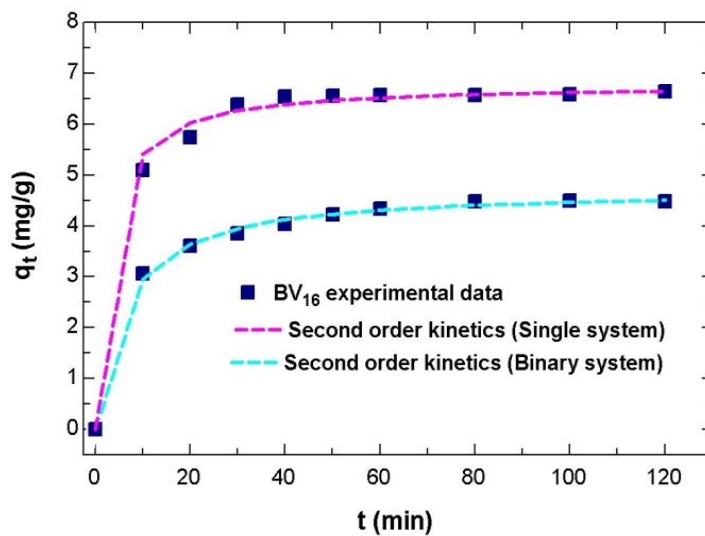


Fig. 94 Kinetics of the adsorption of BV₁₆ (20 mg L⁻¹) on *vermicompost* in single and binary dye solution at 25 C° (Source: Ref (8) Khalilzadeh Shirazi E et al. (2019))

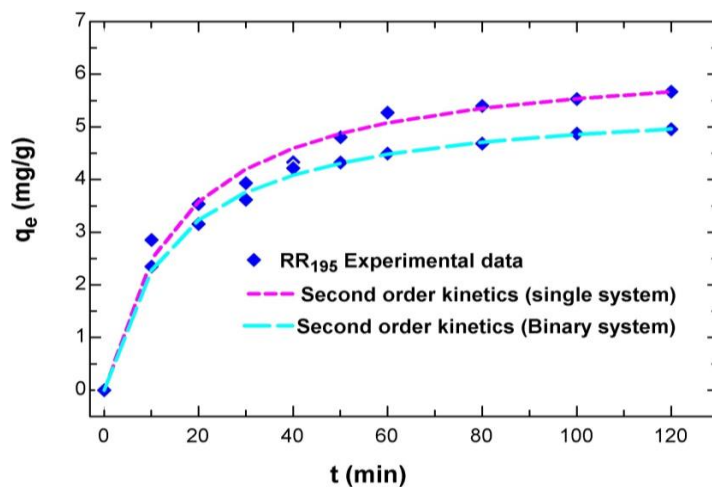


Fig. 95 Kinetics of the adsorption of RR₁₉₅ (20 mg L⁻¹) on *charred dolomite* in single and binary dye solution at 25 C° (Source: Ref (8) Khalilzadeh Shirazi E et al. (2019))

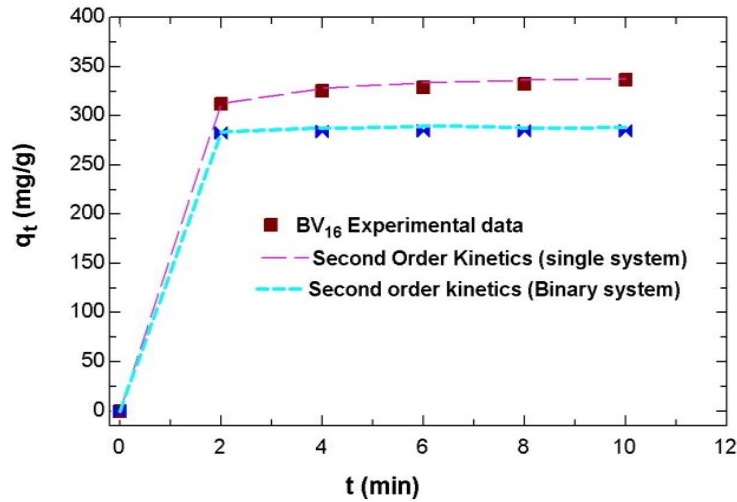


Fig. 96 Kinetics of the adsorption of BV₁₆ (20 mg L⁻¹) on *natural bentonite* in single and binary dye solution at 25 C° (Source: Ref (65) Khalilzadeh Shirazi E et al. (2020))

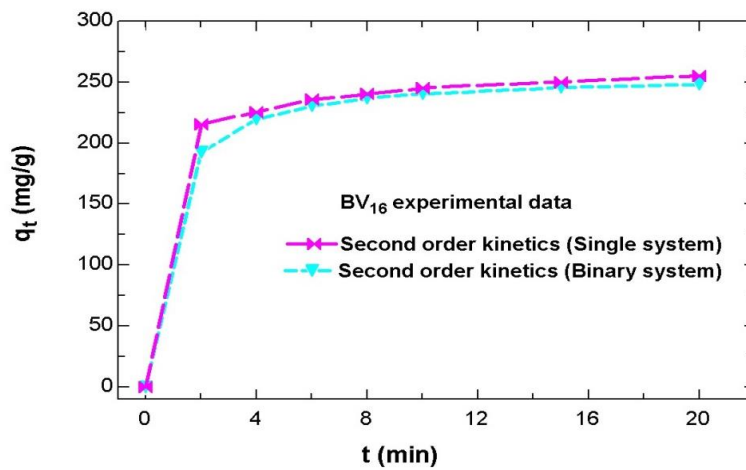


Fig. 97 Kinetics of the adsorption of BV₁₆ (20 mg L⁻¹) on *standard bentonite* in single and binary dye solution at 25 C° (Source: Ref (65) Khalilzadeh Shirazi E et al. (2020))

Kinetic studies on the adsorption of BV₁₆ to natural and to standard bentonite were performed under the same experimental conditions (initial dye concentrations: 20 mg L⁻¹ at varying times). Initially, dye removal was rapid and reached an equilibrium within the first 5 min indicating a high affinity between the cationic BV₁₆ molecules and the surfaces of both kinds of bentonites (12, 65).

As can be seen from Table 27 (similar q_e value for the experimental and model data as well as high values of R²) the adsorption processes in both single and binary dye experiments

fitted well to a pseudo-second-order model. The good fit for this model indicates that chemical adsorption presumably controls the adsorption rate (65, 145).

The adsorption of the dye initially takes place through exchange reactions on the surface. After a complete occupation of the adsorption sites, dye molecules diffuse into the layers of bentonite where they can undergo ion-exchange and/or complexation reactions. With regards to the reaction mechanism, ion exchange may involve positively charged groups ($-\text{NR}_3^+$ or $-\text{NH}^+=\text{N}-$) in BV_{16} and Na^+ ions in bentonite (65, 110).

3.7.4 Adsorption of dyes on the mixed sorbent in binary dye solutions

Since the two sorbents are not capable to adsorb dyes with the same charge as the surface charge of the sorbent, a sorbent system consisting of VC mixed with CD (1:1) was examined with regard to its potential to remove the cationic and anionic dye simultaneously in one step (8).

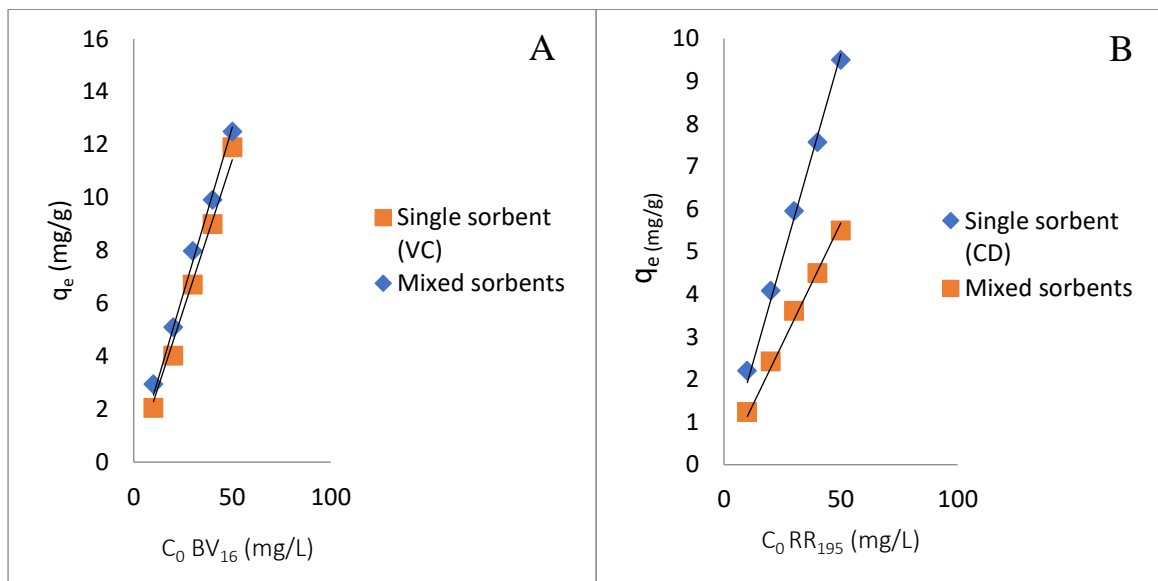


Fig. 98 Adsorption capacity of BV_{16} (A) and RR_{195} (B) to single and mixed sorbent systems

$\text{BV}_{16}: q_{Vermi}^{BV16} = 0.253 C_0^{BV16}$	$R^2 = 0.99$	$\text{RR}_{195}: q_{Vermi}^{RR195} = 0.192 C_0^{BV16}$	$R^2 = 0.993$
$\text{BV}_{16}: q_{Mixed}^{BV16} = 0.228 C_0^{BV16}$	$R^2 = 0.993$	$\text{RR}_{195}: q_{Mixed}^{RR195} = 0.113 C_0^{BV16}$	$R^2 = 0.99$

(Source: Ref (8) Khalilzadeh Shirazi E et al. (2019))

Results and Discussion

The removal efficiencies and adsorption capacities of vermicompost for BV₁₆ (10-50 mg L⁻¹) in the presence of RR₁₉₅ at a fixed concentration (20 mg L⁻¹) were approximately similar to those obtained for the mixed sorbent VC+CD (Table 28), and also the slopes in the q_e-c₀-graph obtained for the single sorbent system and for mixed sorbents were similar (Fig. 97 A) (8, 62). However, in the binary solution consisting of RR₁₉₅ (10-50 mg L⁻¹) and BV₁₆ at a fixed concentration (20 mg L⁻¹) the efficiency of charred dolomite to adsorb RR₁₉₅ decreased slightly in the presence of vermicompost (Table 28, Fig. 98 B) indicating a potential inhibitory impact of vermicompost on the adsorption of RR₁₉₅ on charred dolomite (8).

Table 28 Efficiencies of mixed adsorbents (VC+CD) for removal of BV₁₆ and RR₁₉₅ in single and binary dye solutions (Source: Ref (8) Khalilzadeh Shirazi E et al. (2019))

C₀ in mg L⁻¹		Removal efficiencies of mixed sorbent VC+CD in %	
BV₁₆	RR₁₉₅	BV₁₆	RR₁₉₅
10	0	96.6	0
20	0	90.6	0
30	0	89.2	0
40	0	88.1	0
50	0	85.2	0
10	20	83.6	51.0
20	20	84.1	54.3
30	20	85.6	58.0
40	20	75.6	45.6
50	20	76.1	56.0
0	5	0	91.7
0	10	0	69.7
0	15	0	60.8
0	20	0	53.6
20	5	89.2	84.0
20	10	86.2	55.3
20	15	78.2	55.9
20	30	72.9	41.0

Obviously, the initial surface area of charred dolomite decreases when vermicompost particles settle in the pores of charred dolomite. In conclusion, in binary solutions, the

Results and Discussion

cationic dye (BV₁₆) has a high tendency to adsorb onto vermicompost, whereas the anionic dye (RR₁₉₅) is preferentially adsorbed onto charred dolomite. Moreover, most of the removal efficiencies of the mixed sorbent system determined for each of these dyes were > 70% (with an average of 71.7 %) (Table 28), proving that the cationic and the anionic dye can be removed simultaneously and efficiently from aqueous solution with this novel mixed sorbent system. As many adsorbents can readily adsorb various mixed organic dyes but are generally poor at selectively removing the targeted organic dye (8).

Table 29 Removal efficiencies of mixed adsorbents (NB+CD)/(SB+CD) for BV₁₆ and RR₁₉₅ in single and binary dye solutions (Source: Ref (65) Khalilzadeh Shirazi E et al. (2020))

C₀ in mg/L		Removal efficiencies of mixed sorbent NB+CD in %		Removal efficiencies of mixed sorbent SB+CD in %	
BV₁₆	RR₁₉₅	BV₁₆	RR₁₉₅	BV₁₆	RR₁₉₅
10	0	99.20	0	98.40	0
20	0	72.61	0	70.53	0
30	0	43.20	0	41.34	0
40	0	38.85	0	35.01	0
50	0	32.90	0	29.84	0
10	20	81.23	72.85	70.34	81.84
20	20	73.24	78.36	71.32	71.69
30	20	67.50	71.46	74.24	65.43
40	20	58.38	77.58	73.85	55.04
50	20	59.99	70.95	71.56	56.23
0	5	0	71.21	0	72.54
0	10	0	57.24	0	61.04
0	15	0	51.75	0	50.39
0	20	0	41.47	0	43.66
0	30	0	38.47	0	36.54
20	5	91.34	73.86	90.54	71.65
20	10	92.31	77.34	93.45	78.23
20	15	85.99	72.72	82.11	70.32
20	30	78.32	66.50	76.21	65.92

Single sorbents are not efficient to remove dyes if their surface charge is the same as the charge of the respective dye. Thus, two mixed sorbent systems consisting of natural or standard bentonite and charred dolomite (NB+CD and SB+CD) in optimized ratios were investigated for their potential to simultaneously remove the cationic and anionic dyes from the binary dye solutions. The cationic BV₁₆ is preferentially adsorbed on natural and standard bentonite, whereas the anionic RR₁₉₅ was well adsorbed on charred dolomite, proving selective adsorption. The results given in Table 29 show that both dyes can be removed efficiently from aqueous solution in one step with this new mixed sorbent system: most of the removal efficiencies of the mixed sorbent system determined for the cationic and the anionic dye were > 70% (with an average of 81%) (Table 29). Furthermore, in the case of the binary solutions consisting of BV₁₆ in variable concentrations (10-50 mg L⁻¹) and RR₁₉₅ in a non-variable concentration of 20 mg L⁻¹, the removal efficiencies of neither natural bentonite nor standard bentonite for BV₁₆ changed significantly if charred dolomite was present as the second adsorbent (65).

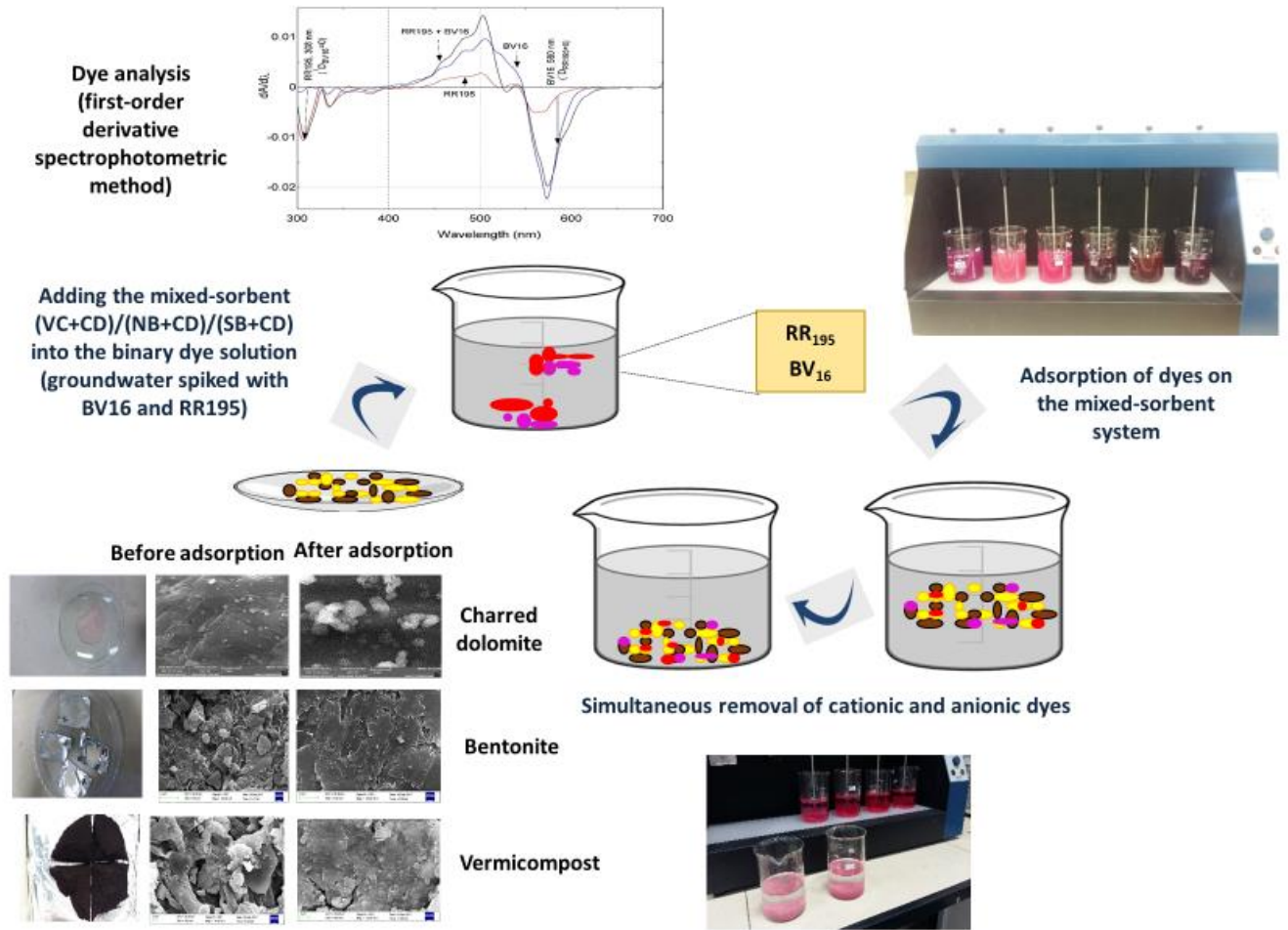


Fig. 99 Conceptual scheme of the proposed method for dye elimination from water with mixed sorbents in single and binary dye solutions

(Source: Ref (8) Khalilzadeh Shirazi E et al. (2019))

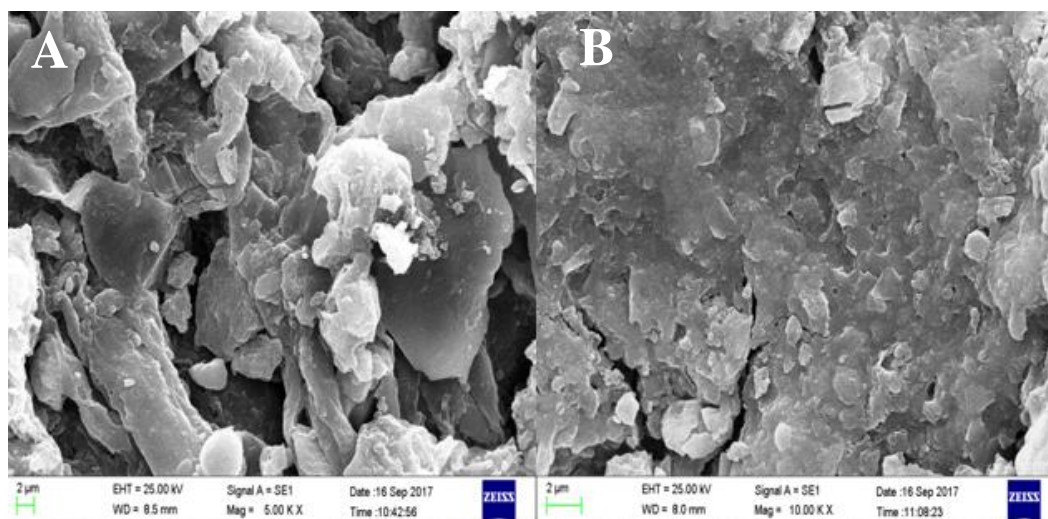


Fig. 100 Field emission scanning electron microscopic (FESEM) images of vermicompost (negative surface charge) before (A) and after (B) adsorption of the positively charged dye (BV_{16}) (Source: Ref (8) Khalilzadeh Shirazi E et al. (2019))

The FESEM images of vermicompost before and after BV_{16} adsorption are shown in Fig. 100 A and B, respectively. Fig. 100 A is an image of the pristine vermicompost showing a porous nature and irregular morphology characteristic of an agro-waste which has been described before (8, 58, 59, 120). This image in Fig. 100 B indicates an effective adsorption of dye molecules into the pores of the adsorbent leading to a less porous surface (8, 59, 120, 124).

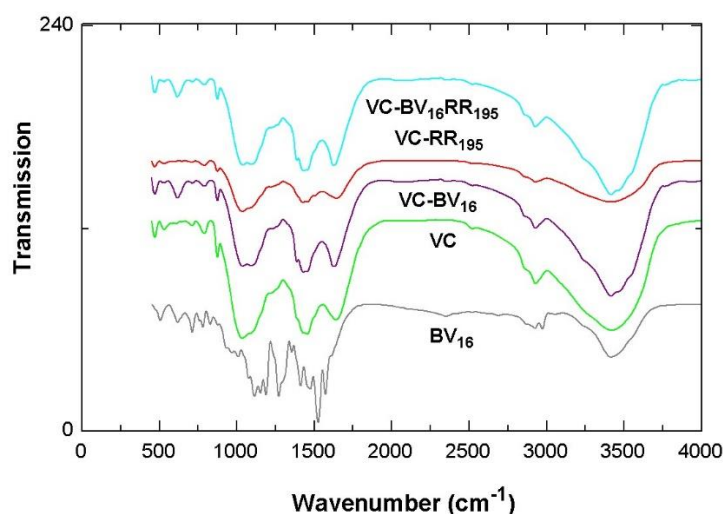


Fig. 101 FTIR spectra of vermicompost (VC) before and after adsorption of BV₁₆ and/or RR₁₉₅ (Source: Ref (8) Khalilzadeh Shirazi E et al. (2019))

Fourier transform infrared (FTIR) spectra of vermicompost were recorded in the range of 400-4,000 cm⁻¹ at room temperature. Fig. 101 shows the FTIR spectra of vermicompost samples before and after adsorption of BV₁₆ and RR₁₉₅ from single and binary dye solutions. The most pronounced bands for pristine vermicompost (VC) are observed in the regions of 3,500 and 3,000 cm⁻¹ which can be ascribed to the stretching vibration of N-H bonds from amines and amides as well as to alcoholic, phenolic and carboxy O-H bonds. In the range of 3,000 to 2,800 cm⁻¹, the absorption can be mainly assigned to the vibration of C-H bonds from aliphatic groups. The absorption at 1,639 cm⁻¹ can be attributed to C=C and C=O vibrations. The bands between 1,100 and 1,000 cm⁻¹ (1,035 cm⁻¹) are characteristic of the C-O bond stretching in polysaccharide or polysaccharide-like substances and Si-O bonds of silicates present in the vermicompost structure (8, 58).

The FTIR spectrum of vermicompost loaded with BV₁₆ alone (VC-BV₁₆) and the spectrum of the adsorbent with BV₁₆ together with RR₁₉₅ (VC-BV₁₆RR₁₉₅) are very similar indicating selective adsorption of BV₁₆ interacting with the respective functional groups of the adsorbent mentioned above. This influence of functional groups in the chemical adsorption process was demonstrated also in some previous works (8, 58, 120, 124, 146).

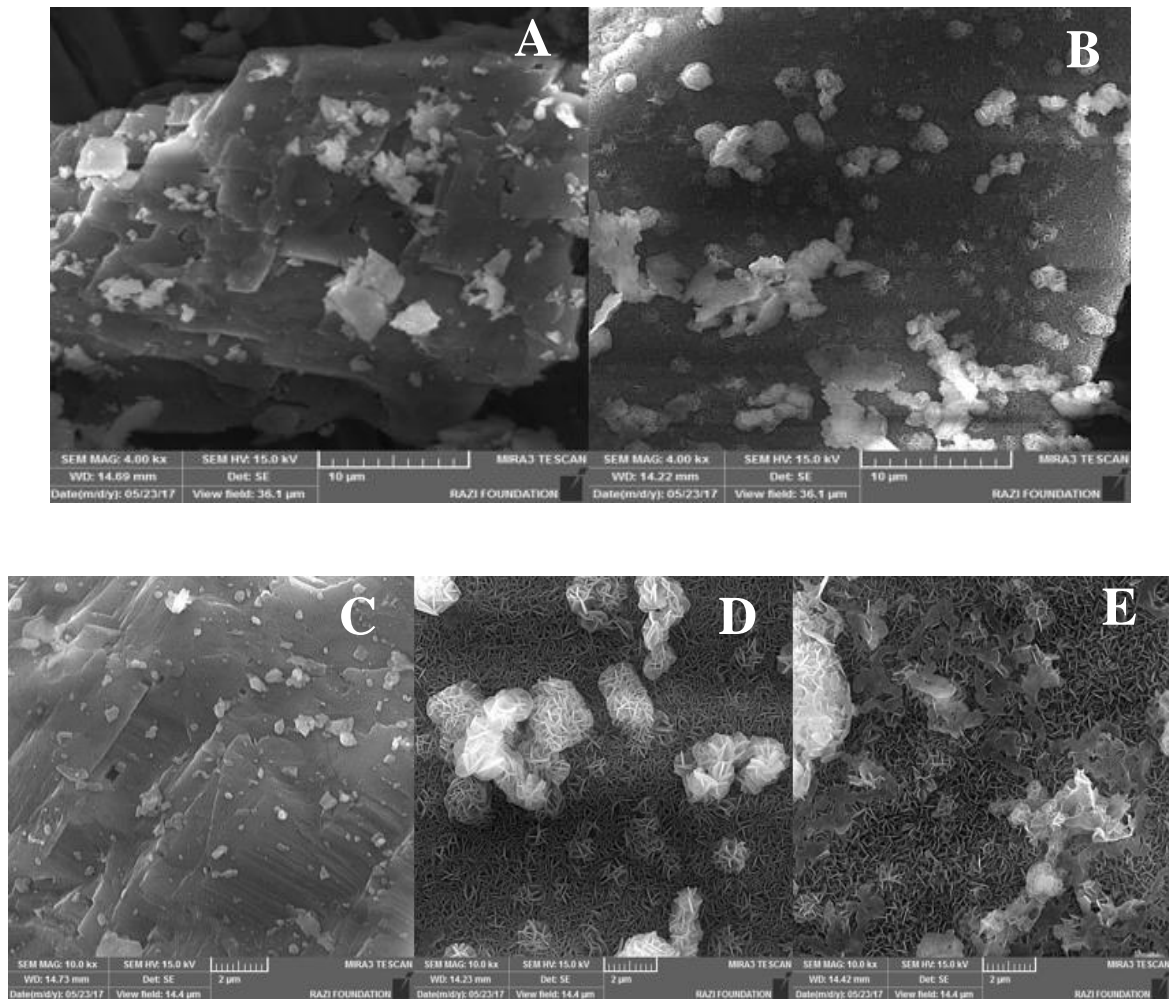


Fig. 102 Field emission scanning electron microscopic (FESEM) images of *charred dolomite* before (A, C) and after (B, D, E) adsorption of the oppositely charged dye RR₁₉₅ (Source: Ref (8, 13) Khalilzadeh Shirazi E et al. (2018), Khalilzadeh Shirazi E et al. (2019))

The typical morphology of charred dolomite with a plain and approximately compacted and stratified surface with sharp edges and crumbly nature can be seen in Fig. 102 A and C (27). The creation of new pores and voids on the surface of charred dolomite and noticeable change in the surface structure of the sample specifies the adsorption of RR₁₉₅ on charred dolomite (Fig. 102 B, D and E) (8, 13).

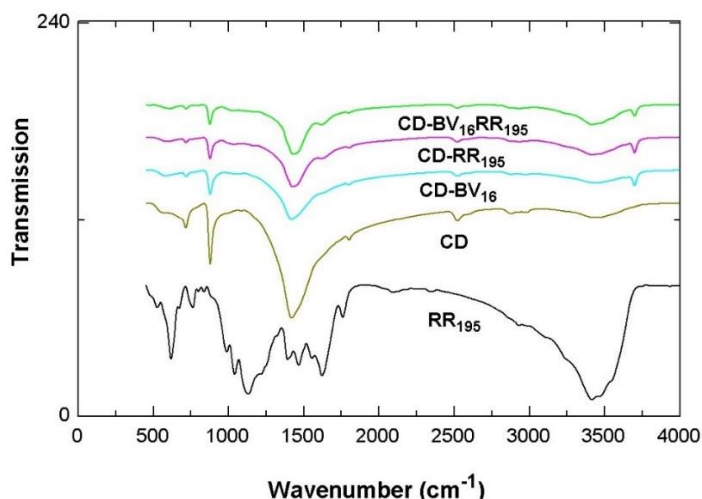


Fig. 103 FTIR spectra of *charred dolomite* (CD) before and after adsorption of BV₁₆ and/or RR₁₉₅ (Source: Ref (8) Khalilzadeh Shirazi E et al. (2019))

Fourier transform infrared (FTIR) spectra of charred dolomite was recorded in the range of 400 - 4,000 cm⁻¹ at room temperature. Fig. 103 shows the FTIR spectra of charred dolomite samples before and/or after adsorption of BV₁₆ and RR₁₉₅ from single and binary dye solutions.

The spectrum of pristine charred dolomite shows the main absorption band at ca. 1,418 cm⁻¹ which is related to the C-O vibrations of the carbonate ion. Bands around 2,500 cm⁻¹ can be assigned to water molecules bonded to the sample. The adsorption at 3,428 cm⁻¹ which can be attributed to OH⁻ bonds indicates possible sorption of RR₁₉₅ molecules to dolomite through hydrogen bonding/chemisorption (electrostatic attraction) in the single and binary dye solution. The absorption band at ca. 3,698 cm⁻¹ in the spectrum of charred dolomite after the adsorption of RR₁₉₅ which does not occur in the spectrum of “dye-unloaded” dolomite- can be attributed to O-H- vibrations originating from the hydration of the charred dolomite sample and possible adsorption of RR₁₉₅ molecules via chemisorption (8, 62).

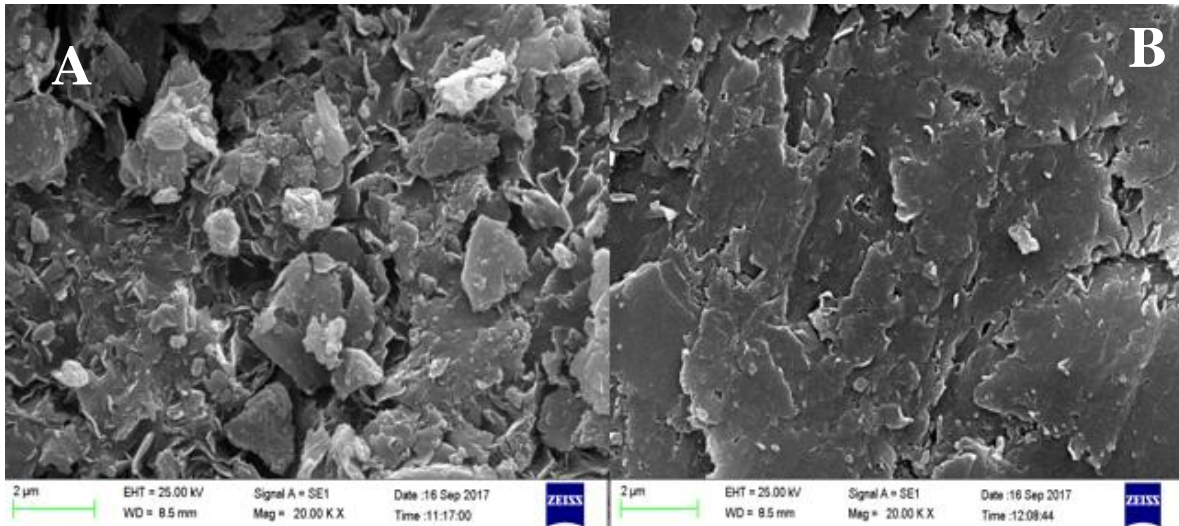


Fig. 104 Field emission scanning electron microscopic (FESEM) images of *natural bentonite* before (A) and after (B) adsorption of the oppositely charged dye (BV₁₆) (Source: Ref (65) Khalilzadeh Shirazi E et al. (2020))

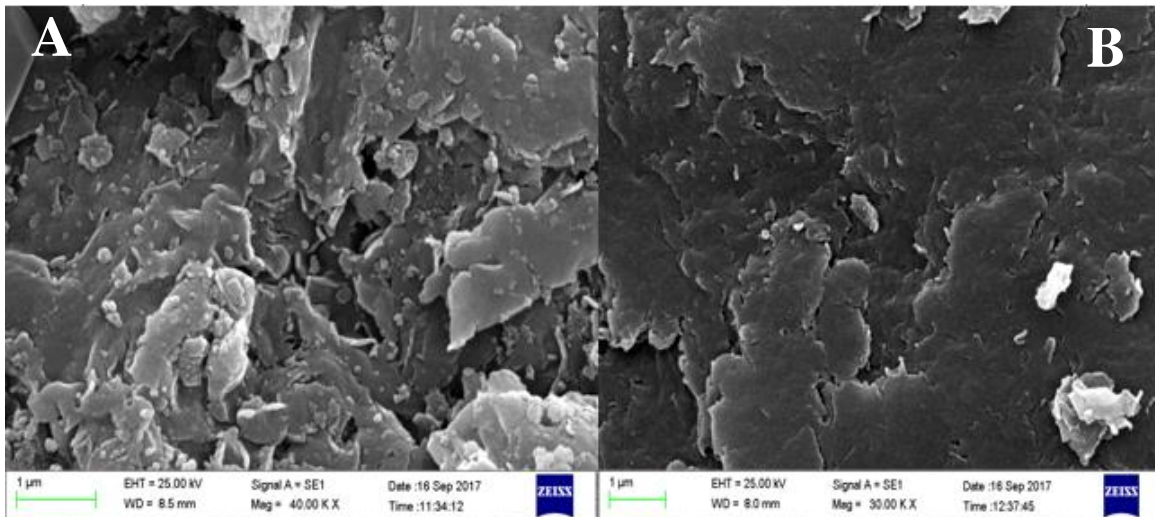


Fig. 105 Field emission scanning electron microscopic (FESEM) images of *standard bentonite* before (A) and after (B) adsorption of the oppositely charged dye (BV₁₆) (Source: Ref (65) Khalilzadeh Shirazi E et al. (2020))

The SEM images of natural bentonite and standard bentonite before and after the adsorption of BV₁₆ are shown in Figs. 104 (A-B) and 105 (A-B), respectively. Fig. 104 A and 105 A are the SEM of the pristine natural and standard bentonite depicting an irregular morphology and sheet-like structure containing various size particles (147).

Figs. 104 B and 105 B indicate an effective adsorption of the cationic BV₁₆ molecules into the pores of the adsorbents resulting in a less porous and more homogenous surface. This suggests that the dye-adsorbed bentonite surface after dye adsorption is coated by dye molecules (65, 127).

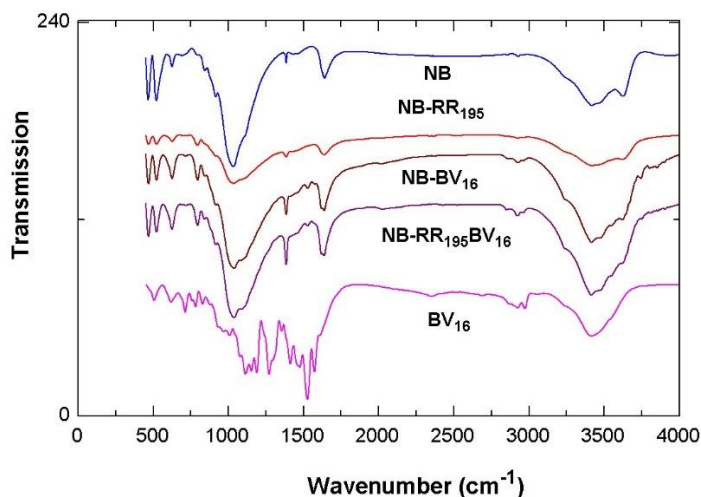


Fig. 106 FTIR spectra of *natural bentonite* before and after adsorption of BV₁₆ and/or RR₁₉₅ (Source: Ref (65) Khalilzadeh Shirazi E et al. (2020))

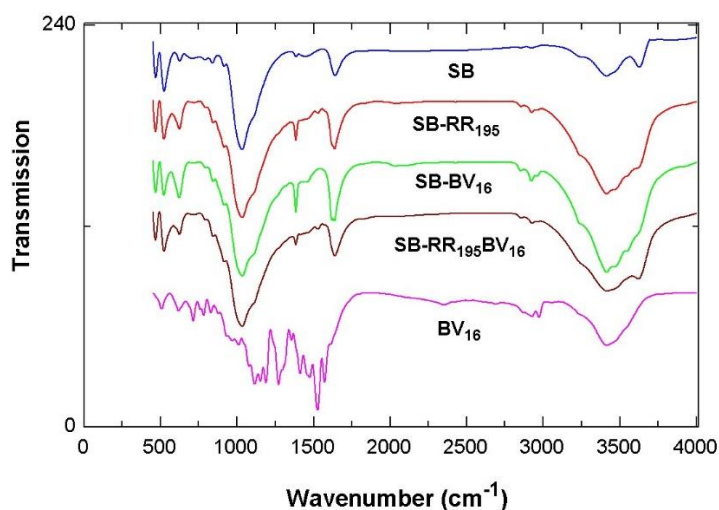


Fig. 107 FTIR spectra of *standard bentonite* before and after adsorption of BV₁₆ and/or RR₁₉₅ (Source: Ref (65) Khalilzadeh Shirazi E et al. (2020))

Fourier transform infrared (FTIR) spectra of natural bentonite, standard bentonite and charred dolomite were recorded in the range of 400 - 4,000 cm⁻¹ at room temperature before and after adsorption of BV₁₆ and RR₁₉₅ in single and binary dye solutions. Fig. 106 shows

the FTIR spectra of natural bentonite samples and Fig. 107 that of standard bentonite samples. IR absorptions at ca. 524, 466, and 917 cm^{-1} which can be attributed to Al · O · Si, Si · O · Si and Al · Al · OH vibrations confirm the presence of montmorillonite. Bands in the region of 3,800 - 3,400 cm^{-1} can be ascribed to the stretching vibration of O.H bonds. The FTIR spectra of both types of bentonites show two bands in this region (3,624.8 cm^{-1} and 3,416 cm^{-1}). The FTIR spectrum of natural bentonite loaded with solely BV₁₆ and the spectrum of this adsorbent with BV₁₆ together with RR₁₉₅ are very similar indicating selective adsorption of BV₁₆ via an interaction with the respective functional groups of the adsorbent mentioned above. Analogous results were obtained for standard bentonite. This influence of functional groups on the chemical adsorption process was demonstrated also in some previous works (65, 127, 148).

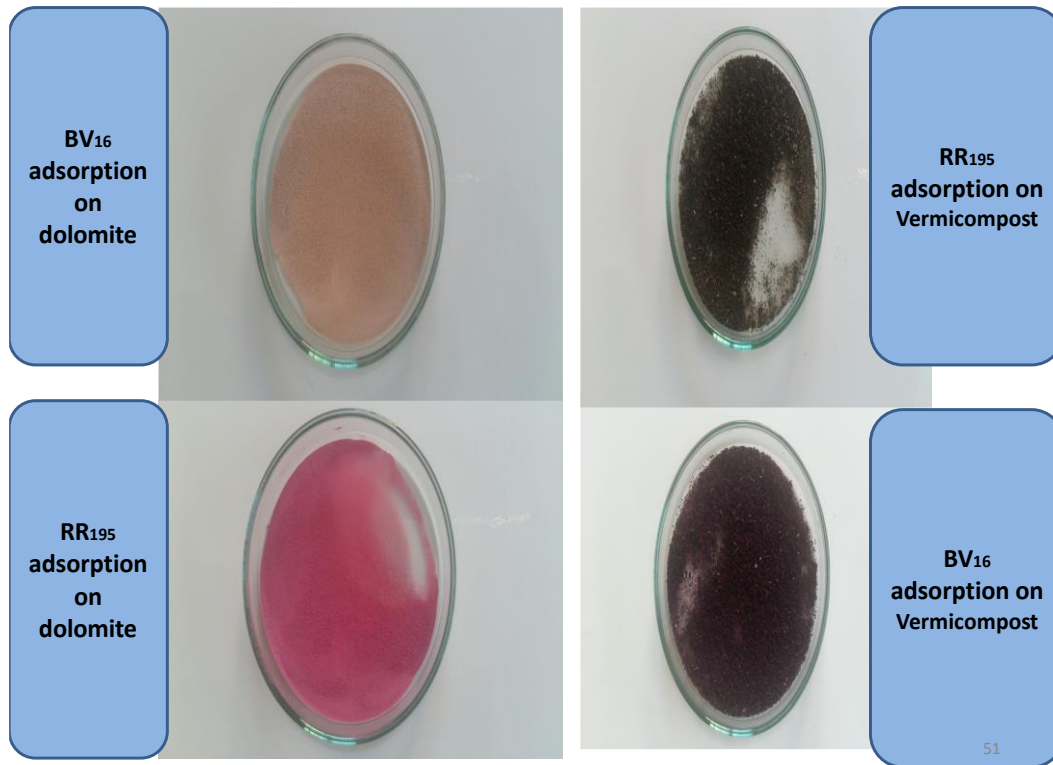


Fig. 108 Adsorption of BV₁₆ on charred dolomite (A), adsorption of RR₁₉₅ on charred dolomite (B), adsorption of RR₁₉₅ on vermicompost (C), adsorption of BV₁₆ on vermicompost (D)



Fig. 109 Removal of RR₁₉₅ with charred dolomite by stirring the suspension in a Jar Tester

Summary of chapter 3

Characterization of the adsorbents

The characterization of the adsorbents showed that vermicompost has a high content of total organic matter (48.13%), high humidity (63%) and a low surface area ($2.91 \text{ m}^2 \text{ g}^{-1}$). The main constituents of charred dolomite were MgO and CaO and in natural bentonite SiO_2 (59.87%) and Al_2O_3 (11.01%) dominated which are supposed to be mainly responsible for the adsorption of the dyes from the solution. The specific surface area for natural powdered bentonite, standard bentonite, charred dolomite and natural granular bentonite was 1205.3, 238.34, 11.88 and $41.83 \text{ m}^2 \text{ g}^{-1}$, respectively. Analysis by X-ray diffractometer (XRD) for mineral analysis of the granular bentonite revealed that the natural material has a phase composition, including the constituents of montmorillonite, clinoptilolite, kaolinite and muscovite-illite, with the main phase being montmorillonite (8, 65).

Characterization of the real wastewater from acrylic-fiber dyeing at Acryl Tab CO.

The wastewater already pretreated by coagulation-flocculation, characterized by a yellowish-orange color, SAC numbers of 20.2 m^{-1} (436 nm), 6.4 m^{-1} (525 nm) and 3.9 m^{-1} (620 nm), an alkaline pH of 11.6 and a COD value of 890 mg L^{-1} was obtained from Acryl Tab CO. It was investigated and treated with natural granular bentonite in batch and fixed-bed column studies.

Batch adsorption studies on real textile wastewater

In the batch studies, the optimized amount of natural granular bentonite for color removal from wastewater was 5 g/L . The adsorption processes followed satisfactorily a pseudo-second-order kinetics and was in agreement with the Langmuir model for all three wavelengths investigated.

The results from the batch experiments showed that the color removal was 88.1% ($\text{SAC}_{436 \text{ nm}}$), 70.3% ($\text{SAC}_{525 \text{ nm}}$) and 71.8% ($\text{SAC}_{620 \text{ nm}}$) and under the optimum conditions, COD concentration was decreased from initial 890 mg L^{-1} to 403 mg L^{-1} , i.e. 54.7% of COD was removed.

Fixed-bed column adsorption experiments

The experimental breakthrough curves for different bed heights and flow rates in fixed-bed column studies indicated that the influent flow rate of 5 mL min^{-1} using a column filled with granular bentonite with a bed height of 20 cm is the best condition for the reduction of color and COD. Breakthrough times of the color removal using adsorbent bed heights of 5, 10 and 20 cm were 360, 540 and 960 min, for the flow rate of 5 ml min^{-1} , respectively. The respective exhaustion times were 600, 840 and 1140 min. It was concluded that the breakthrough times and exhaustion times increased with the increase of the adsorbent bed height and the decrease of the flow rate which is related to the better contact and interaction of the bulk solution with the adsorbent, improving the mass transfer of the dye molecules which lowers the concentration of the dye in the effluent.

Reuse of the treated textile wastewater in the textile industry

By treatment in the fixed-bed adsorption column a color concentration corresponding $32 \text{ mg Pt-Co L}^{-1}$ was obtained which is below the determined limited value for discharge according to Iranian standards. The SAC values of the treated effluent decreased to 3.9 for $\text{SAC}_{436 \text{ nm}}$, 1.5 for $\text{SAC}_{525 \text{ nm}}$ and to 1.4 for $\text{SAC}_{620 \text{ nm}}$ which is also German discharge limits.

The color of the treated effluent was above detection limits ("non-visible") necessary for a general reuse as suggested by the AquaFit4Use project. The COD of the effluent after treatment decreased from 890 mg L^{-1} to 382 mg L^{-1} which lies in the allowed COD range of "low-quality water". Therefore, considering color and COD values as well as other parameters such as heavy metals, total hardness and chlorine of the treated wastewater from the continuous fixed-bed filled with granular bentonite and of the water which is normally reused at the Acryl Tab company, the treated water from the fixed-bed adsorption process can be suggested to be used in the studied industry for rinsing the fibers in the pretreatment step, washing down the equipment and for washing the floors.

Fixed-bed column design by the scale-up approach

With reference to the data obtained from the calculations based on the scale-up approach, the design column has an area of $A = 0.84 \text{ m}^2$ and a diameter of $d = 1.04 \text{ m}$. The height of the design column can be between 3.12 m to 5.12 m. According to the results from 5 cm, 10 cm and 20 cm bentonite bed height at pilot-scale, the design column can treat 37.5 m^3 , 56.25 m^3 and 100 m^3 of wastewater, respectively in 6 h, 9 h and 16 h (at break through

points) using 2287 kg, 4569.6 kg and 9150.4 kg of bentonite which is required for the treatment of wastewater with a flow rate of $150 \text{ m}^3 \text{ d}^{-1}$. As the company works mainly in 2 working shifts, 6098 kg bentonite (5 cm bed height), 8123.73 kg bentonite (10 cm bed height) and 9150.4 kg bentonite (20 cm bed height) is required to treat the generated wastewater.

Reusing the spent bentonite in lightweight aggregates production

The $\text{SiO}_2/\Sigma\text{Flux}$ ratio of the green granules made of the spent adsorbent was ca. 2. This shows the ability of the material to bloat and lets expect a high viscosity of the melted material during sintering.

The products (LWAs) made with the spent material were comparable to those made with the standard natural clay in terms of technical properties such as density, water absorption and compressive strength.

Life cycle assessment (LCA) and Monte Carlo analysis for comparing textile wastewater treatment with bentonite and activated carbon

Monte Carlo simulation method concluded that 3.81 kg of activated carbon is required to treat 1 m^3 of textile wastewater (in relation to 86.6 kg bentonite). Different disposal scenarios which were studied by LCA indicated that the lowest environmental impact is related to the scenario of reusing bentonite in LECA (single score: 1.81) but regeneration of activated carbon concluded 235 which it is about 130 times worse than reusing the spent bentonite in LECA production.

From the economic point of view, Monte Carlo analysis concluded that the treatment of 1 m^3 textile wastewater with bentonite is much cheaper than using AC.

Regarding carbon footprint assessment, the highest amount of the emitted carbon dioxide is concluded in the scenario of "spent activated carbon landfilling" and the lowest amount is concluded in "reusing the spent bentonite in LECA".

Batch adsorption studies on dye-spiked groundwater

Adsorption of dyes on the single sorbent and mixed sorbent in binary dye solutions

In both single and binary dye experiments, charred dolomite (having a positive surface charge), i.e. natural Persian dolomite thermally treated at ca. 800 °C, vermicompost and also natural untreated bentonite (having a negative surface charge) have a high potential to remove anionic and cationic fabric dyes from contaminated groundwater, with preference for the respective dye with the opposite charge, respectively. Thus, charred dolomite is very efficient to remove the reactive dye RR₁₉₅ from water and negatively charged adsorbents such as vermicompost and natural bentonite are very effective adsorbents to remove the cationic dye BV₁₆ from water, whereas the dye with the same charge as the adsorbent has only a very low affinity. Electrostatic attraction is likely to play the main role in the mechanism of the adsorption process.

The experimental results not only revealed interactions between the dyes and the adsorbents but also mutual effects between the dyes BV₁₆ and RR₁₉₅ themselves. Interestingly, in binary dye solutions, the degree of adsorption of RR₁₉₅ on bentonite increased considerably in the presence of BV₁₆, which can be interpreted as synergism. In a similar synergistic way, RR₁₉₅ caused a double increase in the degree of adsorption of bentonite toward BV₁₆. On the other hand, when charred dolomite was used as the adsorbent, RR₁₉₅ enhanced the adsorption of the cationic dye BV₁₆. However, RR₁₉₅ relatively reduced the adsorption of BV₁₆ to vermicompost.

The adsorption data were used to determine adsorption isotherms and kinetic curves for single and binary dye experiments.

The behavior of all adsorbents in single and binary dye experiments could well be described by the Langmuir adsorption model. However, in the case of the adsorption of BV₁₆ on vermicompost in a binary dye system, it was found that the Freundlich model is in good agreement with the experimental data. The adsorption processes totally hinge on the initial dye concentration. Kinetic measurements suggest a pseudo-second-order kinetics as the most acceptable one in single and binary dye solutions, which implies that chemisorption dominates the dye uptake process, and that the reaction rate is proportional to the concentration of adsorbent and adsorbate (8, 65).

Using mixed adsorbents, the effect of different mass ratios of the two adsorbents was investigated in order to reach the optimal removal efficiency. Regarding the system vermicompost/charred dolomite, a ratio of 50:50 was selected, and concerning charred dolomite/natural bentonite, the ratio concluded from optimized adsorbent amounts (obtained from experiments with single dye solutions) was chosen.

These two systems, CD+VC (consisting of a 50:50 mixture of charred dolomite and vermicompost) and CD+NB (a mixture of charred dolomite and natural bentonite in optimized ratios), were successfully used for the simultaneous removal of two charged fabric dyes (the cationic dye BV₁₆ and the anionic dye RR₁₉₅) from contaminated groundwater. The results showed that for both dyes more than half of the removal efficiencies determined for both dyes onto the mixed sorbents were >70%, highlighting that these mixed sorbents are highly efficacious for simultaneous removal of cationic and anionic dyes from contaminated groundwater (8, 65).

High removal efficiencies were obtained using the mixed sorbent approach. In the experiments using single sorbent/single dye and single sorbent/binary dye also a high efficiency for the removal of the dyes from groundwater spiked with a textile effluent from the dyeing section of a textile plant was observed.

Further lab-scale experiments under optimal adsorption conditions with groundwater spiked with one of the dyes were performed to study the reusability of the materials. In terms of the reuse capability of the adsorbents, vermicompost and natural bentonite proved to be efficient sorbents which allow a high number of adsorption-desorption cycles stressing their economic and environmental advantage.

In a series of preliminary bench-scale experiments with single dye solutions optimum operation conditions were determined. In the single dye experiments, BV₁₆ was not removed by charred dolomite, and RR₁₉₅ was not removed by either of the two kinds of bentonites and vermicompost due to the same charge of the dye and the adsorbent.

References (Published papers):

Khalilzadeh Shirazi E, Metzger J.W, Fischer K, Hassani A.H, Design and cost analysis of batch adsorber systems for removal of dyes from contaminated groundwater using natural low-cost adsorbents, *International Journal of Industrial Chemistry*, Vol. 11, 101–110, 2020.

Khalilzadeh Shirazi E, Metzger J.W, Fischer K, Hassani A.H, Simultaneous removal of a cationic and an anionic textile dye from water by a mixed sorbent of vermicompost and Persian charred dolomite, *Chemosphere*, Vol. 234, 618-629, 2019.

Khalilzadeh Shirazi E, Metzger J.W, Fischer K, Hassani A.H, Removal of cationic and anionic dyes from single and binary dye systems with Persian charred dolomite using first-order derivative spectrophotometer analysis method, *International Journal of Advances in Science Engineering and Technology*, Vol. 6 (4), 2018.

Khalilzadeh Shirazi E, Metzger J.W, Fischer K, Hassani A.H, Removal of textile dyes from single and binary component systems by Persian bentonite and a mixed adsorbent of bentonite/charred dolomite, *Colloids and Surfaces A: Physicochemical and Engineering Aspects*, Vol. 598, 124807, 2020.

4. Summary and Outlook

This thesis highlights the effectiveness of a mineral material “granular bentonite” as a natural adsorbent in the decolorization and reduction of the pollution load (COD) of wastewater produced in the Iranian textile company of Acryl Tab. The wastewater originating from the dyeing process of acrylic fiber is pretreated at the Acryl Tab CO. by means of coagulation/flocculation.

A series of pilot-scale fixed-bed columns packed with granular bentonite were designed. They operated for treating real colored wastewater. It was found that the performance of the fixed-bed column is considerably influenced by the influent flow rate and the bed height of the column. Increasing the column bed height resulted in increasing both breakthrough time and exhaustion time of the column bed, whereas the studied parameters decreased with increasing the influent flow rate. For the practical application at the industry studied, the scale-up method based on the data obtained from the breakthrough curves of the pilot-scale column studies was used to design a larger packed-bed column. In addition, experimental studies have been carried out to understand the fundamental mechanisms and kinetics of the adsorption.

Due to the high removal efficiency of color, fixed-bed adsorption using granular bentonite can be considered as a very good option for treating this kind of acrylic fiber dyeing effluent. Important quality parameters, including color and COD, fulfilled the required demands for reuse of the treated wastewater for washing applications in the textile industry. Other parameters such as heavy metal concentrations and total hardness not only were comparable with that of the water which is normally used in the Acryl Tab CO. but even lower. Furthermore, compared to other conventional technologies such as AOPs and activated carbon, the advantages of this approach include low investment costs as well as low energy consumption and a low consumption of chemicals. In the near future, the Iranian textile industry will be forced to improve the quality of the generated wastewater for both discharge into the environment and reuse. As most industries in Iran nowadays have economic problems, using an adsorption system obviates the need to apply more expensive treatment technologies. This method would enable the industry to decrease the cost and space requirements needed for the effluent treatment as well as less consumption of groundwater for process water in the industry considering the water shortage crises in Iran.

In general, treatment of textile wastewater with a combination of a good biological treatment system and adsorption might be a better option. In other words, an adsorption step better not be used as the only treatment method. However, regarding the textile industries in Iran which most of them (including Acryl Tab CO.) do not have any biological treatment system in their wastewater treatment plant and in practice (operation and maintenance) are not able to have an

efficient biological treatment system, using an environmental-friendly and cost-effective adsorbent compared to the common adsorbent activated carbon is reasonable. Based on the LCA and Monte Carlo analysis, using the natural granular bentonite showed a much more environmentally friendly and cheaper alternative compared to activated carbon for the treatment of acrylic fiber dyeing wastewater in Acryl Tab CO. This approach can be very useful for medium to small-scale industries in Iran, to avoid the continuation of causing a lot of harm to the environment. Interestingly, the spent bentonite landfilling in LCA concluded less environmental impacts compared to the regeneration of the spent activated carbon used in textile wastewater treatment which can be ascribed to the intensive consumption of energy and electricity in the production and regeneration of activated carbon. Nevertheless, aimed at minimizing the environmental impacts, reusing the spent bentonite in LECA production was investigated in this thesis.

The spent adsorbent showed a good potential to be used as a raw material for manufacturing LWAs. The sintered aggregates made from the spent adsorbent resulted in approximately similar technical performance in terms of water absorption, compressive strength and density when compared to the commercial LECA available in Iran. The spent adsorbent as a novel raw material can bring about a new market line for its application as LWAs in the construction industry such as lightweight concrete. The reuse of the secondary material generated from the treatment process will translate into the conservation of natural resources as well as landfill diversion.

In the LCA study for using bentonite in textile wastewater treatment and reusing the spent bentonite in LWAs, the distances between the mine, Acryl Tab CO and LECA CO were considered. The results showed that using bentonite for textile wastewater treatment with the scenario of reusing the spent bentonite in LECA was the best scenario compared to the other studied scenarios from the environmental and economic perspectives. Nonetheless, close to the LECA factory, there are some important industrial areas with acrylic textile dyeing industries which can bring about even lower emission of CO₂ due to the relatively shorter distances between the wastewater treatment plants and the LECA factory and in general due to the reduced weight of lightweight concretes produced from LWAs in transportation.

All in all, it is recommended to assess the possible environmental impacts of incorporating waste materials into products such as LWAs for further investigations. Particularly, the risks of reuse and recycling strategies posed on the environment must be evaluated to avoid the development of new potential sources of pollution (90).

The main results obtained and the innovative character of the preliminary studies achieved can be summarized as follows:

1. the development of an analytical method (first-order derivative spectrophotometry) for the simultaneous analysis of the two fabric dyes BV₁₆ and RR₁₉₅ in binary dye solutions (8),
2. the adsorption of the cationic dye BV₁₆ on vermicompost with high removal efficiency in single dye solutions (8),
3. the adsorption of the cationic dye BV₁₆ on vermicompost in binary dye solutions with high removal efficiency (8),
4. the adsorption of the anionic dye RR₁₉₅ on charred dolomite in single dye solutions with high removal efficiency (8),
5. the adsorption of the anionic dye RR₁₉₅ on charred dolomite in binary dye solutions with high removal efficiency (8),
6. the adsorption of the cationic dye BV₁₆ on charred dolomite (both positively charged) enabled by the presence of the anionic dye RR₁₉₅ (synergistic effect) (8),
7. the adsorption of the cationic dye BV₁₆ on natural Persian bentonite in binary dye solutions with high removal efficiency (65),
8. a doubling of the adsorption capacity of both standard and natural bentonite for the cationic dye BV₁₆ in the presence of the anionic dye RR₁₉₅ (synergistic effect) (65),
9. simultaneous removal of BV₁₆ and RR₁₉₅ (oppositely charged dyes) with high removal efficiency from dye-spiked groundwater using mixed adsorbent systems (8, 65).

Novel mixed natural low-cost materials available in Iran for water treatment were investigated. Two dyes commonly used in the dyeing section of a textile factory could successfully be removed from dye-spiked groundwater. Selective and simultaneous removal of oppositely charged (i.e. cationic and anionic) dyes was possible. It was demonstrated that mixed adsorbent systems could be successfully used for the remediation of dye-contaminated groundwater which shows the potential of such mixtures for textile wastewater treatment and thereby the sustainable protection of water resources (65).

Taking into account that the total removal of the compounds sometimes is not needed and some useful chemicals are required to be recycled in industrial waste streams, these novel adsorption materials with a high selectivity towards targeted dyes and the ability to retrieve useful chemicals during the treatment of industrial wastewater in the controlled separation of dye mixtures have currently received many attentions. Since, many adsorbents can readily adsorb

various mixed organic dyes, but are typically poor at selectively removal of the targeted organic dyes (149).

Moreover, multiple components including cationic and anionic dyes are commonly present in real wastewater systems and they cannot be eliminated simultaneously by one sorbent. In order to achieve high removal efficiency for both of dyes with opposite charges, it is important to use oppositely charged materials at the same time (33).

Studying different adsorbents and pre-screening for adsorbents and choice of best-performing materials

The comprehensive literature review demonstrated that various natural and engineered materials have been proposed as adsorbents for dye removal from water, most of them from single dye solutions, and some of them also from binary dye solutions. Some researchers investigated the application of mixed sorbents for dye removal from binary dye solutions. However, all the mixed sorbents studied were nanomaterials and/or chemically modified and/or magnetically tailored sorbents that pose various chemicals such as surfactants, acids or bases, and the like as secondary contaminants to the environment. Their required removal causes further costs. Moreover, some of the mixed sorbents studied only can remove one type of dye (i.e. solely cationic or solely anionic dyes). For some of them the dye elimination efficiency is low, and for others maximum number of regeneration cycles is low.

The novel concept proposed in this thesis overcomes the disadvantage of other adsorbents requiring chemicals necessary for modification and/or of being expensive and/or of having low removal efficiencies and/or low number of regeneration cycles. Using the adsorbents investigated, it is possible to remove cationic and anionic dyes simultaneously by selective adsorption and with high removal efficiency. To my knowledge none of the mixed sorbents reported in literature so far demonstrated all the advantages mentioned above at the same time, specifically considering the application of the proposed mixed adsorbents systems for the removal of dyes from dye-spiked groundwater.

The dye removal capacity of each of the adsorbents natural bentonite, charred dolomite and vermicompost was tested in single dye experiments with dye-spiked deionized water. The investigation of dolomite included different raw and charred dolomitic products of the factory. They were prepared and the best-performing material with regard to removal efficiency and adsorption capacity was selected. The results showed that unlike charred dolomite, raw dolomite cannot adsorb the dyes effectively. Therefore, charred dolomite was chosen to proceed with the experiments with binary dye solutions and for using it in mixed sorbents.

With reference to literature, Na-bentonite has a higher adsorption capacity for most kinds of dyes in aqueous solutions than Ca-bentonite. Thus, Na-bentonite was selected to study the removal of dyes from aqueous solutions.

In a further step, the dye removal efficiency and the adsorption capacity of each material were determined. The capability of these adsorbents to remove the dyes from dye-spiked groundwater in single dye experiments in the new (groundwater) matrix was assessed. Regarding the adsorption of dyes on all materials in both matrices, the results showed that the adsorbents can remove the oppositely charged dyes with high elimination efficiency and that they have a very negligible capability to adsorb the dyes with a charge identical to their surface charge.

Regeneration of the adsorbents

Further lab-scale experiments were performed to determine the maximum reuse capability of the adsorbents. Eight successive adsorption-desorption steps, involving regeneration steps with 1 N HCl, prove the practicability and economic advantage of natural biosorbent vermicompost. The efficiency of vermicompost to remove the cationic dye BV₁₆ from the aqueous solution kept roughly constant during the first five cycles (~4% reduction), it decreased by ~9% after eight cycles. Unlike charred dolomite, natural bentonite (eluent: 1 N HCl) can be used multiply. After five cycles there was only a ~7% reduction of the efficiency to remove the cationic dye BV₁₆ using natural and 9% using standard bentonite. The efficiency of charred dolomite (eluent: 1 N NaOH) to remove RR₁₉₅ decreased significantly to ca. 50% already after three cycles (8, 65).

References (Published papers):

Khalilzadeh Shirazi E, Metzger J.W, Fischer K, Hassani A.H, Design and cost analysis of batch adsorber systems for removal of dyes from contaminated groundwater using natural low-cost adsorbents, *International Journal of Industrial Chemistry*, Vol. 11, 101–110, 2020.

Khalilzadeh Shirazi E, Metzger J.W, Fischer K, Hassani A.H, Simultaneous removal of a cationic and an anionic textile dye from water by a mixed sorbent of vermicompost and Persian charred dolomite, *Chemosphere*, Vol. 234, 618-629, 2019.

Khalilzadeh Shirazi E, Metzger J.W, Fischer K, Hassani A.H, Removal of cationic and anionic dyes from single and binary dye systems with Persian charred dolomite using first-order derivative spectrophotometer analysis method, *International Journal of Advances in Science Engineering and Technology*, Vol. 6 (4), 2018.

Khalilzadeh Shirazi E, Metzger J.W, Fischer K, Hassani A.H, Removal of textile dyes from single and binary component systems by Persian bentonite and a mixed adsorbent of bentonite/charred dolomite, *Colloids and Surfaces A: Physicochemical and Engineering Aspects*, Vol. 598, 124807, 2020.

5. References

- 1) Vandevivere PC, Bianchi R, Verstraete W, Treatment and reuse of wastewater from the textile wet-processing industry: Review of emerging technologies, *Journal of Chemical Technology and Biotechnology*, Vol. 72 (4), 289-302, 1998.
- 2) Sharma A, Syed Z, Brighu U, Gupta AB, Ram C, Adsorption of textile wastewater on alkali-activated sand, *Journal of Cleaner Production*, Vol. 220, 23-32, 2019.
- 3) Santos SCR, Oliveira ÁFM, Boaventura RAR, Bentonitic clay as adsorbent for the decolourisation of dyehouse effluents, *Journal of Cleaner Production*, Vol. 126, 667-676, 2016.
- 4) Crini G, Non-conventional low-cost adsorbents for dye removal: A review, *Bioresource Technology*, Vol. 97 (9), 1061-1085, 2006.
- 5) Stawiński W, Węgrzyn A, Dańko T, Freitas O, Figueiredo S, Chmielarz L, Acid-base treated vermiculite as high-performance adsorbent: Insights into the mechanism of cationic dyes adsorption, regeneration, recyclability and stability studies, *Chemosphere*, Vol. 173, 107-115, 2017.
- 6) Khalilzadeh Shirazi E, Metzger J.W, Fischer K, Hassani A.H, Design and cost analysis of batch adsorber systems for removal of dyes from contaminated groundwater using natural low-cost adsorbents, *International Journal of Industrial Chemistry*, Vol. 11, 101-110, 2020.
- 7) Wang X, Jiang C, Hou B, Wang Y, Hao C, Wu J, Carbon composite lignin-based adsorbents for the adsorption of dyes, *Chemosphere*, Vol. 206, 587-596, 2018.
- 8) Khalilzadeh Shirazi E, Metzger J.W, Fischer K, Hassani A.H, Simultaneous removal of a cationic and an anionic textile dye from water by a mixed sorbent of vermicompost and Persian charred dolomite, *Chemosphere*, Vol. 234, 618-629, 2019.
- 9) Mohammed N, Grishkewich N, Waeijen HA, Berry RM, Tam KC, Continuous flow adsorption of methylene blue by cellulose nanocrystal-alginate hydrogel beads in fixed bed columns, *Carbohydrate Polymers*, Vol. 136, 1194-1202, 2016.
- 10) Salinas T, Durruty I, Arciniegas L, Pasquevich G, Lanfranconi M, Orsi I, Alvarez V, Bonanni S, Design and testing of a pilot scale magnetic separator for the treatment of textile dyeing wastewater, *Journal of Environmental Management*, Vol. 218, 562-568, 2018.
- 11) Abidi N, Errais E, Duplay J, Berez A, Jrad A, Schäfer G, Ghazi M, Semhi K, Trabelsi-Ayadi M, Treatment of dye-containing effluent by natural clay, *Journal of Cleaner Production*, Vol. 86, 432-440, 2015.

References

- 12) Hu QH, Qiao SZ, Haghseresht F, Wilson MA, Lu GQ, Adsorption study for removal of basic red dye using bentonite, *Industrial and Engineering Chemistry Research*, Vol. 45 (2), 733-738, 2006.
- 13) Khalilzadeh Shirazi E, Metzger J.W, Fischer K, Hassani A.H, Removal of cationic and anionic dyes from single and binary dye systems with Persian charred dolomite using first-order derivative spectrophotometer analysis method, *International Journal of Advances in Science Engineering and Technology*, Vol. 6 (4), 2018.
- 14) Errais E, Duplay J, Elhabiri M, Khodja M, Ocampo R, Baltenweck-Guyot R, Darragi F, Anionic RR₁₂₀ dye adsorption onto raw clay: Surface properties and adsorption mechanism, *Colloids and Surfaces A: Physicochemical and Engineering Aspects*, Vol. 403, 69-78, 2012.
- 15) Chu H, Wang Z, Liu Y, Application of modified bentonite granulated electrodes for advanced treatment of pulp and paper mill wastewater in three-dimensional electrode system, *Journal of Environmental Chemical Engineering*, Vol. 4 (2), 1810-1817, 2016.
- 16) Patel H, Fixed-bed column adsorption study: a comprehensive review, *Applied Water Science*, Vol. 9 (45), 2019.
- 17) Schönberger H, State of the art of the co-incineration of waste-derived fuels and raw materials in clinker/cement plants, *Habilitation Treatise* (2021), <https://elib.uni-stuttgart.de/handle/11682/11568> (accessed 25 June 2022).
- 18) Quina MJ, Almeida MA, Santos R, Bordado JM, Quinta-Ferreira RM, Compatibility analysis of municipal solid waste incineration residues and clay for producing lightweight aggregates, *Applied Clay Science*, Vol. 102, 71-80, 2014.
- 19) Dondi M, Cappelletti P, D'Amore M, de Gennaro R, Graziano SF, Langella A, Raimondo M, Zanelli C, Lightweight aggregates from waste materials: Reappraisal of expansion behavior and prediction schemes for bloating, *Construction and Building Materials*, Vol. 127, 394-409, 2016.
- 20) Moreno-Maroto JM, González-Corrochano B, Alonso-Azcárate J, Rodríguez L, Acosta A, Development of lightweight aggregates from stone cutting sludge, plastic wastes and sepiolite rejections for agricultural and environmental purposes, *Journal of Environmental Management*, Vol. 200, 229-242, 2017.
- 21) Kayranli B, Adsorption of textile dyes onto iron-based waterworks sludge from aqueous solution; isotherm, kinetic and thermodynamic study, *Chemical Engineering Journal*, 173 (3), 782-791, 2011.
- 22) DíazGómez-Treviño AP, Martínez-Miranda V, Solache-Ríos M, Removal of remazol yellow from aqueous solutions by unmodified and stabilized iron modified clay, *Applied Clay Science*, Vol. 80-81, 219-225, 2013.

References

- 23) Christie R. M, Environmental aspects of textile dyeing. 1st edition, Woodhead Publishing Series in Textiles, Elsevier Science, 2007.
- 24) Yagub MT, Sen TK, Afroze S, Ang HM, Dye and its removal from aqueous solution by adsorption: A review, *Advances in Colloid and Interface Science*, Vol. 209, 172-184, 2014.
- 25) Hunger K (Ed.), *Industrial dyes: chemistry, properties, applications*, WILEY-VCH, 2003.
- 26) Integrated Pollution Prevention and Control (IPPC), Reference Document on Best Available Techniques for the Textiles Industry, European Commission, 2003.
- 27) Ziane S, Marouf-Khelifa K, Benmekki H, Schott J, Khelifa A, Removal of a reactive textile azo dye by dolomitic solids: kinetic, equilibrium, thermodynamic, and FTIR studies, *Desalination and Water Treatment*, Vol. 56 (3), 695-708, 2015.
- 28) Vanaamudan A, Pathan N, Pamidimukkala P, Adsorption of Reactive Blue 21 from aqueous solutions onto clay, activated clay and modified clay, *Desalination and Water Treatment*, Vol. 52 (7-9), 1589-1599, 2014.
- 29) Carneiro PA, Osugi ME, Fugivara CS, Boralle N, Furlan M, Zanoni MVB, Evaluation of different electrochemical methods on the oxidation and degradation of Reactive Blue 4 in aqueous solution, *Chemosphere*, Vol. 144, 327-337, 2017.
- 30) Holkar CR, Jadhav AJ, Pinjari DV, Mahamuni NM, Pandit AB, A critical review on textile wastewater treatments: Possible approaches, *Journal of Environmental Management*, Vol. 182, 351-366, 2016.
- 31) Kant R, Textile dyeing industry an environmental hazard, *Natural Science*, Vol. 4 (1), 22-26, 2012.
- 32) Schönberger H, Schäfer T, Best Available Techniques in the Textile Industry, UBA. Texte, 14/2023(2003), <https://www.umweltbundesamt.de/sites/default/files/medien/publikation/short/k2274.pdf> (accessed 23.06.2022).
- 33) Yu JX, Zhu J, Feng LY, Chi RA, Simultaneous removal of cationic and anionic dyes by the mixed sorbent of magnetic and non-magnetic modified sugarcane bagasse, *Journal of Colloid and Interface Science*, Vol. 451, 153-160, 2015.
- 34) Qiao S, Hu Q, Haghseresht F, Hu X, Lu GQ (Max), An investigation on the adsorption of acid dyes on bentonite based composite adsorbent, *Separation and Purification Technology*, Vol. 67 (2), 218-225, 2009.
- 35) GilPavas E, Correa-Sanchez S, Assessment of the optimized treatment of indigo-polluted industrial textile wastewater by a sequential electrocoagulation-activated carbon adsorption process, *Journal of Water Process Engineering*, Vol. 36, 101306, 2020.

References

- 36) Khan S, Malik A, Environmental and Health Effects of Textile Industry Wastewater, In: Malik A, Grohmann E, Akhtar R (Eds.), Environmental Deterioration and Human Health, Springer, Dordrecht, 2014.
- 37) Mahmoodi NM, Synthesis of core-shell magnetic adsorbent nanoparticle and selectivity analysis for binary system dye removal, Journal of Industrial and Engineering Chemistry, Vol. 20 (4), 2050-2058, 2014.
- 38) Pal P, Industrial Water Treatment Process Technology, Industrial Water Treatment Process Technology, 2017.
- 39) Paździor K, Klepacz-Smółka A, Wrębiak J, Liwarska-Bizukojc E, Ledakowicz S, Biodegradability of industrial textile wastewater - Batch tests, Water Science and Technology, 74 (5), 1079-1087, 2016.
- 40) Tchobanoglous G, Burton FL, Stensel HD, Metcalf & Eddy, Incl. (Eds.), Wastewater Engineering: Treatment and Reuse, McGraw-Hill 4th edition, 2003.
- 41) Manual Best Management Practices for Pollution Prevention in the Textile Industry, EPA/625/R-96/004, 1996.
- 42) Noroozi B, Sorial GA, Bahrami H, Arami M, Adsorption of binary mixtures of cationic dyes, Dyes and Pigments, 76 (3), 784-791, 2008.
- 43) Soares PA, Batalha M, Souza SMAGU, Boaventura RAR, Vilar VJP, Enhancement of a solar photo-Fenton reaction with ferric-organic ligands for the treatment of acrylic-textile dyeing wastewater, Journal of Environmental Management, Vol. 152, 120-131, 2015.
- 44) Navin PK, Kumar S, Mathur M, Textile wastewater treatment: A critical review, In: International Journal of Engineering Research & Technology (IJERT), Vol. 6 (11), 2018.
- 45) Anjaneyulu Y, Sreedhara Chary N, Samuel Suman Raj D, Decolourization of industrial effluents - Available methods and emerging technologies - A review, Reviews in Environmental Science and Biotechnology, Vol. 4, 245-273, 2005.
- 46) Rahmani Z, Kermani M, Gholami M, Jafari AJ, Mahmoodi NM, Effectiveness of photochemical and sonochemical processes in degradation of basic violet 16 (BV₁₆) dye from aqueous solutions, Iranian Journal of Environmental Health Science and Engineering, Vol. 9, 2012.
- 47) Silva LGM, Moreira FC, Souza AAU, Souza SMAGU, Boaventura RAR, Vilar VJP, Chemical and electrochemical advanced oxidation processes as a polishing step for textile wastewater treatment: A study regarding the discharge into the environment and the reuse in the textile industry, Journal of Cleaner Production, Vol. 198, 430-442, 2018.
- 48) Bhagavathi Pushpa T, Vijayaraghavan J, Sardhar Basha SJ, Sekaran V, Vijayaraghavan K, Jegan J, Investigation on removal of malachite green using

References

- EM based compost as adsorbent, *Ecotoxicology and Environmental Safety*, Vol. 118, 177-182, 2015.
- 49) Robinson T, McMullan G, Marchant R, Nigam P, Remediation of dyes in textile effluent: A critical review on current treatment technologies with a proposed alternative, *Bioresource Technology*, Vol. 77 (3), 247-255, 2001.
- 50) Worch E (Ed), *Adsorption technology in water treatment: Fundamentals, processes, and modeling*, De Gruyter, 2012.
- 51) Liu L, Zhang B, Zhang Y, He Y, Huang L, Tan S, Cai X, Simultaneous removal of cationic and anionic dyes from environmental water using montmorillonite-pillard graphene oxide, *Journal of Chemical & Engineering Data*, 60 (5), 1270-1278, 2015.
- 52) Crini, G, Lichtfouse E, Wilson LD, Morin-Crini N, Adsorption-Oriented Processes Using Conventional and Non-conventional Adsorbents for Wastewater Treatment. In: Crini G, Lichtfouse E (eds), *Green Adsorbents for Pollutant Removal, Environmental Chemistry for a Sustainable World*, Springer, Cham, Vol. 18, 23-71, 2018.
- 53) An S, Liu X, Yang L, Zhang L, Enhancement removal of crystal violet dye using magnetic calcium ferrite nanoparticle: Study in single- and binary-solute systems, *Chemical Engineering Research and Design*, Vol. 94, 726-735, 2015.
- 54) Lian L, Guo L, Guo C, Adsorption of Congo red from aqueous solutions onto Ca-bentonite, *Journal of Hazardous Materials*, Vol. 161 (1), 126-131, 2009.
- 55) Abuzerr S, Darwish M, Mahvi AH, Simultaneous removal of cationic methylene blue and anionic reactive red 198 dyes using magnetic activated carbon nanoparticles: Equilibrium, and kinetics analysis, *Water Science and Technology*, Vol. 2017 (2), 534-545, 2018.
- 56) Ziane S, Bessaha F, Marouf-Khelifa K, Khelifa A, Single and binary adsorption of reactive black 5 and Congo red on modified dolomite: Performance and mechanism, *Journal of Molecular Liquids*, Vol. 249, 1245-1253, 2018.
- 57) Nourmoradi H, Avazpour M, Ghasemian N, Heidari M, Moradnejadi K, Khodarahmi F, Javaheri M, Mohammadi Moghadam M, Surfactant modified montmorillonite as a low-cost adsorbent for 4-chlorophenol: Equilibrium, kinetic and thermodynamic study, *Journal of Taiwan Institute of Chemical Engineers*, Vol. 59, 244-251, 2016.
- 58) De Godoi Pereira M, Korn M, Santos BB, Ramos MG, Vermicompost for tinted organic cationic dyes retention, *Water, Air, and Soil Pollution*, Vol. 200 (1-4), 227-235, 2009.

References

- 59) Pereira MG, Arruda MAZ, Vermicompost as a natural adsorbent material: Characterization and potentialities for cadmium adsorption, *Journal of the Brazilian Chemical Society*, Vol. 14 (1), 39-47, 2003.
- 60) Karaca S, Gürses A, Ejder M, Açıkyıldız M, Adsorptive removal of phosphate from aqueous solutions using raw and calcinated dolomite, *Journal of Hazardous Materials*, Vol. 128, 273-279, 2006.
- 61) Salameh Y, Albadarin AB, Allen S, Walker G, Ahmad MNM, Arsenic (III,V) adsorption onto charred dolomite: Charring optimization and batch studies, *Chemical Engineering Journal*, Vol. 259, 663-671, 2015.
- 62) Albadarin AB, Mangwandi C, Al-Muhtaseb AH, Walker GM, Allen SJ, Ahmad MNM, Kinetic and thermodynamics of chromium ions adsorption onto low-cost dolomite adsorbent, *Chemical Engineering Journal*, Vol. 179, 193-202, 2012.
- 63) Walker GM, Hansen L, Hanna JA, Allen SJ, Kinetics of a reactive dye adsorption onto dolomitic sorbents, *Water Research*, Vol. 37 (9), 2081-2089, 2003.
- 64) Vimonses V, Lei S, Jin B, Chow CWK, Saint C, Kinetic study and equilibrium isotherm analysis of Congo Red adsorption by clay materials, *Chemical Engineering Journal*, Vol. 148 (2-3), 354-364, 2009.
- 65) Khalilzadeh Shirazi E, Metzger J.W, Fischer K, Hassani A.H, Removal of textile dyes from single and binary component systems by Persian bentonite and a mixed adsorbent of bentonite/charred dolomite, *Colloids and Surfaces A: Physicochemical and Engineering Aspects*, Vol. 598, 124807, 2020.
- 66) Titchou FE, Akbour RA, Assabbane A, Hamdani M, Removal of cationic dye from aqueous solution using Moroccan pozzolana as adsorbent: Isotherms, kinetic studies, and application on real textile wastewater treatment, *Groundwater for Sustainable Development*, Vol. 11, 100405, 2020.
- 67) Xia L, Zhou S, Zhang C, Fu Z, Wang A, Zhang Q, Wang Y, Liu X, Wang X, Xu W, Environment-friendly *Juncus effusus*-based adsorbent with a three-dimensional network structure for highly efficient removal of dyes from wastewater, *Journal of Cleaner Production*, Vol. 259, 120812, 2020.
- 68) Bener S, Atalay S, Ersöz G, The hybrid process with eco-friendly materials for the treatment of the real textile industry wastewater, *Ecological Engineering*, Vol. 148, 105789, 2020.
- 69) Núñez J, Yeber M, Cisternas N, Thibaut R, Medina P, Carrasco C, Application of electrocoagulation for the efficient pollutants removal to reuse the treated wastewater in the dyeing process of the textile industry, *Journal of Hazardous Materials*, Vol. 371, 705-711, 2019.
- 70) Xu Z, Cai JG, Pan BC, Mathematically modeling fixed-bed adsorption in aqueous systems, *Journal of Zhejiang University: Science A*, Vol. 14 (3), 155-176, 2013.

References

- 71) Patel H, Comparison of batch and fixed bed column adsorption: a critical review, *International Journal of Environmental Science and Technology*, 2021.
- 72) Wibulswas R, Batch and fixed bed sorption of methylene blue on precursor and QACs modified montmorillonite, *Separation Purification Technology*, Vol. 39 (1-2), 3-12, 2004.
- 73) Reynolds TD, Richards PA, *Unit operations and processes in environmental engineering*, PWS series in engineering, 2nd ed, 1996.
- 74) <https://www.imperial.ac.uk/people/k.madani>
- 75) Madani K, Water management in Iran: what is causing the looming crisis?, *Journal of Environmental Studies and Sciences*, Vol. 4 (4), 315-328, 2014.
- 76) Hasanbeigi A, Hasanabadi A, Abdorrazaghi M, Comparison analysis of energy intensity for five major sub-sectors of the Textile Industry in Iran, *Journal of Cleaner Production*, Vol. 23 (1), 186-194, 2012.
- 77) Rahmani Z, Gholami M, Determination of quality and quantity textile industry wastewater located in 21 area (zone) and comparison their effluent with environmental protection organization standards in 1389, *Iran Occupational Health*, Vol. 10 (4), 25-32, 2013.
- 78) Soares PA, Silva TFCV, Ramos Arcy A, Souza SMAGU, Boaventura RAR, Vilar VJP, Assessment of AOPs as a polishing step in the decolourisation of bio-treated textile wastewater: Technical and economic considerations, *Journal of Photochemistry and Photobiology A: Chemistry*, Vol. 317, 26-38, 2016.
- 79) Vajnhandl S, Valh JV, The status of water reuse in European textile sector, *Journal of Environmental Management*, Vol. 141, 29-35, 2014.
- 80) AquaFit4Use, 2010. Public results: Water quality demands in paper, chemical, food and textile companies, <http://www.aquafit4use.eu>, accessed in 19th June 2017.
- 81) Schönberger H, Technique combinations to meet the ambitious ZDHC Wastewater Guidelines, *Proceedings of the Colloquium on Textile Wastewater Management 2018-09-18/Integrated Best Available Wastewater Management in the Textile Industry*, Stuttgarter Berichte zur Siedlungswasserwirtschaft, Band 241, ISBN 978-3-8356-7411-0, Vulkan-Verlag GmbH, Essen, 35-70, 2018.
- 82) Fashandi H, Pakravan HR, Latifi M, Application of modified carpet waste cuttings for production of eco-efficient lightweight concrete, *Construction and Building Materials*, Vol. 198, 629-637, 2019.
- 83) Galán-Arboledas RJ, Cotes-Palomino MT, Bueno S, Martínez-García C, Evaluation of spent diatomite incorporation in clay based materials for lightweight bricks processing, *Construction and Building Materials*, Vol. 144, 327-337, 2017.

References

- 84) Ducman V, Mirtič B, The applicability of different waste materials for the production of lightweight aggregates, *Waste Management*, Vol. 29 (8), 2361-2368, 2009.
- 85) Tuan BLA, Hwang CL, Lin KL, Chen YY, Young MP, Development of lightweight aggregate from sewage sludge and waste glass powder for concrete, *Construction and Building Materials*, Vol. 47, 334-339, 2013.
- 86) Ayati B, Molineux C, Newport D, Cheeseman C, Manufacture and performance of lightweight aggregate from waste drill cuttings, *Journal of Cleaner Production*, Vol. 208, 252-260, 2019.
- 87) Liu P, Farzana R, Rajarao R, Sahajwalla V, Lightweight expanded aggregates from the mixture of waste automotive plastics and clay, *Construction and Building Materials*, Vol. 145, 283-291, 2017.
- 88) González-Corrochano B, Alonso-Azcárate J, Rodríguez L, Lorenzo AP, Torío MF, Ramos JJT, Corvinos MD, Muro C, Valorization of washing aggregate sludge and sewage sludge for lightweight aggregates production, *Construction and Building Materials*, Vol. 116, 252-262, 2016.
- 89) Piszcz-Karaś K, Klein M, Hupka J, Łuczak J, Utilization of shale cuttings in production of lightweight aggregates, *Journal of Environmental Management*, Vol. 231, 232-240, 2019.
- 90) Ayati B, Ferrándiz-Mas V, Newport D, Cheeseman C, Use of clay in the manufacture of lightweight aggregate, *Construction and Building Materials*, Vol. 162, 124-131, 2018.
- 91) Mamathoni P, Harding KG, Environmental performance of extended activated sludge and sequential batch reactor using life cycle assessment, *Cleaner Environmental Systems*, Vol. 2, 100039, 2021.
- 92) Coats ER, Watkins DL, Kranenburg D, A Comparative Environmental Life-Cycle Analysis for Removing Phosphorus from Wastewater: Biological versus Physical/Chemical Processes, *Water Environment Research*, Vol. 83 (8), 2011.
- 93) Galvez-Martos JL, Schoenberger H, An analysis of the use of life cycle assessment for waste co-incineration in cement kilns, *Resources, Conservation and Recycling*, Vol. 86, 118-131, 2014.
- 94) Gabarrell X, Font M, Vicent T, Caminal G, Sarrà M, Blánquez P, A comparative life cycle assessment of two treatment technologies for the Grey Lanaset G textile dye: Biodegradation by *Trametes versicolor* and granular activated carbon adsorption, *International Journal of Life Cycle Assessment*, Vol. 17, 613-624, 2012.
- 95) <https://www.iso.org/obp/ui/#iso:std:iso:14040:ed-2:v1:en>

References

- 96) Bories C, Vedrenne E, Paulhe-Massol A, Vilarem G, Sablayrolles C, Development of porous fired clay bricks with bio-based additives: Study of the environmental impacts by Life Cycle Assessment (LCA), *Construction and Building Materials*, Vol. 125, 1142-1151, 2016.
- 97) Sun S, Ertz M, Life cycle assessment and Monte Carlo simulation to evaluate the environmental impact of promoting LNG vehicles, *MethodsX*, Vol. 7, 101046, 2020.
- 98) <http://www.worddyevaryety.com/basic-dyes-violet-16.html>.
- 99) <http://www.worddyevaryety.com/reactive-dyes/reactive-red-195.html>
- 100) Jain R, Mathur M, Sikarwar S, Mittal A, Removal of the hazardous dye rhodamine B through photocatalytic and adsorption treatments, *Journal of Environmental Management*, Vol. 85 (4), 956-964, 2007.
- 101) DIN – German Institute for Standardization, DIN EN ISO 7887:2012-04, Wasserbeschaffenheit – Untersuchung und Bestimmung der Färbung, 2012.
- 102) Rice EW, Baird RB, Eaton AD, Clesceri LS, Standard Methods for the Examination of Water and Wastewater, American Public Health Association (APHA), American Water Works Association, Water Environment Federation 22nd edition, 2012.
- 103) Acabaracan S, Vergili I, Kaya Y, Demir G, Barlas H, Removal of color from textile wastewater containing azo dyes by Fentons reagent, *Fresenius Environmental Bulletin*, Vol. 11 (10 b), 840-843, 2002.
- 104) Hazen A, The measurement of the colors of natural waters, *Journal of the American Chemical Society*, Vol, 18 (3), 264-275, 1896.
- 105) Turabik M, Adsorption of basic dyes from single and binary component systems onto bentonite: Simultaneous analysis of Basic Red 46 and Basic Yellow 28 by first order derivative spectrophotometric analysis method, *Journal of Hazardous Materials*, Vol. 158 (1), 52-64, 2008.
- 106) Wang S, Ng CW, Wang W, Li Q, Hao Z, Synergistic and competitive adsorption of organic dyes on multiwalled carbon nanotubes, *Chemical Engineering Journal*, Vol. 197, 34-40, 2012.
- 107) McKay G, Hadi M, Samadi MT, Rahmani AR, Aminabad MS, Nazemi F, Adsorption of reactive dye from aqueous solutions by compost, *Desalination and Water Treatment*, Vol. 28 (1-3), 164-173, 2011.
- 108) Nestic AR, Velickovic SJ, Antonovic DG, Characterization of chitosan/montmorillonite membranes as adsorbents for Bezactiv Orange V-3R dye, *Journal of Hazardous Materials*, Vol. 209-210, 256-263, 2012.

References

- 109) Amini M, Younesi H, Bahramifar N, Biosorption of nickel(II) from aqueous solution by *Aspergillus niger*: Response surface methodology and isotherm study, *Chemosphere*, Vol. 75 (11), 1483-1491, 2009.
- 110) Bulut E, Özacar M, Şengil IA, Equilibrium and kinetic data and process design for adsorption of Congo Red onto bentonite, *Journal of Hazardous Materials*, Vol. 154 (1-3), 613-622, 2008.
- 111) Hu X, Jia L, Cheng J, Sun Z, Magnetic ordered mesoporous carbon materials for adsorption of minocycline from aqueous solution: Preparation, characterization and adsorption mechanism, *Journal of Hazardous Materials*, Vol. 362, 1-8, 2019.
- 112) Nadeem K, Guyer GT, Dizge N, Polishing of biologically treated textile wastewater through AOPs and recycling for wet processing, *Journal of Water Process Engineering*, Vol. 20, 29-39, 2017.
- 113) Ozdemir O, Turan M, Turan AZ, Faki A, Engin AB, Feasibility analysis of color removal from textile dyeing wastewater in a fixed-bed column system by surfactant-modified zeolite (SMZ), *Journal of Hazardous Materials*, Vol. 166 (2-3), 647-654, 2009.
- 114) Moreno-Maroto JM, Uceda-Rodríguez M, Cobo-Ceacero CJ, Cotes-Palomino T, Martínez-García C, Alonso-Azcárate J, Studying the feasibility of a selection of Southern European ceramic clays for the production of lightweight aggregates, *Construction and Building Materials*, Vol. 237, 117583, 2020.
- 115) EPA. www.epa.gov. Risk-Based Screening Table, 2015
- 116) Contescu C, Adhikari S, Gallego N, Evans N, Biss B, Activated Carbons Derived from High-Temperature Pyrolysis of Lignocellulosic Biomass, C (Basel), *Journal of Carbon Research*, 4 (3), 2018.
- 117) Bazan A, Nowicki P, Półrolniczak P, Pietrzak R, Thermal analysis of activated carbon obtained from residue after supercritical extraction of hops, *Journal of Thermal Analysis and Calorimetry*, Vol. 125, 1199-1204, 2016.
- 118) Cho JH, Kim YS, Jeon S bin, Seo JB, Jung JH, Oh KJ, Improvement of thermal regeneration of spent granular activated carbon using air agent : Application of sintering and deoxygenation, *Korean Journal of Chemical Engineering*, Vol. 31 (9), 1641-1650, 2014.
- 119) Cuhadaroglu D, Uygun OA, Production and characterization of activated carbon from a bituminous coal by chemical activation, *African Journal of Biotechnology*, Vol. 7 (20), 3703-3710, 2008.
- 120) Zhu W, Du W, Shen X, Zhang H, Ding Y, Comparative adsorption of Pb²⁺ and Cd²⁺ by cow manure and its vermicompost, *Environmental Pollution*, Vol. 227, 89-97, 2017.

References

- 121) Cuhadaroglu D, Uygun OA, Production and characterization of activated carbon from a bituminous coal by chemical activation, *African Journal of Biotechnology*, Vol. 7 (20), 3703-3710, 2008.
- 122) Zhu W, Du W, Shen X, Zhang H, Ding Y, Comparative adsorption of Pb^{2+} and Cd^{2+} by cow manure and its vermicompost, *Environmental Pollution*, Vol. 227, 89-97, 2017.
- 123) Zhang J, Ma X, Yuan L, Zhou D, Comparison of adsorption behavior studies of Cd^{2+} by vermicompost biochar and $KMnO_4$ modified vermicompost biochar, *Journal of Environmental Management*, Vol. 256, 109959, 2020.
- 124) Sinha RK, Herat S, Valani D, Chauhan K, Earthworms - The environmental engineers: Review of vermiculture technologies for environmental management and resource development, *International Journal of Global Environmental Issues*, Vol. 10 (3-4), 265-292, 2010.
- 125) Paradelo R, Vecino X, Moldes AB, Barral MT, Potential use of composts and vermicomposts as low-cost adsorbents for dye removal: an overlooked application, *Environmental Science and Pollution Research*, Vol. 26, 21085-21097, 2019.
- 126) De Godoi Pereira M, Cardoso de Souza Neta L, Ferreira Fontes MP, Nascimento Souza A, Carvalho Matos T, de Lima Sachdev R, dos Santos V, Oliveira da Guarda Souza M, Almeida Santana de Andrade MV, Marinho Maciel Paulo G, Nardy Ribeiro J, Flores Nardy Ribeiro AV, An overview of the environmental applicability of vermicompost: From wastewater treatment to the development of sensitive analytical methods, Vol. 2014, *The Scientific World Journal*, 2014.
- 127) Turabik M, Gozmen B, Removal of basic textile dyes in single and multi-dye solutions by adsorption: Statistical optimization and equilibrium isotherm studies, *Clean Soil Air Water*, Vol. 41 (11), 1080-1092, 2013.
- 128) Adeyemo AA, Adeoye IO, Bello OS, Adsorption of dyes using different types of clay: a review, *Applied Water Science*, Vol. 7 (2), 543-68, 2017.
- 129) Patel H, Vashi RT, Fixed-Bed Column Studies of Dyeing Mill Wastewater Treatment Using Naturally Prepared Adsorbents, *Characterization and treatment of textile wastewater*, 127-145, 2015.
- 130) Zhang Y, Jin F, Shen Z, Wang F, Lynch R, Al-Tabbaa A, Adsorption of methyl tert-butyl ether (MTBE) onto ZSM-5 zeolite: Fixed-bed column tests, breakthrough curve modelling and regeneration, *Chemosphere*, Vol. 220, 422-431, 2019.

References

- 131) Wibulswas R, Batch and fixed bed sorption of methylene blue on precursor and QACs modified montmorillonite, *Separation Purification Technology*, Vol. 39 (1-2), 3-12, 2004.
- 132) Moreno-Maroto JM, González-Corrochano B, Alonso-Azcárate J, Martínez García C, A study on the valorization of a metallic ore mining tailing and its combination with polymeric wastes for lightweight aggregates production, *Journal of Cleaner Production*, Vol. 212, 997-1007, 2019.
- 133) Lyra GP, dos Santos V, de Santis BC, Rivaben RR, Fischer C, Pallone EM de JA, Rossignolo JA, Reuse of sugarcane bagasse ash to produce a lightweight aggregate using microwave oven sintering, *Construction and Building Materials*, Vol. 222, 222-228, 2019.
- 134) EPA-452/F-03-022. Air Pollution Control Technology. Fact sheet. EPA-CICA Fact Sheet.
- 135) Van der Sloot HA, Hoede D, Cresswell DJF, Barton JR, Leaching behaviour of synthetic aggregates, *Waste Management*, Vol. 21 (3), 221-228, 2001.
- 136) González-Corrochano B, Alonso-Azcárate J, Rodas M, Effect of thermal treatment on the retention of chemical elements in the structure of lightweight aggregates manufactured from contaminated mine soil and fly ash, *Construction and Building Materials*, Vol. 35, 497-507, 2012.
- 137) Giro-Paloma J, Mañosa J, Maldonado-Alameda A, Quina MJ, Chimenos JM, Rapid sintering of weathered municipal solid waste incinerator bottom ash and rice husk for lightweight aggregate manufacturing and product properties, *Journal of Cleaner Production*, Vol. 232, 713-721, 2019.
- 138) Ju WJ, Shin D, Park H, Nam K, Environmental compatibility of lightweight aggregates from mine tailings and industrial by products, *Metals*, Vol. 7 (10), 2017.
- 139) Xu G, Liu M, Li G, Stabilization of heavy metals in lightweight aggregate made from sewage sludge and river sediment, *Journal of Hazardous Materials*, Vol. 260, 74-81, 2013.
- 140) Al-Degs Y, Khraisheh MAM, Allen SJ, Ahmad MN, Walker GM, Competitive adsorption of reactive dyes from solution: Equilibrium isotherm studies in single and multisolite systems, *Chemical Engineering Journal*, Vol. 128 (2-3), 163-167, 2007.
- 141) Alimohamadi M, Abolhamd G, Keshtkar A, Pb(II) and Cu(II) biosorption on *Rhizopus arrhizus* modeling mono- and multi-component systems, *Minerals Engineering*, 18 (13-14), 1325-1330, 2005.
- 142) Yu JX, Cai XL, Feng LY, Xiong WL, Zhu J, Xu YL, Zhang YF, Chi RA, Synergistic and competitive adsorption of cationic and anionic dyes on polymer

References

- modified yeast prepared at room temperature, *Journal of the Taiwan Institute of Chemical Engineers*, Vol. 57, 98-103, 2015.
- 143) Deihimi N, Irannajad M, Rezai B, Equilibrium and kinetic studies of ferricyanide adsorption from aqueous solution by activated red mud, *Journal of Environmental Management*, Vol. 227, 277-285, 2018.
- 144) Zhou Q, Wang M, Adsorption-desorption characteristics and pollution behavior of reactive X-3B red dye in four Chinese typical soils, *Journal of Soils and Sediments*, Vol. 10, 1324-1334, 2010.
- 145) Luo L, Shen K, Xu Q, Zhou Q, Wei W, Gondal MA, Preparation of multiferroic Co substituted BiFeO_3 with enhanced coercive force and its application in sorption removal of dye molecules from aqueous solution, *Journal of Alloys and Compounds*, Vol. 558, 73-76, 2013.
- 146) Inyinbor AA, Adekola FA, Olatunji GA, Adsorption of Rhodamine B dye from aqueous solution on *Irvingia gabonensis* biomass: Kinetics and thermodynamics studies, *South African Journal of Chemistry*, Vol. 68, 115-125, 2015.
- 147) Bhattacharyya KG, Sen Gupta S, Sarma GK, Kinetics, equilibrium isotherms and thermodynamics of adsorption of Congo red onto natural and acid-treated kaolinite and montmorillonite, *Desalination and Water Treatment*, Vol. 53 (2), 530-542, 2015.
- 148) Al-Khatib L, Fraige F, Al-Hwaiti M, Al-Khashman O, Adsorption from aqueous solution onto natural and acid activated bentonite, *American Journal of Environmental Sciences*, Vol. 8 (5), 510-522, 2012.
- 149) Zhang C, Li P, Huang W, Cao B, Selective adsorption and separation of organic dyes in aqueous solutions by hydrolyzed PIM^{-1} microfibers, *Chemical Engineering Research and Design*, Vol. 109, 76-85, 2016.

Appendix

A1. Recovery studies for the first-order derivative spectrophotometry experiments

To evaluate the accuracy of the first-order derivative spectrophotometry in determining the dye concentrations in binary solutions, the recovery studies were carried out. Different concentrations of the binary dye solutions consisting of BV₁₆ and RR₁₉₅ were prepared, and the first-order derivative spectra of the binary mixtures were determined. The results are summarized in Table A1. The recoveries, errors and average percentage errors (all in %) of the theoretical concentrations (C_t) compared to the measured concentrations (C_m) were calculated using Eq. 1-3, respectively. In Eq. 3, N is the number of measurements.

$$\text{Recovery (\%)} = \frac{C_m}{C_t} \times 100 \quad (1)$$

$$\text{Error (\%)} = \frac{C_m - C_t}{C_t} \times 100 \quad (2)$$

$$C (\%) = \frac{\sum_{i=1}^N C_m - C_t / C_t}{N} \quad (3)$$

(105).

Table A. 1 Results of the percentage recovery, error and average error values for the concentrations of BV₁₆ and RR₁₉₅ in binary mixtures obtained from first-order derivative spectra

Theoretical mgL ⁻¹		Measurement in mgL ⁻¹		Recovery %		Error %	
C _{RR195}	C _{BV16}	C _{RR195}	C _{BV16}	RR ₁₉₅	BV ₁₆	RR ₁₉₅	BV ₁₆
2	2	2	2.1	100	105	0	5
2	4	2	3.9	100	97.5	0	-2.5
2	6	1.9	5.7	95	95	-5	-5
2	8	1.9	8.1	95	101.2	-5	1.25
2	10	1.9	9.9	95	99	-5	-1
2	2	2	2.1	100	105	0	5
4	2	3.9	1.9	97.5	95	-2.5	-5
6	2	6.2	2	103.3	100	3.33	0

Appendix

Theoretical mgL ⁻¹		Measurement in mgL ⁻¹		Recovery %		Error %	
8	2	8.2	1.9	102.5	95	2.5	-5
10	2	10.1	1.9	101	95	1	-5
2	2	2	2.1	100	105	0	5
4	4	4.2	4	105	100	5	0
6	6	6.2	6.1	103.3	101.6	3.33	1.66
8	8	8.2	7.9	102.5	98.7	2.5	-1.25
10	10	10.1	10.2	101	102	1	2
						2.4*	2.9*

*Average percentage error

As can be seen in Table A1, the recoveries for the determination of the concentrations of the dyes BV₁₆ and RR₁₉₅ in binary mixtures by the first-order derivative spectrophotometry were in the range of 95-105% and the average percentage errors (%) were 2.9 and 2.4% for BV₁₆ and RR₁₉₅, respectively. With reference to the recovery studies, it can be indicated that the concentrations of BV₁₆ and RR₁₉₅ concentrations in binary mixtures can be accurately determined using derivative spectrophotometry (8, 105).

A2. Studies on the reuse of adsorbents

Dye-loaded vermicompost and dye-loaded natural and standard bentonite were contacted to aqueous HCl (10 mL; 0.1 M) and dye-loaded charred dolomite was contacted to NaOH (10 mL; 0.1 M). After stirring the suspensions (200 rpm; 10 min) the adsorbents were filtered via filter paper. After separating the adsorbents, they were washed by deionized water for the subsequent following adsorption experiments. The amount of the dyes desorbed was determined using spectrophotometry (8, 65).

A3. pH points of zero charge (pH_{pzc}) of the adsorbents

The drift method was used to determine the pH_{pzc} of the adsorbents. Each adsorbent (0.1 g) was added to a NaCl solution (0.1 M; 50 mL) which initially had been adjusted to a pH between 2 and 10 using either NaOH or HCl (both 0.1 M). After shaking the suspensions for 24 h, the final pH values were measured. pH_{pzc} is the pH for which ΔpH (difference between initial and final pH) is zero. The pH_{pzc} was obtained as the pH at the point of intersection of the curve obtained by plotting Δ pH versus the initial pH axis (65).



Fig. A 1 Drift method test
(Laboratory of Water and Wastewater Treatment at Azad University in Iran)

A4. Effect of pH on absorbance and λ_{\max}

To find out if pH influences the absorbance of dye solutions, experiments were performed at different pH values from acidic to basic.

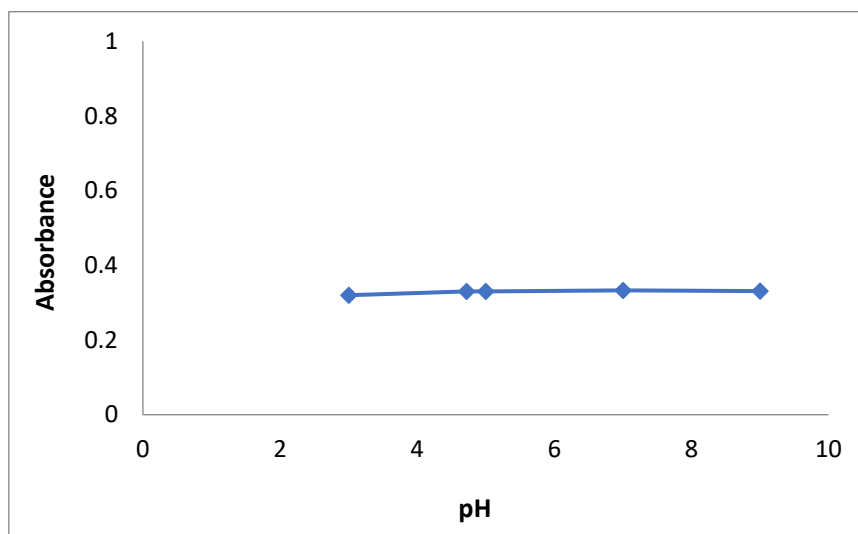


Fig. A 2 Effect of changes of pH on the absorbance of reactive red 195 at 540 nm, 20 mg L⁻¹

As can be seen in Fig. A2 the absorbance at 540 nm for RR₁₉₅ keeps constant at pH values between 3 and 9. Therefore, RR₁₉₅ is not sensitive to pH in that range.

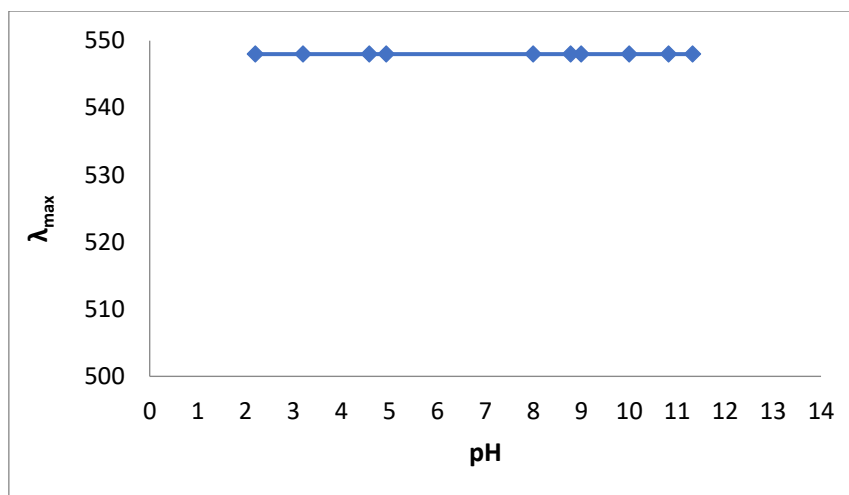


Fig. A 3 Effect of changes of pH on λ_{\max} of basic violet 16 (BV₁₆), 20 mg L⁻¹

For a solution of BV₁₆ (20 mg L⁻¹) λ_{\max} keeps constant within a pH range of 2 to 11. Therefore, it is not sensitive to pH.

A5. Reuse studies

From the aspect of sustainability as well as from an economical point of view it is desirable to have adsorbents available which can be regenerated or reused in a large number of cycles. Therefore, the regeneration capabilities of vermicompost, charred dolomite and the two kinds of bentonites were examined in experiments performing subsequent adsorption-desorption cycles. Desorption experiments were carried out to assess the maximum reuse capability of the natural adsorbents for the removal of the fabric dyes (20 mg L⁻¹ each).

The desorption cycles for regeneration were performed with HCl (0.1 M) and NaOH (0.1 M) as eluents. It could be shown that BV₁₆ strongly adsorbs to vermicompost, but it can be hardly removed from vermicompost by the eluents applied. Obviously, a high proportion of dye molecules irreversibly binds to the vermicompost adsorption sites and cannot be remobilized by HCl leading to a low percentage of recovery of the dye. The efficiency of vermicompost to remove BV₁₆ from the aqueous solution kept roughly constant during the five adsorption-desorption cycles (~4% reduction), it decreased by ~9% after eight cycles. In contrast, the efficiency of charred dolomite for the removal of RR₁₉₅ decreased significantly already after three adsorption-desorption cycles (~ 50%).

The limited amount of dye which could be desorbed from both kinds of bentonites proves a strong interaction and a high affinity between the cationic dye and the negative clay surface. After five cycles there was only a ~7% reduction of removal efficiency for the cationic dye BV₁₆ using natural bentonite, and 9% using standard bentonite; after eight cycles there was a reduction of the efficiency by 25% for natural and 30% for standard bentonite (8, 65).

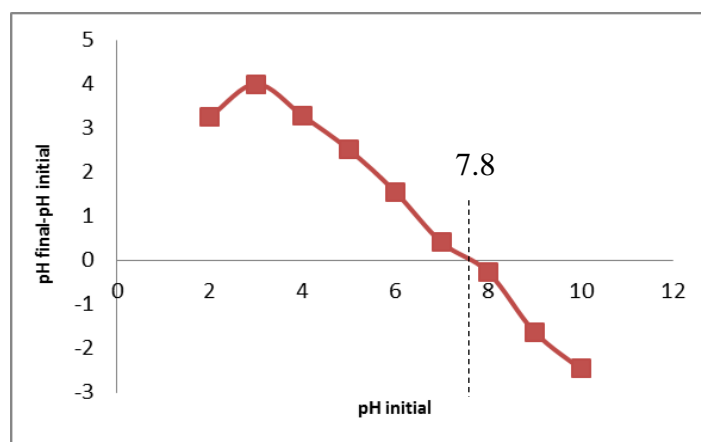
A6. pH points of zero charge (pH_{pzc}) of the adsorbents

Fig. A 4 pH_{pzc} of a suspension of vermicompost in water

In general, humic materials such as vermicompost have a great number of negative charges, which are responsible for elevated PZC.

A suspension of vermicompost in water had a pH_{PZC} of ca. 7.8. At this pH the surface is “neutral”. At a $\text{pH} > \text{pH}_{\text{pzc}}$, the charge of the adsorbent surface converts to negative (deprotonation) and it changes to positive (protonation) at a $\text{pH} < \text{pH}_{\text{PZC}}$. The measurement of the Zeta potential shows that the surface of vermicompost at the pH where the experiments were performed is negatively charged, allowing it to interact with positively charged molecules (see Fig. A4). Thus, the electrostatic attraction can explain the strong adsorption of cationic dyes on this adsorbent.

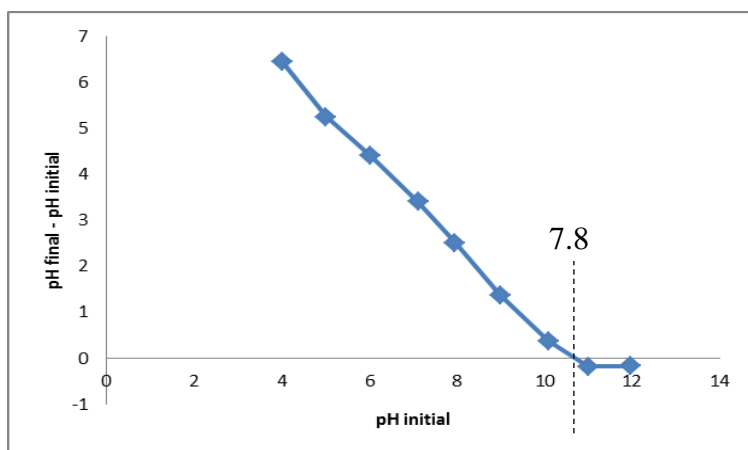


Fig. A 5 pH_{pzc} of a suspension of charred dolomite in water

The pH_{PZC} of charred dolomite determined was 10.8; below this pH, the surface of charred dolomite is positively charged due to protonation (see Fig. A5). Thus, based on electrostatic attraction negatively charged molecules like anionic dyes strongly adsorb to charred dolomite.

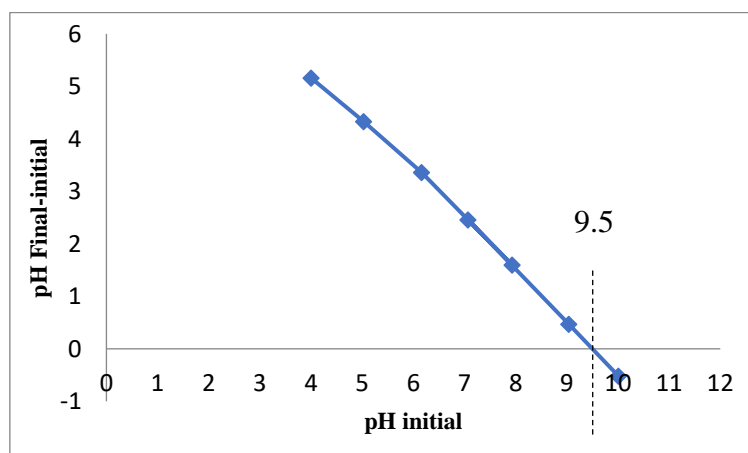


Fig. A 6 pH_{pzc} of a suspension of natural bentonite in water

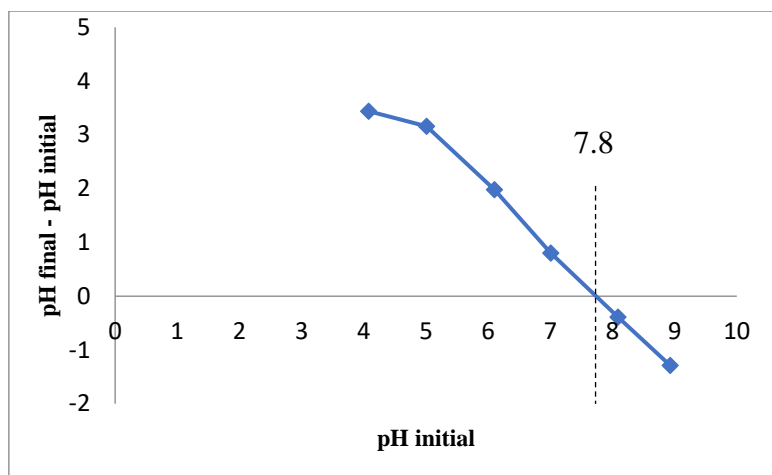


Fig. A 7 pH_{pzc} of a suspension of standard bentonite in water

A suspension of natural bentonite and standard bentonite had a pH_{PZC} of ca. 9.5 and 7.8, respectively (see Fig. A6 and A7). At a $pH > pH_{pzc}$, the charge of the adsorbent surface converts to negative and it changes to positive at a lower $pH <$ the pH_{PZC} . In the case of bentonite, the permanent negative net charges on the bentonite surface generated by the isomorphous substitutions (Al^{3+} for Si^{4+} in the tetrahedral layer and Mg^{2+} for Al^{3+} in the octahedral layer) are independent of pH. Hence, based on electrostatic attraction the cationic dye can strongly interact with bentonite within a broad range of $pH > pH_{PZC}$ (65).

**Verzeichnis der in der Schriftenreihe
„Stuttgarter Berichte zur Siedlungswasserwirtschaft“
seit 2008 erschienenen Veröffentlichungen**

Band 192	Siedlungswasserwirtschaftliches Kolloquium an der Universität Stuttgart	Zukunftsfähige Wasserversorgung – Von der lokalen zur globalen Herausforderung 22. Trinkwasserkolloquium am 14.02.2008 (2008) 116 S., 29 Abb., 4 Tab. (34,80 €)
Band 193	Hassan H. Shawly	Urban Water – Integrated Resource Planning to Meet Future Demand in Jeddah – Saudi Arabia (2008) 182 S., 38 Abb., 30 Tab. (34,80 €)
Band 194	Holger Kauffmann	Arsenelimination aus Grundwasser (2008) 151 S., 55 Abb., 22 Tab. (34,80 €)
Band 195	Siedlungswasserwirtschaftliches Kolloquium an der Universität Stuttgart	Betrieb und Sanierung von Entwässerungssystemen 83. Siedlungswasserwirtschaftliches Kolloquium am 09.10.2008 (2008) 160 S., 45 Abb. 7 Tab. (34,80 €)
Band 196	Siedlungswasserwirtschaftliches Kolloquium an der Universität Stuttgart	Von der Ressource bis zum Lebensmittel höchster Qualität 23. Trinkwasserkolloquium am 12.02.2009 (2009) 151 S., 59 Abb., 17 Tab. (34,80 €)
Band 197	Khaja Zillur Rahman	Treatment of arsenic containing artificial wastewater in different laboratory-scale constructed wetlands (2009) 184 S., 36 Abb., 10 Tab. (34,80 €)
Band 198	Juliane Gasse	Quantifizierung der Emissionen aus Abwasseranlagen und deren Auswirkungen auf die hygienische Qualität von Fließgewässern (2009) 220 S., 66 Abb., 77 Tab. (34,80 €)
Band 199	Siedlungswasserwirtschaftliches Kolloquium an der Universität Stuttgart	Abwasserbewirtschaftung im Spannungsfeld politischer, klimatischer und technischer Entwicklungen 84. Siedlungswasserwirtschaftliches Kolloquium am 08.10.2009 (2009) 213 S., 56 Abb., 24 Tab. (34,80 €)
Band 200	Darla Nickel	Erfassung und Bewertung des Einflusses von gebietsstrukturellen Eigenschaften auf Trinkwasserpreise (2009) 174 S., 27 Abb., 43 Tab. (34,80 €)

Band 201	Siedlungswasserwirtschaftliches Kolloquium an der Universität Stuttgart	Grundwasser und Grundwasserleiter – Nutzungskonflikte und Lösungsansätze 24. Trinkwasserkolloquium am 25.02.2010 (2010) 168 S., 81 Abb., 12 Tab. (34,80 €)
Band 202	Alexander Weideler	Phosphorrückgewinnung aus kommunalem Klärschlamm als Magnesium-Ammonium-Phosphat (MAP) (2010) 165 S., 69 Abb., 15 Tab. (34,80 €)
Band 203	Siedlungswasserwirtschaftliches Kolloquium an der Universität Stuttgart	Kanalsanierung – Werterhalt durch Wissensvorsprung 1. Stuttgarter Runde am 15.04.2010 (2010) 70 S., 26 Abb., 16 Tab. (24,80 €)
Band 204	Siedlungswasserwirtschaftliches Kolloquium an der Universität Stuttgart	Regenwasserbehandlung in Abwasseranlagen – Prozesse und Lösungsansätze 85. Siedlungswasserwirtschaftliches Kolloquium am 14.10.2010 (2010) 213 S., 73 Abb., 11 Tab. (34,80 €)
Band 205	Fabio Chui Pressinotti	Anpassung der Tropfkörpertechnologie an heiße Klimazonen (2010) 196 S., 82 Abb., 22 Tab. (34,80 €)
Band 206	Siedlungswasserwirtschaftliches Kolloquium an der Universität Stuttgart	Herausforderungen und Lösungen für die Wasserversorgung - Wettbewerb, Versorgungssicherheit, Innovation, Effizienzsteigerung 25. Trinkwasserkolloquium am 24.02.2011 (2011) 160 S., 47 Abb., 1 Tab. (34,80 €)
Band 207	Siedlungswasserwirtschaftliches Kolloquium an der Universität Stuttgart	Kanalsanierung – Werterhalt durch Wissensvorsprung 2. Stuttgarter Runde am 14.04.2011 (2011) 80 S., 27 Abb., 1 Tab. (24,80 €)
Band 208	Siedlungswasserwirtschaftliches Kolloquium an der Universität Stuttgart	Neue Verfahren und Betriebsstrategien in der Abwasserbehandlung 86. Siedlungswasserwirtschaftliches Kolloquium am 13.10.2011 (2011) 172 S., 71 Abb., 25 Tab. (34,80 €)
Band 209	Siedlungswasserwirtschaftliches Kolloquium an der Universität Stuttgart	Wasserversorgung und Energie – Nutzungskonflikte; Management und Technik zur Optimierung der Energieeffizienz 26. Trinkwasserkolloquium am 16.02.2012 (2012) 156 S., 81 Abb., 15 Tab. (34,80 €)

- Band 210** Geremew Sahilu Gebrie
Integrated Decision Support Tools for Rural Water Supply based on Ethiopian Case-Studies
(2012) 310 S., 101 Abb., 110 Tab.
(34,80 €)
- Band 211** Siedlungswasserwirtschaftliches Kolloquium an der Universität Stuttgart
Mikroschadstoffe und Nährstoffrückgewinnung – Praxiserfahrungen und Umsetzungspotenzial in der Abwasserreinigung
87. Siedlungswasserwirtschaftliches Kolloquium am 11.10.2012
(2012) 102 S., 44 Abb., 19 Tab.
(34,80 €)
- Band 212** Christian Johannes Locher
Anaerobe Behandlung von Abwasserkonzentraten aus der Halbstoffherzeugung von Papierfabriken
(2012), 206 S., 67 Abb., 40 Tab.
(34,80 €)
- Band 213** Siedlungswasserwirtschaftliches Kolloquium an der Universität Stuttgart
Trinkwasserqualität und Gewässerschutz – Trinkwasserverordnung, Gewässerschutzkonzepte, Spurenstoffe
27. Trinkwasserkolloquium am 21.02.2013
(2013) 134 S., 77 Abb., 10 Tab.
(34,80 €)
- Band 214** Olaf Jerzy Kujawski
Entwicklung eines anlagenweiten Steuerungs- und Regelungskonzeptes für Biogasanlagen
(2013) 238 S., 78 Abb., 35 Tab.
(34,80 €)
- Band 215** Siedlungswasserwirtschaftliches Kolloquium an der Universität Stuttgart
Kanalsanierung – Werterhalt durch Wissensvorsprung
3. Stuttgarter Runde am 18.04.2013
(2013) 84 S., 109 Abb., 2 Tab.
(24,80 €)
- Band 216** Iosif Mariakakis
A two stage process for hydrogen and methane production by the fermentation of molasses
(2013) 202S., 33 Abb., 34 Tab.
(34,80 €)
- Band 217** Siedlungswasserwirtschaftliches Kolloquium an der Universität Stuttgart
Management des urbanen Wasserhaushalts – mehr als nur Kanalnetzplanung
88. Siedlungswasserwirtschaftliches Kolloquium am 10.10.2013
(2013) 178 S., 74 Abb., 18 Tab.
(34,80 €)
- Band 218** Özgül Demet Antakyali
An Evaluation of Integrated Wastewater and Solid Waste Management in Large Tourist Resorts
(2013) 185 S., 71 Abb., 59 Tab.
(34,80 €)
- Band 219** Siedlungswasserwirtschaftliches Kolloquium an der Universität Stuttgart
Zukünftige Herausforderungen für die Wasserversorgung – Vom Klimawandel über die Demografie bis hin zur Organisation
28. Trinkwasserkolloquium am 13.02.2014
(2014) 150 S., 45 Abb., 7 Tab.
(34,80 €)

- Band 220** Siedlungswasserwirtschaftliches Kolloquium an der Universität Stuttgart
Kanalsanierung – Werterhalt durch Wissensvorsprung / Grundlagen, Konzepte und Innovation
4. Stuttgarter Runde am 10.04.2014
(2014) 108 S., 90 Abb.
(24,80 €)
- Band 221** Siedlungswasserwirtschaftliches Kolloquium an der Universität Stuttgart
Energiepotenziale kommunaler Kläranlagen erkennen, nutzen und kritisch bewerten
89. Siedlungswasserwirtschaftliches Kolloquium am 09.10.2014
(2014) 146 S. 58 Abb., 11 Tab.
(34,80 €)
- Band 222** Kristy Peña Muñoz
Integrated sludge management concepts for green energy production in wastewater treatment plants in Heujotzingo City, Mexico
(2014) 268 S., 34 Abb., 79 Tab.
(34,80 €)
- Band 223** Siedlungswasserwirtschaftliches Kolloquium an der Universität Stuttgart
Zukunftsfähigkeit und Sicherheit der Wasserversorgung – Ressourcen / Tarife / Neue Technologien
29. Trinkwasserkolloquium am 26.02.2015
(2015) 132 S., 76 Abb., 32 Tab.
(34,80 €)
- Band 224** Timo Pittmann
Herstellung von Biokunststoffen aus Stoffströmen einer kommunalen Kläranlage
(2015) 244 S., 54 Abb., 53 Tab.
(34,80 €)
- Band 225** Siedlungswasserwirtschaftliches Kolloquium an der Universität Stuttgart
Wasser Schutz Mensch
5. Aqua Urbanica und 90. Siedlungswasserwirtschaftliches Kolloquium am 07. und 08.10.2015
(2015) 338 S., 147 Abb., 28 Tab.
(34,80 €)
- Band 226** Sebastian Tews
Aerob-biologische und oxidative Verfahren zur Behandlung von Membrankonzentraten aus der Holzstoff- und Altpapieraufbereitung
(2015) 245 S., 62 Abb., 31 Tab.
(34,80 €)
- Band 227** Peace Korshiwor Amoatey
Leakage Management in the Urban Water Supply System of Ghana: Estimation and Detection Modeling
(2015) 245 S., 67 Abb., 62 Tab.
(34,80 €)
- Band 228** Sebastian Platz
Charakterisierung, Abtrennung und Nachweis von Pulveraktivkohle in der Abwasserreinigung
(2015) 256 S., 74 Abb., 51 Tab.
(34,80 €)
- Band 229** Siedlungswasserwirtschaftliches Kolloquium an der Universität Stuttgart
3 Jahrzehnte Trinkwasserkolloquium
3 Jahrzehnte Entwicklung in Wasserversorgung und Gewässerschutz
30. Trinkwasserkolloquium am 18.02.2016
(2016) 160 S., 78 Abb., 3 Tab.
(34,80 €)

- Band 230** Siedlungswasserwirtschaftliches Kolloquium an der Universität Stuttgart
Stickstoffelimination auf kommunalen Kläranlagen im Spannungsfeld von Gewässerschutz, Energieeffizienzsteigerung und Industrieabwässern
91. Siedlungswasserwirtschaftliches Kolloquium am 13.10.2016
(2016) 132 S., 38 Abb., 15 Tab.
(34,80 €)
- Band 231** Siedlungswasserwirtschaftliches Kolloquium an der Universität Stuttgart
Stand des Umwelt- und Arbeitsschutzes bei der Verchromung von Metall und Kunststoff
Kolloquium zum integrierten industriellen Umwelt- und Arbeitsschutz am 30.11.2016
(2016) 126 S., 54 Abb., 9 Tab.
(34,80 €)
- Band 232** Mehari Goitom Haile
Accounting for Uncertainties in the Modelling of Emissions from Combined Sewer Overflow Structures
(2016) 197 S., 93 Abb., 22 Tab.
(34,80 €)
- Band 233** Eduard Rott
Untersuchungen zur Elimination von Phosphor aus phosphonathaltigen Industrieabwässern
(2016) 258 S., 57 Abb., 26 Tab.
(34,80 €)
- Band 234** Kenan Güney
Investigating Water Reusability in Cotton Processing Textile Dye-house by Applying Membrane Filtration
(2017) 219 S., 64 Abb., 57 Tab.
(34,80 €)
- Band 235** Siedlungswasserwirtschaftliches Kolloquium an der Universität Stuttgart
Risiken in der Wasserversorgung
Vorsorge/Management/Minimierung/Kommunikation
31. Trinkwasserkolloquium am 06.04.2017
(2017) 132 S., 79 Abb., 6 Tab.
(34,80 €)
- Band 236** Pengfei Wang
Phosphorus recovery from wastewater via struvite crystallization in a fluidized bed reactor: Influence of operating parameters and reactor design on efficiency and product quality
(2017) 202 S., 72 Abb., 20 Tab.
(34,80 €)
- Band 237** Siedlungswasserwirtschaftliches Kolloquium an der Universität Stuttgart
Chemikalienmanagement und Umweltschutz in der textilen Kette
Kolloquium zur nachhaltigen Textilproduktion am 21.09.2017
(2017) 174 S., 48 Abb., 9 Tab. (34,80 €)
- Band 238** Siedlungswasserwirtschaftliches Kolloquium an der Universität Stuttgart
Spurenstoffe im Regen- und Mischwasserabfluss
Abwasserkolloquium 2017 am 26.10.2017
(2017) 130 S., 48 Abb., 13 Tab.
(34,80 €)

- Band 239** Marie Alexandra Launay
Organic micropollutants in urban wastewater systems during dry and wet weather – Occurrence, spatio-temporal distribution and emissions to surface waters
(2018) 240 S., 65 Abb., 38 Tab.
(34,80 €)
- Band 240** Asya Drenkova-Tuhtan
Phosphorus Elimination and Recovery from Wastewater with Reusable Nanocomposite Magnetic Particles
(2018) 259 S., 78 Abb., 25 Tab.
(34,80 €)
- Band 241** Siedlungswasserwirtschaftliches Kolloquium an der Universität Stuttgart
Integrated Best Available Wastewater Management in the Textile Industry
Colloquium on Textile Wastewater Management 2018-09-19
(2018) 182 S., 99 Abb., 14 Tab.
(34,80 €)
- Band 242** Siedlungswasserwirtschaftliches Kolloquium an der Universität Stuttgart
Spurenstoffe und antibiotikaresistente Bakterien – Schnittstelle Abwasserent- und Wasserversorgung
Abwasserkolloquium 2018 am 08.11.2018
(2018) 118 S., 26 Abb., 8 Tab.
(34,80 €)
- Band 243** Karen Mouarkech
Combined energy and phosphorus recovery from black water, co-substrates and urine
(2019) 296 S., 69 Abb., 107 Tab.
(34,80 €)
- Band 244** Siedlungswasserwirtschaftliches Kolloquium an der Universität Stuttgart
Minimisation of Wastewater Emission from Textile Finishing Industries
Colloquium on Textile Wastewater Management 2019-09-19
(2019) 148 S., 60 Abb., 20 Tab.
(34,80 €)
- Band 245** Siedlungswasserwirtschaftliches Kolloquium an der Universität Stuttgart
Ansprüche an die Siedlungswasserwirtschaft – Kernaufgaben versus weitergehende Anforderungen
Abwasserkolloquium 2019 am 10.10.2019
(2019) 143 S., 43 Abb., 2 Tab.
(34,80 €)
- Band 246** Siedlungswasserwirtschaftliches Kolloquium an der Universität Stuttgart
Sichere Trinkwasserversorgung trotz Klimawandel - wie resilient sind unsere Systeme und wo besteht Handlungsbedarf?
32. Trinkwasserkolloquium am 20.02.2020
(2020) 107 S., 52 Abb.
<http://dx.doi.org/10.18419/opus-10799>
- Band 247** Michael Seeger
Entwicklung und Validierung eines CSB-basierten und temperatursensitiven Bemessungsansatzes für Tropfkörper – Untersuchungen an technischen und halbtechnischen Tropfkörpern in warmen Klimazonen
(2020) 308 S., 63 Abb., 46 Tab.
<http://dx.doi.org/10.18419/opus-10942>

- Band 248** Stephan Wasielewski
Ammoniumrückgewinnung aus Schlammwasser mittels Ionenaustausch an Klinoptilolith (2021) 273 S., 40 Abb., 52 Tab.
<http://dx.doi.org/10.18419/opus-11464>
- Band 249** Jovana Husemann
Development of a Decision Support Tool for Integrated Wastewater and Organic Material Flows Management in the Scope of Circular Economy (2021) 216 S., 52 Abb., 30 Tab.
<http://dx.doi.org/10.18419/opus-11891>
- Band 250** Tobias David Reinhardt
Adsorptive Removal of Phosphonates and Orthophosphate From Membrane Concentrate Using Granular Ferric Hydroxide (2022) 214 S., 43 Abb., 18 Tab.
<http://dx.doi.org/10.18419/opus-12183>
- Band 251** Nikolai Otto
Evaluierung eines UV-A-LED-Panelreaktor-konzepts für Photo-Oxidationsverfahren in der (Ab-)Wasserreinigung (2022) 387 S., 84 Abb., 42 Tab.
<http://dx.doi.org/10.18419/opus-12353>
- Band 252** Manuel Christian Krauß
Entwicklung einer Methodik zur Bewertung von Trinkwassertarifen für Privathaushalte in Deutschland (2022) 308 S., 117 Abb., 32 Tab.
<http://dx.doi.org/10.18419/opus-12407>
- Band 253** Elham Khalilzadeh Shirazi
Investigations on the applicability of bentonite, dolomite and vermicompost as natural adsorbents for the decolorization of textile wastewater (2023) 238 S., 109 Abb., 30 Tab.



Forschungs- und Entwicklungsinstitut für
Industrie- und Siedlungswasserwirtschaft
sowie Abfallwirtschaft e.V. (FEI)